Développement de nouveaux ingrédients naturels à visée nutraceutique à partir de co-produits de l'industrie oléicole

Aurelia Malapert

▶ To cite this version:

Aurelia Malapert. Développement de nouveaux ingrédients naturels à visée nutraceutique à partir de co-produits de l'industrie oléicole. Autre. Université d'Avignon, 2017. Français. NNT : 2017AVIG0268 . tel-03630655
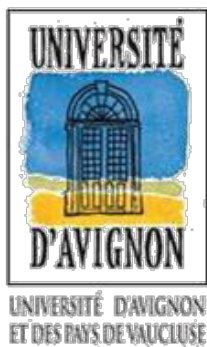
HAL Id: tel-03630655
https://hal.inrae.fr/tel-03630655

Submitted on 15 Feb 2023

Université d'Avignon et des Pays du Vaucluse

Ecole doctorale 536 – Sciences et Agrosciences

THESE

Présentée pour obtenir le grade de Docteur en Sciences

de l'Université d'Avignon et des Pays de Vaucluse

Spécialité: Chimie

Développement de nouveaux ingrédients naturels à visée nutraceutique à partir de co-produits de l'industrie oléicole

par

Aurélia MALAPERT

Le 22 décembre 2017

<u>Composition du jury:</u>

Rapporteur	Mme Amiot-Carlin Marie-Josèphe	UMR MOISA, Montpellier SupAgro
Rapporteur	Mr Rouillon Régis	Université de Perpignan
Examinateur	Mr Jacques Artaud	Aix-Marseille Université
Examinateur	Mr Dangles Olivier	Université d'Avignon
Directeur	Mme Tomao Valérie	Université d'Avignon
Co-directeur	Mme Reboul Emmanuelle	UMR NORT, Aix-Marseille Université
Invité	Mr Pinatel Christian	Centre Technique de l'Olivier

NOTES

Je souhaite adresser mes premiers remerciements à ma directrice de thèse le Dr Valérie Tomao. On a traversé moult péripéties mais on n'est toujours restée sur la barque. Je tiens également à remercier ma co-directrice de thèse le Dr Emmanuelle Reboul qui a toujours été présente, malgré la distance. Je vous remercie toutes deux pour m'avoir accueillie au sein de leur équipe respective. Ces travaux ont été permis grâce à votre accompagnement et votre confiance. J'adresse aussi mes plus sincères remerciements au Pr Olivier Dangles pour avoir toujours eu un regard bienveillant sur moi tout au long de cette thèse et pour toute l'aide que vous nous avez apportée; je vous en suis très reconnaissante. Je remercie également le Dr Nathalie Soumille pour sa gentillesse, sa douceur et son dynamisme ! Aussi, je remercie le Dr Raphaël Plasson pour sa sympathie et sa constance.

Je remercie pareillement le Pr Jacques Artaud pour avoir fait partie du comité de suivi de thèse et pour les conseils que vous nous avez apportés.

Je tiens également à remercie Mr Jean-Benoît Hugues, directeur du Moulin Castelas, pour avoir su être disponible nous avoir fourni les grignons d'olive. Je remercie la Structure Fédérative de Recherches TERSYS pour le financement de la thèse. Mes remerciements s'adressent aussi à Mr Pinatel Christian, directeur technique du Centre Technique de l'Olivier ainsi qu'à Mr André Souteyrat, président de l'Afidol, pour leur expertise et leur soutien apportés à ces travaux.

J'ai eu la chance de rencontrer et collaborer avec des personnes d'autres laboratoires. Trois jours à Toulouse m'ont permis de faire la connaissance du Dr Mallorie Tourbin de l'ENSIACET. Merci pour ta participation, ton aide et ta pédagogie. Aussi, je remercie le Pr Alain Thièry de l'IMBE, pour son soutien dans nos recherches et nos conversations enrichissantes.

Je remercie aussi particulièement le Pr Farid Chemat, directeur du laboratoire GREEN, pour m'avoir permis de participer au projet européen OliveNet et d'intégrer dans ce cadre, le laboratoire Natac à Madrid pour quatre mois. Cette expérience a été très enrichissante pour moi. Je tiens également à remercier Manu et Karine pour leur soutien et leur sympathie !

Je remercie de la même façon tous les laboratoires du bâtiment B, pas un seul ne m'a pas donné un conseil ou prêté du matériel… Le laboratoire « Chimie de l'art » de Cathy Vieillescazes, avec Carole et ses doux parfums et Céline pour son aide et sa pédagogie ; le

laboratoire IBMM très « rock » de Grégory Durand, avec Simon et Sthéphane toujours prêts à prendre de leur temps pour rendre des services et donner des conseils.

J'ai eu la chance de faire partir de l'équipe MicroNut et de passer beaucoup de temps à l'INRA en très bonne compagnie ! Je ne remercierai jamais assez Michèle, Béa, Christian, Pascale pour leur aide, leur soutien et leur amitié qui m'est chère. Aussi, je remercierai particulièrement Michèle et Béa de m'avoir fait une jolie place dans leur bureau et pour leur amitié! Béa, peu importe la ville ou le pays, on arrivera toujours à se retrouver…

Je remercie de la même façon toutes les personnes que j'ai côtoyé au sein du Domaine INRA St Paul comme Véronique, Jean-François, Domi, Eric, Claire, Romain, Thibaut et tous les autres qui ont toujours su dire un mot ou faire un sourire, ce qui m'a permis de me sentir parfaitement bien à l'INRA. Je remercie aussi très sincèrement Sylvie Serino et Emilie Rubio du laboratoire PSH pour leur aide et pour avoir toujours mis à disposition leur matériel pour moi.

« La vie n'est pas un long fleuve tranquille », la thèse non plus ! J'ai eu toutefois la chance durant ces trois années de rencontrer de superbes personnes et de bénéficier de leur soutien, leur conseil et leur sympathie. Je remercie tous mes collègues doctorants, Anne-Gaëlle, Magali et Cassandra pour leur sincère amitié. Caroline, je n'ai pas oublié ton tatouage ^^, et je te remercie pour ta joie et ton sourire, un véritable rayon de soleil ! Léa, Alice, Vincent, Natacha avec qui j'ai toujours apprécié échanger quelques mots. Je remercie également Jean-Baptiste avec qui tout a commencé et qui a été d'un grand soutien notamment en 1ère année, Hitomi pour sa douceur incomparable à une autre, Christophe, Valentin, Anaïs et aussi Elodie qui ont su me redonner le plaisir à prendre une pause « thé » ! Et à manger des bonbons ! Je remercie également Marie avec qui j'ai eu la chance de partager ma 2ème année de thèse et qui nous a confectionné un tas de petits gâteaux, tous plus bons les uns que les autres ! Je remercie bien entendu Gaëtan, toujours prêt à organiser un pot et qui a eu la gentillesse de venir me rendre visite à Madrid !

J'ai eu la chance de partager mes enseignements avec Salma mais surtout de partager de superbes conversations et soirées qu'on s'engagera à perdurer bien entendu. Merci aussi à toi, Gildas, pour ton quotidien « Never Give Up ». Tu as toujours su remotiver les troupes ! Je remercie tous les thésards et post-docs pour la cohésion et l'entre-aide constante entre nous. D'ailleurs sans ça, on n'y arriverait peut-être pas !

Le bâtiment A, the other side of the bridge… Que de bons moments passés avec vous, mes chers amis biologistes… Sandrine, Emmanuelle, Félicie, Franck, David, Marine et Saad. Je peux assurément dire qu'il n'y a pas une seule matinée où nous n'avons pas ri à gorge déployée. On en a dit des bêtises ! Mais vous avez toujours su aussi me conseiller et me soutenir. Je vous adore.

Je remercie donc très sincèrement Manue, Charlotte et Marion de l'équipe NORT, pour leur incroyable joie de vivre. De véritables donneuses d'ondes positives ! Sans oublier Marielle qui est juste fantastique ! J'ai beaucoup appris à vos côté et les moments passés avec vous ont fait partie des meilleurs de ma thèse.

No hablaba español antes de venir a Natac. Hoy, puedo intentarlo. Muchas gracias a Pini por organizar mi llegada, a Esther y Picas con quienes he trabajado, por sus consejos y amabilidad. Agredezco a José y Natalia por sus sonrisas y por enseñarme palabras no siempre elegantes! Mis grandes gracias son para Alejandra y Manu con quienes he disfrutado muchos agradables momentos. Sé que volveremos a vernos.

Je tiens à remercier tous mes amis « hors-thèse » ! On se suit depuis l'école primaire ou le collège, et ce n'est pas près de s'arrêter. Mais plus particulièrement, je remercie Fagule, Zophia et Princesse Tom-Tom. Que ce soit pour mon mariage ou pour les études (les deux choses dans lesquelles on ne m'attendait pas!), vous avez toujours cru en moi et su m'accompagner.

Pour finir, je remercie très chaleureusement ma famille. J'ai la chance d'avoir un grand frère et quatre sœurs tous plus formidables les uns que les autres. Vous avez tous été des modèles pour moi pour diverses raisons. Mes sincères compliments vont bien entendu à mes parents pour avoir réalisé la tribu et pour nous avoir toujours soutenus dans nos choix.

Enfin, je remercie infiniment mon mari, Cyprien. Tu es là depuis le début de la thèse. On ne savait pas dans quoi on s'embarquait, les trajets Nyons-Avignon quotidiens… Ça n'a pas toujours été facile, mais tu as toujours su être constant. J'admire encore la patience que tu as eue à mon égard. Tu sais combien je suis sincère quand je te dis ce tout simple mot mais qui signifie tant : « Merci ».

« Qui vit en paix avec lui-même

vit en paix avec l'univers »,

Marc-Aurèle

Publications

Review

An overview of the analysis of phenolic compounds found in olive mill by-products, Aurélia Malapert, Emmanuelle Reboul, Olivier Dangles, Valérie Tomao, *Trends in chromatography*, 10, 81-94, **2016**.

Articles

Direct and rapid profiling of biophenols in olive pomace by UHPLC-DAD-MS, Aurélia Malapert, Michèle Loonis, Emmanuelle Reboul, Olivier Dangles, Valérie Tomao, *Journal of Food Analytical Methods*, **2017**. *DOI: 10.1007/s12161-017-1064-2*.

Characterization of Hydroxytyrosol-β-cyclodextrin complexes complexes in solution and in the solid state, a potential bioactive ingredient, Aurélia Malapert, Emmanuelle Reboul, Mallorie Tourbin, Olivier Dangles, Alain Thiéry, Fabio Ziarelli, Valérie Tomao, *Food chemistry*, **2017** (*under review*).

One-step extraction of tyrosol and hydroxytyrosol from aqueous solution using β-cyclodextrin in the solid state, Aurélia Malapert, Emmanuelle Reboul, Olivier Dangles, Valérie Tomao (*future submission*).

New procedure for the biophenols extraction from alperujo using β-cyclodextrin in the solid state, Aurélia Malapert, Emmanuelle Reboul, Olivier Dangles, Valérie Tomao, (*future submission*).

Effect of foods and β-cyclodextrin on the bioaccessibility and the uptake by Caco-2 cells of hydroxytyrosol from either a pure standard or from alperujo, Aurélia Malapert, Valérie Tomao, Olivier Dangles, Emmanuelle Reboul, *Food chemistry*, **2017** (*under review*).

Effect of β-cyclodextrin on the bioaccessibility and the uptake by Caco-2 cells of main phenolic compounds from alperujo, Aurélia Malapert, Marielle Margier, Marion Nowicki, Béatrice Gleize, Olivier Dangles, Valérie Tomao, Emmanuelle Reboul (*imminent submission*).

Oral communication

Complexes using food grade nanomaterials, Aurélia Malapert, Emmanuelle Reboul, Mallorie Tourbin, Alain Thiéry, Olivier Dangles, Valérie Tomao, *C'NANO*, Porquerolles, May 26, **2016**.

Posters

Valorization of olive oil by-product, Aurélia Malapert, Emmanuelle Reboul, Olivier Dangles, Valérie Tomao, *Journées Franco-Italiennes de Chimie*, Avignon, April 25-26, **2016**.

Biophenols extraction from olive mill by-product using β-cyclodextrin: Focusing on the interaction with hydroxytyrosol, Aurélia Malapert, Emmanuelle Reboul, Mallorie Tourbin, Alain Thiéry, Olivier Dangles, Valérie Tomao, *C'NANO*, Porquerolles, May 26-27, **2016**.

Identification of phenolic compounds in two-phase olive pomace by UHPLC-DAD-ESI-MS, Aurélia Malapert, Michèle Loonis, Emmanuelle Reboul, Olivier Dangles, Valérie Tomao, *Réseau Francophone de Métabolomique et Fluxomique*, Montpellier, May 30-June 2, **2016**.

European project

Participation to the European Project "Olive-Net" with duration of 4 months (June 1st – September 30th) in Natac (Madrid, Spain) thanks to a collaboration with the GREEN laboratory (University of Avignon). Olive-Net project: Bioactive compounds from *Olea europaea*: investigation and application in food, cosmetic and pharmaceutical industry (from 2017-03-01 to 2021-02-28).

Integration within the work package 1 "Extraction and purification". Focus on hydroxytyrosol from alperujo.

Ions exchange resins to purify alperujo samples, Aurélia Malapert, Pilar Castro, José Antonio Pérez, Esther de la Fuente, *internal meetings*, Natac, Alcorcón-Madrid, **2017**.

Different formulation additives: Effect on the stability of hydroxytyrosol, Aurélia Malapert, Pilar Castro, Esther de la Fuente, *internal meetings*, Natac, Alcorcón-Madrid, **2017**.

Summary

Summary

General introduction

Phenolic compounds are secondary metabolites naturally synthesized in plants and notably known to act as protective agents against ultraviolet damage or predators. Numerous studies highlighted their potential ability to improve human health, most of them being efficient antioxidants.

Olive oil presents a high interest in the Cretan diet because of its composition of valuable active molecules, such as phenolic compounds. However, it has been proved that only 2% of phenolic compounds are found in olive oil, while the rest remains in the olive mill wastes [1].

Several methods have been developed to extract phenolic compounds from olive mill by-products. Most of them are based on the use of organic solvents, which are recognized efficiently for the phenolic compounds' recovery. However, to minimize environmental impacts, others techniques have been developed, such as steam treatments under high pressure, high temperature or supercritical CO_2, which have led to high phenolic recovery yields [2,3]. Nevertheless, these techniques rest on qualified staff and expensive equipment.

The objective of this thesis is to develop high added value ingredients by valorizing olive mill wastes. The new products would be finally intended for food and nutraceutical industries.

Our work focused on the development of a new process for the extraction and complexation of biophenols from a two-phase olive pomace, called "alperujo". For this purpose, alperujo has been firstly characterized. Its phenolic profile has been determined by UHPLC-DAD-MS and revealed a high hydroxytyrosol and tyrosol content.

β-cyclodextrin (β-CD) has been chosen as a host molecule, as it is commonly used in many nutraceutical and food formulations because of its GRAS (generally recognized as safe) label. In order to study the behavior of phenols from alperujo with β-cyclodextrin, hydroxytyrosol and tyrosol have been chosen as biophenol models.

Second, their properties were investigated in solution in the presence of β-CD; then, solid complexes were obtained using conventional methods such as spray- and freeze-drying and interactions occurring between biophenol and β-CD in the solid complexes were characterized by UV/Vis and ^{13}C CP/MAS NMR spectroscopic studies .

Then, a new procedure using solid β-CD as phenol-extracting agent has been developed to offer a simple and economic way to easily extract antioxidants from liquid plant materials and to preserve their activity. The procedure has been developed and optimized carried out on both model biophenols. Then, the same method has been applied on the aqueous phase of

alperujo (i.e. alperujo juice). This work describes a one-step procedure for the concomitant removal of olive phenols from wastewater and formulation of these micronutrients in a native β-CD matrix. The phenol-rich β-CD powders recovered could be potentially used as food supplements.

Finally, the effects of both β-CD and food on bioaccessibility and bioavailability of HT from either a pure standard or alperujo juice have been evaluated by *in vitro* studies. *In vitro* digestion and absorption by Caco-2/TC7 cells studies have been also carried out for the other main phenolic compounds from alperujo, i.e. hydroxytyrosol-O-β-glucoside, tyrosol, caffeic acid and *p*-coumaric acid.

The first part of that thesis introduce the olive mill wastes, their phenolic compounds and their current valorization pathways. Generalities about β-cyclodextrin and the inclusion complex formation as well as the main fate of phenolic compounds after ingestion are developed afterwards. In the second part, the experimental approaches are exhibited, results and discussion are presented. The characterization of alperujo is described. A one-step extraction procedure of phenols using native β-CD in the solid state has been developed with biophenol model solutions. Then, the same procedure is applied on alperujo juice. The *in vitro* digestion of phenolic compounds from alperujo and their intestinal absorption by Caco-2/TC7 monolayer cells is the final results of this work.

Chapter I. State of the art

I-Olive pomace: Origin and description

1   Olive oil production

After harvest, cleaning and washing of olives, different steps follow:

1.1   Crushing

Olive crushing leads to an olive paste by tearing the drupe tissues. The older crushing technique was based on a stone mortar system and has been identified in antiques vestiges [1]. Because of its impracticality, it was then replaced by edge mills. The principle rests on the grindstone strength applied on olives linked to its weight and movements. The stone rotation formerly realized by the driving strength of animals (also called "mill with blood") was replaced by electrical systems, putting in movement several grindstones. However, this kind of mills is not suitable for industrial demands. Thus, they are nowadays used only for familial and rural productions. Metallic crushers mostly are a part of industrial-scale mills (Figure I.1). The prominent edges of metallic arms associated with the rotation speed (from 1000 to 3000 rotations per minutes) allow to rip the olives. Olive particles can then go through the railing pores of the crusher cavity and reach the kneading compartment.

Figure I.1. Hammers crushers

1.2   Kneading

Kneading leads to coalesce oil droplets in the olive paste. The bigger the droplets are, the easier the oil extraction is. To facilitate this operation, the olive paste can be heated to 27°C, i.e. the temperature limit to receive the "cold pressure" label designation. Kneading is commonly done with an endless screw for almost 30 minutes (Figure I.2).

(a)	**(b)**
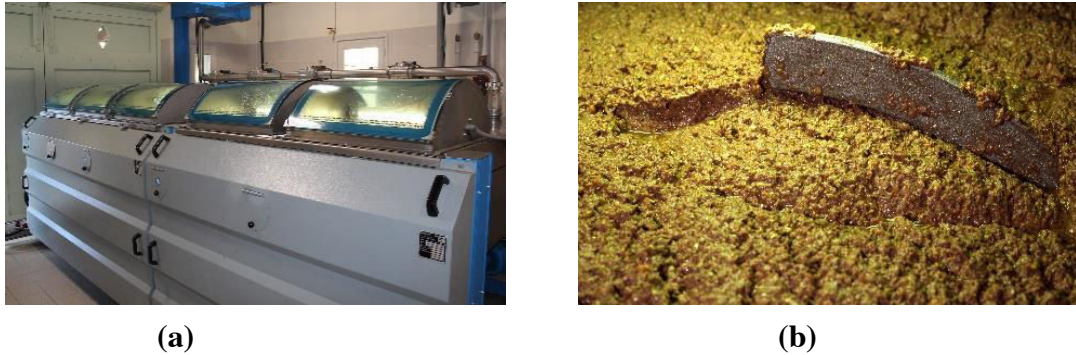
Figure I.2. Mixer of Castelas Mill (a), kneading of olive paste (b)

1.3   Oil extraction

The olive oil extraction consists of a solid-liquid separation of the homogeneous olive paste. Various techniques exist and are closely linked to the kind of mills.

1.3.1   Traditional press mill

Traditional press mill uses mechanical power to extract olive oil. Olive paste is successively placed between carpets of coconut or synthetic fibres, called "scourtins". The whole is pressed by a hydraulic strength that generates two fractions:

- A solid phase composed of olive pieces which is called "olive pomace".
- A liquid phase composed of vegetation and process waters and olive oil. After decantation, oil is recovered on the top. The residual waters are called "olive mill wastewaters" (OMWW).

1.3.2   Three-phase centrifuge system

Three-phase centrifuge system has been developed to improve the olive oil production. Olive paste passes through a first horizontal centrifuge called "decanter". The liquid fraction recovered goes then through a second faster vertical centrifuge, which separates olive oil from water. Three products are generated, i.e. olive oil, olive pomace and OMWW. This system needs a large addition of water, which increases the final wastewaters amount (80 to 120 L per 100 kg of olives).

1.3.3   Two-phase centrifuge system

Developed in the 90s, the two-phase centrifuge system is only composed of an efficient horizontal centrifuge whose power allows the olive oil recovery without adding water. This system has been developed to reduce the OMWW quantity. This process is rested on the intrinsic vegetation waters of olives [2]. By opposition with the three-phase system, two-phase

14

centrifuge system generates only two products, namely the olive oil and a semi-solid residue, composed of olive fruit pieces and the vegetation water, called two-phase olive pomace or "alperujo". The mill effluent production can be reduced by over half. In the dry Mediterranean landscape, two-phase centrifuge mills bring many advantages, using water only for the olive cleaning. In Spain, two-phase centrifuge system represents 90% of olive oil mills and this technology still increases in Greece and France [3].

2   Olive mill by-products

The olive oil production as well as the wastes quantity i.e. olive pomace and OMWW, are dependent on the types of mill (Table I.1).

The olive oil constitutes around 20% of processed olives while the olive mill wastes can represent up to 100% [4].

Table I.1. Olive oil and by-products production according to the kind of mills

Products	Traditional mill	Three-phase centrifuge mill	Two-phase centrifuge mill
Olive oil (kg/100kg of olive)	20-22	20-23	20-23
Olive pomace (kg/100kg of olive)	25-40	45-57	72-85
Olive mill wastewaters (L/100kg of olive)	40-60	60-120	0-10

2.1   Olive mill wastewaters

OMWW are characteristic of traditional and three-phase centrifuge mills which need water addition. They are almost absent in two-phase centrifuge mills. OMWW composed of process and vegetation waters reach from 40 L to 120 L per 100 kg of olives according to the type of mill [3,5]. Process water can be added in several steps to improve the olive oil extraction from the paste [6]. OMWW is a red-brown liquid waste mainly composed of water (80-92%) [3,7], solid olive fragments and a low quantity of olive oil. Physicochemical characteristics of OMWW depend on the olive oil extraction conditions, the olive variety and all environmental parameters and cultural practices [8,9]. Bouknana *et al*. (2014) observed that many physicochemical characteristics of OMWW did not depend only on the variety and cultural conditions, but also on the kind of mills [9].

2.2   Olive pomace

Olive pomace is mainly composed of skin, pulp and seeds pieces which give it a doughy texture. Olive pomace currently presents a great economic interest to be used as a low-cost raw material for several ends.

The olive pomace production is linked to the oil extraction process. In the case of two-phase system, the centrifugation is enough both to extract olive oil and produce only one waste composed of olive pieces and vegetation water [2,3,10,11].

OMWW and olive pomace are the main wastes associated with the olive oil production. Their physicochemical characteristics and their phenolic compound composition have been described on a mini-review published in the journal of "Trends and chromatography". Their main valorization pathways are quoted beyond.

3   An overview of the analysis of phenolic compounds found in olive mill by-products

Abstract

Disposal of olive mill by-products is associated with several environmental problems in the Mediterranean area where the cultivation of olive trees is extensive. Indeed, olive oil production generates large volumes of wastes with the composition depending on processing conditions, agricultural specificities and season. Nevertheless, olive oil wastes also represent a promising source of bioactive phenolic compounds, well known for their health benefits in terms of antioxidant and anti-inflammatory properties. To reduce the environmental impact of olive oil production and promote the industrial development of olive phenols, efficient methods for the fractionation of olive oil by-products and the analysis of their phenolic composition must be developed. This mini-review focuses on one of the most efficient methods for the structural analysis of olive phenols, i.e. liquid chromatography coupled with a diode array detector and up-to-date mass spectrometry.

3.1   Introduction

Considered as the most ancient cultivated tree in the world, olive tree is now at the 24th place among the most cultivated trees with 1.5 billion trees and more than 2000 cultivars [12–16]. In the 2015 season, the ever-growing olive oil production reached nearly 3000 tons, essentially from the Mediterranean basin, which provides optimal conditions for olive growth. The composition of olive oil depends not only on the environmental factors (variety of tree, geography, climate etc.) but also on the processing techniques used for olive oil production. The same applies to the by-products generated. Olive oils are extracted from olive fruits by crushing them, kneading the resulting paste and separating the oily phase (Figure I.3).
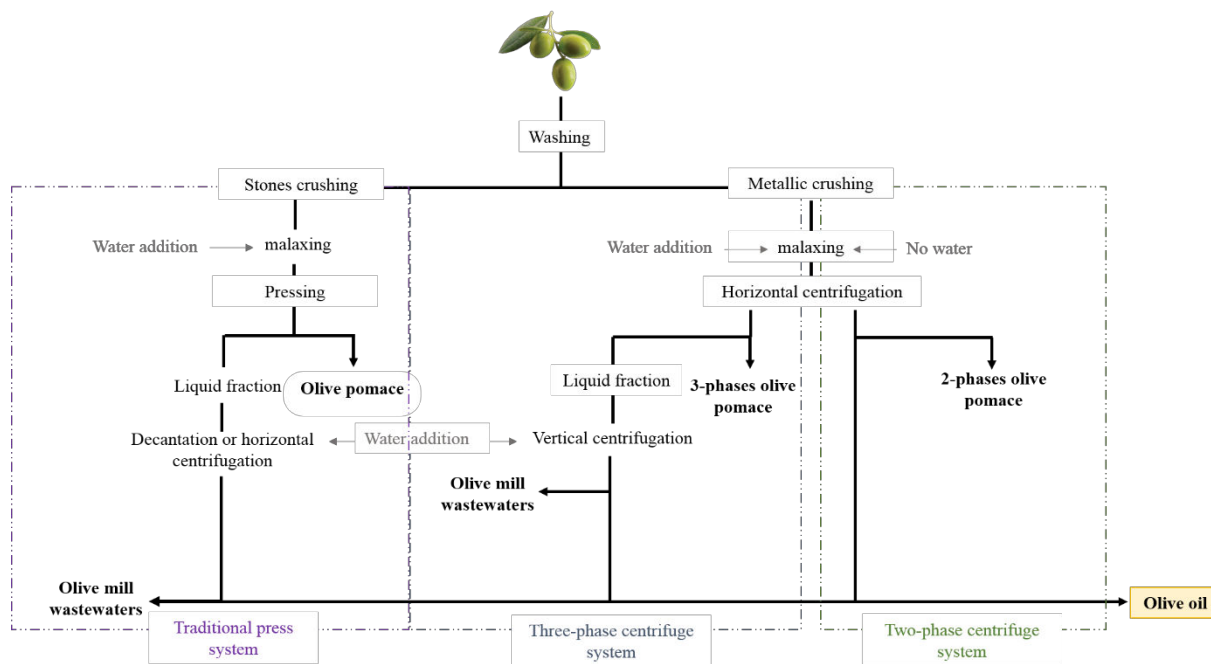
Figure I.3. General plan of olive oil production

The crushing is carried out by discontinuous stone mill in the case of traditional processing or continuous metal crusher when processed using modern devices. Metallic systems accelerate the grinding process, thus increasing daily production volumes. The choice of the crushing technique has a great importance because it leads to chemically different virgin oils in terms of quality parameters such as organoleptic properties or content of biophenols [17].

The olive paste obtained after crushing is triturated before phase separation using different processes. This kneading step influences the oil composition because of the partition phenomena between oil and the aqueous and solid phases, and because of the activity of olive enzymes released during crushing [18]. Then, the mixture is pressed between fiber disks allowing for a solid phase called "pomace" composed of solid olive fragments, and a liquid phase mainly containing olive oil and water. The last step consists of decantation or centrifugation of the liquid part with added water leading to olive oil and wastewaters.

To address the increasing demand for olive oil, continuous two- and three-phase processes were introduced, based on successive horizontal and vertical centrifugations directly applied after the kneading step. Initially designed three-phase mills require water addition to enhance the extraction yield and generate a solid by-product, wastewaters and olive oil [1,11]. As the high volume of wastewater generated by this system is a major drawback, a new generation of olive oil mill was developed with an efficient horizontal centrifugal system not requiring water addition. Here, olive oil is separated from a wet solid residue of crushed olives

[3,19]. This single olive waste is considered a semi-solid by-product composed of vegetation water and solid olive pieces [2,3,19,20]. The two-phase system has the advantage of not needing to dilute the water-soluble olive phenols. However, whatever the process used for phase separation, most biophenols end up in olive by-products, rather than olive oil [21,22].

Wet olive pomace obtained from two-phase mills represents a lower volume of by-products and thus has a minimal environmental impact. These by-products have a potential for agro-industrial development, in particular for their high concentration of specific phenols (also present in oil in low concentration) explored as a source of natural antioxidants in the human diets [23].

The possible valorization of olive phenols has prompted many investigations to chemically characterize the by-products from olive oil mills. The aim of the current mini-review is to provide updated information on the composition of olive mill by-products as deduced from the analysis by liquid chromatography coupled with a diode array detector and a high performance mass spectrometer such as a quadrupole time-of-flight mass spectrometer (QTOF-MS/MS).

3.2   Characterization of olive by-products

The main characteristics of OMWW and pomace are summarized in table I.2.

Table I.2. Main physicochemical characteristics of olive mill wastes

Parameters	Ranges of values	References
pH	4.4-6.8[a] 4.7-5.7[b] 2.2-6.0[c]	[1[c],3[b],11[a,c],24[b],25[c],26[a]]
Water content (% of FM)	49.6-75.0[a] 40.0-55.0[b] 80.0-92.0[c]	[3[b],4[a],7[b],19[c],27[c],28[a]]
Seed (% of FM)	12.0-18.0[a] 15.0-45.0[b]	[3[a],11[b]]
Pulp (% of FM)	10.0-15.0[a] 12.0-35.0[b]	[3[a,b]]
Dry matter (% of FM)	30.7-64.1[a] 70.2-94.4[b] 6.3-12.8[c]	[3[b],10[c],19[a],24[b],29[a],30[c]]
Ash (% of FM)	1.4-4.0[a] 1.7-4.0[b] 0.6-4.7[c]	[3[a,b,c],10[c],31[b]]

Oil (% of FM)	2.0-5.0[a] 2.5-8.7[b] 0.16-1.25[c]	[2[c],3[b],10[c],11[a],19[a,b]]
Phenolic content (% of FM standard equivalent)	0.021-0.26[a,b] 0.098-1.013[c]	[32[a,b],33[c],34[a,b],35[c]]
Phenolic content after extraction by AcOEt (% of FM – mass yield)	0.58-1.12[a,b] 0.12-1.5[b,c]	[36[c],37[a,b],38[c]]

FM: fresh matter; [a]: Two-phase olive pomace; [b]: Three-phase olive pomace; [c]: OMWW.

All by-products have a brown color, an high water content and are mildly acidic. The large range of values for each parameter may be explained by the multiplicity of environmental factors (olive variety, climatic condition, harvesting time etc.), agricultural and olive oil processing conditions [8,39–41]. However, olive mill wastewaters are more acidic (pH 2.2-6.6) than the other by-products (pH 4.4-6.8). For all other reported parameters, olive mill wastewaters are also significantly different from pomace, whatever the process used.

Generally, the total phenolic content of olive wastes (with or without extraction) is estimated by the colorimetric Folin-Ciocalteu method and expressed as a concentration of standard equivalent [30,42]. The solubility of biophenols controls their distribution in olive oil and wastes. Depending on whether it is produced by two-phase or three-phase centrifugal mills, the olive pomace is or is not rinsed by water. This step enriches olive mill wastewaters in biophenols and impoverishes the solid pomace (three-phase system) or generates a semi-solid waste enriched in biophenols (two-phase processing). Standard deviations on the phenolic content are large due to several kinds of wastes and extraction methods, but these values clearly confirm that olive mill wastes are a rich source of biophenols.

The biological activity of olive oil by-products has been addressed in several studies. For instance, Anter *et al*. (2014) have shown that olive pomace protects against the genotoxic activity of hydrogen peroxide [43]. Ramos *et al*. (2013) have demonstrated that an olive waste extract rich in hydroxytyrosol (HT) shows an antiproliferative activity against breast cancer cells [44]. However, given the current knowledge on the bioavailability of dietary phenols, it is now clear that olive phenols are not delivered to human cells for biological activity under their native forms but as a mixture of metabolites. Hence, any study that does not take into account this metabolism of olive phenols in humans obviously lacks biological significance.

3.3   Recovery of phenols from olive mill by-products

For their valorization, biophenols of olive mill by-products must be extracted. Some researchers have investigated the extraction of biophenols from olive by-products using matrices selected according to their adsorption and desorption capacities. Thus, Ena *et al*. (2012) tested granular activated charcoal and an algae powder (Azolla) to extract phenols from olive mill wastewaters. A higher quantity of HT was recovered with the activated charcoal but the total phenolic content was higher with the Azolla powder [45]. Olive biophenols were also extracted using successive filtration steps [46] and/or elution on adsorbent resins [47,48]. Another way consists in applying a thermal process such as thermal evaporation after successive filtration stages and passage through a series of adsorbent resins [43–45]. Michailof *et al*. (2008) succeeded in the selective extraction of phenols such as caffeic acid. Puoci *et al*. (2012) extracted 80% pure gallic acid from olive mill wastewaters by elution on molecularly imprinted polymers [49,50]. A low pH favors the release of the free forms of phenols, thus increasing the total phenolic content extracted [51]. Biophenols are generally extracted into polar solvents such as methanol [52], ethyl acetate [38,51], ethanol [53–56] And water. Extraction can be assisted by ultrasons [57] or microwaves [58] or carried out in the Soxhlet apparatus [38] under optimized temperature conditions. For example, Alu'Datt *et al*. (2010) obtained a maximal extraction yield from olive pomace with methanol at 70 °C in 12 h whereas ethyl acetate came up as the best solvent in the study by Kalogerakis *et al*. (2013) [52,59]. Using Soxhlet extraction, Sannino *et al*. (2013) succeeded in obtaining a highly pure HT from olive mill wastewaters [38]. Steam treatments under high pressure and high temperature led to phenol-rich aqueous phase [37,60]. This process gave high extraction rates under optimal conditions (180 °C, 90 min) as reported by Aliakbarian *et al*. (2011) [20]. Superheated liquids of different polarity were also used for the extraction of olive phenols. Pérez-Serradilla *et al*. (2008) used *n*-hexane and a methanol-water mixture (80:20) for the respective extraction of fatty acids and HT (2.2 g/kg) [61]. Lozano-Sanchez *et al*. (2014) optimized extraction in ethanol-water by using pressurized liquid extraction at temperatures ranging from 40 to 175 °C, the highest yield being obtained at 120 °C with 50% ethanol [56].

3.4   Characterization of phenols from olive mill by-products

The interest in natural phenols has been increasing over the past few decades, due to the elucidation of their many important roles in plants and possibly also in humans via a diet rich in plant products [62]. Apart from the basic Folin-Ciolateu method, liquid chromatography

coupled with a diode array detector is the next most common technique for the characterization of phenols in plant extracts. Generally, the separation is performed using binary solvent systems consisting of a gradient elution with acidified water and methanol or acetonitrile on a reverse phase column. By means of high performance liquid chromatography coupled with a diode array detector (HPLC-DAD), Fernández-Bolaños *et al.* (1998) and Aranda *et al.* (2007) identified 20 phenolic compounds in olive stones and 26 in dried olive pomace, respectively [63,64]. Lafka *et al.* (2011) used HPLC-DAD analyses to compare the extraction efficacy of different solvents in the recovery of biophenols from olive mill waste [55]. Rubio-Senent *et al.* (2013) applied the same analysis to their phenolic extract obtained from steam-treated olive oil waste and Suarez *et al.* (2009) identified 23 biophenols in olive pomace after ultrasound-assisted extraction [60,65].

However, DAD only provides limited structural information as many phenols display similar UV spectra [66]. Electrospray ionization mass spectrometry (ESI-MS) is then often used as an additional detector. Rubio-Senent *et al.* (2013) and Obied *et al.* (3007) separated and identified 26 phenolic compounds in olive pomace and 52 compounds in dried olive pomace, respectively using HPLC-DAD-MS [60,66]. D'Antuono *et al.* (2014) achieved separation and identification of 23 compounds in 36 min by HPLC-DAD and HPLC-MS [46]. Lozano-Sánchez *et al.* (2014) extracted phenolic compounds from the solid residue obtained after olive oil filtration. By means of HPLC-DAD coupled to an electrospray ionization time-of-flight mass spectrometry (ESI-TOF/MS), they identified 25 compounds in 27 min [56]. Peralbo-Molina *et al.* (2012) identified 51 phenolic compounds from olive pomace in 26.5 min using LC-QTOF-MS/MS [67]. To characterize some specific compounds, mass selective detector (MSD) can be coupled to the LC system. Ghayth *et al.* (2014) characterized flavonoids from olive pomace in 18min [68]. MS analyses are commonly carried out in the negative mode.

Although much more rarely, capillary electrophoresis has also been used. Priego-Capote *et al.* (2004) and Bonoli *et al.* (2003) identified and quantified phenolic compounds in olive pomace (8.68 mg/g) and olive oil (0.066-0.527 mg/mL), respectively [42,69]. Finally, gas chromatography (GC) is sometimes used but requires prior derivatization of the samples to make them volatile enough. Using GC-MS, Deeb-Ahmad *et al.* (2012) identified and quantified seven phenolic compounds in olive mill wastewaters, among which was HT at a concentration of 315.9 mg/L [36].

Table I.3 is an exhaustive listing of phenolic compounds identified in olive mill wastewaters and olive pomace, as well as their UV and mass data in negative mode. Olive phenols are highly diverse and range from simple compounds such as phenolic acids and alcohols to much more complex compounds such as tannins. They show maximal UV absorption around 280 nm and additional absorption around 330 nm for hydroxycinnamic acid derivatives.

Table I.3. Reported biophenols in olive mill wastes with UV and mass spectral data

Phenolic compounds	λ_{max} nm	m/z [M-H]	Major mass fragments	OMWW	OP	References
Tyrosol (Tyr)	217, 273	137		+	+	[28,65,66,70]
ρ-hydroxybenzoic acid	194, 256	137	93	+	+	[52,71]
Cinnamic acid	265	147	147		+	[67]
Vanillin	279, 320	151	123	+	+	[28,37,65,70]
4-hydroxyphenylacetic acid	280	151	123,108		+	[72]
Oxidized hydroxytyrosol	232, 280	151			+	[56]
Hydroxytyrosol (HT)	234, 278	153	123, 97	+	+	[28,60,65,70]
Protocatechuic acid	260, 294	153	109, 45	+	+	[52,71,73]
ρ-coumaric acid	223, 307	163	135,119	+	+	[37,65,66,74]
o-coumaric acid	273, 323	163	163		+	[66]
Vanillic acid	257, 289	167	123,108	+	+	[51,65,70]
3,4-Dihydroxyphenylacetic acid	234, 278	167	151, 123, 109, 59	+		[37,71]
Gallic acid	266, 271	169	125, 97	+	+	[32,67]
3,4-Dihydroxy-phenyl glycol	214, 234, 278	169	151	+	+	[46,60,75]
Shikimic acid		173	173		+	[67]
Esculetin	228, 257, 349	177			+	[68]
Caffeic acid	240, 299, 324	179	163, 135, 45	+	+	[65,66,73]
Dihydrocaffeic acid		181	181	+		[71]
Homovanillic acid	223, 276	181	181, 137, 122	+	+	[66]
2,6-Dimethoxybenzoic acid		181	137,166	+		[71]
Dialdehydic form of decarboxymethyl elenolic acid		183	139, 95	+	+	[46,56]
Dihydroxymandelic acid	239	183		+		[28,64]
Quinic acid	239	191	173, 127, 111, 103	+	+	[56,71]
Ferulic acid	233, 292, 320	193	149,134		+	[66]
3,4-DHPEA-AC	234, 280	195	153, 137, 123, 77, 68	+	+	[37,65]
Homoveratric acid		195	151	+		[71]
Syringic acid	220, 272	197	153	+	+	[32,67,71]
Hydroxylated products of dialdehydic form of decarboxymethyl elenolic acid	240	199	181, 155, 111		+	[46,56,75]
3,4,5-trimethoxybenzoic acid	260	211		+		[28,70]
(+)-Erythro-1-(4-hydroxy-3-methoxy)phenyl-1,2,3-propanetriol		213	195,151	+	+	[66,76]

Aldehydic form of decarboxyl elenolic acid		215	197,153		+	[75]
Sinapic acid	233, 322	223		+	+	[28,52,66]
3,4,5-Trimethoxycinnamic acid		237	133,103	+		[71]
Elenolic acid	240	241	209, 165, 139, 127, 121, 101, 95	+	+	[56,65,75]
Hydroxylated form of elenolic acid	240	257	213, 181, 137		+	[56]
Apigenin	221, 263, 335	269	277, 161, 153, 139	+	+	[66,70]
Naringenin	300	271		+		[28]
Luteolin	251, 345	285	241, 199, 175, 151	+	+	[21,66,75]
Tyrosol glucoside	237, 275	299	179, 137, 119	+	+	[67]
Quercetin	369	301	265, 247, 147, 97	+	+	[28,72,77]
ρ-HPEA-EDA (Oleocantal)	230, 280	303	285, 183, 179, 165, 59	+	+	[56,65,75]
Taxifolin		303	285, 177		+	[67]
Hydroxytyrosol hexoside	236, 276	315	179, 153, 135, 161		+	[65,72,77]
3,4-DHPEA-EDA (Oleacein)	230, 280	319	249, 195, 183, 139, 95, 69	+	+	[56,65,75]
Lactone (ester with hydroxytyrosol)		321	185	+	+	[56,65,75]
Decarboxymethyl 10-hydroxy-oleuropein aglycone	230, 280	335	199, 155, 111	+	+	[56,70,74]
Caffeoyl-hexose	239, 318	341	179, 135	+	+	[66]
Oleuropein aglycone hemiacetal	198, 224, 275	351	137, 119		+	[60]
Chlorogenic acid	240, 298, 324	353	191, 179, 161		+	[72]
Pinoresinol	236, 279	357	339, 151	+	+	[21,28,66]
Oleuropein aglycone derivative		359	153, 123		+	[78]
7-Deoxyloganic acid		359	359		+	[67]
Ligstroside aglycone (ρ-HPEA-EA)		361	329, 291, 259, 241	+	+	[65,78]
Acetal of 3,4-DHPEA-EDA	242, 281	365	229, 153, 138	+	+	[70,74]
Loganin acid		375	15, 1113		+	[67]
Oleuropein aglycone	236, 282	377	345, 327, 307, 275, 149	+	+	[28,37,65]
Oleuropein aglycone derivative	238, 284	377	197, 153, 179, 119, 89	+	+	[44,72,73]
Hydroxytyrosol acyclodihydroelenolate		381	363, 349, 245, 227		+	[77]
secologanin		387	387		+	[67]
Oleoside	236	389	345, 209, 165, 121, 101	+	+	[46,79]
Secologanoside	260, 294	389	345, 167, 123, 108		+	[37,75]
Loganin		389	151, 113		+	[67]
Methyl oleuropein aglycone		391	345, 272		+	[80]
Deoxyloganic acid lauryl ester	244	393	349, 331, 225		+	[81]
10-hydroxy-oleuropein aglycone	236, 282	393			+	[56]
Secologanic acid		401	401		+	[67]
Oleoside 11-methyl-ester		403	223, 179, 119, 101	+	+	[28,72,75]

1-β-D-glucopyranosyl acyclodihydroelenolic	237, 312	407	389, 375, 357, 313, 161	+	+	[72,78]
ME 3,4-DHPEA-EA		409	377, 275		+	[65]
1-acetoxy-pinoresinol	238, 279	415	373, 371, 151, 123	+	+	[21,37]
Oleoside dimethylester		417	417		+	[67]
Elenolic acid derivative	242	423	423, 241, 197, 137		+	[60]
Apigenin-7-O-glucoside	220, 263, 335	431	431, 265, 199, 179	+	+	[65,67,70]
Quercetin arabinose	330	433	433, 301		+	[60]
Luteolin-7-O-glucoside	256, 349	447	285	+	+	[65,72,82]
Luteolin-4-O-glucoside	270, 339	447	285		+	[72]
Quercitrin	251, 342	447	301, 300		+	[66]
Oleanolic acid		455	407		+	[75]
Maslinic acid		471	423, 405, 393		+	[75]
Hydroxytyrosol diglucoside		475	245, 153		+	[67]
Isoverbascoside residue	275, 327	477	459, 367, 161	+		[83]
Verbascoside residue		477	459, 367, 161	+		[83]
Hydroxytyrosol rhamnoside		481	481, 265, 153		+	[67]
Oleoside riboside		505	505, 389, 345		+	[67]
Demethylligstroside	250	509	509		+	[37]
Ligostroside	224, 280	523	361, 291, 259, 101	+	+	[28,37]
Ligstroside derivative		523	453, 421, 363, 299	+	+	[84]
Demethyloleuropein	247, 280	525	509, 389, 243, 211, 181		+	[37]
Oleuropein derivative		527	377		+	[67]
Comselogoside	192, 230, 312	535	491, 389, 345, 265, 163	+	+	[57,60]
6-deoxyhexopyranosyl-oleoside		535	517, 491, 390, 345, 325		+	[72]
ρ-coumaric derivative	230, 310	535	205, 145, 117			[37]
Loganic acid glucoside		537	375, 179		+	[67]
Oleuropein derivative	214, 234, 278	537	403, 361, 223, 151, 123		+	[37]
Oleuropein derivative		539	507, 469, 437, 377, 315		+	[84]
Oleuropein	198, 232, 282	539	377, 307, 275, 223	+	+	[28,73]
Oleuroside	243, 280	539	377, 307, 275		+	[77]
Oleuroside isomer		539	469, 437, 315		+	[75]
Hydro-oleuropein		541	405, 137, 123		+	[78]
Dihydro-oleuropein		543	525, 513, 377, 151		+	[67,75,78]
Caffeoyl-6'-secologanoside	198, 328	551	507, 389, 385, 341, 303		+	[37,57]
Oleoside glucoside		551	507, 239, 209		+	[67]
10-hydroxyoleuropein	214, 234, 278	555	223, 151, 123		+	[37,67,85]
6-O-[(2E)-2,6-Dimethyl-8-hydroxy-2-octenoyloxy] secologanoside	214, 234, 278	557	539, 345, 167		+	[75,85]
Glycosyl-methyloleoside	220, 264	565	385	+	+	[75]
Loganin glucoside		569	389, 313		+	[67]
Apigenin-7-rutinoside	212, 254, 350	577	431, 371, 269	+	+	[21,28,77]
Luteolin-7-rutinoside	200, 254, 349	593	447, 285, 181	+	+	[21,28,72,77]

Luteolin-4'-O-rutinoside		593			+	[66]
Cyanidin-3-O-rutinoside	200, 225, 280	595			+	[37]
Quercetin-3-O-arabinoglucoside	256, 355	595			+	[68]
Rutin	219, 253, 353	609	463, 301, 179		+	[72,82]
Hesperidin	221, 281, 327	609	463, 377, 361		+	[52]
Verbascoside/acteoside	198, 238	623	461, 179, 161		+	[72,82]
Isoverbascoside/isoacteoside	250, 290, 328	623	461, 161	+	+	[83,86]
Verbascoside derivative		637	461, 315, 193, 175		+	[86]
β-hydroxy-verbascoside/ β-hydroxy-isoverbascoide	240, 300, 332	639	639, 621, 461, 179	+		[83]
β-Ethyl-hydroxy-verbascoside		667	621, 487, 459, 179		+	[86]
Nüzhenide	249, 275	685	523, 453, 421, 403	+	+	[66,87]
Oleuropein diglucoside		701	539, 377, 307, 275		+	[72]
Neo-nüzhenide		701	539		+	[75,78]
Nüzhenide 11-methyl-oleoside		1071	909, 839, 771, 685, 523		+	[75]
Oleuropein dimer		1075	1075		+	[88]
Oleuropein trimer		1615	1615		+	[88]
Oleuropein tetramer		2153	2153		+	[88]
Oleuropein pentamer		2691	2691		+	[88]

OMW: olive mill wastewaters ; OP: olive pomace; 3,4-DHPEA-AC: 3,4-dihydroxyphenylethanol-acetate; HPEA-EDA: p-hydroxyphenylethanol-elenolic acid dialdehyde; ρ-HPEA-EA: ρ-hydroxyphenylethanol-elenolic acid mono-aldehyde; ME 3,4-DHPEA-EA: methyl 3,4-dihydroxyphenylethanol-elenolic acid monoaldehyde.

3.4.1   Phenyl alcohols and their derivatives

Tyrosol (Tyr) and hydroxytyrosol (HT), which differ only by a hydroxyl group, are the simplest phenols present in the three kinds of olive mill by-products (two-phase olive pomace, three-phase olive pomace and olive mill wastewaters). With its catechol group, HT presents a high antioxidant potential. Many studies have shown the potential capacity of this molecule to fight certain cancers and to reduce the risk of cardiovascular disease and diabetes [89,90]. El Abbassi *et al*. (2012) estimated HT and Tyr contents from pretreated olive mill wastewaters as equal to 54.7 to 69.6% and 4.6 to 6.3% of the total phenolic content, respectively [30]. In the same way, Fernández-Bolaños *et al*. (1998) identified these two phenyl alcohols as the main biophenols in steam-treated olive stone extracts [63]. The additional hydroxyl group causes a bathochromic shift in the UV spectrum between Tyr ($\lambda_{max} = 273$ nm) and HT ($\lambda_{max} = 278$ nm). HT acetate (3,4-DHPEA-AC, m/z 195, having the same fragment ions as HT) has an antioxidant activity similar to HT [91]. There exist oxidized forms of these phenyl alcohols in olive mill by-products, for example, the ion pattern at m/z = 151 corresponding to the HT *o*-quinone or *p*-quinonemethide. Another important phenyl alcohol largely found in olive mill wastes is

3,4-dihydroxyphenylglycol (*m/z* = 169) [46,75,92], probably formed by water addition to the HT *p*-quinonemethide. This compound too has a strong antioxidant potential [93].

3.4.2 Benzoic and cinnamic acids

Belonging to the phenolic acid family, benzoic and cinnamic acids are characterized by a phenyl unit with at least one hydroxyl group and an acid function. They differ from each other by a supplementary double bond separating the acid function from the phenyl in the case of cinnamic acids (Figure I.4).

Benzoic acids	R1	R2	Cinnamic acids
Benzoic acid	H	H	Cinnamic acid
Protocatechuic acid	OH	OH	Caffeic acid
Vanillic acid	OCH3	OH	Ferulic acid
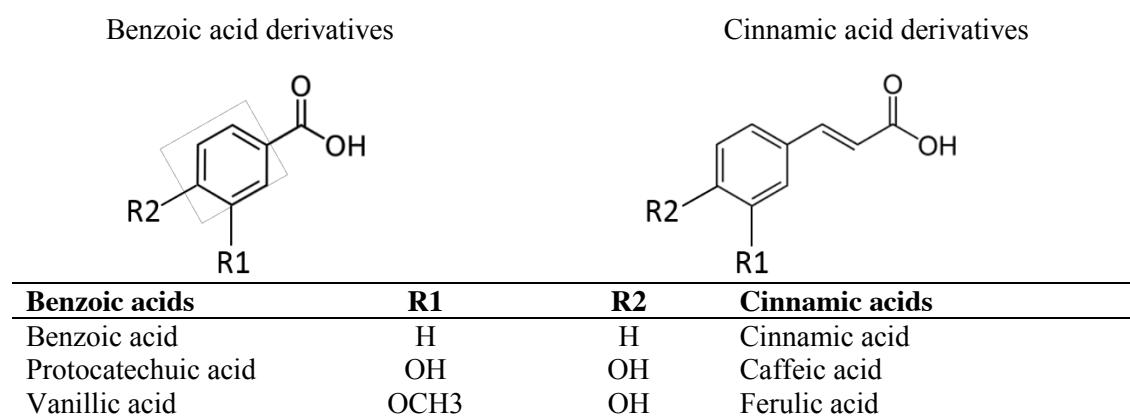
Figure I.4. Chemical structures of benzoic and cinnamic acids

This family presents large numbers of interesting antioxidant molecules such as chlorogenic acid and quinic acid which are recognized as carcinogenic and cardiovascular disease inhibitors [94] These classes relate to simple biophenols including caffeic, coumaric or ferulic acids for cinnamic acids, and vanillic and protocatechuic acids for benzoic acids as well as complex biophenols including verbascoside and its derivatives. Structures of aglycon and glycosides such as caffeic acid at m/z 179 and caffeoyl-hexoside at m/z 341 produce ion fragments at m/z 179 and 135 relative to the caffeoyl unit. Other structural modifications such as methylation of phenolic hydroxyl groups may be present. Vanillic acid and syringic acid (m/z 197) belonging to the benzoic acid family and ferulic acid and sinapic acid (m/z 223) as cinnamic acid derivatives have been widely reported.

Cinnamic acids are often found in high quantities in olive by-products, particularly caffeic acid which was quantified by Deeb *et al*. (2012) as equal to 140 mg per liter of olive mill wastewaters [36]. Other cinnamic acid derivatives commonly present in large amounts in olive by-products are hydroxycinnamic acid i.e. *ρ*-coumaric acid (the most widespread isomer) and its *o*-coumaric acid isomer. They differ from each other by their UV spectra, with maximum absorbances around 310nm and 320nm, respectively.

Olive mill by-products also contain quinic acid (m/z 191) and shikimic acid (m/z 173) which are simple benzoic acids. Quinic acid is part of the composition of large numbers of others phenolic compounds, by esterification with, for example, ferulic acid, coumaric acid or also caffeic acid. Shikimic acid is also widely present in plants acting as a precursor for many biosynthesis pathways. Indeed, the shikimic acid pathway is known for the synthesis of aromatic amino acids and phenylpropanoids [95,96].

As quoted before, verbascoside also called acteoside (m/z 623), with a more complex structure than these simple benzoic and cinnamic acids, is an ester formed with the phenylethanoid HT, the phenylpropanoid caffeic acid and the rhamnopyranosyl glucopyranose. Verbacoside, widely found in plants as a water-soluble compound, is abundant in olive mill by-products [51,97]. Innocenti *et al.* (2006) quantified verbascosides equivalent to 87% of the total phenolic content of the olive pomace used in their study and identified for the first time *β*-ethyl-hydroxy-verbascoside at m/z 639 [86]. Some derivatives of verbascoside can also be found, as Cardinali *et al.* (2012) have shown in olive mill wastewater [83]. They identified verbascoside and isoverbascoside residue at m/z 477 and oxidized forms of verbascoside and isoverbascoside at m/z 621. They also established the presence of several *β*-hydroxyverbacosides and *β*-hydroxyisoverbascosides identifiable by a higher mass of 16 Da (m/z 639) corresponding to the supplementary hydroxyl group and their mass fragments similar to verbascoside.

3.4.3   Iridoids, secoiridoids and their derivatives

Formed by the secondary metabolism of terpenes, iridoids have a cyclopentane ring linked with a pyrane ring, whereas secoiridoids are distinguished from iridoids by the cleavage of the cyclopentane ring [98,99]. These secondary metabolites are commonly found in all plants in glycosidic forms. The most known secoiridoid in olive and its mill by-products is the 3,4-dihydroxyphenyl ethyl alcohol-elenolic acid di-aldehyde (3,4-DHPEA-EDA) called oleuropein (m/z 539), which is a secoiridoid glucoside attached with a HT unit. Many oleuropein derivatives have been detected in olive mill by-products. These compounds were characterized by the ion fragments at m/z 377 corresponding to the oleuropein aglycon residue and m/z 539 Da corresponding to its glycoside form. In this way, several oleuropein derivatives were identified as hydro-oleuropein (m/z 541), dihydro-oleuropein (m/z 543), 10-hydroxyoleuropein (m/z 555) or other oleuropein aglycone derivatives such as methyl oleuropein aglycone (m/z 393).

Several other iridoid and secoiridoid derivative molecules are found in all olive mill by-products, such as loganin (m/z 389) which is an iridoid glycoside, secologanoside (m/z 389) which is a secoiridoid glycoside, oleocanthal (m/z 303) which is an ester of Tyr with a structure similar to oleuropein, oleoside (m/z 389) and elenolic acid (m/z 241) which are part of several iridoids and secoiridoids, and their derivatives. Other than glycoside, simple phenols can be linked to these (seco)iridoids; for example, comselogoside corresponding to a *ρ*-coumaroyl unit linked to a secologanoside. The presence of this hydroxycinnamic acid resulted in a λ_{max} around 310 nm. Another secoiridoid called nüzhenide (m/z 685), composed of an elenolic acid and/or a Tyr unit, is mainly found in olive seed [100,101].

3.4.4   Elenolic acids and their derivatives

Elenolic acid (m/z 241) is not a phenolic polar compound but could act as a maturity marker of olives [102]. Elenolic acids are commonly found in the composition of oleuropein, ligstrosides and their derivative compounds, where they are in the form of esters with phenyl alcohols. At m/z 183 the dialdehydic form of decarboxymethyl elenolic acid was identified which corresponds to a moiety of ligstroside or oleuropein without Tyr or HT, respectively. This dialdehydic form of decarboxymethyl elenolic acid, either free or linked to HT, is known to inhibit the lactic acid bacteria during the brine storage of olives [103].

3.4.5   Flavonoids and anthocyanins

Flavonoids are characterized by two aromatic cycles (A and B) linked together with a central heterocyclic pyran ring (C) (Figure I.5). The UV-Vis spectrum of flavonoids is usually represented by a first absorbance at around 270 nm-290 nm as is the case with most of the phenolic compounds, and a second band around 310 nm-350 nm for flavones and 350 nm-385 nm for flavonols [104].

Mainly responsible for the plant color, they are known to act as a protective agent against UV radiations and bacterial attacks [105].
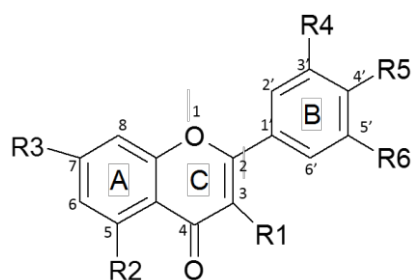
Flavonoids	R1	R2	R3	R4	R5	R6
Apigenin	H	OH	OH	H	OH	H
Luteolin	H	OH	OH	OH	OH	H
Quercetin	OH	OH	OH	OH	OH	H
Quercitrin	O-Deoxy-Rha	OH	OH	H	OH	OH
Rutin	O-Glc-Glc	OH	OH	H	OH	OH

Rha: rhamnose ; Glc: glucose

Figure I.5. Chemical structure of some flavonoids

Flavonoids, aglycone and glycosides, essentially belonging to flavonols (rutin, quercetin, quercitrin), flavones (luteolin, apigenin), flavanone (naringenin, hesperidin) and flavanolol (taxifolin) are listed in table 2. Flavonols and dihydroflavonols have a hydroxyl group on carbon 3 (R1) and differ by the presence (flavonol) or absence (dihydroflavonol) of the double bond between C2 and C3.

The antioxidant properties of flavonoids are mainly due to the hydroxyl units on the aromatic rings (A and B). Flavonoids can also be present in glucoside forms, linked to hexose units (rhamnose, glucose, rutinose (glucose linked with a rhamnose unit). In this way, we can distinguish luteolin aglycone (m/z 285), apigenin aglycon (m/z 269) and their glycosidic forms with hexose unit (+ 162 Da) or rutinoside unit (+ 324 Da – H_2O) in C4 or C7 isomers.

Anthocyanins such as cyanidin-3-glucoside (m/z 595), responsible for the dark pigmentation of olive fruits, occur in olive waste in low quantities. Anthocyanins differ from flavonoids by the absence of the ketone unit (C4) and correspond to the red colors whereas flavonoids correspond to yellow-orange colors.

3.4.6   Lignans

Belonging to the large family of phenolic compounds, lignans possess two phenylpropanoid units linked in C8-C8' [106]. Pinoresinol (mz 357) and 1-acetoxy-pinoresinol (mz 415) are found in oil due to their liposoluble nature and in low quantities in olive by-products [37].

Overall, olive mill wastewaters and olive pomace contain lots of biophenols belonging to several phenolic families. The main biophenols identified in olive mill by-products are HT

and Tyr (phenyl alcohol), hydroxycinnamic acids such as caffeic, ferulic and coumaric acids, verbascosides and several iridoids and secoiridoids such as elenolic acid, oleoside, ligstroside and oleuropein derivatives. In addition to olive pomace and olive mill wastewaters, other byproducts of olive industry such as olive leaves and twigs may be valuable sources of bioactive compounds. Researches show that these two olive farming wastes can be used for animal feed, in particular they are suitable if they are supplemented with proteins [107,108], as bulking agents for compost [109] or as a source of antioxidants [110–113].

3.5   Conclusion

Olive mill by-products cause major environmental problems due to their complex and variable chemical composition and due to the large quantities produced with a seasonal character. Nevertheless, these wastes are rich in bioactive compounds and in particular in phenolic compounds. Olive oil by-products could be considered as a no-cost source of these target compounds. Biophenols potentially extractable from olive mill by-products are numerous and varied depending upon the cultivar, the geographical area of cultivation, the seasonal conditions and type of production process as revealed by the large available literature reviewed in this paper. Different methodologies including spectroscopic and chromatographic techniques have been used not only to develop efficient recovery mechanisms but also to identify, isolate and structurally elucidate novel olive phenolic compounds. The ultimate objective of all these research studies is to contribute to the advancement of knowledge that will allow in the future, both to use these co-products as high-value molecules with interesting functionalities and also to find ways to contribute in reducing the environmental impact of olive oil by-products.

4   Valorization of olive mill wastes

Olive pomace and OMWW are the main olive by-products. They could be used as rich sources of phenolic compounds (mini-review published in Trends of chromatography). Nowadays, the main current industrial managements of olive mill wastes are the second oil extraction and the energy production. Nevertheless, many studies showed that olive mill wastes could be considered as a high value by-product for number of other applications.

4.1   Industrial applications

4.1.1   Second oil extraction

The olive oil content of olive pomace ranges from 2.0% to 8.7% [2,3]. Olive pomace is generally extracted after drying. *n*-Hexane is commonly used to extract oil from dried olive pomace. This management is more suitable for olive pomace from traditional press and three phase centrifuge systems, while the wet two phase olive pomace (i.e. alperujo) is difficult and costly to dry. *Krokida et al.* (2002) suggested a rotary dryer allowing to reduce the obstruction of pores observed in the classical dryers. But this method is a high energy consumer [114,115]. Others worked on high-pressure and high temperature processes to avoid solvents [20]. A physical extraction process based on horizontal axis centrifuges has been developed to recover olive-pomace oil from alperujo. The centrifugal force firstly causes the solids spread onto the rotor walls and their move towards the conical end of the rotor [116]. The final exhausted solid waste can be managed as biomass for the energy production [117].

4.1.2   Fuel

Olive-pomace oil can be used as the raw material for the biofuel production. Fatty acids can be esterified at 50°C for an hour with sulfuric acid as catalyser [118,119]. Steam or microbial lipase pretreatment of olive pomace can enhance the oil and glycerol contents respectively in order to increase the biodiesel production yield [119–121]. The fuel produced is biodegradable but has a very low heat value.

4.1.3   Energy recovery

The combustion is the simple way to manage solid olive by-products. Defatted olive pomace has a high calorific power (4000 kCal/kg). The energy produced can be thermal or electric and supplies several olive mills [117]. The main disadvantage of this valorization pathway is the air pollution. Nevertheless, this management is a low-cost operation and solid residues have a high thermal efficiency.

4.1.4   Application on soil

Because of their high organic matter and potassium contents, OMWW and olive pomace can be directly applied on soil as fertilizers [20,109]. The spreading is easy and direct. However, due to their low pH, mineral salts and phenolic composition, these wastes can be toxic to both plants and microorganisms. Furthermore, unpleasant odors can occur [19].

Composting includes an aerobic biodegradation of organic matter which is turned into rich-humus. OMWW and olive pomace should be firstly mixed with bulking agents as wheat straw or sheep manure. These mixtures are good fertilizers with a high level of humification [122,123]. The microbiota involved in the process is able to degrade phenolic compounds and modify the organic matter. Thus, the compost of olive mill wastes exhibits satisfying results [26]. Furthermore, spreading olive pomace in olive fields for many years could increase the oil content in the olive drupes and could improve the olive production [124].

4.1.5   Animal Feed

Olive pomace is indigestible to ruminants because of its high content in indigestible fibers and its low protein content. Olive pomace should be dried and defatted. The next sieving and grinding remove less digestible seed shells. The rumen activity can participate in improving the protein intake by synthetizing microbial proteins [107,108]. Furthermore, a solid-state fermentation could significantly increase the protein content of olive pomace and reduce the phenolic content, also responsible for its low digestibility [29,125]. , Finally, high quality olive pomace in terms of pro-oxidant/oxidant ratio can be used as feedstuff and improve the meat quality [126].

4.1.6   Activated charcoal

Solid olive mill wastes can be used to produce activated charcoal. Oil-exhausted olive pomace is carbonized at 850°C and physically activated either with carbon dioxide or steam at 800°C [45,127]. Other activation exist, such as with phosphoric acid but it has a high environmental impact [128]. These activated charcoals display a high adsorption capacity. However, this management is not profitable due to the cost-value ratio.

4.1.7   Biogas production

Anaerobic digestion of olive mill wastes is the most common way for the biogas exploitation, such as biohydrogen [129] or biomethane [4,33]. Pretreatments such as

ultrasounds, photon, thermal or acid hydrolysis favor the release of sugar monomers from resistant ligno-cellulosic components that increases the biogas production yield [130,131]. More rarely, steam treatment can be used on olive mill by-products to produce hydrogen or methane [132–134]. Phenolic content as well as the Total Chemical Oxygen Demand (TCOD) can be firstly reduced by microorganisms to optimize the gas production [135–137]. These valorization pathways bring good outputs but are expensive.

4.2 Laboratory scale

4.2.1 Substrate for microorganisms' cultivation

Olive wastes can be used as nutritive sources for microorganisms' cultivation due to their high organic matter content such as sugars, polyphenols, pectin, lipids. Altieri *et al.* (2009) succeeded the cultivation of *Agaricus bisporus* on a substrate composed of olive pomace [136]. It is recommended to pasteurize and to supplement olive mill wastes with a bulking agent as a supplementary carbon source [137,138]. Furthermore, the enzymatic activity of mushrooms, such as polyphenol oxidases, is able to decrease the toxicity of olive mill wastes by removing their phenolic compounds [138–140].

4.2.2 Alcohol

Olive wastes are suitable for the production of methanol, ethanol or mannitol due to their high fermentable sugars contents [141,142]. Exhausted and dried olive pomace or fresh pretreated pomace can be used [143]. Biologic processes, such as an ethanol fermentation with *S. cereviseae*, allow to obtain bioalcohol from olive pomace [144]. Thermal and/or acid pretreatment can be used at first to improve the alcohol production yield [120].

4.2.3 Sugars

Pectin, cellulose and hemicellulose are common polysaccharides found in olive mill by-products. Their extraction is carried out with a hydrolysis followed by an alcohol precipitation. Dietary fibers are recovered in the alcohol-insoluble residue [54,145]. Pectin, which is often used in industries as gelling agents, can be extracted from olive pomace with the same efficiency than others already used such as pectins from apple or citrus [146]. A hydrothermal treatment before the acid hydrolysis can enhance the polysaccharides recovery [147]. Other polysaccharides are extracted by a alcohol precipitation process such as arabinan [148,149] xanthan [150] or pullulan [151].

4.2.4 Dye

Some studies focused on olive mill wastes as natural sources of colorants, i.e. the flavonoids. The process is simple and consists in rinsing olive wastes with warm water and drying the aqueous fraction in a fine powder. In the case of OMWW, its direct application on textile could be possible without a drying step [152,153].

4.2.5 Others

Based on the microorganisms' activity, OMWW and olive pomace can be used as a carbon source to synthetize biosurfactants [154], enzymes [34,155], flavors [156] or biopolymers [157]. Some pretreatments are generally performed such as a fermentation step to reduce the phenolic content, a hydrolysis to increase the free sugars content, a steam treatment or ultrasounds to enhance the production yield [158–161].

II-Beta-cyclodextrin as a host for inclusion complex

1   History

Cyclodextrins (CDs) are known for over a century. Antoine Villiers (1854-1932), a French pharmacist-chemist, discovered CDs in 1891 by studying the enzymes' activities on various carbohydrates. He focused on the use of butyric ferment (*Bacillus amylobacter*) on potato starch and observed the formation of crystals, which turned out to be dextrins. He observed that they were low water-soluble substances, resistant to acid and able to be recovered by an ethanol precipitation. Villiers named these crystalline substances 'cellulosine', in reason of its physicochemical similarities with cellulose [162–164].

Schardinger Franz (1853-1920), an Austrian chemist and bacteriologist, worked on food poisoning generated by heat-resistant micro-organisms. One of his researches was the bacterial degradation of starch. In 1903, he discovered that high thermal resistance bacteria were able to degrade starch and form similar crystals than those previously observed by Villiers. Schardinger distinguished two types of dextrins by their ability to form complexes with iodine molecules that generated two different colours. He named such particles crystalline dextrin A (grey-green coloured complex) and crystalline dextrin B (reddish purple coloured complex) [165].

Following these studies, the first X-ray analyses showed that CDs are cyclic oligosaccharides and that starch is degraded by cyclodextrin glucosyl transferases. Many studies have been led on starch degradation and dextrins to improve their production yields. For example, Wilson *et al*. (1943) showed that dextrin production yield was better for starches with a high amylose/amylopectin ratio [162,166].

2   Structure and main physicochemical properties

The structure of CDs is represented by a hydrophilic external surface and a hydrophobic cavity. These cyclic oligosaccharides shaped like a truncated cone are able to receive hosts. CDs are called 'cage molecules' (Figure I.6).
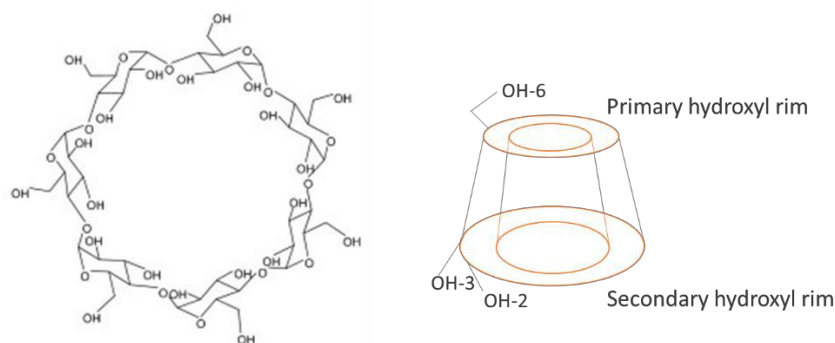
Figure I.6. Chemical structure, conical shape and hydroxyl rims of β-CD

The main native CDs are α-CD, β-CD and γ-CD, composed of 6, 7 and 8 monomeric units of glucopyranose connected by α-1,4-glycosidic bonds, respectively. They are in the form of homogeneous and non-hygroscopic powder [167]. Their hydroxyl groups are steered to the exterior of the cavity, primary hydroxyl groups (6-OH) being on the narrow rim, the secondary hydroxyl groups on the other side rim [168,169]. In solution, hydroxyl groups form hydrogen bonds with water molecules generating a hydration shell around solubilized CDs [170]. Cavity of CDs are more hydrophobic and rather apolar, being constituted by carbon and hydrogen atoms and glycosidic oxygen bridges. The non-bonding electron pairs of the oxygen in the etheroxyde bonds are steered towards the cavity inside, that produces a high electron density and participates in the hydrophobic character of its interior [171].

Table I.4 presents the main characteristics of these three CDs [167].

Table I.4. Main physicochemical characteristics of α-CD, β-CD and γ-CD

	α-CD	β-CD	γ-CD
Structure			
Glucopyranose units	6	7	8
Formula	$C_{36}H_{60}O_{30}$	$C_{42}H_{70}O_{35}$	$C_{48}H_{80}O_{40}$
Molecular weight (g.mol^{-1})	973	1135	1297
Water solubility at 25°C (g.L^{-1})	145	18.5	232
Outer diameter (Å)	14.6	15.4	17.5
Cavity diameter (Å) Inner rim - Outer rim	4.5 - 5.3	6.0 - 6.5	7.5 - 8.5
Height of torus (Å)	7.9	7.9	7.9
Cavity volume (Å^3)	174	262	427

3   Inclusion complex

Encapsulation is defined as the trapping of a substance in another one. This principle is based on the host-guest relationship and considers a minimum of two molecules. The success of this interaction depends on several parameters such as the sizes of the cavity and the guest molecule and its physicochemical properties such as hydrophobicity [90,172].

3.1   Determination of the stoichiometry (Job's method)

CDs can act as a host agent and form inclusion complexes with selected compounds. Due to their hydrophobic cavity, CDs generally include more lipophilic molecules through non-covalent interactions such as hydrophobic, electrostatic or Van der Walls forces and hydrogen bonds [173].

Stoichiometry is defined as the number of guest and host molecules interfering in one complex. In solution, the most common complex provides a 1:1 stoichiometry, implying one CD molecule and one guest molecule. 1:2 guest-CD complexes can be formed when the guest is too large relative to the CD cavity. By opposition, 2:1 guest-CD complex occurs when two guest molecules can enter in the same CD cavity (Figure I.7).

1:1 Complex   1:2 Complex   2:1 Complex
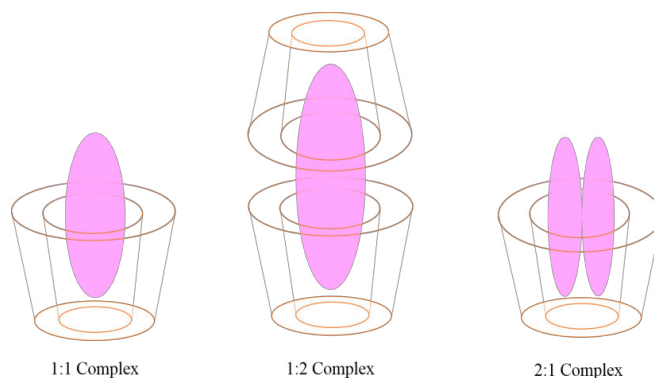
Figure I.7. Main inclusion complexes

UV-Vis spectrophotometry is a suitable technique to determine the stoichiometry of the inclusion complex. The polarity changes of the guest included within a CD cavity shift the maximum wavelength and affect the final molar absorption coefficient (ε) of the complex [174].

The Job's method, also known as the method of continuous variation, consists in mixing equimolar solutions of CD and of guest compound by varying the molar fraction r between 0 and 1, while keeping the total volume and the total concentration constant. The absorbance changes are plotted against r [175]. A maximum at r = 0.5 corresponds to a 1:1 guest:host stoichiometry. In the case of 1:2 and 2:1 complexes, the top of the curve is for r = 0.37 and r = 0.67 respectively (Figure I.8).
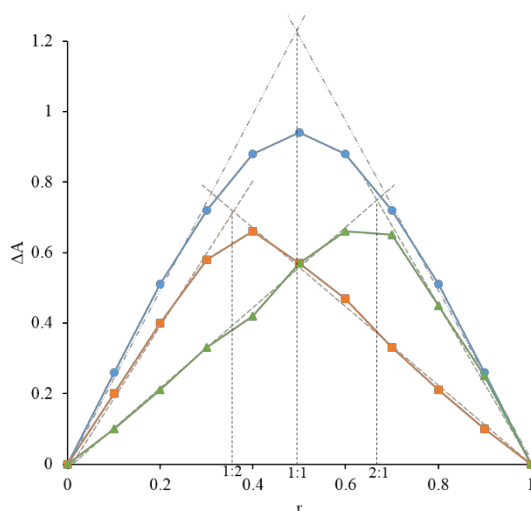
Figure I.8. Models of Job's plots for 1:1, 1:2 and 2:1 guest-host complexes

3.2   Determination of the association constant

The non-covalent interactions between the host and the guest allow a dynamic equilibrium to exist. This reversible phenomenon can be expressed by the calculation of the association constant K [173]. K can be determined by the spectrophotometric method of Benesi-Hildebrand [176]. For a 1:1 stoichiometry, this method allows to express K as detailed below:

$$G \quad + \quad H \quad \overset{Ka}{\leftrightarrow} \quad G - H$$

and

$$K = \frac{[G - H]}{[G][H]}$$

Where: G = guest; H = host; G-H = guest-host complex

The absorbance variations (1/ΔA) are plotted against the CD concentration according to the Benesi-Hildebrand double reciprocal plot:

$$\frac{1}{\Delta A} = \frac{1}{\Delta \varepsilon C K [CD]} + \frac{1}{\Delta \varepsilon C}$$

Where: C = total guest concentration, $\Delta A = A - A_0$, A_0 = absorbance of guest alone = $\varepsilon_{guest} C$, $\Delta \varepsilon = \varepsilon_{guest\text{-}CD} - \varepsilon_{guest}$

K is stronger as the guest's affinity for the host is. This is often observed in very polar solvents, which conduce guest molecules (less polar than the solvent) to enter in CD cavity. In general, the affinity of CDs for a guest compound and K are high for hydrophobic molecules or their hydrophobic moieties [90,177].

3.3   Inclusion complex solubility

CD inclusion complex formation enhances the water solubility of the guest molecules. Higuchi and Connors developed a method to evaluate the solubilization ability of CD (Figure I.9). A-type profiles are obtained when the solubility of the guest compound increases with the CD concentration. A_L subtype concerns complexes with a 1:1 stoichiometry described by a linear relation between the guest solubility and the CD concentration. Complexes with more than one molecule of CD give the A_P subtype. The interpretation of A_N subtype profiles is delicate, including notably the effect of solute-solvent interactions. B-type profiles describe the formation of inclusion complex with a poor solubility. B_I subtype diagram concerns water insoluble complexes, while B_S-type describes the formation of complexes with limited solubility [169,178].
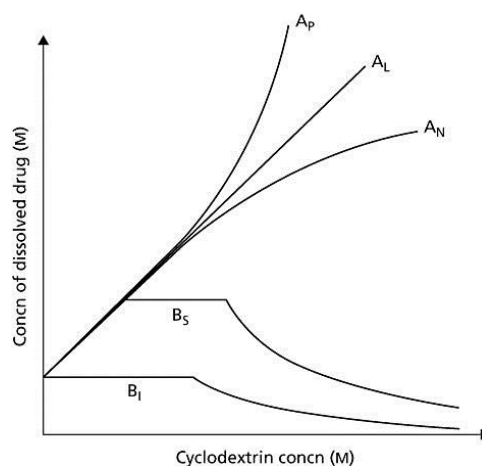
Figure I.9. Type of phase solubility diagram

3.4   Preparation of inclusion complexes in the solid state

Solid complexes are often more suitable for many industrial applications. The main inclusion complexation approaches are presented below.

3.4.1   <u>Drying processes</u>

The most common methods used for the recovery of solid-state complexes are drying processes such as spray-drying and freeze-drying. Before drying, guest and CD are mixed in aqueous solution. A minimal water-solubility of guests is required.

Spray-drying is a fast method based on the conversion of a bulk liquid into small droplets dispersed into a hot drying gas stream. Water is eliminated by evaporation and solid particles are recovered. This technology is usually used to form solid-state β-CD inclusion

complex. Spray-drying produces low-sized particles (less than 40μm) and represents almost 80% of the inclusion complex production [172].

Freeze-drying is a slower process based on the water removal by sublimation. This technology ensures the stability and the preservation of the original properties of the products. It occurs at low temperature (-50°C) and it is more required for heat-sensitive compounds. This technique is less applied than spray-drying because of its higher cost and the long dehydration period required (generally 20 hours). Thereby, freeze-drying is preferentially reserved for high-value compounds [179].

3.4.2   Kneading

This method involves mixing guest and CD in semi-solid form. Solid guest is continuously added to a CD paste. The complexation occurs within 1 to 2 hours. Finally, the paste is dried. However, it is not easily used in large scale production [180–182].

3.4.3   Co-precipitation

The co-precipitation method is especially designed for non-water-soluble compounds. They are dissolved in organic solvent and added dropwise into a CD water-solution under stirring. A second method is to solubilize guest compounds in a hot β-CD-saturated aqueous. Precipitate is then recovered after cooling to room temperature [180,183].

3.4.4   Solvent evaporation

Two miscible solutions of guest and CD molecules are mixed. CDs are commonly solubilized in aqueous solution, while the guest molecule is dissolved in alcohol. The whole is mixed for a long time (24h) and then the solvent is evaporated under vacuum at less than 50°C. This method is considered alternative to the spray-drying process [184,185].

3.4.5   Solid phase complexation

Guest and CD in solid form are vigorously stirred with high level of mechanical energy and solid complexes are finally recovered. However, the analysis of the final product often showed a superposition of the individual characteristics of each compound, as an adsorption phenomenon, due to insufficient energy provided [186]. This method is less efficient that kneading or solvent evaporation methods, although it still allows to increase the water solubility of the guest compound [187].

3.5   Applications of inclusion complexes in the solid state

3.4.6.1. Research stage

Research is mainly based on inclusion of lipophilic substances such as lipids, aroma and dyes [188]. Many works have been led on curcumin complexation with CDs. Mangolim *et al*. (2014) showed that the co-precipitation method was more efficient to form curcumin-β-CD inclusion complex than freeze-drying and evaporation methods, exhibiting a high complexation efficiency (74%) and a photostability increase of 18% [189]. Jantarat *et al*. (2014) observed that evaporation and freeze-drying methods were more suitable to form inclusion complexes between curcumin and a hydroxypropyl derivative of β-CD (HP-β-CD). They obtained a total curcumin content in the inclusion complex up to 88 % in both cases [190]. Mohan *et al*. (2012) studied the freeze drying and physical mixture methods to form curcumin inclusion complexes with HP-β-CDs. They confirmed the inclusion complexation by Raman spectroscopy even if the true encapsulated curcumin content was evaluated as less than 2.5% in any case [191].

Other studies focused on small hydrophilic phenolic compounds. Martínez-Alonso *et al*. (2015) characterized the inclusion complex formation between gallic acid derivatives and β-CD by UV-Vis spectroscopy. They analyzed the spectral shift upon increasing concentration of β-CD. They observed a higher efficiency of β-CD to form inclusion complexes with propyl and butyl gallates than with gallate [192]. Olga *et al*. (2015) worked on the potential competition between ferulic and gallic acid to be including into HP-β-CD by spray-drying. Inclusion complex formation was observed in both cases and preferentially for ferulic acid when it was simultaneously mixed with gallic acid [193]. As for Liu *et al*. (2016), they observed the water solubility of cinnamic acids (ferulic, *p*-coumaric and caffeic acids) linearly increased with the β-CD concentration, displaying a typical A_L. Moreover, they observed that these three cinnamic acids inserted their phenyl moieties inside the hydrophobic cavity of β-CD [194].

Other works focused on the ability of CD inclusion complexes to protect and extract valuable compounds from plant extracts. Ratnasooriya and Rupasinghe (2012) compared α-CD, β-CD and γ-CD to extract (poly)phenols from grapes and their pomace. First, they used CDs in extraction solvents, i.e. water or 80% ethanol, and increased the extraction yield of (poly)phenols from grape pomace compared to the control. Second, they worked on the application of β-CD as a pre-treatment. They added several concentrations of β-CD to the grape mash and samples were incubated for 12 hours at room temperature before pressing. They obtained a higher phenolic recovery for a β-CD amount up to 0.5% (w/w) compared to the

control. For other compounds, such as flavonoids and stilbenes, adding β-CD until 2% (w/w) enhanced their extraction yield prior to press [111]. Kalogeropoulos *et al*. (2010) extracted flavonoids from a *Hypericum perforatum* (St John's wort) with β-CD. They succeeded to extract up to 35 % of quercetin by mixing plant extract and β-CD (1:4 mass ratio) in aqueous solution and successively freeze-drying the mix [195]. Mantegna *et al*. (2012) optimized the (poly)phenols extraction from *Polygonum cuspidatum* by using ultrasounds and a β-CD water solution as extraction solvent [196].

Finally, some studies focused on the ability of solid CDs to extract components from water and wastewaters. Insoluble polymers of CDs or CDs coated on insoluble structures have shown to be efficient to remove organic pollutants, especially the water soluble aromatic molecules [197–199].

3.4.6.2. *Industrial stage*

α-CD, β-CD, γ-CD and some derivatives are labeled as GRAS (generally recognized as safe), and are found in several nutraceutical or food products. Their use is under regulations which vary depending on countries. For instance, these three kinds of CDs can be commercialized in USA, being on the GRAS list, whereas they belong to the *Novel Foods* list in Australia [177]. The European Food Safety Agency (EFSA) reevaluated β-CD as a food additive (E 459) and considered that the current acceptable daily intake (ADI) of 5 mg/kg of body weight per day could be kept, based on the available toxicological database [200], while Joint FAO/WHO Expert Committee on Food Additives (JECFA) calculated for European consumers a total intake of 65 g/person/day of α-CD as ingredient and additive (E457); γ-CD (E458) is recognized as a food ingredient under Regulation (EC) No 258/97. JECFA classifies α-CD and γ-CD as "Allowed Daily Intakes not specified" [201].

Pharmaceutical industry is the first sector which used CDs to protect and to preserve the active molecules. CDs ensure their shelf life, optimize their delivery and can enhance their bioavailability [90]. Nutraceutical industry similarly uses CDs. Nutraceutical products lead to improve the nutrition by formulating dietary supplements, including minerals, vitamins, antioxidants... The main reasons for the use of CDs are their abilities to enhance solubility, stability and activity of the encapsulated compounds [202]. The type of guest compounds to encapsulate determines the kind of CD to use. γ-CD is expensive but suitable to form inclusion complexes with vitamins or vitamin-likes (as coenzyme Q10), carotenoids, flavonoids. γ-CD complexes with vitamin E, coenzyme Q10 or omega 3-rich fish oil are already marketed by

Wacker Chemie [201,203]. α-CD and β-CD are more commonly used to complex the hydrosoluble vitamins B [204] and fatty alcohols such as policonasol [205]. β-CD is especially recognized to encapsulate antioxidants such as for example, cinnamic acids [194], tea-catechins [206]. In all instances, these encapsulations tend to improve the bioavailability of each guest compound [201]. α-CD and β-CD are generally not hydrolyzed by human salivary and pancreatic amylases and can reach the intestinal compartment where CDs are entirely metabolized by the microflora fermentation [207,208].

The global world CDs markets currently is almost 6 tons, mainly assigned for food industry [209]. Food sectors used CDs to reduce unpleasant odors or bitter tastes, by enwrapping the bad-tasting molecule in the CD cavity; the strong hydration on the outer surface of the complex also reduces its attachment on bud receptors. For example, CDs can be mixed with coffee or tea to reduce the bitter taste occurring after an over-cook or extended-stand [210]. Otherwise, CDs can be used to retain desirable flavors during storage of bakery products or during mastication. In this way, CDs cavity can receive and protect dietary fats from loss or damage, avoiding the rancidness [211]. For instance, OmegaDry® Cranberry contains various active compounds of cranberry seed oil encapsulated in γ-CD (Wacker Chemie AG, CAVAMAX®). CDs can also act as an extraction agent to remove cholesterol from dairy foods that improves their nutritional characteristics. It is commonly executed by filtering milk through crosslinked β-CD beads prepared by silanization [177]. Also, CDs are sometimes found in food formulation to enhance the solubility of components or to improve the stability of emulsions. CDs can then act in industries as a multifunctional GRAS and efficient ingredients for food quality preservation and improvement.

Due to these properties, CDs are also found in cosmetic industry by acting as solubilizing agents (vegetal oils or vitamins), penetration enhancers for transdermal molecules delivery or to reduce unpleasant smell, to control release of fragrances, to stabilize emulsion or to protect the guest active compound [212].

3.4.6.3. Researches on interactions between CDs and olive phenolic compounds

Olive biophenols are very interesting in reason of their antioxidant potential and their ability to scavenge radical oxygen species. Encapsulation could preserve their integrity and enhance their stability. In this way, some studies worked on the encapsulation of standard phenolic compounds commonly found in olive and derivatives. Efmorfopoulou *et al*. (2004) evaluated the oleuropein complexation as well as the interaction between *trans*-cinnamic acid

with the three main CDs in aqueous solution by light scattering. They determined the inclusion complex formation according to the turbidity of aqueous model systems. As Barão *et al.* (2014), they observed than β-CD was more suitable for the complexation of both these phenolic compounds, followed by γ-CD and α-CD. They determined optimal conditions as 1:1 stoichiometry, one hour and pH 4 for *trans*-cinnamic complexation and neutral pH for oleuropein. Efmorfopoulou *et al.* (2004) mixed olive oil spiked with *trans*-cinnamic acid with a 2% aqueous solution of β-CD (v/v) and recovered a precipitate of solid inclusion complex by centrifugation. Thus, they succeeded to recover 98% of *trans*-cinnamic acid from olive oil in the precipitate [213,214]. Moraes *et al.* (2011) worked on the CD inclusion complex of phenolic compounds from olive oil, focusing on oleuropein as well. Once again, β-CD was more efficient for the oleuropein complexation, having a higher association constant than α-CD. They obtained the best complexation yield by mixing β-CD and oleuropein in 2:1 molar ratio [215]. López-García *et al.* (2010) produced β-CD inclusion complexes with HT and enhanced its photostability in solution [216]. García-Padial *et al.* (2013) focused on the solid-state complexation of Tyr with β-CD or β-CD derivatives by co-evaporation and kneading. They also studied the sorption of Tyr on a β-CD polymer crosslinked with epichlorohydrin. Co-evaporating and kneading complexes had similar X-ray diffraction profiles, showing the disappearance of the Tyr crystalline structure peak. They also succeeded to quickly retain almost 1mg of Tyr per gram of polymer [217].

Other researchers tried to form CDs inclusion complex with polyphenols from olive plant extracts. In this way, Rescifina *et al.* (2010) compared β-CD and caffeine to form complexes with polyphenols from olive oil. They observed that β-CD was able to form complexes from 1:1 stoichiometry in aqueous solution with different values for association constants according to the biophenols [218]. Mourtzinos *et al.* (2007) worked on the possibility of β-CD to encapsulate an oleuropein-rich extract from olive leaves. They succeeded to form inclusion complexes with a high content of oleuropein by mixing the leaf extract with β-CD and freeze-drying the whole. Finally, CD complex increased the water solubility of biophenols, in particular of oleuropein [110]. The ability of CDs to form water-soluble inclusion complex has also been used to optimize polyphenols extractions. In this way, Mourtzinos *et al.* (2016) used HP-β-CD and glycerin as co-solvents for the extraction of polyphenol from olive leaves [219].

III-Post ingestion future of phenolic compounds

Many studies have observed that some chronic diseases, such as cardiovascular diseases, are much represented in countries of Northern Europe than Southern ones. Concomitantly, southern diets such as the Mediterranean diet, often appear more balanced as they are richer in fruits and vegetables, and contain vegetable fats such as olive oil instead of animal fats. It has been further showed that it is the intrinsic composition of the Mediterranean diet, and especially its content in plant products and vegetal oils rich in unsaturated fatty acids, fibers and antioxidants, that makes it good and recommended for health [220,221].

Among the natural antioxidants present in fruits and vegetables, phenolic compounds have attracted researchers' interest. In particular, several studies have focused on the ability of phenolic compounds to participate to the prevention of several human diseases, such as diabetes, cardiovascular diseases or tumors. Even if they are not considered as essential yet, phenolic compounds seem to contribute to human health [221,222].

However, the biological activities of a given molecule only exist if the component resists to the digestion and is absorbed by the organism to be finally transported to a specific site. The bioavailability of a component is defined as the quantity that is absorbed and can reach a target tissue to exert its biological properties. Bioavailability depends on two major steps. First, the fraction of molecules released from the food matrix to the aqueous phase of the bolus during the digestion process, which becomes available to be absorbed from the lumen to the blood circulation through the intestinal epithelial barrier, is defined as the bioaccessible part of the component. Second, the quantity that is absorbed and circulates in organism to reach target tissues, is considered as the bioavailable part of the component [223].

Both bioaccessibility and bioavailability are correlated to the initial amount of the molecules ingested. Their absorption rates are closely linked to the nature of bioactive components and their possible interactions with other nutrients, digestive enzymes, enterocytes and cellular transporters in the gastrointestinal lumen [224]. For example, interactions between polyphenols and the gut-microbiota can lead to metabolites that can be better absorbed but have different biological activities [221]. All these interactions modify the bioaccessibility and bioavailability of the involved phenolic compound and affect their functionalities.

1   Fate of phenolic compounds during the digestion-absorption process

As previously described, the bioaccessible fraction of a compound is its released amount from the food matrix in the gastrointestinal lumen and can thereby be available for intestinal absorption [225]. So, bioaccessibility is controlled by different factors involved from food mastication in the mouth compartment to absorption in the intestinal compartment. All compartments produce and release digestive fluids that contribute to the liberation and or modification of the active components.

1.1   First compartment of digestion: the Mouth

In the mouth, both mastication and saliva incorporation into the food collaborate to destroy the food matrix and prepare its arrival in the stomach compartment.

1.1.1   Mechanical breakdown of food

The oral step is mainly associated with the food oral breakdown executed by mechanical destruction. The latter is allowed by mastication, i.e. biting and chewing. More precisely, jaw closings, teeth involvement (tearing and cutting) as well as tongue pressing are assigned with the food size reduction to smaller particles, from centimeter scale to sub-millimeter scale. These oral mechanisms depend on individuals' oral physiological conditions. It has been proved than individuals with strong tongue muscle will destroy and reduce food by using more tongue whereas other persons with low tongue muscle will involve mainly teeth to destroy food [226].

The oral mechanical destruction occurs mostly for solid and soft solid foods, which cannot be swallowed as they are. The swallowing is only allowed with the saliva participation, wetting food bolus and finally making possible its transportation to the stomach. Reducing food size also maximizes the digestion from the stomach, increasing the surface exchange area. Moreover, the food destruction leads to free flavors (taste and aroma), which can finally be detected by the taste buds and olfactory receptors, this phenomenon increases with the size reduction and the duration of mastication phase [227]. When the mastication is more intensive and longer, lower are the food textures and rheology, and more dominant is the saliva impregnation. Furthermore, the particle size reduction improves the gastrointestinal absorption of food molecules by increasing the surface area of food matrix [228].

1.1.2   Implication of saliva and enzymes

Human saliva, whose daily production is between 1.0 and 1.5L, is a complex system composed of water (99%), electrolytes, proteins, micelles, lipids, bacterial and cells from oral

epithelium. Human saliva is defined as a colloidal mixture maintaining oral health and facilitating food intake. Saliva acts as a buffering, lubricating and protective agent and participates actively of the wetting of solid and soft solid foods to allow the swallowing. The saliva-food mixture constitutes the food bolus. Prolin-rich mucins which compose Human saliva have gel properties and then participate actively for oral cavity and food surface lubrication [229].

Saliva is also composed of two enzymes: a lipase and a α-amylase. These enzymes interact respectively with lipids and starches. Secreted from Ebner's glands of the tongue, salivary human lipase is few in quantity but able to hydrolyze medium to long chain triglycerides to form free fatty acids. Due to the very low concentration of lipase in human saliva, researchers suspect that the lipase activity is not efficient for the lipid digestion but participate in the release of fatty acids, leading to their detection by specific receptors. This phenomenon leads to fat and cream perception in the oral cavity [230]. Their perception could also be allowed by physical mechanisms based on textural feature [231]. The main enzymatic mechanisms that occur in the oral cavity are linked to the presence of α-amylase (calcium metalloenzyme) in the human saliva. α-amylase is abundant and highly active in oral conditions. It is able to hydrolyze (1-4) bonds of both amylose and amylopectin that are the main components of starch to form free small sugars molecules, such as maltose. The sweetness sense during consumption of starch-foods (rice, bread …) is a result of the α-amylase activity. Moreover, α-amylase participates intensively to the food breakdown by hydrolyzing carbohydrates [232,233].

These physical and enzymatic activities occur at different rate caused by the differences of foods (structure, composition…) as well as the differences between each individual.

1.1.3   Interaction with phenolic compounds

Phenolic compounds, often present in fruits and vegetables, can be found in the oral cavity and interact with components of oral environment, such as those of saliva.

During the consumption of polyphenol-rich foods or beverage, phenolic compounds are able to interact with salivary proteins to form aggregates, which destabilize emulsion and reduce oral lubrication leading to astringency perception. Proline-rich proteins are the main protein in human saliva, which are able to form stable complexes with phenolic compounds, resulting in the dryness and roughness perception [234]. This phenomenon can be considered as the first mammalian defense against ingested polyphenols. Moreover, it appears that polyphenols can

strongly bind with salivary proteins as much as their number of aromatic rings, their size and their hydrophobicity increase [235]. Polyphenols addition in foods and beverages such as wine often improves the sensory quality and the color stability. Ferrer-Gallego *et al*. (2015) thus studied the effect of flavonol addition on wine astringency and their interaction with human saliva. They focused on the quercetin-3-*O*-glucoside addition to white and red wines, and observed an increase of astringency, greenness and bitterness in both cases [236]. Genovese *et al*. (2015) observed that phenolic compounds from olive oil affected the release of retronasal aroma in the mouth reducing the headspace release of almost all volatile compounds. This property could be due to the low affinity of olive oil phenolic compounds toward mucin which could then link volatile compounds. It has also been hypothesized that biophenols could directly interact with aroma compounds [237]. All these interactions tend to reduce the bioavailability of the reacting phenolic compounds.

Phenolic compounds (depending on their structures) can inhibit the activity of α-amylase leading to reduce the carbohydrates digestion and/or further absorption. Xiao *et al*. (2011) showed that methylation on hydroxyl groups increases the capacity of phenolic compounds to interact with α-amylase, while glycosylation enhanced or, on the contrary, decreased the affinity of isoflavone and flavonols for this enzyme, respectively [224,238].

1.2   The Stomach

1.2.1   Gastric mechanisms

The stomach is composed of parietal, zymogen and surface epithelial/mucus neck cells that are responsible of HCl, pepsinogen and mucus glycoprotein secretions, respectively. These secretions are controlled by transepithelial transducing cells. For instance, gastrin cells located in the antral part of stomach, produce the gastrin hormone inducing acid secretions into the lumen. System regulations (neural and endocrine reflexes) allow the mix between secretions and foods [239]. The stomach is thus the second main compartment for the food disintegration during the digestion after the oral step. In fact, stomach-wall muscle contractions, the acid environment as well as the enzyme interactions largely participate to the food breakdown [227]. The smaller the food particles size is, the better will be the gastric digestion efficiency. Drechsler *et al*. (2016) observed undamaged and fine potatoes debris particles after gastric digestion, meaning that the breakdown resulted on surface damage mechanisms. Moreover, the more-time exposure with gastric juices also leads to reduce the potato particles size because of the matrix softening and pepsin action [240]. This enzyme, resulting in the selective cleavage

of the parent pepsinogen, initiates protein digestion, hydrolyzing peptide bonds. Its activity is optimal for acidic pH and leads to reduce the food particle size and to release peptides [241,242]. Besides, the action of the gastric lipase leads to the hydrolysis of a part of the ingested triglycerides and to the formation of a gastric emulsion that is stabilized by both lipid digestion products and peptides produced via pepsin-catalyzed hydrolysis [243].

1.2.2   Gastric fate of phenolic compounds

Almost all phenolic compounds reach the stomach in their intact forms. The food matrix disruption in the stomach leads to an increased surface area of solid particles, which enhances the ability of phenolic compounds to interact with other food compounds or digestive enzymes. Besides, the effect of gastric digestion on the antioxidant potential of phenolic compounds has been studied. Attri *et al*. (2017) worked on the digestion of several fruit juices and observed that both the total phenolic content and the antioxidant activity were increased after simulating gastric digestion containing pepsin. This study thus revealed that gastric digestion allowed the liberation of small active phenolic compounds [244].

As previously said, polyphenols are commonly bonded to food components, especially fibers in non-processed plants, reducing their bioaccessibility and bioavailability. However, these properties can precisely be used for producing resistant complexes to protect and transport phenolic compounds [245]. Liu *et al*. (2016) worked on the ability of starch nanoparticles to load and preserve polyphenols during digestion. The *in vitro* release study revealed that the free polyphenols quickly diffused through the dialysis membrane, while the complexes presented three release successive steps: i) a first liberation of polyphenols, followed by ii) a potential release of soft-adsorbed phenolic compounds on the starch surface and iii) a slow diffusion of phenolic compounds from the nanoparticles [246]. Gastric digestive enzymes such as amylases were able to digest some starches, while the resistant ones were reaching the large intestine [224].

Phenolic compounds highly interact with digestive enzymes. Therefore, *in vitro* and *in vivo* studies showed interactions between polyphenols and digestive enzymes. Many studies focused on the interaction between gastric enzymes and (poly)phenols. For instance, tea catechins, such as epigallocatechin gallate (EGCG), can interact with pepsin. As observed by Cui *et al*. (2015), the binding affinity varies according to their conformation, the number and the position of hydroxyl and aromatic groups as well as their structure and orientation [247]. Non-covalent bonds are generally involved in the binding process of (poly)phenols to these

enzymes. These interactions generally cause the proteolysis decrease in the stomach and lead to reduce the food digestibility [248,249].

Finally, Kanner *et al.* (2017) studied the potential benefits of several fruits and vegetables on the gastric redox homeostasis in the stomach. Postprandial oxidative stress (POS) occurs commonly after red-meat rich-lipid meal consumption and results in susceptible damage for the human organism. In fact, the peroxidation of red-meat generates reactive cytotoxic aldehydes such as the malondialdehyde. Most of them are produced in the stomach and can thereby be absorbed in the intestine causing transient endothelial dysfunction, inflammation and cellular oxidative stress; which can lead to important risks of cardiovascular diseases. Kanner *et al.* worked on the ability of over 50 foods to reduce the POS, comparing results obtained from simulating gastric fluid (SGF) assays with the *in vivo* analyses of malondialdehyde amount in human blood after meat meal consumption. They observed that many fruits and vegetables could reduce the postprandial oxidative stress, especially fruits such as black olive drupes, blackberry and cranberries, which exhibited a reduced POS Index (rPOSI) (180 per 100g of fresh matter). This ability was in exergue with their higher total phenol content, up to 100 mg of catechin equivalent per 100g of fresh matter. However, it also appeared that low-phenolic concentration could exert a pro-oxidant activity in presence of iron-ions. [250].

1.3   The Intestine

1.3.1   Physical description

The intestine, which primarily function is to absorb nutrients, is described like a heterogeneous barrier of cellular and extracellular components. Intestinal epithelium and the underlying lamina propria form the intestine mucosa. Several types of epithelial cells are present, such as the absorptive enterocytes and goblet cells secreting mucus, which is the major extracellular component. Mucus lubricates the intestinal walls facilitating the food passage. It also acts as a protective agent of the intestinal barrier, protecting epithelial cells against the digestive enzymes present in the lumen and avoiding the bacteria adhesion onto the epithelium and their entry into the lamina propria. Mucus is also composed of antimicrobial peptides and antibodies which ensure the epithelial health [251,252].

The epithelial monolayer is folded into crypts and villi that optimize the exchange surface. The intestinal epithelial is considered as the largest interface between the body and the environment [253]. The enterocyte monolayer acts as a physical barrier against the crossing of

most components, in particular the most of hydrophilic and/or big molecules, which cannot generally cross the intestinal barrier without a specific transporter. Epithelial cells are linked together through adherent and tight junctions, as well as underlying desmosomes. Transmembrane proteins compose the tight junctions, forming an extracellular selective barrier. Many regulations occur in the intestine to control its permeability. [251].

Food acts as a regulator of the intestinal barrier functions. In fact, dietary antigens can modulate physiological functions like tight junction permeability, transport activity, immune functions etc. Interestingly, (poly)phenols can modify the transport of glucose, by inhibiting the glucose transporters or increasing the integrity of the intestinal barrier by enhancing the Transepithelial Electrical Resistance (TER), reducing paracellular efflux and/ or increasing the tight junction proteins expressions [251].

Both pancreatic juice and bile, secreted by the pancreas and the liver, respectively, are released at the duodenal level following a meal. The pancreatic juice contains all the enzymes required to fully hydrolyze foods into nutrients (i.e. proteases, lipases, amylases, ribonucleases, etc.). Bile contains biliary salts that act like detergent to solubilize lipid digestion products and allow their absorption [254].

1.3.2   Luminal metabolism of polyphenols

The mild-alkaline conditions of intestinal phases can be deleterious for phenolic compounds. For instance, anthocyanins and flavonoids are generally stable at low pH but are converted into chalcone at pH > 4. However, chalcone can be degraded into phenolic acids that explains the low bioavailability of the initial anthocyanins after reaching the gastrointestinal tract [255]. Nevertheless, other phenolic compounds can be stable at mild-alkaline pH or their degradation can generate other interesting antioxidants. Stanisavljević *et al*. (2015) observed an important decrease of anthocyanins from chokeberry juice in duodenal juice while the final concentrations of studied cyanidins were higher than those in the gastric juice. This can be explained by the degradation of procyanidin oligomers into monomeric compounds [256]. Attri *et al*. (2017) also observed that the total phenolic content and the antioxidant activity of fruit juices were higher after intestinal phase than the gastric phase, and attributed differences of the total phenolic content and antioxidant activity between fruit juices to the different levels of bounded polyphenols to other food components. The highest antioxidant activity in the intestine phases can be resulted of the polyphenols transformation into other more active molecules (Attri *et al*., 2017).

Polyphenols are also able to interact with gastrointestinal enzymes in this compartment, including α-chymotrypsin and trypsin [250]. Besides, number of polyphenols can interact with lipases, reducing fat acid adsorption [257,258].

At this level, phenolic glycosides can be hydrolyzed to liberate smaller phenolic moieties. The most important enzyme involved in the luminal metabolism pathway of (poly)phenols is the lactose phlorizin hydrolase (LPH). Located at the luminal side of the brush border, it can release aglycones from glucosides by a glucosidase activity. For instance, it has been observed on flavonoids that LPH can release the flavonoid skeleton from its sugar [259,260].

1.3.3 Intestinal absorption of polyphenols

The physicochemical properties of the nutrients govern their transport mechanisms [261,262]. The molecule has to be soluble in the mucus to interact with the intestinal barrier and cross it according to its molecular weight and size, its stability and charge distribution [253]. Phenolic glycosides, in reason of their size, polarity and hydrogen bonds, are generally not absorbed, while the aglycones released after luminal hydrolysis can more easily cross the intestinal barrier [228,263,264]. In a general manner, the aglycone transport is affected by its own structure. For example, it appeared that hydrophobic anthocyanins are preferably transported through the intestinal barrier than hydrophilic ones [255].

The absorption of small phenolic compounds and/or their metabolites mainly occurs in the small intestine. Four main transport pathways through the intestinal barrier exist: the passive diffusion, the paracellular transport in tight junctions, the facilitated transcellular transport and the active transport mediated by receptors [221,224] (Figure I.10).
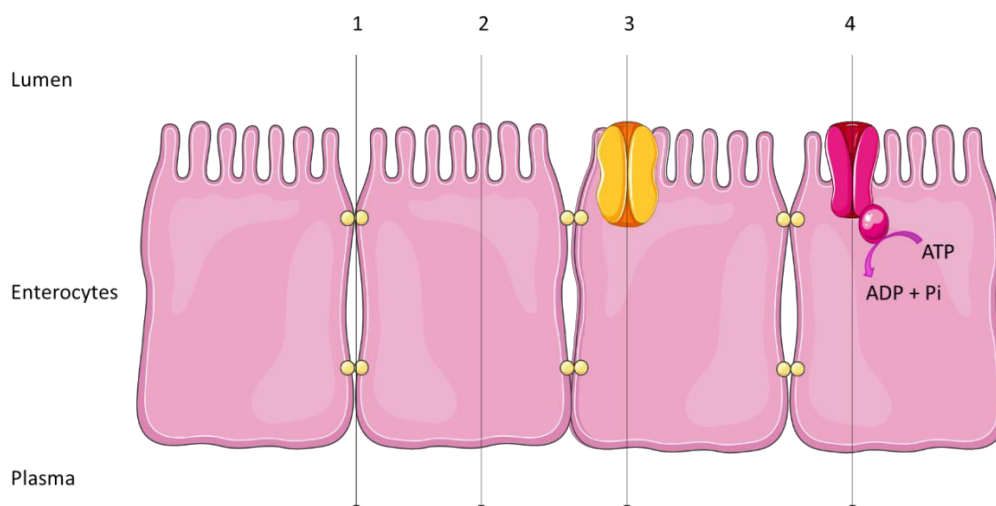
(1): paracellular transport through tight junctions; (2): passive diffusion; (3): facilitated transport (ex: SL transporter); (4): energy-dependent active transport (ex: ABC transporter)

Figure I.10. Illustration of different modes of transport of phenolic compounds through the enterocytes

The paracellular transport is linked to the pore size of tight junctions. Electrochemical and osmotic gradients across epithelium cause water movements that induce small molecules absorption through the tight junction pores. Thus, both steric conformation and hydrophobicity of molecules are important parameters for paracellular transport [265]. The passive diffusion is also intended for low weight and hydrophobic or neutral molecules.

The other polyphenol transports are mediated by transmembrane pumps, channels and carriers [251]. Organic anion transporters (OATs), organic anion transporters polypeptides (OATPs) and monocarboxylic transporters (MCTs) are commonly involved in (poly)phenol absorption. They belong to the solute carriers (SLCs) family and are located in the cell membranes. These transporters are generally implicated in the absorption, uptake and elimination of molecules by facilitated transport pathways. They do not need energy for molecule transport, which is driven by electrochemical gradient. Indeed, ions/solute gradients created across the membrane are the indispensable energy for this transporter activity, and it has been showed that SLC activity increases by decreasing the extracellular pH [266,267]. OATs are responsible of bidirectional transports. The transport of polyphenols occurs against the concentration gradient and can result in the increase of the molecules content in the blood circulation (or in contrary in the lumen, see "efflux paragraph" below).

Besides, some active transporters, i.e. transporters requiring ATP hydrolysis for their functioning such as ATP binding cassette (ABC) transporters are also able i) to allow the

absorption of phenolic compounds (such as the multidrug resistance associated protein 3 (MRP3 or ABCC3) involved among others in the active transport of resveratrol [268,269]) or ii) to efflux them back to the lumen (see below) [221,224].

Even if glycosides are generally weakly absorbed by enterocytes, SGLT1 transporter, present on the apical side of the brush border and belonging to the active sodium-dependent glucose transporter (SGLT) family, has been involved in the transport of some (poly)phenol glucosides [263].

1.3.4   Metabolism in the enterocyte cytosol

Together with the liver, the intestine is a main site for orally ingested compound metabolism, including phenols and xenobiotics. These transformations are indeed a common way to excrete in urines absorbed xenobiotic molecules by making them more hydrosoluble (detoxification pathway).

The phenolic compounds metabolism is divided in two main phases. Firstly, phenolic compounds can be slightly modified (phase I). The enzymatic pathway predominantly involved in the (poly)phenol metabolism is the cytochrome P450 (CYP450), responsible of several modifications. Most of them are reduction, oxidation, hydrolysis, hydration, methylation [270,271]. Furthermore, a cytosolic β-glucosidase (CBG) can hydrolyze the glycosides which are transported through SGLT1 [272].

Phase II of the metabolism corresponds to the conjugation of absorbed phenolic compounds [268] and this phase represents the most part of the phenolic metabolism. Phase II may be preceded or not by phase I reactions. The three main conjugates are a sulfate, glucuronide and methyl moiety [273].

UDP-glucuronyltransferases (UGTs) mediate the glucuronidation of xenobiotics such as phenolic compounds, facilitating their removal. Their active site is in the lumen side. Glucuronidation generally consists in the conjugation between a glucuronic acid unit and a nucleophilic functional group (such as a hydroxyl group) onto the aroma ring. Multiple glucuronide isomers can exist when the molecule exhibits several hydroxyl groups. Human UGTs are divided in two main families according to their amino acid sequences. UGT1A9 would be implicated in the glucuronidation of bulky polyphenols such as flavonoids, while UGT1A6 could preferentially act on simple and plane phenols. Uridine diphosphoglucuronic acid (UDP-glucuronic acid) is the indispensable cofactor for the glucuronidation. It is

transported into the endoplasmic reticulum where membrane-bonds UGTs can transfer the glucuronic acid moiety by an ester linkage. Uridine diphosphate is then released subsequently to this reaction (Figure I.11) [274,275].
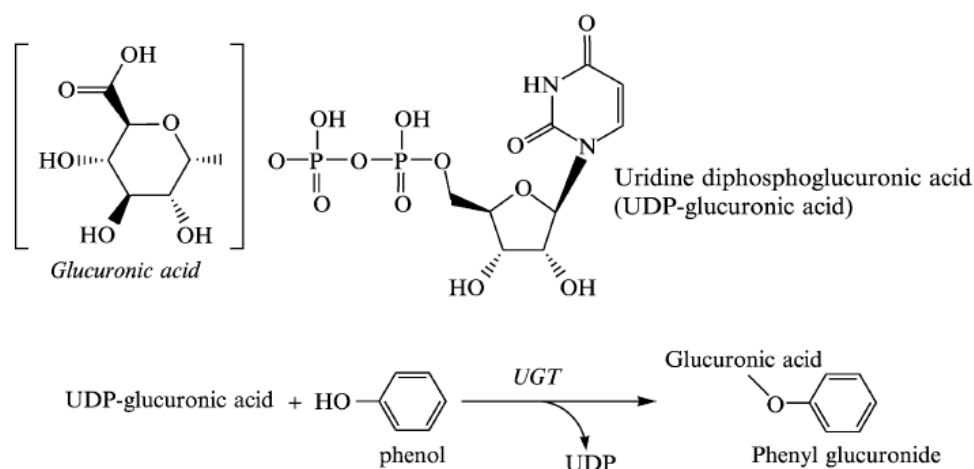
Figure I.11. Glucuronidation of phenols

Another detoxifying conjugation is the sulfation commonly mediated by sulfatotransferase (SULT) enzymes. This transfer can also occur on a hydroxyl group of the phenolic compounds. Sulfation has the same goal: to increase the water solubility of endobiotics and xenobiotics to improve their excretion. As for glucuronidation, sulfation needs a cofactor (3'-phosphoadenylsulfate (PAPS)) to transfer a sulfate moiety to a phenol by an ether linkage. The products are then the sulfated metabolite and the 3'phosphoadenosine-5'-phosphate (PAP) (Figure I.12) [274]. Two families of SULTs exist according their amino acid sequences. Moreover, SULTs can be found bounded into the endoplasmic reticulum or in the cytosol. The cytosolic SULTs are generally more active [276]. Furthermore, metabolism can occur on other aromatic compounds derivatives such as quinones. They need to be reduced into hydroquinone before conjugation. The detoxification of quinone by an electron transfer can be catalyzed by NAD(P)H-dependent quinone oxidoreductases using the abundant NAD(P)H in cells as an electron donor. Then, glucuronidation and sulfation can happen onto hydroxyl groups of hydroquinone.
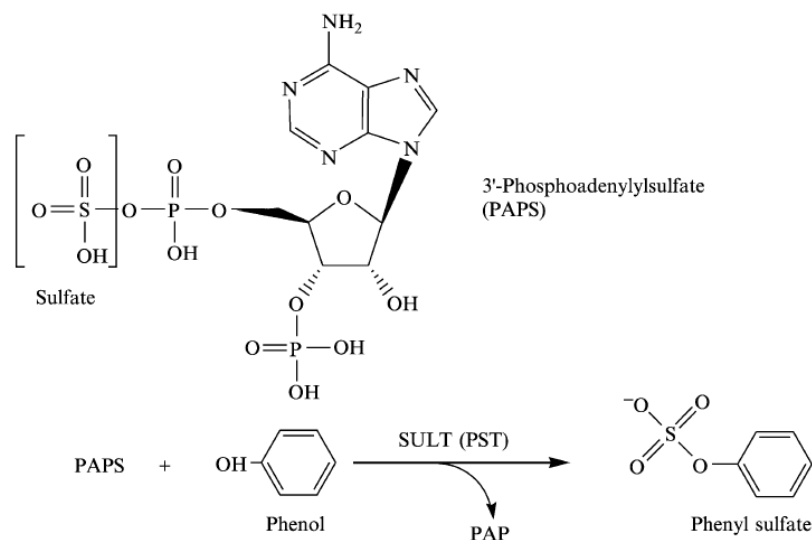
Figure I.12. Sulfation of phenols

While glucuronidation and sulfation are the main metabolism pathways of phenolic compounds, other conjugations exist. Methylation is a less frequent one. However, it can be the main metabolism pathway for some simple phenolic compounds. For instance, main HT intestinal metabolite is homovanillyl alcohol, which is its mono-methylated form [277]. The methylation of phenolic compounds is mediated by catechol-O-methyl transferases (COMT). These magnesium-dependent enzymes can be found in the cytosolic side or bound into the endoplasmic reticulum. The soluble COMT is the predominant form expressed in intestinal cells [276].

1.3.5   Efflux

Efflux can be defined as the flowing out a molecule from the cytoplasm to the lumen. Only active transport pathway controls the efflux of phenolic compounds. The main proteins involved in the efflux transport are p-glycoproteins (p-gp, ex: MDR1), multidrug resistance associated proteins (ex: MRP2) and breast cancer resistant proteins (BCRP, ex: ABCG2) belonging to the ABC transporter family. They are unidirectional transporters using ATP as a driving force for these active transporters. The glucuronides and sulfates previously formed (phase II metabolism) are too hydrophilic to cross through cellular membrane by passive diffusion [268]. BCRP and MRP2 transporters are involved in metabolite efflux into lumen. Furthermore, it has been shown that these efflux transporters and UGTs or SULTs are often coupled to optimize the elimination efficiency [278,279]. Efflux transport participates to the commonly observed poor bioavailability of polyphenols since they actively drive (poly)phenols back into the lumen [280]. The high affinity of efflux transporters for (poly)phenols has been

yet considered to modulate drug efflux in multidrug-resistant (MDR) cancer cells. For instance, certain flavonoids inhibit efflux pathways, such as p-gp, and lead to enhance the therapeutic effects by increasing the drug absorption [281].

Figure I.13 presents the main absorption and metabolism mechanism of phenolic compounds in the small intestine.
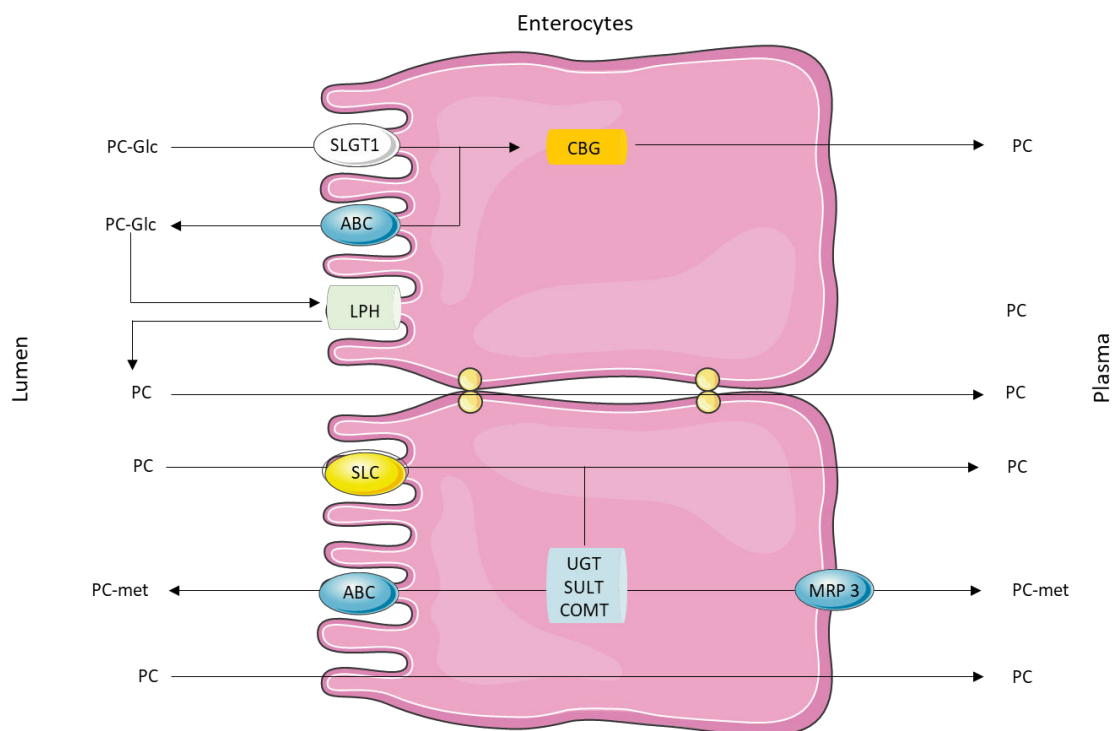
PC: phenolic compound; PC-Glc: PC-glucoside; PC-met: PC sulfate/glucuronide/methyl metabolites

Figure I.13. Main mechanisms for the absorption and metabolism of (poly)phenols in the small intestine

1.3.1   Colonic fate

The major part of phenolic compounds and the bonded phenolic compounds generally attain the large intestine, where they can be metabolized in smaller forms that can potentially reach the blood stream.

The hypothesis of a passage of phenolic compounds through the large intestine is widely studied. In the colon, a high metabolism activity occurs degrading complex phenolic compounds in simple aglycone forms that are finally able to either exert their activity in the colic lumen or reach the blood stream [228]. Bresciani *et al*. (2017) assessed the *in vivo* absorption of a capsule of a (poly)phenol mix from fruit juices. Despite the high complexity and variability of the *in vivo* results, they proposed a "global" curve of (poly)phenol absorption

taking to account the totality of quantified phenolic metabolites (Figure I.14). The gastro-intestinal tract absorption (1-2h) was lower compared to that in the colon (5-10h after the capsule consumption), which highlights a potential interaction between microbiota and the (poly)phenolic compounds [282].
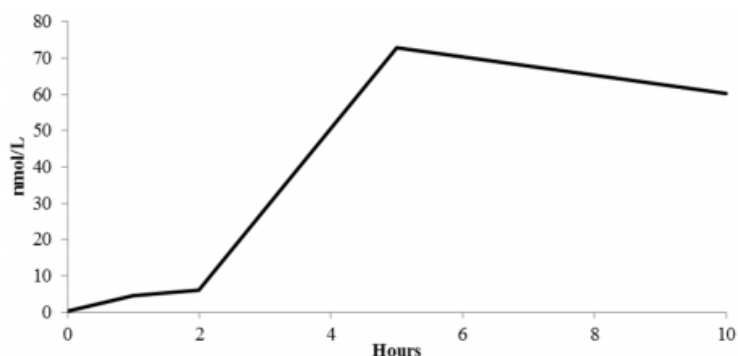
Figure I.14. Global curve of circulating (poly)phenols metabolites

Renouf *et al.* (2014) observed a low plasmatic apparition of intact chlorogenic and phenolic acids that got along with a rapid gastrointestinal absorption. Furthermore, they obtained a two-peaks kinetic of chlorogenic acid metabolites indicating there are two metabolism places, i.e. the small intestine and the colon. The earlier peak described a low plasmatic absorption of caffeic, ferulic and isoferulic acids. Dihydroferulic and dihydrocaffeic acids, which were the major chlorogenic acid metabolites found in bloodstream after a coffee consumption, needed a long-time to be detected. That supposed a colonic metabolism occurred for these two molecules [283].

To resume, the following figure (I.15) roughly presents the general steps involved in digestion and absorption of phenolic compounds in humans.

Rich-polyphenol
food

Mastication: physical breakdown
Saliva impregnation
First enzymes activity (α-amylase)

Oral cavity

Acidic environment
Desintegration of food matrix
Enzymatic hydrolysis (pepsin, amylase)

Stomach

Liver
Pancreas

Large intestine
Intensive metabolism by colonic
microflora fermentation
Absorption of aglycone, small phenols

Colon

Duodenum

Jejunum

Ileum

Small intestine
Midle alkaline environment
Weak absorption of aglycone, small phenols
Metabolism (methyl, sulfate, glucuronide)

Rectum

Elimination of the most of phenolic
compounds and their metabolites in
faeces and urines.

Anus

Figure I.15. Scheme of main steps involved in the digestion of phenolic compounds

The large class of phenolic compounds presents several families of molecules, with different specific properties which influence their final bioaccessibility and absorption through the epithelial barrier of the gastro-intestinal tract. However, their distributions in foods as well as their concentrations have also effects on their bioavailability and bioactivity.

2 Dietary factor influencing the bioaccessibility and bioavailability of phenolic compounds

Food and food processes determine the environment of bioactive compounds during its digestion, from the mouth to the intestine. The fate of natural bioactive compounds is highly dependent on their nature, the food matrix and the food process, which determine their environment and their potential interactions with other components [225].

2.1   Influence of phenolic compounds nature and food origin

Bioaccessibility and bioavailability are dependent on the molecule structure, its stereochemistry, size and hydrophobicity. For example, Tsukagoshi *et al*. (2016) compared the uptake of two phenolic compounds, i.e. hydroxyl derivatives of benzoic and of cinnamic acids by Caco-2 cells. They observed that the uptake of benzoic and cinnamic acids highly decreased when there were two hydroxyl groups on the benzene ring. Moreover, the position of hydroxyl groups controlled the uptake rate. In fact, in the case of a hydroxyl group in *m*-position, the benzoic acids absorption was unmodified, while strong decreases from 40% to 89% were observed when for a *p*-position or an *o*-position respectively. In the case of cinnamic acids, a hydroxyl group in *m*-position significantly decreased its uptake whereas a methoxy group (OCH_3) increased it. A methoxy group seemed then to enhance the uptake of cinnamic acids *via* MCTs [284]. Bresciani *et al*. (2017) worked on the bioavailability of a capsule containing polyphenols from fruits juices. They mainly observed conjugated metabolites, which were differently absorbed and found in the plasma according to their nature. For example, flavonol metabolites were essentially formed from the first part of the gastro-intestinal tract and were detectable in the circulatory system within 1 or 2 h after capsule ingestion, while flavonones, such as naringenin and hesperetin, showed two absorption peaks resulting of a double phase metabolism. The same observation was realized for ferulic acid, which is a hydroxycinnamic acids metabolite resulting to the COMT activity [282]. Moreover, phenolic compounds are generally linked to a glycoside or esterified that ensures a better stability. In literature, many studies demonstrated that glycosidic forms of specific antioxidants are commonly more bioaccessible during digestion steps making them more suitable to be potentially absorbed into

61

the enterocytes [285]. Unfortunately, as said previously, it was often revealed that free aglycones go easier through the intestinal barrier to reach the blood stream, while (poly)phenol-glycosides are often too big to cross, no specific enzymes being able to cleave the glycosidic bonds [222,286]. Donovan *et al.* (2006) observed the importance of the sugar type and location linked to flavonoids skeleton for controlling their absorption site [287]. Zhao *et al.* (2003) concluded that the molecular size of the sugar esters influences the rate and absorption site of ferulic acid. In their cases, a complex sugar esterification (such as arabinose, xylose) caused the targeting of phenolic compounds to the large intestine [288].

Phenolic compounds profile and concentration can be different within a same plant in reason of its cultivar. For example, chlorogenic acid has been always found in 33 sour cherry cultivars but its quantity varied. Furthermore, according to their localization (peel, pulp, seed, leaves, tubers), the phenolic compounds amount differs as shown by Truong *et al.* (2007) in a study on sweet potatoes [289]. However, an abundant antioxidant is not necessarily efficiently bioaccessible and bioavailable. The *in vivo* phenolic compound effects are dependent of its concentration but also in which form it is absorbed [286].

The absorption of ingested phenolic compounds is also dependent on the matrix in which they are embedded. Excepted for a pure compound, (poly)phenols are naturally mixed with other intrinsic components such as carbohydrates, lipids and proteins that play an important role in their accessibility, release and stability. In liquid matrices (such as beverages), phenolic compounds can easier exert their healthy effect while they have to be firstly extracted from a solid matrix to be bioaccessible [228,290]. As evoked previously, phenolic compounds are highly able to form complexes with polysaccharides such as matrix fibers. Indeed, they are naturally bounded to cell wall components in plants [228,286]. Fibers, which are indigestible cell wall components, are known to interfere with phenolic compounds and modify their post-ingestion fate. These heterogeneous functional compounds are mainly distinguished according to their water solubility: soluble dietary fibers such as pectin, some hemicellulose, gums, mucilage, etc. and insoluble dietary fibers comprising hemicellulose, cellulose and lignin. Phenolic compounds mainly remain bounded to fibers what reduces their activity and their release in the gastrointestinal tract [291]. Van der Waals-type interactions are the main forces involved in the interaction between phenolic compounds and dietary fibers. There are electrostatic interactions involving hydroxyl groups of phenolic compounds, London interactions involving non-polar groups of both components and ionic interactions [228]. Phenolic hydroxyl groups are also able to form ether bonds with fibers. Moreover, non-covalent

bonds can be found between them according their origins. It is considered that the release rate of antioxidants from fibrous complexes is proportionally dependent on the solute gradient and inversely proportional to the particle size. The physical state, structure and surface are also involved in the phenolic release from fibrous particles [228].

Thr food components recognized to interact with phenolic compounds such as starch or proteins, can be used for producing protective and stable complexes of active compounds [292–294]. Sengul *et al*. (2014) worked on the *in vitro* digestion of pomegranate and observed that the protein-rich foods like milk, yogurt, meat protein or bread reduced the total phenolic content in the post gastric and undialyzed fractions. The bioaccessibility and bioavailability of phenolic compounds were then reduced. They also observed inhibiting effects of lactose and starch from milk, yogurt and bread respectively demonstrating the possible interactions between phenolic compounds and these food constituents [295]. Finally, fats naturally present in plant or added to food preparations have an important role in the phenolic compounds bioaccessibility and bioavailability. In fact, fats participate to the micellization of hydrophobic phenolic compounds, essential step as for the absorption of lipophilic components [224].

Phenolic compounds linked to indigestible food components are commonly not bioavailable in the small intestine. Thus, most phenolic compounds finally reach the colon where indigestible carbohydrates and proteins can be degraded by the bacterial microflora and breakdown products such as polyphenol aglycones are released [286].

In reason of these interactions between phenolic compounds and components of foods, industrial and home food processes have been recognized to improve their bioaccessibility and finally their potential absorption in the gastrointestinal tract by cleaving these interactions.

2.2   Influence of food processing

It is assumed that storage and some food processes cause nutrient decrease from a food matrix, while they can increase the free phenolic compounds content. Indeed, food processing, such as peeling, grinding, heating, freezing or boiling can disrupt cells walls and bonds with food components, which increase the release of (poly)phenols. However, (poly)phenols can be damaged during these processes [225].

The phenolic content and composition in food processing are time-dependent. For example, it has been observed that the chlorogenic acid content in coffee beans decreased with the roasting time. However, increases of quinic and caffeic acids, which are the two moieties of chlorogenic acid, happened in the same time. So, the roasting process and its duration caused

the production of both these active metabolites [296,297]. Another example is the blanching of vegetables that causes the leaching of antioxidants into surrounding boiling water [298]. Fermentation has also shown beneficial effects on the phenolic compounds bioavailability by increasing the phenolic compounds release from the food matrix [299,300]. Otherwise, thermal treatments often lower polyphenol content because of the thermal sensitivity of these molecules. Thus, decreasing time and temperature of the thermal treatment proved to be more suitable for antioxidant preservation of phenolic water-soluble fraction of some selected vegetables (spinach, Chinese cabbage, white cabbage…) [301]. Overall, thermal sensitivity of antioxidants is dependent of their nature, the food matrices in which they are and the type of thermal processing method itself. Sharma K. *et al*. (2015) studied the temperature effect on antioxidants in onions powders. They observed a positive effect of temperature up to 120°C on the flavonoids content, which decreased at 150°C. The first phenomenon could be due to the plant wall cell breakdown and then the release of flavonoids and phenolic compounds, the second to the degradation of the molecules. Also, industrial thermal treatment can cause the formation of monomers by hydrolysis of C-glycoside bonds of flavoinoids, increasing total flavonoid content. After a certain temperature, the loss of total flavonoids content indicated that some of them were certainly degraded. The same observations were made for the total phenolic content. Thermal processes, such as sauteing, frying or roasting cause the release of (poly)phenols by cleaving esterified and glycosylated bonds. Nevertheless, excessive temperatures degraded the antioxidants [302].

Vallverdú-Queralt *et al*. (2014) studied the effect of home cooking on antioxidant capacity of homemade tomato sauces. They compared the time-dependent effects as well as those of olive oil supplementation (5% or 10%) to the sauces. They focused on phenolic acids from tomato such as caffeic, ferulic, coumaric acids and some flavonoids as quercetin, rutin, naringenin. Olive oil brought Tyr and HT into the tomato sauces. Results showed that antioxidant capacity (DPPH assay) of the tomato sauces at 95°C decreased over time and the results were similar in presence of 5% or 10% of olive oil. The phenolic content was slightly higher when olive oil was added at 10% but phenolic acids content decreased (except for caffeic acid) as well as the flavonoids content at 95°C, in a time-dependent manner. Indeed, the thermal treatment can cause in parallel the enhancement of reactive oxygen species in the food, which can be captured by (poly)phenols. This can explain the abrupt reduction of quercetin content compared to the other focused flavonoids whose the hydroxy-function at the C-ring is blocked by a sugar moiety. Heat improved the hydrolysis of glycosides bonds and the release of cell

wall components, which likely explains the increase in caffeic acid concentrations. Kinetics comparison between HT and Tyr content led to conclude that Tyr was most stable to thermal-oxidation. Its concentration continued to increase during 60 min as a degradation product of Tyr derivatives present in olive oil, whereas HT content increased up to 30 min and thereafter decreased. The thermal sensitivity of HT could be explained by the presence of a catechol unit for HT, that makes it more antioxidant than Tyr, and thus it was the first compound to be oxidized [303].

The growing consumer demands for natural and fresh-like products, new food processing has been developed to respect both food quality and integrity. Among them, High Pressure Processing (HPP) is mainly used for solid foods while High-Pressure Homogenizing (HPH) is used for liquid matrix. During the pressure procedures, the compression of the pressure-transmitting fluid (often water) causes the increase of the intrinsic temperature; also it stays lower than in thermal treatments. Pressure treatments lead to decrease the molecular volume and modify both cell walls and membrane integrity. These modifications allow a better extractability of nutrients and phenolic compounds from food matrices. Other technologies bring energy into the foods to enhance their nutrient and phenolic contents releases. Pulsed Electrified Fields (PEF) or Ultrasounds (US) have been already industrially used for producing safe foods while preserving their general structure. All these non-thermal food processes improve the phenolic compounds bioaccessibility [304].

To summarize, different extrinsic and intrinsic parameters such as the nature of phenolic compounds, the composition and structure of food matrix, the type of food processing and the bolus composition control the phenolic compounds absorption. Because of wide range of (poly)phenols and the complex food matrices, a specific food processing can either enhance or reduce their bioavailability. However, it generally appears that food processing can improve their extractability disrupting cell walls and membranes, although it can modify the (poly)phenol content and profile.

3   *In vitro* determination of the bioaccessibility and the bioavailability of phenolic compounds

Different techniques exist from the simplest simulated models to *in vivo* clinical studies. *In vivo* bioavailability studies consist in analyzing the blood and/or urine to determine how components are absorbed, i.e. in what quantity, in which compartment and their metabolism. Bresciani *et al.* (2017) studied the *in vivo* absorption of a phenolic compounds pool and

observed that their absorption rate and their metabolism are also closely dependent on the characteristics of each individual. They especially determined colonic metabolites and observed that the bioconversions of these antioxidants were different according to the characteristic and composition of colonic microbiota. All these inter-individual differences lead to obtain a wide range of bioavailability results and a lot of variability about the (poly)phenol metabolism, the timing of their appearance and finally their potential health benefits involving the colonic metabolism. Besides, *in vivo* assays meet ethical and economical obstacles in addition to the difficulty to be repeatable and to interpret data. Therefore, many numbers of *in vitro* methods have been developed to mimic physiological conditions and determine the bioaccessibility and bioavailability of targeted phenolic compounds. These methods provide a lot of information, especially when the model is close to *in vivo* situations even if some parameters (genre, age, and other physiological status) cannot be simulated. *In vitro* methods allow to specifically study the impact of food preparation and cooking, the interaction of the food matrix with other internal components, the stability and the metabolism of a molecule in the gastrointestinal tract [305].

Four methods are usually used to determine the bioaccessibility and/or bioavailability of a component. These are solubility, dialysis, *in vitro* gastrointestinal digestion model, and study in Caco-2 monolayer cells that mimics the intestinal absorption [305]. This last method can be preceded by one of the *in vitro* digestion models.

3.1 Determination of *in vitro* bioaccessibility

Bioaccessibility is closely dependent to the molecule extractability and its stability in the gastrointestinal tract. It is calculated as a mass ratio between the final solubilized intestinal amount against its initial administered mass [306].

Solubility, dialyzability and *in vitro* digestion are three static models which can bring primarily information on the simple food matrices digestion.

Solubility method results in the sample centrifugation and the analysis of the supernatant. This phase represents the soluble fraction which could be bioaccessible, the rest remaining in the precipitate [307].

Dialyzability was initially developed to study the bioaccessibility of iron and low molecular weight minerals from food matrix. It involves a membrane with a specific molecular weight cut off after the gastric digestion. Gastric or pancreatic juice is then added and the final bioaccessibility of irons and small minerals can be measured in the dialysate. Gil-Izquierdo A. *et al*. (2002) developed a dialysis method to determine the bioaccessibility of phenolic

compounds from non-liquid foods and compared their results to a precedent method developed by Miller *et al*. (1981). They optimised the contact between the food and the dialysis tubing, placing both in a same polyethylene tube. They also improved the equipment to change the medium (addition of enzymes, pH). They notably succeeded to reach pH near 7 in the dialyzed and non-dialyzed fractions. However, they observed a smaller dialyzed fraction in the case of strawberry jam probably because of its high sugar content making more difficult the diffusion through the membrane. Water from dialysis tubing naturally diffused to the food phase to equilibrate sugar content that decreased the dialysis fraction volume and increased the one of non-dialysed fraction. This phenomenon reduced the phenolic content in the dialysed fraction [308]. The *in vitro* dialyzability results have then to be taken with caution, as food compounds such as sugars and salts affect the diffusion of targeted molecules through the membrane.

In vitro digestion models were developed to reproduce the different parameters (pH, digestion secretions) in the various phases of the digestion. In usual models, the oral phase is mimicked using synthetic saliva at pH 7.5. Then, the gastric phase is reproduced by adding pepsin to the solution and by rectifying the pH at 4.0 or less. Finally, to mimic the duodenal step, the sample is neutralized near to pH 6.0, before adding pancreatin and bile. Pancreatin is a mix of several pancreatic enzymes such as amylases, lipases, ribonucleases and proteases. The addition of bile provides bile salts that are necessary for the digestion of lipophilic compounds [309–311].

These static methods simulate a limited number of physiological conditions (pH, temperature, etc.) without taking account of physical processes as shearing, mixing, peristalsis or other changes [312]. However, they have been recognized as suitable methods to simply analyse sample digestion, but they are sometimes too far from the real *in vivo* conditions. In reason of these lacks, researchers and industrials develop several multi-compartmental dynamic models.

- Dynamic Gastric Model (DGM) is a vertical alignment system performing in real-time the digestion of foods. The time and the secretions are determined based on the nature of foods and their estimated residence-times in each compartment. The acid and enzymes secretions depend on the bolus composition and the fill volume of the stomach. This system represents the both parts of the Human stomach i.e. the fondus and the antrum by distinguishing among other their respective peristalsis, higher for the distal part (antrum). The intensive peristalsis leads to decrease the food particles size, facilitating the bolus emptying to the duodenum. DGM system can represent this gradual particle size reduction as well as the *in vivo* gastric sieving, retained

longer bigger particles to extend their size reduction. When duodenal step is studied, the gastric sample is recovered and subjected to a static intestinal model [313,314].

- Horizontal models can avoid the particles gravity but are not representative of the real body position during the digestion process. TNO Intestinal Model (TIM) is a kind of horizontal dynamic digestion method. Four compartments representing stomach, duodenum, jejunum and ileum follow each other in series, simulating a continuous digestion. They are connected by peristaltic valve pumps that allow the controlled transfer of bolus from a compartment to another. Alternative pressures on flexible compartment walls allow to mix the content for each step. This first system part is controlled by a first computer (TIM1) and allows the recovery of aliquot from each fraction to determinate the bioaccessibility. Finally, the non-digestive fraction reaches the large intestine, representing by a second computer (TIM2) and is recovered for the study of its colonic fermentation. One of the most interesting advantages of this technique is the ability to recover any fraction at any time. Moreover, it can be possible to recover the digest at last TIM1 step to evaluate the bioavailability onto a human intestinal cell model [305].

- Beaker model reminds in any way the static methods. Stirred beakers are used to mimic the gastrointestinal digestion in the DIDGI systems. The DIDGI system has been developed by Institut National de la Recherche Agronomique (INRA). The stomach and the intestine are represented by two successive compartments where transit-time, secretions, pH and stirring are controlled by a computer. The flow of meal, of secretions (HCl, Na_2CO_3, digestive enzymes, biles) as well as the emptying of each compartment are controlled by several sensors and are regulated by specific computer-controlled peristaltic pumps. Air can be purged by nitrogen to mimic anaerobic conditions and the gastric sieving can also be simulated by a holed Teflon membrane before the transfer pump between the both compartments. The Stomach Regulation and Monitoring (StoRM) software controls in setting up all DIDGI parameters according to *in vivo* data from the literature. DIDGI system is a suitable dynamic model to mimic the gastric and intestinal digestion of foods, making also possible the atmosphere control. The glass beakers allow to visually follow the digestion process and results have been validated against *in vivo* data. However, some disadvantages occur as the absence of peristalsis and the differences with the real gastrointestinal anatomy [315].

In all these cases, shear and stirring forces are applied to the bolus when it passes to the stomach and the small intestine. However, the stirred approach in the beaker system does not allow to represent the real *in vivo* physical forces in the stomach. Because of their large numbers of studied parameters, such as peristalsis, body temperature, pH of gastric and pancreatic steps,

digestive juices, transit times, gastrointestinal models are known to be more representative of the component bioaccessibility in contrast to static models. However, they are much more difficult to implement. Samples recovered from all these methods can finally be applied onto *in vitro* cell models to evaluate the gastrointestinal bioavailability of nutrients.

Table I.5. Main in vitro methods for determining bioaccessibility and bioavailability (adapted from Etcheverry et al., 2012 [305])

In vitro method	Measurement	Advantages	Limitations
Solubility	Bioaccessibility	▪ Simple to do ▪ Relatively inexpensive ▪ Easy to conduct ▪ Does not required specific equipment	▪ Sometimes not a reliable indicator of bioavailability ▪ Cannot assess rate of uptake or absorption or transport kinetics ▪ Cannot measure nutrient or food component competition at the site of absorption
Dialyzability	Bioaccessibility	▪ Simple to do ▪ Relatively inexpensive ▪ Easy to conduct ▪ Does not required specific equipment	▪ Cannot assess rate of uptake or absorption or transport kinetics ▪Cannot measure nutrient or food component competition at the site of absorption
Static gastrointestinal models	Bioaccessibility Bioavailability when coupled to intestinal cells	▪ Easy to conduct ▪ Does not required specific equipment ▪ Allows the collection of digest at any step of the digestive system	▪ Less representative of the physiological conditions than the dynamic gastrointestinal models
Dynamic gastrointestinal models	Bioaccessibility Bioavailability when coupled to intestinal cells	▪ Many digestion parameters (peristalsis, body temperature etc.) ▪ Allows the collection of digest at any step of the digestive system	▪ Expensive ▪ Few validation studies
Caco-2 cell model	Intestinal absorption	▪ Allows the study of competitions and metabolism at the site of absorption	▪ Requires trained personnel with knowledge of cell culture methods

3.2   Determination of *in vitro* absorption

The intestinal absorption of phenolic compounds can be modeled by *in vitro* methods to get insights about their transport, their distribution and their metabolism by enterocytes. Different methods exist; from the noncellular approach to the cellular ones.

- The biomimetic artificial membrane permeability assay (BAMBA) method is a noncellular approach which allows to measure of passive transport. In this method, a filter is impregnated of both solutions of phospholipid and cholesterol and analyses consist in evaluating the amount of the compounds that move from one side to the other one of the filter [316].

- Caco-2 cells are the more common model to evaluate the *in vitro* intestinal absorption of a molecule. They derive from human colonic adenocarcinoma cells and are recognized to be a reliable, simple and low-cost model for absorption studies. Caco-2 cells are able to polarize, mimicking the intestinal barrier, when they grow on a semi-permeable membranes during about 21 days of culturing [317]. Transwell inserts allow the study of three compartments that are the apical side, the cells and the basolateral side representing the gut lumen, the intestinal epithelium and the blood circulation, respectively. Among the isolated clones from Caco-2 cell line, TC7 clone has been designed as providing the most homogeneous and functional population, and which develops more intercellular junctions that are representative of the small intestine [318]. Many enzymes which are commonly found in the small intestine are produced, such as carboxylase, peptidase, CYP450 isoenzymes, glutathione-S-transferase, SULTs, UGTs for example [319]. Thus, the metabolism of phenolic compounds by Caco-2/TC7 cells can be rather accurately comparable to what happens in intestinal cells. Indeed, glucuronide, sulphated, methylated and other metabolites have been found in many studies [261,320]. Although all *in vivo* parameters of the intestinal absorption cannot be represented by an *in vitro* approach, Caco-2 cells culture is the most frequently and most successfully method to investigate the post-ingestion fate of nutrients [321]. It is a reliable model for the intestinal transport and metabolism (phases I and II) of phenols [273].

- HT29 cells, which also derived from human carcinoma cells, are another type of cellular model to determine the *in vitro* absorption of nutrients. After confluence, a few portion (< 5%) of differentiated mucin-producing goblet cells and absorptive cells can be observed. According to the culture conditions, differentiations can occur for example by acquiring the morphology of enterocytes or goblet cells [322].

- Co-culturing HT29 with Caco-2 allow to get around the lack of mucin production by the Caco-2 cell model, which is an important parameter of the *in vivo* intestinal barrier. HT-29 MTX cells are a stable homogeneous differentiated mucin-secreting clone. These goblet cells are glandular epithelial cells responsible of mucus secretion [253,323]. This approach appears to be more suitable for the *in vitro* absorption of nutrients such as flavonoids by favouring paracellular transport [261].

To summarize, the term of "bioavailability" thus depends on several steps including gastro-intestinal digestion, absorption, metabolism, tissues distribution and bioactivity of the component [273]. To benefit of their health activity, phenolic compounds must be released from food matrix and adsorbed through intestinal epithelium [324] so it is important to determine (poly)phenol bioavailability. The *in vitro* bioavailability can be determined by coupling to an *in vitro* bioaccessibility study (such as a static digestion model) to an absorption model (such as Caco-2 cells in culture). A major problem related to the *in vitro* bioavailability studies is usually the dose applied. Indeed, the amount administered should be representative of physiological conditions, although this could lead to detection issue. Therefore, some *in vitro* bioavailability results must be extrapolated with great care [272].

References

1. Kapellakis IE, Tsagarakis KP, Crowther JC. 2008. Olive oil history, production and by-product management. *Rev. Environ. Sci. Biotechnol.* 7:1–26.

2. Niaounakis M, Halvadakis CP. 2006. *Olive processing waste management literature review and patent survey*. Elsevier, Amsterdam; London.

3. Dermeche S., Nadour M., Larroche C., F. Moulti-Mati, Michaud P. 2013. Olive mill wastes: Biochemical characterizations and valorization strategies. *Process Biochem.* 48:1532–1552.

4. Toscano P, Montemurro F. 2012. Olive Mill By-Products Management. In Muzzalupo Innocenzo, ed., *Olive Germplasm - Olive Cultiv. Table Olive Olive Oil Ind. Italy*. InTech.

5. Azbar N, Bayram A, Filibeli A, Muezzinoglu A, Sengul F, Ozer A. 2004. A review of waste management options in olive oil production. *Crit. Rev. Environ. Sci. Technol.* 34:209–247.

6. CAR/PP. 2000. *Prévention de la pollution dans la Production d'Huile d'Olive*. Centre d'Activité Régionale pour la Production Propre, Espagne:142p.

7. Perez J, De La Rubia T, Hamman OB, Martinez J. 1998. Phanerochaete flavido-alba laccase induction and modification of manganese peroxidase isoenzyme pattern in decolorized olive oil mill wastewaters. *Appl. Environ. Microbiol.* 64:2726–2729.

8. Aggoun M, Arhab R, Cornu A, Portelli J, Barkat M, Graulet B. 2016. Olive mill wastewater microconstituents composition according to olive variety and extraction process. *Food Chem.* 209:72–80.

9. Bouknana D, Hammouti B, Salghi R, Jodeh S, Zarrouk A, Warad I, Aouniti A, Sbaa M. 2014. Physicochemical characterization of olive oil mill wastewaters in the eastern region of Morocco. *J Mater Env. Sci.* 5:1039–1058.

10. Di Giovacchino L. 2000. Technological aspects. *Handb. Olive Oil*. Springer, pp 17–59.

11. Di Giovacchino L. 2010. *Tecnologie di lavorazione delle olive in frantoio: rese di estrazione e qualità dell'olio*. Tecniche nuove, Milano.

12. Breton C.M., Medail F., Pinatel C., Bervillé A. 2006. From olive tree to oleaster: origin and domestication of *Olea europaea* L. in the Mediterranean basin. *Cah. Agric.* 15:329–336.

13. COI. 2015. Production mondiale annuelle.

14. Ellstrand. 2003. Dangerous liaisons? When cultivated plants matae withy their wild relatives. *Schneider SS Johns Hopkins Univ. Press*.

15. Liphschitz N, Gophna R, Hartman M, Biger G. 1991. The beginning of olive (Olea europaea) cultivation in the old world: A reassessment. *J. Archaeol. Sci.* 18:441–453.

16. Ollivier D., Pinatel C., Ollivier V., Artaud J. 2014. Composition en acides gras et en triglycérides d'huiles d'olive vierges de 34 variétés et 8 Appellations d'Origine Françaises et de 2 variétés étrangères implantées en France: Constitution d'une banque de données (1ère partie). *Olivae*.:36–48.

17. Veillet S, Tomao V, Bornard I, Ruiz K, Chemat F. 2009. Chemical changes in virgin olive oils as a function of crushing systems: Stone mill and hammer crusher. *Comptes Rendus Chim.* 12:895–904.

18. Gómez-Rico A, Inarejos-García AM, Salvador MD, Fregapane G. 2009. Effect of Malaxation Conditions on Phenol and Volatile Profiles in Olive Paste and the Corresponding Virgin Olive Oils (*Olea europaea* L. Cv. *Cornicabra*). *J. Agric. Food Chem.* 57:3587–3595.

19. Roig A, Cayuela ML, Sánchez-Monedero MA. 2006. An overview on olive mill wastes and their valorisation methods. *Waste Manag.* 26:960–969.

20. Aliakbarian B, Casazza AA, Perego P. 2011. Valorization of olive oil solid waste using high pressure–high temperature reactor. *Food Chem.* 128:704–710.

21. Obied HK, Allen MS, Bedgood DR, Prenzler PD, Robards K, Stockmann R. 2005a. Bioactivity and Analysis of Biophenols Recovered from Olive Mill Waste. *J. Agric. Food Chem.* 53:823–837.

22. Rodis PS, Karathanos VT, Mantzavinou A. 2002. Partitioning of Olive Oil Antioxidants between Oil and Water Phases. *J. Agric. Food Chem.* 50:596–601.

23. EFSA Panel on Dietetic Products, Nutrition and Allergies (NDA). 2011. Scientific Opinion on the substantiation of health claims related to olive oil and maintenance of normal blood LDL-cholesterol concentrations (ID 1316, 1332), maintenance of normal (fasting) blood concentrations of triglycerides (ID 1316, 1332), maintenan: Olive oil related health claims. *EFSA J.* 9:2044.

24. Bernal MP, García-Gomez A, Roig A, Paredes C, Cegarra J, Sangiorgi F. 2000. Changes in the composition of the wastes generated by different systems of the olive oil industry. *Proc 9th Intern Conf FAO ESCORENA Netw. Recycl. Agric. Munic. Ind. Residues Agric. RAMIRAN.*, pp 220–222.

25. Daâssi D, Lozano-Sánchez J, Borrás-Linares I, Belbahri L, Woodward S, Zouari-Mechichi H, Mechichi T, Nasri M, Segura-Carretero A. 2014. Olive oil mill wastewaters: Phenolic content characterization during degradation by Coriolopsis gallica. *Chemosphere.* 113:62–70.

26. Federici E, Pepi M, Esposito A, Scargetta S, Fidati L, Gasperini S, Cenci G, Altieri R. 2011. Two-phase olive mill waste composting: Community dynamics and functional role of the resident microbiota. *Bioresour. Technol.* 102:10965–10972.

27. Frankel E, Bakhouche A, Lozano-Sánchez J, Segura-Carretero A, Fernández-Gutiérrez A. 2013. Literature Review on Production Process To Obtain Extra Virgin Olive Oil Enriched in Bioactive Compounds. Potential Use of Byproducts as Alternative Sources of Polyphenols. *J. Agric. Food Chem.* 61:5179–5188.

28. Leouifoudi I, Zyad A, Amechrouq A, Oukerrou MA, Mouse HA, Mbarki M. 2014. Identification and characterisation of phenolic compounds extracted from Moroccan olive mill wastewater. *Food Sci. Technol. Camp.* 34:249–257.

29. Alhamad MN, Rababah TM, Al-u'datt M, Ereifej K, Esoh R, Feng H, Yang W. 2012. The physicochemical properties, total phenolic, antioxidant activities, and phenolic profile of fermented olive cake. *Arab. J. Chem.* doi:10.1016/j.arabjc.2012.07.002.

30. El-Abbassi A, Kiai H, Hafidi A. 2012. Phenolic profile and antioxidant activities of olive mill wastewater. *Food Chem.* 132:406–412.

31. Vlyssides A., Loizides M, Karlis P. 2004. Integrated strategic approach for reusing olive oil extraction by-products. *J. Clean. Prod.* 12:603–611.

32. Cioffi G, Pesca MS, De Caprariis P, Braca A, Severino L, De Tommasi N. 2010. Phenolic compounds in olive oil and olive pomace from Cilento (Campania, Italy) and their antioxidant activity. *Food Chem*. 121:105–111.

33. Filidei S, Masciandaro G, Ceccanti B. 2003. Anaerobic digestion of olive oil mill effluents: evaluation of wastewater organic load and phytotoxicity reduction. *Water. Air. Soil Pollut*. 145:79–94.

34. Salgado JM, Abrunhosa L, Venâncio A, Domínguez JM, Belo I. 2014. Screening of winery and olive mill wastes for lignocellulolytic enzyme production from *Aspergillus* species by solid-state fermentation. *Biomass Convers. Biorefinery*. 4:201–209.

35. El-Abbassi A, Kiai H, Raiti J, Hafidi A. 2014. Cloud point extraction of phenolic compounds from pretreated olive mill wastewater. *J. Environ. Chem. Eng*. 2:1480–1486.

36. Deeb AA, Fayyad MK, Alawi MA. 2012. Separation of Polyphenols from Jordanian Olive Oil Mill Wastewater. *Chromatogr. Res. Int*. 2012:1–8.

37. Rubio-Senent F, Rodríguez-Gutíerrez G, Lama-Muñoz A, Fernández-Bolaños J. 2012. New Phenolic Compounds Hydrothermally Extracted from the Olive Oil Byproduct Alperujo and Their Antioxidative Activities. *J. Agric. Food Chem*. 60:1175–1186.

38. Sannino F, De Martino A, Capasso R, El Hadrami I. 2013. Valorisation of organic matter in olive mill wastewaters: Recovery of highly pure hydroxytyrosol. *J. Geochem. Explor*. 129:34–39.

39. Franco MN, Galeano-Díaz T, López Ó, Fernández-Bolaños JG, Sánchez J, De Miguel C, Gil MV, Martín-Vertedor D. 2014. Phenolic compounds and antioxidant capacity of virgin olive oil. *Food Chem*. 163:289–298.

40. Essiari, Zouhair, Chimi. 2014. Contribution à l'étude de la typicité des huiles d'olive vierges produites dans la région de Sais (Maroc). *119.*:8–22.

41. Servili M, Taticchi A, Esposto S, Sordini B, Urbani S. 2012. Technological Aspects of Olive Oil Production. In Muzzalupo, I, ed., *Olive Germplasm - Olive Cultiv. Table Olive Olive Oil Ind. Italy*. InTech.

42. Priego-Capote F, Ruiz-Jiménez J, Luque de Castro M. 2004. Fast separation and determination of phenolic compounds by capillary electrophoresis–diode array detection. *J. Chromatogr. A*. 1045:239–246.

43. Anter J, Tasset I, Demyda-Peyrás S, Ranchal I, Moreno-Millán M, Romero-Jimenez M, Muntané J, Luque de Castro MD, Muñoz-Serrano A, Alonso-Moraga Á. 2014. Evaluation of potential antigenotoxic, cytotoxic and proapoptotic effects of the olive oil by-product 'alperujo', hydroxytyrosol, tyrosol and verbascoside. *Mutat. Res. Toxicol. Environ. Mutagen*. 772:25–33.

44. Ramos P, Santos SAO, Guerra ÂR, Guerreiro O, Felício L, Jerónimo E, Silvestre AJD, Neto CP, Duarte M. 2013. Valorization of olive mill residues: Antioxidant and breast cancer antiproliferative activities of hydroxytyrosol-rich extracts derived from olive oil by-products. *Ind. Crops Prod*. 46:359–368.

45. Ena A, Pintucci C, Carlozzi P. 2012. The recovery of polyphenols from olive mill waste using two adsorbing vegetable matrices. *J. Biotechnol*. 157:573–577.

46. D'Antuono I, Kontogianni VG, Kotsiou K, Linsalata V, Logrieco AF, Tasioula-Margari M, Cardinali A. 2014. Polyphenolic characterization of olive mill wastewaters, coming

from Italian and Greek olive cultivars, after membrane technology. *Food Res. Int.* 65:301–310.

47. Agalias A, Magiatis P, Skaltsounis A-L, Mikros E, Tsarbopoulos A, Gikas E, Spanos I, Manios T. 2007. A New Process for the Management of Olive Oil Mill Waste Water and Recovery of Natural Antioxidants. *J. Agric. Food Chem.* 55:2671–2676.

48. Kaleh Z, Geißen S-U. 2016. Selective isolation of valuable biophenols from olive mill wastewater. *J. Environ. Chem. Eng.* 4:373–384.

49. Michailof C, Manesiotis P, Panayiotou C. 2008. Synthesis of caffeic acid and p-hydroxybenzoic acid molecularly imprinted polymers and their application for the selective extraction of polyphenols from olive mill waste waters. *J. Chromatogr. A.* 1182:25–33.

50. Puoci F, Scoma A, Cirillo G, Bertin L, Fava F, Picci N. 2012. Selective extraction and purification of gallic acid from actual site olive mill wastewaters by means of molecularly imprinted microparticles. *Chem. Eng. J.* 198–199:529–535.

51. De Marco E, Savarese M, Paduano A, Sacchi R. 2007. Characterization and fractionation of phenolic compounds extracted from olive oil mill wastewaters. *Food Chem.* 104:858–867.

52. Alu'datt MH, Alli I, Ereifej K, Alhamad M, Al-Tawaha AR, Rababah T. 2010. Optimisation, characterisation and quantification of phenolic compounds in olive cake. *Food Chem.* 123:117–122.

53. Bouaziz M, Jemai H, Khabou W, Sayadi S. 2010. Oil content, phenolic profiling and antioxidant potential of Tunisian olive drupes. *J. Sci. Food Agric.* 90:1750–1758.

54. Galanakis CM, Tornberg E, Gekas V. 2010. Recovery and preservation of phenols from olive waste in ethanolic extracts. *J. Chem. Technol. Biotechnol.* 85:1148–1155.

55. Lafka T-I, Lazou AE, Sinanoglou VJ, Lazos ES. 2011. Phenolic and antioxidant potential of olive oil mill wastes. *Food Chem.* 125:92–98.

56. Lozano-Sánchez J, Castro-Puyana M, Mendiola J, Segura-Carretero A, Cifuentes A, Ibáez E. 2014. Recovering Bioactive Compounds from Olive Oil Filter Cake by Advanced Extraction Techniques. *Int. J. Mol. Sci.* 15:16270–16283.

57. Jerman KT, Mozetič VB. 2011. Ultrasonic Extraction of Phenols from Olive Mill Wastewater: Comparison with Conventional Methods. *J. Agric. Food Chem.* 59:12725–12731.

58. Pérez-Serradilla JA, Japón-Luján R, Luque de Castro MD. 2007. Simultaneous microwave-assisted solid–liquid extraction of polar and nonpolar compounds from alperujo. *Anal. Chim. Acta.* 602:82–88.

59. Kalogerakis N, Politi M, Foteinis S, Chatzisymeon E, Mantzavinos D. 2013. Recovery of antioxidants from olive mill wastewaters: A viable solution that promotes their overall sustainable management. *J. Environ. Manage.* 128:749–758.

60. Rubio-Senent F, Rodríguez-Gutiérrez G, Lama-Muñoz A, Fernández-Bolaños J. 2013. Phenolic extract obtained from steam-treated olive oil waste: Characterization and antioxidant activity. *LWT - Food Sci. Technol.* 54:114–124.

61. Pérez-Serradilla JA, Japón-Luján R, Luque de Castro MD. 2008. Static–dynamic sequential superheated liquid extraction of phenols and fatty acids from alperujo. *Anal. Bioanal. Chem.* 392:1241–1248.

62. Reis Giada M de L. 2013. Food Phenolic Compounds: Main Classes, Sources and Their Antioxidant Power. In Morales-Gonzalez, JA, ed., *Oxidative Stress Chronic Degener. Dis. - Role Antioxid.* InTech.

63. Fernandez-Bolanos J, Felizón B, Brenes M, Guillén R, Heredia A. 1998. Hydroxytyrosol and tyrosol as the main compounds found in the phenolic fraction of steam-exploded olive stones. *J. Am. Oil Chem. Soc.* 75:1643–1649.

64. Aranda E, García-Romera I, Ocampo JA, Carbone V, Mari A, Malorni A, Sannino F, De Martino A, Capasso R. 2007. Chemical characterization and effects on Lepidium sativum of the native and bioremediated components of dry olive mill residue. *Chemosphere.* 69:229–239.

65. Suárez M, Romero M-P, Ramo T, Macià A, Motilva M-J. 2009. Methods for Preparing Phenolic Extracts from Olive Cake for Potential Application as Food Antioxidants. *J. Agric. Food Chem.* 57:1463–1472.

66. Obied HK, Bedgood DR, Prenzler PD, Robards K. 2007. Chemical screening of olive biophenol extracts by hyphenated liquid chromatography. *Anal. Chim. Acta.* 603:176–189.

67. Peralbo-Molina Á, Priego-Capote F, Luque de Castro MD. 2012. Tentative Identification of Phenolic Compounds in Olive Pomace Extracts Using Liquid Chromatography–Tandem Mass Spectrometry with a Quadrupole–Quadrupole-Time-of-Flight Mass Detector. *J. Agric. Food Chem.* 60:11542–11550.

68. Ghayth R. 2014. Recovery of high yield flavonoids rich extract from two-phase Chemlali olive pomace. *J. Food Stud.* 3:25–39.

69. Bonoli M, Montanucci M, Toschi TG, Lercker G. 2003. Fast separation and determination of tyrosol, hydroxytyrosol and other phenolic compounds in extra-virgin olive oil by capillary zone electrophoresis with ultraviolet-diode array detection. *J. Chromatogr. A.* 1011:163–172.

70. Suárez M, Macià A, Romero M-P, Motilva M-J. 2008. Improved liquid chromatography tandem mass spectrometry method for the determination of phenolic compounds in virgin olive oil. *J. Chromatogr. A.* 1214:90–99.

71. Bianco A, Buiarelli F, Cartoni G, Coccioli F, Jasionowska R, Margherita P. 2003. Analysis by liquid chromatography-tandem mass spectrometry of biophenolic compounds in olives and vegetation waters, Part I. *J. Sep. Sci.* 26:409–416.

72. Cardoso SM, Guyot S, Marnet N, Lopes-da-Silva JA, Renard CM, Coimbra MA. 2005. Characterisation of phenolic extracts from olive pulp and olive pomace by electrospray mass spectrometry. *J. Sci. Food Agric.* 85:21–32.

73. Rubio-Senent F, Rodríguez-Gutiérrez G, Lama-Muñoz A, Fernández-Bolaños J. 2013. Chemical characterization and properties of a polymeric phenolic fraction obtained from olive oil waste. *Food Res. Int.* 54:2122–2129.

74. de la Torre-Carbot K, Jauregui O, Gimeno E, Castellote AI, Lamuela-Raventós RM, López-Sabater MC. 2005. Characterization and Quantification of Phenolic Compounds in Olive Oils by Solid-Phase Extraction, HPLC-DAD, and HPLC-MS/MS. *J. Agric. Food Chem.* 53:4331–4340.

75. Kanakis P, Termentzi A, Michel T, Gikas E, Halabalaki M, Skaltsounis A-L. 2013. From Olive Drupes to Olive Oil. An HPLC-Orbitrap-based Qualitative and Quantitative Exploration of Olive Key Metabolites. *Planta Med.* 79:1576–1587.

76. DellaGreca M, Previtera L, Temussi F, Zarrelli A. 2004. Low-molecular-weight components of olive oil mill waste-waters. *Phytochem. Anal.* 15:184–188.

77. Obied HK, Bedgood DR, Prenzler PD, Robards K. 2007. Bioscreening of Australian olive mill waste extracts: Biophenol content, antioxidant, antimicrobial and molluscicidal activities. *Food Chem. Toxicol.* 45:1238–1248.

78. Rubio-Senent F, Martos S, Lama-Muñoz A, Fernández-Bolaños JG, Rodríguez-Gutiérrez G, Fernández-Bolaños J. 2015. Isolation and identification of minor secoiridoids and phenolic components from thermally treated olive oil by-products. *Food Chem.* 187:166–173.

79. Herrero M, Temirzoda TN, Segura-Carretero A, Quirantes R, Plaza M, Ibañez E. 2011. New possibilities for the valorization of olive oil by-products. *J. Chromatogr. A.* 1218:7511–7520.

80. García-Villalba R, Carrasco-Pancorbo A, Oliveras-Ferraros C, Vázquez-Martín A, Menéndez JA, Segura-Carretero A, Fernández-Gutiérrez A. 2010. Characterization and quantification of phenolic compounds of extra-virgin olive oils with anticancer properties by a rapid and resolutive LC-ESI-TOF MS method. *J. Pharm. Biomed. Anal.* 51:416–429.

81. Rigane G, Bouaziz M, Sayadi S, Ben Salem R. 2012. Identification and characterization of a new iridoid compound from two-phase Chemlali olive pomace. *Eur. Food Res. Technol.* 234:1049–1054.

82. Mulinacci N, Innocenti M, La Marca G, Mercalli E, Giaccherini C, Romani A, Erica S, Vincieri FF. 2005. Solid Olive Residues: Insight into Their Phenolic Composition. *J. Agric. Food Chem.* 53:8963–8969.

83. Cardinali A, Pati S, Minervini F, D'Antuono I, Linsalata V, Lattanzio V. 2012. Verbascoside, Isoverbascoside, and Their Derivatives Recovered from Olive Mill Wastewater as Possible Food Antioxidants. *J. Agric. Food Chem.* 60:1822–1829.

84. Cardoso SM, Falcão SI, Peres AM, Domingues MRM. 2011. Oleuropein/ligstroside isomers and their derivatives in Portuguese olive mill wastewaters. *Food Chem.* 129:291–296.

85. Obied HK, Prenzler PD, Robards K. 2008. Potent antioxidant biophenols from olive mill waste. *Food Chem.* 111:171–178.

86. Innocenti M, Marca G la, Malvagia S, Giaccherini C, Vincieri FF, Mulinacci N. 2006. Electrospray ionisation tandem mass spectrometric investigation of phenylpropanoids and secoiridoids from solid olive residue. *Rapid Commun. Mass Spectrom.* 20:2013–2022.

87. Silva S, Gomes L, Leitao F, Coelho AV, Boas LV. 2006. Phenolic Compounds and Antioxidant Activity of *Olea europaea* L. Fruits and Leaves. *Food Sci. Technol. Int.* 12:385–395.

88. Cardoso SM, Guyot S, Marnet N, Lopes-da-Silva JA, Silva AM, Renard CM, Coimbra MA. 2006. Identification of oleuropein oligomers in olive pulp and pomace. *J. Sci. Food Agric.* 86:1495–1502.

89. Jemai H, El Feki A, Sayadi S. 2009. Antidiabetic and Antioxidant Effects of Hydroxytyrosol and Oleuropein from Olive Leaves in Alloxan-Diabetic Rats. *J. Agric. Food Chem.* 57:8798–8804.

90. Zhongxiang Fang, Bhesh Bhandari. 2010. Encapsulation of polyphenols – a review. *Trends Food Sci. Technol.* 21:510–523.

91. Gordon MH, Paiva-Martins F, Almeida M. 2001. Antioxidant Activity of Hydroxytyrosol Acetate Compared with That of Other Olive Oil Polyphenols. *J. Agric. Food Chem.* 49:2480–2485.

92. Rodríguez G, Lama A, Jaramillo S, Fuentes-Alventosa JM, Guillén R, Jiménez-Araujo A, Rodríguez-Arcos R, Fernández-Bolaños J. 2009. 3,4-Dihydroxyphenylglycol (DHPG): An Important Phenolic Compound Present in Natural Table Olives. *J. Agric. Food Chem.* 57:6298–6304.

93. Rodríguez G, Rodríguez R, Fernández-Bolaños J, Guillén R, Jiménez A. 2007. Antioxidant activity of effluents during the purification of hydroxytyrosol and 3,4-dihydroxyphenyl glycol from olive oil waste. *Eur. Food Res. Technol.* 224:733–741.

94. Olthof MR, Hollman PC, Zock PL, Katan MB. 2001. Consumption of high doses of chlorogenic acid, present in coffee, or of black tea increases plasma total homocysteine concentrations in humans. *Am. J. Clin. Nutr.* 73:532–538.

95. Fraser CM, Chapple C. 2011. The Phenylpropanoid Pathway in Arabidopsis. *Arab. Book.* 9:e0152.

96. Vogt T. 2010. Phenylpropanoid Biosynthesis. *Mol. Plant.* 3:2–20.

97. Alipieva K, Korkina L, Orhan IE, Georgiev MI. 2014. Verbascoside — A review of its occurrence, (bio)synthesis and pharmacological significance. *Biotechnol. Adv.* 32:1065–1076.

98. Dinda B, Debnath S, Banik R. 2011. Naturally occurring iridoids and secoiridoids. An updated review, part 4. *Chem. Pharm. Bull. (Tokyo).* 59:803–833.

99. Haris Omar S. 2010. Oleuropein in Olive and its Pharmacological Effects. *Sci. Pharm.* 78:133–154.

100. Servili M, Baldioli M, Selvaggini R, Macchioni A, Montedoro G. 1999. Phenolic Compounds of Olive Fruit: One- and Two-Dimensional Nuclear Magnetic Resonance Characterization of Nüzhenide and Its Distribution in the Constitutive Parts of Fruit. *J. Agric. Food Chem.* 47:12–18.

101. Silva S, Gomes L, Leitão F, Bronze M, Coelho AV, Boas LV. 2010. Secoiridoids in olive seed: characterization of nüzhenide and 11-methyl oleosides by liquid chromatography with diode array and mass spectrometry. *Grasas Aceites.* 61:157–164.

102. Esti M, Cinquanta L, La Notte E. 1998. Phenolic compounds in different olive varieties. *J. Agric. Food Chem.* 46:32–35.

103. Medina E, Romero C, Brenes M, García P, de Castro A, García A. 2008. Profile of anti-lactic acid bacteria compounds during the storage of olives which are not treated with alkali. *Eur. Food Res. Technol.* 228:133–138.

104. Tsimogiannis D, Samiotaki M, Panayotou G, Oreopoulou V. 2007. Characterization of flavonoid subgroups and hydroxy substitution by HPLC-MS/MS. *Molecules.* 12:593–606.

105. Kumar S, Pandey AK. 2013. Chemistry and Biological Activities of Flavonoids: An Overview. *Sci. World J.* 2013:1–16.

106. Cunha WR, Bastos JK, e Silva MLA, Veneziani RCS, Ambrósio SR. 2012. *Lignans: Chemical and Biological Properties.* INTECH Open Access Publisher.

107. Molina-Alcaide, Nefzaoui. 1996. Recycling of Olive Oil By-Products: Possibilities of Utilization in Animal Nutrition. *Int. Biodeterior. Biodegrad.*:227–235.

108. Molina-Alcaide E, Yáñez-Ruiz DR. 2008. Potential use of olive by-products in ruminant feeding: A review. *Anim. Feed Sci. Technol*. 147:247–264.

109. Nefzaoui A. 1991. Valorisation des sous-produits de l'olivier. *Options Méditerranéennes–Série A*. 16:101–08.

110. Mourtzinos I, Salta F, Yannakopoulou K, Chiou A, Karathanos VT. 2007. Encapsulation of Olive Leaf Extract in β-Cyclodextrin. *J. Agric. Food Chem*. 55:8088–8094.

111. Ratnasooriya CC, Rupasinghe HPV. 2012. Extraction of phenolic compounds from grapes and their pomace using β-cyclodextrin. *Food Chem*. 134:625–631.

112. Stamatopoulos K, Chatzilazarou A, Katsoyannos E. 2013. Optimization of Multistage Extraction of Olive Leaves for Recovery of Phenolic Compounds at Moderated Temperatures and Short Extraction Times. *Foods*. 3:66–81.

113. Talhaoui N, Gómez-Caravaca AM, León L, De la Rosa R, Segura-Carretero A, Fernández-Gutiérrez A. 2014. Determination of phenolic compounds of 'Sikitita' olive leaves by HPLC-DAD-TOF-MS. Comparison with its parents 'Arbequina' and 'Picual' olive leaves. *LWT - Food Sci. Technol*. 58:28–34.

114. Krokida MK, Maroulis ZB, Kremalis C. 2002. Process design of rotary dryers for olive cake. *Dry. Technol*. 20:771–788.

115. Rodríguez-Gutiérrez G, Rubio-Senent F, Lama-Muñoz A, García A, Fernández-Bolaños J. 2014. Properties of Lignin, Cellulose, and Hemicelluloses Isolated from Olive Cake and Olive Stones: Binding of Water, Oil, Bile Acids, and Glucose. *J. Agric. Food Chem*. 62:8973–8981.

116. Moral PS, Méndez MVR. 2006. Production of pomace olive oil. *Grasas Aceites*. 57:47–55.

117. Intini F., Kühtz S., Rospi G. 2011. Energy recovery of the solid waste of the olive oil Industries–LCA analysis and carbon footprint assessment. *J. Sustain. Energy Environ*. 2.:157–166.

118. Che F, Sarantopoulos I, Tsoutsos T, Gekas V. 2012. Exploring a promising feedstock for biodiesel production in Mediterranean countries: A study on free fatty acid esterification of olive pomace oil. *Biomass Bioenergy*. 36:427–431.

119. Lama-Muñoz A, Álvarez-Mateos P, Rodríguez-Gutiérrez G, Durán-Barrantes MM, Fernández-Bolaños J. 2014. Biodiesel production from olive–pomace oil of steam-treated alperujo. *Biomass Bioenergy*. 67:443–450.

120. Abu Tayeh H, Najami N, Dosoretz C, Tafesh A, Azaizeh H. 2014. Potential of bioethanol production from olive mill solid wastes. *Bioresour. Technol*. 152:24–30.

121. Yücel Y. 2011. Biodiesel production from pomace oil by using lipase immobilized onto olive pomace. *Bioresour. Technol*. 102:3977–3980.

122. Muktadirul Bari Chowdhury AKM, Akratos CS, Vayenas DV, Pavlou S. 2013. Olive mill waste composting: A review. *Int. Biodeterior. Biodegrad*. 85:108–119.

123. Tomati U, Galli E, Fiorelli F, Pasetti L. 1996. Fertilizers from composting of olive-mill wastewaters. *Int. Biodeterior. Biodegrad*. 38:155–162.

124. Fernández-Hernández A, Roig A, Serramiá N, Civantos CG-O, Sánchez-Monedero MA. 2014. Application of compost of two-phase olive mill waste on olive grove: Effects on soil, olive fruit and olive oil quality. *Waste Manag*. 34:1139–1147.

125. Brozzoli V, Bartocci S, Terramoccia S, Contò G, Federici F, D'Annibale A, Petruccioli M. 2010. Stoned olive pomace fermentation with Pleurotus species and its evaluation as a possible animal feed. *Enzyme Microb. Technol.* 46:223–228.

126. Dal Bosco A, Mourvaki E, Cardinali R, Servili M, Sebastiani B, Ruggeri S, Mattioli S, Taticchi A, Esposto S, Castellini C. 2012. Effect of dietary supplementation with olive pomaces on the performance and meat quality of growing rabbits. *Meat Sci.* 92:783–788.

127. Raposo R, Ruiz-Moreno MJ, Garde-Cerdán T, Puertas B, Moreno-Rojas JM, Zafrilla P, Gonzalo-Diago A, Guerrero RF, Cantos-Villar E. 2016. Replacement of sulfur dioxide by hydroxytyrosol in white wine: Influence on both quality parameters and sensory. *LWT - Food Sci. Technol.* 65:214–221.

128. Hjaila K, Baccar R, Sarrà M, Gasol CM, Blánquez P. 2013. Environmental impact associated with activated carbon preparation from olive-waste cake via life cycle assessment. *J. Environ. Manage.* 130:242–247.

129. Ntaikou I, Kourmentza C, Koutrouli EC, Stamatelatou K, Zampraka A, Kornaros M, Lyberatos G. 2009. Exploitation of olive oil mill wastewater for combined biohydrogen and biopolymers production. *Bioresour. Technol.* 100:3724–3730.

130. Battista F, Mancini G, Ruggeri B, Fino D. 2016. Selection of the best pretreatment for hydrogen and bioethanol production from olive oil waste products. *Renew. Energy.* 88:401–407.

131. Pintucci C, Giovannelli A, Traversi ML, Ena A, Padovani G, Carlozzi P. 2013. Fresh olive mill waste deprived of polyphenols as feedstock for hydrogen photo-production by means of *Rhodopseudomonas palustris* 42OL. *Renew. Energy.* 51:358–363.

132. Casanovas A, Galvis A, Llorca J. 2015. Catalytic steam reforming of olive mill wastewater for hydrogen production. *Int. J. Hydrog. Energy.* 40:7539–7545.

133. Tosti S, Cavezza C, Fabbricino M, Pontoni L, Palma V, Ruocco C. 2015. Production of hydrogen in a Pd-membrane reactor via catalytic reforming of olive mill wastewater. *Chem. Eng. J.* 275:366–373.

134. Fernández-Rodríguez MJ, Rincón B, Fermoso FG, Jiménez AM, Borja R. 2014. Assessment of two-phase olive mill solid waste and microalgae co-digestion to improve methane production and process kinetics. *Bioresour. Technol.* 157:263–269.

135. Gharsallah N, Labat M, Aloui F, Sayadi S. 1999. The effect of *Phanerochaete chrysosporium* pretreatment of olive mill waste waters on anaerobic digestion. *Resour. Conserv. Recycl.* 27:187–192.

136. Altieri R, Esposito A, Parati F, Lobianco A, Pepi M. 2009. Performance of olive mill solid waste as a constituent of the substrate in commercial cultivation of *Agaricus bisporus*. *Int. Biodeterior. Biodegrad.* 63:993–997.

137. Mansour–Benamar M, Savoie J-M, Chavant L. 2013. Valorization of solid olive mill wastes by cultivation of a local strain of edible mushrooms. *C. R. Biol.* 336:407–415.

138. Ruiz-Rodriguez A, Soler-Rivas C, Polonia I, Wichers HJ. 2010. Effect of olive mill waste (OMW) supplementation to *Oyster* mushrooms substrates on the cultivation parameters and fruiting bodies quality. *Int. Biodeterior. Biodegrad.* 64:638–645.

139. Garcıa Garcıa I, Jimenez Pena PR, Bonilla Venceslada JL, Martın Martın A, Martın Santos MA, Ramos Gomez E. 2000. Removal of phenol compounds from olive mill wastewater

using *Phanerochaete chrysosporium*, *Aspergillus niger*, *Aspergillus terreus* and *Geotrichum candidum*. *Process Biochem*. 35:751–758.

140. Ntougias S, Baldrian P, Ehaliotis C, Nerud F, Antoniou T, Merhautová V, Zervakis GI. 2012. Biodegradation and detoxification of olive mill wastewater by selected strains of the mushroom genera *Ganoderma* and *Pleurotus*. *Chemosphere*. 88:620–626.

141. Ballesteros I, Oliva JM, Saez F, Ballesteros M. 2001. Ethanol production from lignocellulosic byproducts of olive oil extraction. *Appl. Biochem. Biotechnol*. 91:237–252.

142. Heinrich A. 2007. Production of Ethanol by an Integrated Valorization of Olive Oil Byproducts. The Role of Phenolic Inhibition (2 pp). *Environ. Sci. Pollut. Res. - Int*. 14:5–6.

143. Fernández-Bolaños J, Rodríguez G, Gómez E, Guillén R, Jiménez A, Heredia A, Rodríguez R. 2004. Total Recovery of the Waste of Two-Phase Olive Oil Processing: Isolation of Added-Value Compounds. *J. Agric. Food Chem*. 52:5849–5855.

144. Fernandes MC, Torrado I, Carvalheiro F, Dores V, Guerra V, Lourenço PML, Duarte LC. 2016. Bioethanol production from extracted olive pomace: dilute acid hydrolysis. *Bioethanol*. 2.

145. Herrero ML, Vallejo MD, Sardella MF, Deiana AC. 2015. Acid Pretreatment of Two Phase Olive Mill Waste to Improve Bioavailable Sugars: Conditions Optimization Using Response Surface Methodology. *Waste Biomass Valorization*. 6:37–44.

146. Rubio-Senent F, Rodríguez-Gutiérrez G, Lama-Muñoz A, García A, Fernández-Bolaños J. 2015. Novel pectin present in new olive mill wastewater with similar emulsifying and better biological properties than citrus pectin. *Food Hydrocoll*. 50:237–246.

147. Rubio-Senent F, Rodríguez-Gutiérrez G, Lama-Muñoz A, Fernández-Bolaños J. 2015. Pectin extracted from thermally treated olive oil by-products: Characterization, physico-chemical properties, *in vitro* bile acid and glucose binding. *Food Hydrocoll*. 43:311–321.

148. Cardoso SM, Silva AMS, Coimbra MA. 2002. Structural characterisation of the olive pomace pectic polysaccharide arabinan side chains. *Carbohydr. Res*. 337:917–924.

149. Coimbra MA, Cardoso SM, Lopes-da-Silva JA. 2010. Olive Pomace, a Source for Valuable Arabinan-Rich Pectic Polysaccharides. In Rauter, AP, Vogel, P and Queneau, Y, eds, *Carbohydr. Sustain. Dev. I*. 294, Springer Berlin Heidelberg, Berlin, Heidelberg, pp 129–141.

150. Lopez MJ, Moreno J, Ramos-Cormenzana A. 2001. *Xanthomonas campestris* strain selection for xanthan production from olive mill wastewaters. *Water Res*. 35:1828–1830.

151. Israilides C, Scanlon B, Smith A, Harding SE, Jumel K. 1994. Characterization of pullulans produced from agro-industrial wastes. *Carbohydr. Polym*. 25:203–209.

152. Elksibi I., Haddar W., Ben Ticha M., Gharbi R., Mhenni M.F. 2014. Development and optimisation of a non conventional extraction process of natural dye from olive solid waste using response surface methodology (RSM). *Food Chem*. 161:345–352.

153. Meksi N, Haddar W, Hammami S, Mhenni MF. 2012. Olive mill wastewater: A potential source of natural dyes for textile dyeing. *Ind. Crops Prod*. 40:103–109.

154. Moya Ramírez I, Tsaousi K, Rudden M, Marchant R, Jurado Alameda E, García Román M, Banat IM. 2015. Rhamnolipid and surfactin production from olive oil mill waste as sole carbon source. *Bioresour. Technol*. 198:231–236.

155. Salgado JM, Abrunhosa L, Venâncio A, Domínguez JM, Belo I. 2016. Combined bioremediation and enzyme production by *Aspergillus sp.* in olive mill and winery wastewaters. *Int. Biodeterior. Biodegrad.* 110:16–23.

156. Guneser O, Demirkol A, Yuceer YK, Togay SO, Hosoglu MI, Elibol M. 2016. Production of flavor compounds from olive oil mill waste by *Rhizopus oryzae* and Candida tropicalis. *Braz. J. Microbiol.* doi:10.1016/j.bjm.2016.08.003.

157. Alsafadi D, Al-Mashaqbeh O. 2017. A one-stage cultivation process for the production of poly-3-(hydroxybutyrate-co-hydroxyvalerate) from olive mill wastewater by *Haloferax mediterranei. New Biotechnol.* 34:47–53.

158. Campanari S, e Silva FA, Bertin L, Villano M, Majone M. 2014. Effect of the organic loading rate on the production of polyhydroxyalkanoates in a multi-stage process aimed at the valorization of olive oil mill wastewater. *Int. J. Biol. Macromol.* 71:34–41.

159. Dionisi D, Carucci G, Papini MP, Riccardi C, Majone M, Carrasco F. 2005. Olive oil mill effluents as a feedstock for production of biodegradable polymers. *Water Res.* 39:2076–2084.

160. Leite P, Salgado JM, Venâncio A, Domínguez JM, Belo I. 2016. Ultrasounds pretreatment of olive pomace to improve xylanase and cellulase production by solid-state fermentation. *Bioresour. Technol.* 214:737–746.

161. Moya Ramírez I, Altmajer Vaz D, Banat IM, Marchant R, Jurado Alameda E, García Román M. 2016. Hydrolysis of olive mill waste to enhance rhamnolipids and surfactin production. *Bioresour. Technol.* 205:1–6.

162. Crini G. 2014. Review: A History of Cyclodextrins. *Chem. Rev.* 114:10940–10975.

163. Riche. 1892. Journal de Pharmacie et de Chimie.:661.

164. Villiers A. 1891. Bulletin de la Société Chimique de Paris. *Sur Transform. Fécule En Dextrine Par Ferment Butyrique.*:468–472.

165. Schardinger F. 1903. Über Thermophile Bakterien aus verschiedenen Speisen und Milch, sowie über einige Umsetzungsprodukte derselben in hohlenhydrathaltigen Nährlösungen, darunter kristallisierte Polysaccharide (Dextrine) aus Stärke. *Z Unters Nahr Genussm.*:865–880.

166. Wilson EJ, Schoch TJ, Hudson CS. 1943. The action of macerans amylose on the fractions from starch. *J. Am. Chem. Soc.*:1380.

167. Szejtli J. 2004. Past, present and futute of cyclodextrin research. *Pure Appl. Chem.* 76.

168. Magnúsdóttir A, Másson M, Loftsson T. 2005. The conventional model of drug/cyclodextrin complex formation (salicylic acid/β-cyclodextrin inclusion complex). *Expert Opin. Drug Deliv.* 2.

169. Uekama K, Hirayama F, Irie T. 1998. Cyclodextrin drug carrier systems. *Chem. Rev.* 98:2045–2076.

170. Winkler RG, Fioravanti S, Ciccotti G, Margheritis C, Villa M. 2000. Hydration of β-cyclodextrin: a molecular dynamics simulation study. *J. Comput. Aided Mol. Des.* 14:659–667.

171. Szejtli J. 1988. *Cyclodextrin Technology.* 1, Springer Netherlands, Dordrecht.

172. Nedovic V, Kalusevic A, Manojlovic V, Levic S, Bugarski B. 2011. An overview of encapsulation technologies for food applications. *Procedia Food Sci.* 1:1806–1815.

173. Oehlke K, Adamiuk M, Behsnilian D, Gräf V, Mayer-Miebach E, Walz E, Greiner R. 2014. Potential bioavailability enhancement of bioactive compounds using food-grade engineered nanomaterials: a review of the existing evidence. *Food Funct*. 5:1341.

174. Khalafi L, Rafiee M. 2013. Cyclodextrin Based Spectral Changes. In Radis-Baptista, G, ed., *Integr. View Mol. Recognit. Toxinology - Anal. Proced. Biomed. Appl*. InTech. doi:10.5772/52824.

175. Job P. 1928. Recherches sur la formation de complexes minéraux en solution et sur leur stabilité. *Ann. Chim*. 9:113–203.

176. Benesi HA, Hildebrand JH. 1949. A Spectrophotometric Investigation of the Interaction of Iodine with Aromatic Hydrocarbons. *J. Am. Chem. Soc*. 71:2703–2707.

177. Astray G, Gonzalez-Barreiro C, Mejuto JC, Rial-Otero R, Simal-Gándara J. 2009. A review on the use of cyclodextrins in foods. *Food Hydrocoll*. 23:1631–1640.

178. Higuchi T, Connors KA. 1965. Phase Solubility Techniques. 4:117–212.

179. Verri WA, Vicentini FTMC, Baracat MM, Georgetti SR, Cardoso RDR, Cunha TM, Ferreira SH, Cunha FQ, Fonseca MJV, Casagrande R. 2012. Flavonoids as Anti-Inflammatory and Analgesic Drugs: Mechanisms of Action and Perspectives in the Development of Pharmaceutical Forms. *Stud. Nat. Prod. Chem*. 36, Elsevier, pp 297–330.

180. Cheirsilp B, Rakmai J. 2017. Inclusion complex formation of cyclodextrin with its guest and their applications. *Biol. Eng. Med*. 2.

181. Ghosh A, Biswas S, Ghosh T. 2011. Preparation and Evaluation of Silymarin β-cyclodextrin Molecular Inclusion Complexes. *J. Young Pharm*. 3:205–210.

182. Yoshii H, Kometani T, Furuta T, Watanabe Y, Linko YY, Linko P. 1998. Formation of inclusion complexes of cycldextrin with ethanol under anhydrous conditions. *Biosci. Biotechnol. Biochem*. 62:2166–2170.

183. Sapkal NP, Kilor VA, Bhursari KP, Daud AS. 2007. Evaluation of some methods for preparing gliclazide-β-cyclodextrin inclusion complexes. *Trop. J. Pharm. Res*. 6:833–840.

184. Kane R, Kuchekar B. 2010. Preparation, physicochemical characterization, dissolution and formulation studies of telmisartan cyclodextrin inclusion complexes. *Asian J. Pharm*. 4:52.

185. Patil JS, Kadam DV, Marapur SC, Kamalapur MV. 2010. Inclusion complex system; a novel technique to improve the solubility and bioavailability of poorly soluble drugs: a review. 2:29–34.

186. Iacovino R, Rapuano F, Caso J, Russo A, Lavorgna M, Russo C, Isidori M, Russo L, Malgieri G, Isernia C. 2013. β-Cyclodextrin Inclusion Complex to Improve Physicochemical Properties of Pipemidic Acid: Characterization and Bioactivity Evaluation. *Int. J. Mol. Sci*. 14:13022–13041.

187. Loh GOK, Tan YTF, Peh K-K. 2016. Enhancement of norfloxacin solubility via inclusion complexation with β-cyclodextrin and its derivative hydroxypropyl-β-cyclodextrin. *Asian J. Pharm. Sci*. 11:536–546.

188. Marques HMC. 2010. A review on cyclodextrin encapsulation of essential oils and volatiles. *Flavour Fragr. J*. 25:313–326.

189. Mangolim CS, Moriwaki C, Nogueira AC, Sato F, Baesso ML, Neto AM, Matioli G. 2014. Curcumin–β-cyclodextrin inclusion complex: Stability, solubility, characterisation by FT-

IR, FT-Raman, X-ray diffraction and photoacoustic spectroscopy, and food application. *Food Chem*. 153:361–370.

190. Jantarat C, Sirathanarun P, Ratanapongsai S, Watcharakan P, Sunyapong S, Wadu A. 2014. Curcumin-Hydroxypropyl-beta-Cyclodextrin Inclusion Complex Preparation Methods: Effect of Common Solvent Evaporation, Freeze Drying, and pH Shift on Solubility and Stability of Curcumin. *Trop. J. Pharm. Res*. 13:1215.

191. Mohan PRK, Sreelakshmi G, Muraleedharan CV, Joseph R. 2012. Water soluble complexes of curcumin with cyclodextrins: Characterization by FT-Raman spectroscopy. *Vib. Spectrosc*. 62:77–84.

192. Martínez-Alonso A, Losada-Barreiro S, Bravo-Díaz C. 2015. Encapsulation and solubilization of the antioxidants gallic acid and ethyl, propyl and butyl gallate with β-cyclodextrin. *J. Mol. Liq*. 210:143–150.

193. Olga G, Styliani C, Ioannis RG. 2015. Coencapsulation of Ferulic and Gallic acid in hp-b-cyclodextrin. *Food Chem*. 185:33–40.

194. Liu B, Zeng J, Chen C, Liu Y, Ma H, Mo H, Liang G. 2016. Interaction of cinnamic acid derivatives with β-cyclodextrin in water: Experimental and molecular modeling studies. *Food Chem*. 194:1156–1163.

195. Kalogeropoulos N, Yannakopoulou K, Gioxari A, Chiou A, Makris DP. 2010. Polyphenol characterization and encapsulation in β-cyclodextrin of a flavonoid-rich Hypericum perforatum (St John's wort) extract. *LWT - Food Sci. Technol*. 43:882–889.

196. Mantegna S, Binello A, Boffa L, Giorgis M, Cena C, Cravotto G. 2012. A one-pot ultrasound-assisted water extraction/cyclodextrin encapsulation of resveratrol from Polygonum cuspidatum. *Food Chem*. 130:746–750.

197. Li H, Meng B, Chai S-H, Liu H, Dai S. 2016. Hyper-crosslinked β-cyclodextrin porous polymer: an adsorption-facilitated molecular catalyst support for transformation of water-soluble aromatic molecules. *Chem Sci*. 7:905–909.

198. Wilson LD, Mohamed MH, Berhaut CL. 2011. Sorption of Aromatic Compounds with Copolymer Sorbent Materials Containing β-Cyclodextrin. *Materials*. 4:1528–1542.

199. Xiaohong LI, Baowei Z, Kun ZHU, Xuekui HAO. 2011. Removal of nitrophenols by adsorption using β-cyclodextrin modified zeolites. *Chin. J. Chem. Eng*. 19:938–943.

200. EFSA Panel on Food Additives and Nutrient Sources added to Food (ANS), Mortensen A, Aguilar F, Crebelli R, Di Domenico A, Dusemund B, Frutos MJ, Galtier P, Gott D, Gundert-Remy U, Leblanc J, Lindtner O, Moldeus P, Mosesso P, Parent-Massin D, Oskarsson A, Stankovic I, Waalkens-Berendsen I, Woutersen RA, Wright M, Younes M, Boon P, Chrysafidis D, Gürtler R, Tobback P, Arcella D, Rincon AM, Lambré C. 2016. Re-evaluation of β-cyclodextrin (E 459) as a food additive. *EFSA J*. 14.

201. Fenyvesi E., Vikmon M, Szente L. 2016. Cyclodextrins in Food Technology and Human Nutrition: Benefits and Limitations. *Crit. Rev. Food Sci. Nutr*. 56:1981–2004.

202. Tiwari G, Tiwari R, Bannerjee S, Bhati L, Pandey S, Pandey P, Sriwastawa B. 2012. Drug delivery systems: An updated review. *Int. J. Pharm. Investig*. 2:2.

203. Uekaji Y, Terao K. 2017. Coenzyme Q10 - gamma cyclodextrin complex is a powerful nutraceutical for anti-aging and health improvements. *Biomed. Res. Clin. Pract*. 2.

204. Saha S, Roy A, Roy K, Roy MN. 2016. Study to explore the mechanism to form inclusion complexes of β-cyclodextrin with vitamin molecules. *Sci. Rep*. 6.

205. Madhavi DL, Kagan DI. 2008. Water dispersible policosanol cyclodextrin complex and method of its production.

206. Ishizu T, Kajitani S, Tsutsumi H, Sato T, Yamamoto H, Hirata C. 2011. Configurational Studies of Complexes of Tea Catechins with Caffeine and Various Cyclodextrins. *Planta Med*. 77:1099–1109.

207. Hatat C, Rambaud AC. 1993. Fate of γ-Cyclodextrin in the Human Intestine.

208. Joint FAO WHO Expert Committee on Food Additives. 2009. *Safety evaluation of certain food additives: [Rome, Italy, from 17 - 26 June 2008]*. World Health Organization, Geneva.

209. Moreira da Silva A. 2009. Cyclodextrins as food additives and ingredients: nutraceutical applications.

210. Szejtli J, Szente L. 2005. Elimination of bitter, disgusting tastes of drugs and foods by cyclodextrins. *Eur. J. Pharm. Biopharm*. 61:115–125.

211. Szente L, Szejtli J. 2004. Cyclodextrins as food ingredients. *Trends Food Sci. Technol*. 15:137–142.

212. Cutrignelli A, Lopedota A, Laquintana V, Franco M, Denora N. 2015. 'Making cosmetics' using cyclodextrins. 10:49–51.

213. Barão CE, Paiva-Martins F, Zanin GM, Moraes FF. 2014. Determination of the inclusion complex constant between oleuropein and cyclodextrins by complexation theory. *J. Incl. Phenom. Macrocycl. Chem*. 78:465–470.

214. Efmorfopoulou E, Rodis P. 2004. Complexation of oleuropein and trans-cinnamic acid with cyclodextrins. *Chem. Nat. Compd*. 40:362–366.

215. Moraes F, Barao C, Zanin G, Paiva-Martins F. Complexation of olive oil antioxidant with cyclodextrins.

216. López-García MÁ, López Ó, Maya I, Fernández-Bolaños JG. 2010. Complexation of hydroxytyrosol with β-cyclodextrins. An efficient photoprotection. *Tetrahedron*. 66:8006–8011.

217. García-Padial M, Martínez-Ohárriz MC, Isasi JR, Vélaz I, Zornoza A. 2013. Complexation of tyrosol with cyclodextrins. *J. Incl. Phenom. Macrocycl. Chem*. 75:241–246.

218. Rescifina A, Chiacchio U, Iannazzo D, Piperno A, Romeo G. 2010. β-Cyclodextrin and Caffeine Complexes with Natural Polyphenols from Olive and Olive Oils: NMR, Thermodynamic, and Molecular Modeling Studies. *J. Agric. Food Chem*. 58:11876–11882.

219. Mourtzinos I, Anastasopoulou E, Petrou A, Grigorakis S, Makris D, Biliaderis CG. 2016. Optimization of a green extraction method for the recovery of polyphenols from olive leaf using cyclodextrins and glycerin as co-solvents. *J. Food Sci. Technol*. 53:3939–3947.

220. Miller MG, Thangthaeng N, Poulose SM, Shukitt-Hale B. 2017. Role of fruits, nuts, and vegetables in maintaining cognitive health. *Exp. Gerontol*. 94:24–28.

221. Rein MJ, Renouf M, Cruz-Hernandez C, Actis-Goretta L, Thakkar SK, da Silva Pinto M. 2013. Bioavailability of bioactive food compounds: a challenging journey to bioefficacy: Bioavailability of bioactive food compounds. *Br. J. Clin. Pharmacol*. 75:588–602.

222. Pandey KB, Rizvi SI. 2009. Plant polyphenols as dietary antioxidants in human health and disease. *Oxid. Med. Cell. Longev.* 2:270–278.

223. Harms H. 2011. Bioavailability and Bioaccessibility as Key Factors in Bioremediation. *Compr. Biotechnol.* Elsevier, pp 83–94. doi:10.1016/B978-0-08-088504-9.00367-6.

224. Domínguez-Avila JA, Wall-Medrano A, Velderrain-Rodríguez GR, Chen C-YO, Salazar-López NJ, Robles-Sánchez M, González-Aguilar GA. 2017. Gastrointestinal interactions, absorption, splanchnic metabolism and pharmacokinetics of orally ingested phenolic compounds. *Food Funct.* 8:15–38.

225. Cilla A, Bosch L, Barberá R, Alegría A. 2017. Effect of processing on the bioaccessibility of bioactive compounds – A review focusing on carotenoids, minerals, ascorbic acid, tocopherols and polyphenols. *J. Food Compos. Anal.* doi:10.1016/j.jfca.2017.01.009.

226. Mosca AC, Chen J. 2016. Food oral management: physiology and objective assessment. *Curr. Opin. Food Sci.* 9:11–20.

227. Chen J. 2009. Food oral processing: A review. *Food Hydrocoll.* 23:1–25.

228. Palafox-Carlos H, Ayala-Zavala JF, González-Aguilar GA. 2011. The Role of Dietary Fiber in the Bioaccessibility and Bioavailability of Fruit and Vegetable Antioxidants. *J. Food Sci.* 76:R6–R15.

229. Ginsburg I, Koren E, Shalish M, Kanner J, Kohen R. 2012. Saliva increases the availability of lipophilic polyphenols as antioxidants and enhances their retention in the oral cavity. *Arch. Oral Biol.* 57:1327–1334.

230. Voigt N, Stein J, Galindo MM, Dunkel A, Raguse J-D, Meyerhof W, Hofmann T, Behrens M. 2014. The role of lipolysis in human orosensory fat perception. *J. Lipid Res.* 55:870–882.

231. Kulkarni BV, Mattes RD. 2014. Lingual lipase activity in the orosensory detection of fat by humans. *AJP Regul. Integr. Comp. Physiol.* 306:R879–R885.

232. Mandel AL, Breslin PAS. 2012. High Endogenous Salivary Amylase Activity Is Associated with Improved Glycemic Homeostasis following Starch Ingestion in Adults. *J. Nutr.* 142:853–858.

233. Woolnough JW, Bird AR, Monro JA, Brennan CS. 2010. The Effect of a Brief Salivary α-Amylase Exposure During Chewing on Subsequent *in vitro* Starch Digestion Curve Profiles. *Int. J. Mol. Sci.* 11:2780–2790.

234. Rossetti D, Yakubov GE, Stokes JR, Williamson A-M, Fuller GG. 2008. Interaction of human whole saliva and astringent dietary compounds investigated by interfacial shear rheology. *Food Hydrocoll.* 22:1068–1078.

235. Baxter NJ, Lilley TH, Haslam E, Williamson MP. 1997. Multiple Interactions between Polyphenols and a Salivary Proline-Rich Protein Repeat Result in Complexation and Precipitation [†]. *Biochemistry (Mosc.).* 36:5566–5577.

236. Ferrer-Gallego R, Soares S, Mateus N, Rivas-Gonzalo J, Escribano-Bailón MT, Freitas V de. 2015. New Anthocyanin–Human Salivary Protein Complexes. *Langmuir.* 31:8392–8401.

237. Genovese A, Caporaso N, Villani V, Paduano A, Sacchi R. 2015. Olive oil phenolic compounds affect the release of aroma compounds. *Food Chem.* 181:284–294.

238. Xiao J, Mao F, Yang F, Zhao Y, Zhang C, Yamamoto K. 2011. Interaction of dietary polyphenols with bovine milk proteins: Molecular structure-affinity relationship and influencing bioactivity aspects. *Mol. Nutr. Food Res*. 55:1637–1645.

239. Dockray GJ. 1999. Topical review. *J. Physiol*. 518:315–324.

240. Drechsler KC, Ferrua MJ. 2016. Modelling the breakdown mechanics of solid foods during gastric digestion. *Food Res. Int*. 88:181–190.

241. Hornbuckle WE, Simpson KW, Tennant BC. 2008. Gastrointestinal Function. *Clin. Biochem. Domest. Anim*. Elsevier, pp 413–457. doi:10.1016/B978-0-12-370491-7.00014-3.

242. Raufman J-P. 2004. Pepsin. *Encycl. Gastroenterol*. Elsevier, pp 147–148. doi:10.1016/B0-12-386860-2/00561-X.

243. Carriere F, Barrowman JA, Verger R, René L. 1993. Secretion and contribution to lipolysis of gastric and pancreatic lipases during a test meal in humans. *Gastroenterology*. 105:876–888.

244. Attri S, Singh N, Singh TR, Goel G. 2017. Effect of *in vitro* gastric and pancreatic digestion on antioxidant potential of fruit juices. *Food Biosci*. 17:1–6.

245. Zhu F, Wang Y-J. 2012. Rheological and thermal properties of rice starch and rutin mixtures. *Food Res. Int*. 49:757–762.

246. Liu C, Ge S, Yang J, Xu Y, Zhao M, Xiong L, Sun Q. 2016. Adsorption mechanism of polyphenols onto starch nanoparticles and enhanced antioxidant activity under adverse conditions. *J. Funct. Foods*. 26:632–644.

247. Cui F, Yang K, Li Y. 2015. Investigate the Binding of Catechins to Trypsin Using Docking and Molecular Dynamics Simulation. In Permyakov, EA, ed., *PLOS ONE*. 10:e0125848.

248. Lamothe S, Azimy N, Bazinet L, Couillard C, Britten M. 2014. Interaction of green tea polyphenols with dairy matrices in a simulated gastrointestinal environment. *Food Funct*. 5:2621–2631.

249. Martinez-Gonzalez AI, Díaz-Sánchez ÁG, Rosa LA de la, Vargas-Requena CL, Bustos-Jaimes I, Alvarez-Parrilla and E. 2017. Polyphenolic Compounds and Digestive Enzymes: *In vitro* Non-Covalent Interactions. *Molecules*. 22:669.

250. Kanner J, Selhub J, Shpaizer A, Rabkin B, Shacham I, Tirosh O. 2017. Redox homeostasis in stomach medium by foods: The Postprandial Oxidative Stress Index (POSI) for balancing nutrition and human health. *Redox Biol*. 12:929–936.

251. De Santis S, Cavalcanti E, Mastronardi M, Jirillo E, Chieppa M. 2015. Nutritional Keys for Intestinal Barrier Modulation. *Front. Immunol*. 6.

252. Sánchez de Medina F, Romero-Calvo I, Mascaraque C, Martínez-Augustin O. 2014. Intestinal Inflammation and Mucosal Barrier Function: *Inflamm. Bowel Dis*. 20:2394–2404.

253. Lea T. 2015. Epithelial Cell Models; General Introduction. In Verhoeckx, K, Cotter, P, López-Expósito, I, Kleiveland, C, Lea, T, Mackie, A, Requena, T, Swiatecka, D and Wichers, H, eds, *Impact Food Bioact. Health Vitro Ex Vivo Models*. Springer International Publishing, Cham, pp 95–102. doi:10.1007/978-3-319-16104-4_9.

254. Boland M. 2016. Human digestion - a processing perspective: Human digestion - a processing perspective. *J. Sci. Food Agric*. 96:2275–2283.

255. Kamiloglu S, Capanoglu E. 2014. *In vitro* gastrointestinal digestion of polyphenols from different molasses (pekmez) and leather (pestil) varieties. *Int. J. Food Sci. Technol.* 49:1027–1039.

256. Stanisavljević N, Samardžić J, Janković T, Šavikin K, Mojsin M, Topalović V, Stevanović M. 2015. Antioxidant and antiproliferative activity of chokeberry juice phenolics during *in vitro* simulated digestion in the presence of food matrix. *Food Chem.* 175:516–522.

257. Li Y-F, Chang Y-Q, Deng J, Li W-X, Jian J, Gao J-S, Wan X, Gao H, Kurihara H, Sun P-H, He R-R. 2016. Prediction and evaluation of the lipase inhibitory activities of tea polyphenols with 3D-QSAR models. *Sci. Rep.* 6.

258. McDougall GJ, Kulkarni NN, Stewart D. 2009. Berry polyphenols inhibit pancreatic lipase activity *in vitro. Food Chem.* 115:193–199.

259. Day AJ, Cañada FJ, Díaz JC, Kroon PA, Mclauchlan R, Faulds CB, Plumb GW, Morgan MR., Williamson G. 2000. Dietary flavonoid and isoflavone glycosides are hydrolysed by the lactase site of lactase phlorizin hydrolase. *FEBS Lett.* 468:166–170.

260. Day AJ, Gee JM, DuPont MS, Johnson IT, Williamson G. 2003. Absorption of quercetin-3-glucoside and quercetin-4′-glucoside in the rat small intestine: the role of lactase phlorizin hydrolase and the sodium-dependent glucose transporter. *Biochem. Pharmacol.* 65:1199–1206.

261. Gonzales GB, Van Camp J, Vissenaekens H, Raes K, Smagghe G, Grootaert C. 2015. Review on the Use of Cell Cultures to Study Metabolism, Transport, and Accumulation of Flavonoids: From Mono-Cultures to Co-Culture Systems: Cell co-cultures for flavonoid research.... *Compr. Rev. Food Sci. Food Saf.* 14:741–754.

262. Roth M, Obaidat A, Hagenbuch B. 2012. OATPs, OATs and OCTs: the organic anion and cation transporters of the SLCO and SLC22A gene superfamilies: OATPs, OATs and OCTs. *Br. J. Pharmacol.* 165:1260–1287.

263. Del Rio D, Rodriguez-Mateos A, Spencer JPE, Tognolini M, Borges G, Crozier A. 2013. Dietary (Poly)phenolics in Human Health: Structures, Bioavailability, and Evidence of Protective Effects Against Chronic Diseases. *Antioxid. Redox Signal.* 18:1818–1892.

264. Denny A, Buttriss J. 2007. *Plant foods and health: focus on plant bioactives : synthesis report no. 4*. European Food Information Resource Consortium (EuroFIR), Norwich.

265. Ménard S, Cerf-Bensussan N, Heyman M. 2010. Multiple facets of intestinal permeability and epithelial handling of dietary antigens. *Mucosal Immunol.* 3:247–259.

266. Hussain S, Sulaiman A, Alhaddad H, Alhadidi Q. 2016. Natural polyphenols: Influence on membrane transporters. *J. Intercult. Ethnopharmacol.* 5:97.

267. Leuthold S, Hagenbuch B, Mohebbi N, Wagner CA, Meier PJ, Stieger B. 2008. Mechanisms of pH-gradient driven transport mediated by organic anion polypeptide transporters. *AJP Cell Physiol.* 296:C570–C582.

268. Liu Z, Hu M. 2007. Natural polyphenol disposition via coupled metabolic pathways. *Expert Opin. Drug Metab. Toxicol.* 3:389–406.

269. Scheepens A, Tan K, Paxton JW. 2010. Improving the oral bioavailability of beneficial polyphenols through designed synergies. *Genes Nutr.* 5:75–87.

270. Gao S, Hu M. 2010. Bioavailability Challenges Associated with Development of Anti-Cancer Phenolics. *Mini Rev. Med. Chem.* 10:550–567.

271. Mukkavilli R, Gundala SR, Yang C, Donthamsetty S, Cantuaria G, Jadhav GR, Vangala S, Reid MD, Aneja R. 2014. Modulation of Cytochrome P450 Metabolism and Transport across Intestinal Epithelial Barrier by Ginger Biophenolics. In Agarwal, R, ed., *PLoS ONE*. 9:e108386.

272. D'Archivio M, Filesi C, Varì R, Scazzocchio B, Masella R. 2010. Bioavailability of the Polyphenols: Status and Controversies. *Int. J. Mol. Sci*. 11:1321–1342.

273. Carbonell-Capella JM, Buniowska M, Barba FJ, Esteve MJ, Frígola A. 2014. Analytical Methods for Determining Bioavailability and Bioaccessibility of Bioactive Compounds from Fruits and Vegetables: A Review: Bioavailability of bioactive compounds…. *Compr. Rev. Food Sci. Food Saf*. 13:155–171.

274. Shangari N, Chan TS, O'Brien PJ. 2005. Sulfation and Glucuronidation of Phenols: Implications in Coenyzme Q Metabolism. *Methods Enzymol*. 400, Elsevier, pp 342–359.

275. Wu B, Kulkarni K, Basu S, Zhang S, Hu M. 2011. First-Pass Metabolism via UDP-Glucuronosyltransferase: a Barrier to Oral Bioavailability of Phenolics. *J. Pharm. Sci*. 100:3655–3681.

276. Janov P, iller M. 2012. Phase II Drug Metabolism. In Paxton, J, ed., *Top. Drug Metab*. InTech. doi:10.5772/29996.

277. Manna C, Galletti P, Maisto G, Cucciolla V, D'Angelo S, Zappia V. 2000. Transport mechanism and metabolism of olive oil hydroxytyrosol in Caco-2 cells. *FEBS Lett*. 470:341–344.

278. Liu W, Feng Q, Li Y, Ye L, Hu M, Liu Z. 2012. Coupling of UDP-glucuronosyltransferases and multidrug resistance-associated proteins is responsible for the intestinal disposition and poor bioavailability of emodin. *Toxicol. Appl. Pharmacol*. 265:316–324.

279. Mazerska Z, Mróz A, Pawłowska M, Augustin E. 2016. The role of glucuronidation in drug resistance. *Pharmacol. Ther*. 159:35–55.

280. Zhang X, Dong D, Wang H, Ma Z, Wang Y, Wu B. 2015. Stable Knock-down of Efflux Transporters Leads to Reduced Glucuronidation in UGT1A1-Overexpressing HeLa Cells: The Evidence for Glucuronidation-Transport Interplay. *Mol. Pharm*. 12:1268–1278.

281. Rodriguez-Proteau R, Mata JE, Miranda CL, Fan Y, Brown JJ, Buhler DR. 2006. Plant polyphenols and multidrug resistance: Effects of dietary flavonoids on drug transporters in Caco-2 and MDCKII-MDR1 cell transport models. *Xenobiotica*. 36:41–58.

282. Bresciani L, Martini D, Mena P, Tassotti M, Calani L, Brigati G, Brighenti F, Holasek S, Malliga D-E, Lamprecht M, Del Rio D. 2017. Absorption Profile of (Poly)Phenolic Compounds after Consumption of Three Food Supplements Containing 36 Different Fruits, Vegetables, and Berries. *Nutrients*. 9:194.

283. Renouf M, Marmet C, Giuffrida F, Lepage M, Barron D, Beaumont M, Williamson G, Dionisi F. 2014. Dose-response plasma appearance of coffee chlorogenic and phenolic acids in adults. *Mol. Nutr. Food Res*. 58:301–309.

284. Tsukagoshi K, Endo T, Kimura O. 2016. Uptake of Hydroxy Derivatives of Benzoic Acid and Cinnamic Acid by Caco-2 cells via Monocarboxylic Acid Transporters. *J. Pharm. Drug Res*. 1:9–18.

285. Boyer J, Brown D, Liu RH. 2005. *In vitro* digestion and lactase treatment influence uptake of quercetin and quercetin glucoside by the Caco-2 cell monolayer. *Nutr. J*. 4.

286. Manach C, Scalbert A, Morand C, Rémésy C, Jiménez L. 2004. Polyphenols: food sources and bioavailability. *Am. J. Clin. Nutr*. 79:727–747.

287. Donovan JL, Manach C, Faulks RM, Kroon PA. 2006. Absorption and Metabolism of Dietary Plant Secondary Metabolites. In Crozier, A, Clifford, MN and Ashihara, H, eds, *Plant Second. Metab*. Blackwell Publishing Ltd, Oxford, UK, pp 303–351. doi:10.1002/9780470988558.ch8.

288. Zhao Z, Egashira Y, Sanada H. 2003. Digestion and Absorption of Ferulic Acid Sugar Esters in Rat Gastrointestinal Tract. *J. Agric. Food Chem*. 51:5534–5539.

289. Truong V-D, McFeeters RF, Thompson RT, Dean LL, Shofran B. 2007. Phenolic Acid Content and Composition in Leaves and Roots of Common Commercial Sweetpotato (Ipomea batatas L.) Cultivars in the United States. *J. Food Sci*. 72:C343–C349.

290. Aguilera Y, Martin-Cabrejas MA, González de Mejia E. 2016. Phenolic compounds in fruits and beverages consumed as part of the mediterranean diet: their role in prevention of chronic diseases. *Phytochem. Rev*. 15:405–423.

291. Parada J, Aguilera JM. 2007. Food Microstructure Affects the Bioavailability of Several Nutrients. *J. Food Sci*. 72:R21–R32.

292. Munin A, Edwards-Lévy F. 2011. Encapsulation of Natural Polyphenolic Compounds; a Review. *Pharmaceutics*. 3:793–829.

293. Robert P, Fredes C. 2015. The Encapsulation of Anthocyanins from Berry-Type Fruits. Trends in Foods. *Molecules*. 20:5875–5888.

294. Zhang L, Cheng H, Zheng C, Dong F, Man S, Dai Y, Yu P. 2016. Structural and release properties of amylose inclusion complexes with ibuprofen. *J. Drug Deliv. Sci. Technol*. 31:101–107.

295. Sengul H, Surek E, Nilufer-Erdil D. 2014. Investigating the effects of food matrix and food components on bioaccessibility of pomegranate (Punica granatum) phenolics and anthocyanins using an in-vitro gastrointestinal digestion model. *Food Res. Int*. 62:1069–1079.

296. Ayelign A, Sabally K. 2013. Determination of chlorogenic acids (CGA) in coffee beans using HPLC. *Am. J. Res. Commun*. 1:78–91.

297. Moon J-K, Yoo HS, Shibamoto T. 2009. Role of Roasting Conditions in the Level of Chlorogenic Acid Content in Coffee Beans: Correlation with Coffee Acidity. *J. Agric. Food Chem*. 57:5365–5369.

298. Chipurura B, Muchuweti M, Manditsera F. 2010. Effects of Thermal Treatment on the Phenolic Content and Antioxidant Activity of Some Vegetables. *Asian J. Clin. Nutr*. 2:93–100.

299. Adetuyi FO, Ibrahim TA. 2014. Effect of Fermentation Time on the Phenolic, Flavonoid and Vitamin C Contents and Antioxidant Activities of Okra (Abelmoschus esculentus) Seeds. *Niger. Food J*. 32:128–137.

300. Nogueira A, Guyot S, Marnet N, Lequéré JM, Drilleau J-F, Wosiacki G. 2008. Effect of alcoholic fermentation in the content of phenolic compounds in cider processing. *Braz. Arch. Biol. Technol*. 51:1025–1032.

301. Roy MK, Takenaka M, Isobe S, Tsushida T. 2007. Antioxidant potential, anti-proliferative activities, and phenolic content in water-soluble fractions of some commonly consumed vegetables: Effects of thermal treatment. *Food Chem*. 103:106–114.

302. Sharma K, Ko EY, Assefa AD, Ha S, Nile SH, Lee ET, Park SW. 2015. Temperature-dependent studies on the total phenolics, flavonoids, antioxidant activities, and sugar content in six onion varieties. *J. Food Drug Anal*. 23:243–252.

303. Vallverdú-Queralt A, Regueiro J, Rinaldi de Alvarenga JF, Torrado X, Lamuela-Raventos RM. 2014. Home Cooking and Phenolics: Effect of Thermal Treatment and Addition of Extra Virgin Olive Oil on the Phenolic Profile of Tomato Sauces. *J. Agric. Food Chem*. 62:3314–3320.

304. Barba FJ, Mariutti LRB, Bragagnolo N, Mercadante AZ, Barbosa-Cánovas GV, Orlien V. 2017. Bioaccessibility of bioactive compounds from fruits and vegetables after thermal and nonthermal processing. *Trends Food Sci. Technol*. doi:10.1016/j.tifs.2017.07.006.

305. Etcheverry P, Grusak MA, Fleige LE. 2012. Application of *in vitro* bioaccessibility and bioavailability methods for calcium, carotenoids, folate, iron, magnesium, polyphenols, zinc, and vitamins B6, B12, D, and E. *Front. Physiol*. 3.

306. Fernández-García E, Carvajal-Lérida I, Pérez-Gálvez A. 2009. *In vitro* bioaccessibility assessment as a prediction tool of nutritional efficiency. *Nutr. Res*. 29:751–760.

307. Liang J, Han B-Z, Nout MJR, Hamer RJ. 2010. *In vitro* solubility of calcium, iron and zinc in relation to phytic acid levels in rice-based consumer products in China. *Int. J. Food Sci. Nutr*. 61:40–51.

308. Gil-Izquierdo A, Zafrilla P, Tomás-Barberán FA. 2002. An *in vitro* method to simulate phenolic compound release from the food matrix in the gastrointestinal tract. *Eur. Food Res. Technol*. 214:155–159.

309. Gleize B, Tourniaire F, Depezay L, Bott R, Nowicki M, Albino L, Lairon D, Kesse-Guyot E, Galan P, Hercberg S, Borel P. 2013. Effect of type of TAG fatty acids on lutein and zeaxanthin bioavailability. *Br. J. Nutr*. 110:1–10.

310. Minekus M, Alminger M, Alvito P, Ballance S, Bohn T, Bourlieu C, Carrière F, Boutrou R, Corredig M, Dupont D, Dufour C, Egger L, Golding M, Karakaya S, Kirkhus B, Le Feunteun S, Lesmes U, Macierzanka A, Mackie A, Marze S, McClements DJ, Ménard O, Recio I, Santos CN, Singh RP, Vegarud GE, Wickham MSJ, Weitschies W, Brodkorb A. 2014. A standardised static *in vitro* digestion method suitable for food – an international consensus. *Food Funct*. 5:1113–1124.

311. Reboul E, Richelle M, Perrot E, Desmoulins-Malezet C, Pirisi V, Borel P. 2006. Bioaccessibility of Carotenoids and Vitamin E from Their Main Dietary Sources. *J. Agric. Food Chem*. 54:8749–8755.

312. Mackie A, Rigby N. 2015. InfoGest Consensus Method. In Verhoeckx, K, Cotter, P, López-Expósito, I, Kleiveland, C, Lea, T, Mackie, A, Requena, T, Swiatecka, D and Wichers, H, eds, *Impact Food Bioact. Health Vitro Ex Vivo Models*. Springer International Publishing, Cham, pp 13–22. doi:10.1007/978-3-319-16104-4_2.

313. Thuenemann EC, Mandalari G, Rich GT, Faulks RM. 2015. Dynamic Gastric Model (DGM). In Verhoeckx, K, Cotter, P, López-Expósito, I, Kleiveland, C, Lea, T, Mackie, A, Requena, T, Swiatecka, D and Wichers, H, eds, *Impact Food Bioact. Health*. Springer International Publishing, Cham, pp 47–59. doi:10.1007/978-3-319-16104-4_6.

314. Wickham MJS, Faulks RM, Mann J, Mandalari G. 2012. The Design, Operation, and Application of a Dynamic Gastric Model. *Dissolution Technol*. 19:15–22.

315. Ménard O, Picque D, Dupont D. 2015. The DIDGI® System. In Verhoeckx, K, Cotter, P, López-Expósito, I, Kleiveland, C, Lea, T, Mackie, A, Requena, T, Swiatecka, D and

Wichers, H, eds, *Impact Food Bioact*. *Health*. Springer International Publishing, Cham, pp 73–81. doi:10.1007/978-3-319-16104-4_8.

316. Miret S. 2004. Comparison of *in vitro* Models for the Prediction of Compound Absorption across the Human Intestinal Mucosa. *J*. *Biomol*. *Screen*. 9:598–606.

317. Sambuy Y, De Angelis I, Ranaldi G, Scarino ML, Stammati A, Zucco F. 2005. The Caco-2 cell line as a model of the intestinal barrier: influence of cell and culture-related factors on Caco-2 cell functional characteristics. *Cell Biol*. *Toxicol*. 21:1–26.

318. Turco L, Catone T, Caloni F, Consiglio ED, Testai E, Stammati A. 2011. Caco-2/TC7 cell line characterization for intestinal absorption: How reliable is this *in vitro* model for the prediction of the oral dose fraction absorbed in human? *Toxicol*. *In vitro*. 25:13–20.

319. Tarko T, Duda-Chodak A, Zajac N. 2013. Digestion and absorption of phenolic compounds assessed by *in vitro* simulation methods. A review. *Rocz. Państw. Zakl. Hig.* 64.

320. Aragonès G, Danesi F, Del Rio D, Mena P. 2017. The importance of studying cell metabolism when testing the bioactivity of phenolic compounds. *Trends Food Sci*. *Technol*. doi:10.1016/j.tifs.2017.02.001.

321. Angelis ID, Turco L. 2011. Caco-2 Cells as a Model for Intestinal Absorption. In Bus, JS, Costa, LG, Hodgson, E, Lawrence, DA and Reed, DJ, eds, *Curr*. *Protoc*. *Toxicol*. John Wiley & Sons, Inc., Hoboken, NJ, USA. doi:10.1002/0471140856.tx2006s47.

322. Martínez-Maqueda D, Miralles B, Recio I. 2015. HT29 Cell Line. In Verhoeckx, K, Cotter, P, López-Expósito, I, Kleiveland, C, Lea, T, Mackie, A, Requena, T, Swiatecka, D and Wichers, H, eds, *Impact Food Bioact*. *Health*. Springer International Publishing, Cham, pp 113–124. doi:10.1007/978-3-319-16104-4_11.

323. Kleiveland CR. 2015. Co-cultivation of Caco-2 and HT-29MTX. In Verhoeckx, K, Cotter, P, López-Expósito, I, Kleiveland, C, Lea, T, Mackie, A, Requena, T, Swiatecka, D and Wichers, H, eds, *Impact Food Bioact*. *Health*. Springer International Publishing, Cham, pp 135–140. doi:10.1007/978-3-319-16104-4_13.

324. Seiquer I, Rueda A, Olalla M, Cabrera-Vique C. 2015. Assessing the bioavailability of polyphenols and antioxidant properties of extra virgin argan oil by simulated digestion and Caco-2 cell assays. Comparative study with extra virgin olive oil. *Food Chem*. 188:496–503.

Chapitre II. Matériels et Méthodes

1   Matériels

1.1   Solvants et réactifs

L'ensemble des réactifs et solvants tilisés au cours des travaux est présenté ci-dessous (Tableau II.1.).

Tableau II.1. Solvants, réactifs et produits utilisés pour les différentes études

Dénomination du produit	CAS	Fournisseur	M(g/mol)
2,2-Diphenyl-1-picryhydrazyl (DPPH)	1898-66-4	Sigma-Aldrich	394,32
Acétate de sodium	204-823-8	Alfa Aesar	136,08
Acétate d'éthyle	141-78-6	Sigma-Aldrich	88,11
Acétonitrile LC/MS	75-05-8	VWR	41,05
Acide 3,4 dihydroxyhydrocinnamique (acide hydrocaféique)	1078-61-1	Sigma-Aldrich	182,17
Acide 3,4 dihydroxyphényl acétique (acide homoprotocatéchuique)	102-32-9	Sigma-Aldrich	168,15
Acide acétique	64-19-7	VWR	60,05
Acide caféique	331-39-5	Sigma-Aldrich	180,16
Acide chlorhydrique 6M	7647-01-0	Fisher	36,46
Acide chlorogénique	327-97-9	Sigma-Aldrich	354,31
Acide cinnamique	140-10-3	Extrasynthèse	148,16
Acide formique	64-18-6	Sigma-Aldrich	46,03
Acide férulique	537-98-4	Extrasynthèse	194,19
Acide *p*-coumarique (acide 4-hydroxycinnamique)	501-98-4	Sarsynthèse	164,16
Acide gallique	149-91-7	Sigma-Aldrich	170,12
Acide homovanillique	306-08-1	Extrasynthèse	182,18
Acide protocatéchuique (acide 3,4-dihydrobenzoïque)	99-50-3	Sigma-Aldrich	154,12
Acide quinique	77-95-2	Fluka	192,17
Acide syringique	530-57-4	Extrasynthèse	198,18
Acide trans-cinnamique	140-10-3	Extrasynthèse	148,16
Acide vanillique	121-34-6	Extrasynthèse	168,15
Alcool homovanillique	2380-78-1	Sigma-Aldrich	168,19
Apigénine	520-36-5	Extrasynthèse	270,24
Apigénine-7-O-glucoside	578-74-5	Extrasynthèse	432,38
β-cyclodextrine	7585-39-9	Roquette	1134,98
Carbonate de sodium	497-19-8	Sigma-Aldrich	105,99
Catéchol	120-80-9	Extrasynthèse	110,12
Célite	61790-53-2	Sigma-Aldrich	60,08
Charbon actif	7440-44-0	Sigma-Aldrich	12,01
DMEM (Milieu Eagle modifié de Dubelcco)	-	ThermoFisher	-
DMSO (Diméthylsulfoxide)	67-68-5	ThermoFisher	78,13
Eau LC/MS	7732-18-5	Fisher	18

Extrait de bile porcine	8008-63-7	Sigma-Aldrich	-
Ethanol 96%	64-17-5	VWR	46,07
Ethanol LC/MS	64-17-5	Sigma-Aldrich	46,07
Folin &Ciocalteu	-	Sigma-Aldrich	-
HBSS (Solution saline équilibrée de Hank)	-	ThermoFisher	-
Hespéridine	520-26-3	Extrasynthèse	610,57
Hexane LC/MS	110-54-3	Sigma-Aldrich	86,18
Hydroxytyrosol	10597-60-1	Sigma-Aldrich	154,16
Lutéoline	491-70-3	Extrasynthèse	286,24
Lutéoline-7-O-glucoside	5373-11-5	Extrasynthèse	448,38
Méthanol LC/MS	67-56-1	Sigma-Aldrich	32
MTT (Méthylthiazolydiphényl-tétrazolium)	57360-69-7	Fisher	335,43
Pancréatine porcine	8049-47-6	Sigma-Aldrich	-
Pepsine	9001-75-6	Sigma-Aldrich	-
PBS (Tampon phosphate salin)	-	ThermoFisher	-
Oleuropéine	32619-42-4	Extrasynthèse	540,53
Rutine	207671-50-9	Sigma-Aldrich	610,52
Sérum Bovin Fétal	-	Biomedia	-
Sulfate de sodium anhydre	7757-82-6	Applichem Panreac	142,04
Taxifolin	480-18-2	Sarsynthèse	304,25
Tyrosol	501-94-0	Extrasynthèse	138,17
Vanillin	121-33-5	Sigma-Aldrich	152,15
Verbascoside	61276-17-3	Extrasynthèse	624,6

1.2 Matériel végétal

Les grignons d'olive utilisés pour ces trois années de thèse proviennent d'une même récolte (2014). Ils sont issus d'olives de la variété Aglandau, cultivés selon les règles de l'agriculture biologique.

Les grignons d'olive (90kg) ont été récoltés au Moulin Castelas, dans les Baux-de-Provence (04, France). Ce moulin est équipé d'un système à centrifugation deux-phases qui permet l'obtention d'un seul sous-produit, les grignons d'olive humides, autrement appelés « alperujo ». Afin de bénéficier d'une haute teneur en composés phénoliques dans les grignons, les olives ont été récoltées et triturées au moulin à la mi-octobre 2014 c'est-à-dire, en début de saison de récolte, les grignons d'olive ont été récupérés ce même jour.

Les grignons d'olive ont été mis dans des sachets hermétiques (contenance 2L) de façon équivalente (300g). L'ensemble a été conservé au congélateur à -18°C avant utilisation.

1.3   Appareillages

1.3.1   Spectrophotomètre UV/Visible

Un spectrophotomètre à barrette de diodes modèle 8453 (Agilent, Germany) équipé d'un support cuve thermostaté Peltier et d'une cuve quartz (parcours optique : 10mm) sous agitation magnétique est utilisé pour l'étude des interactions entre les biophénols et la β-CD ainsi que les dosages des phénols totaux et de l'activité antioxydante. Les coefficients d'extinction molaire des biophénols modèles sont de 1414 $M^{-1}.cm^{-1}$ pour Tyr et de 2568 $M^{-1}.cm^{-1}$ pour HT, mesurés respectivement à 275nm et à 280nm.

1.3.2   Chromatographie et spectrométrie de masse

Un système de chromatographie liquide ultra haute performance (UHPLC) Waters (Waters, USA) couplé à un détecteur « modèle 2996 » à barrettes de photodiodes (Waters, USA) (UHPLC-DAD) muni d'une pompe et d'un contrôleur de gradient « modèle 600 » et une colonne BEH C18 50 x 2,1 mm x 1,7 µm sont utilisés pour l'étude chromatographique de la phase aqueuse des grignons d'olive (autrement appelé « jus »).

Le montage précédent couplé à un spectromètre de masse « modèle esquire 6000 » à ionisation en électrospray (Bruker, USA) (UHPLC-DAD-MS) est utilisé pour l'identification des composés phénoliques du jus et pour les études *in vitro* des digestions et de l'absorption intestinale du jus et de HT.

Les spectres UV obtenus par le détecteur à barrette de photodiode, les temps de rétention couplé aux masses des ions parents et fils de deuxième génération permettent l'identification des principaux composés phénoliques présents dans les grignons d'olive ainsi que des métabolites apparus au cours des études de digestion *in vitro* des composés phénoliques.

1.3.3   Atomisation

Un atomiseur Nano-Spray Dryer B-90 (Büchi, Suisse) longue version (hauteur: 150cm, diamètre: 55cm) équipé d'une membrane vibrante (taille des pores 4-7µm) permettant de réduire la taille des gouttelettes pulvérisées (3-15µm, taille moyenne 5-7µm) est utilisé pour la formation de complexes d'inclusion à l'état solide.

1.3.4   Lyophilisation

Un lyophilisateur ALPHA 1-4 LDplus® (Christ Martin, Allemagne) de capacité 4kg et avec une température de condensateur de -55°C est utilisé pour le séchage d'échantillon et la formation de complexes d'inclusion à l'état solide par sublimation de l'eau.

1.3.5 Microscopie électronique à balayage

Deux microscopes électroniques à balayage (MEB): le modèle FEI XL 30S FEG (Philips, USA) avec un voltage de 1,0kV et le modèle Gemini SEM 500 (Zeiss®, Allemagne) avec un voltage de 3,0kV sont utilisés pour l'étude des structures externes des complexes β-CD-biophénol sous forme solide. Les micrographies sont étudiées par le logiciel Image J.

1.3.6 RMN du solide

Un spectromètre de Résonance Magnétique Nucléaire Avance HD-400 MHz muni d'une sonde commerciale (Bruker, USA) est utilisé pour l'étude des interactions entre les biophénols et la β-CD. Les spectres RMN du ^{13}C en phase solide sont obtenus à une fréquence de résonance ^{13}C de 106 MHz. Les échantillons sont placés dans un rotor en dioxide de zirconium (4mm de diamètre extérieur) tournant à l'angle magique (Magic Angle Spinning, MAS) à une fréquence de 10 kHz.

2 Caractérisation physicochimique des grignons d'olive

2.1 Préparation des échantillons

Les grignons d'olive ont été décongelés avant toutes manipulations. La phase aqueuse des grignons d'olive est obtenue de grignons décongelés (environs 600g) à l'aide d'une presse manuelle. Une maille nylon serrée entoure le tambour et permet une préfiltration du jus. Ce jus de grignons ainsi récupéré est ensuite filtré sur célite. Après avoir été délipidé (100 mL de jus extraits trois fois par 15 mL de *n*-hexane [1], il sert de fraction riche en composés phénoliques pour la suite des travaux.

2.2 Méthodes

2.2.1 pH

Ce paramètre est directement relevé sur la matière fraîche (MF).

2.2.2 Teneur en eau

La teneur en eau des grignons d'olive est déterminée selon la norme AOCS Ja 2a-46 en utilisant un montage Dean-Stark [2]. 100 mL de toluène sont ajoutés à 10g de grignons frais pesées précisément. L'ensemble est chauffé et l'eau de l'échantillon est extraite par distillation. La teneur en eau des grignons d'olive est finalement mesurée dans le réceptacle Dean-Stark gradué et exprimée en pourcentage d'eau dans la matière fraîche, comme suit :

$$Teneur\,en\,eau\,(\%\,MF) = \frac{m_e}{m_f} \times 100$$

Où :

m_e : masse de l'eau (d_{eau} = 1,0) (g).

m_f : masse de la matière fraîche (g).

2.2.3   Teneur en matière sèche

20g de grignons pesés précisément sont séchées à l'étuve à 105°C pendant 24 heures. Les échantillons sont ensuite pesées toutes les 2 heures, après retour à température ambiante dans un dessicateur, jusqu'à obtention d'un ratio m/m inférieur à 10% [3,4]. Les résultats sont exprimés en g de matière sèche pour 100g de matière fraîche :

$$Teneur\,en\,matière\,sèche\,(\%\,MF) = \frac{m_s}{m_f} \times 100$$

Où :

m_s : masse de la matière sèche (g).

m_f : masse de la matière fraîche (g).

2.2.4   Teneur en cendres

La teneur en cendres (matière minérale) est déterminée à partir de grignons préalablement séchés. L'ensemble des échantillons est mis 8 heures à 550°C [5]. Les échantillons sont ensuite pesés toutes les 2 heures, après retour à température ambiante dans un dessicateur, jusqu'à obtention d'un ratio m/m inférieur à 10%. Les cendres sont exprimées en g de cendres pour 100g de grignons frais :

$$Teneur\,en\,cendres\,(\%\,MF) = \frac{m_c}{m_s} \times \%(m_s)$$

Où :

m_c : masse des cendres (g).

m_s : masse de matière sèche (g).

$\%(m_s)$: teneur en matière sèche pour 100g de matière fraîche (%).

2.2.5   Teneur en noyaux et pulpes d'olive

5g de grignons séchés sont tamisés afin de récupérer d'une part les fragments de noyaux et d'autre part les peaux et pulpes d'olive passées au travers du tamis sous forme de poudre. La teneur en noyau est alors exprimée en g de noyau pour 100g de matière fraîche.

$$Teneur\,en\,noyau\,(\%\,MF) = \frac{m_n}{m_s} \times \%(m_s)$$

Où :

m_n : masse noyaux (g).

m_s : masse de la matière sèche (g).

$\%(m_s)$: teneur en matière sèche pour 100g de matière fraîche (%).

La quantité de peau et pulpe d'olive est déterminée comme étant la différence entre la masse de matière sèche initiale et la masse de noyaux d'olive. Elle est exprimée en g de peau et de pulpe pour 100g de grignons frais.

2.2.6 Teneur en huile

La teneur en huile est déterminée selon le protocole standardisé ISO 659 1988. 30g de grignons secs pesés au mg près sont déposés dans une cartouche de cellulose (33 x 100 mm), placée dans la chambre d'extraction d'un montage Soxhlet. L'extraction est réalisée par 200 mL de *n*-hexane contenus dans un ballon de masse connue et est répétée trois fois comme suit : 4 heures, 2 heures et 2 heures. Le *n*-hexane est ensuite évaporé à l'aide d'un évaporateur rotatif. L'huile résiduelle contenue dans les grignons d'olive est exprimée en g d'huile pour 100g de matière fraîche [6].

$$Teneur\,en\,huile\;(\%\,MF) = \frac{m_h}{m_s} \times \%(m_s)$$

Où :
m_h : masse huile (g).
m_s : masse de la matière sèche (g).
$\%(m_s)$: teneur en matière sèche pour 100g de matière fraîche (%).

2.2.7 Extraction des composés phénoliques à l'acétate d'éthyle

L'acétate d'éthyle est un solvant reconnu pour l'extraction des composés phénoliques. 50 mL de jus de grignons délipidé (par 3x15mL de *n*-hexane) et acidifié à pH 2 (par ajout d'acide chlorhydrique 6 M) sont extraits par 50 mL d'acétate d'éthyle pendant 5 minutes à 1000rpm. Après séparation en ampoule à décanter, la phase aqueuse est de nouveau extraite deux fois par 50 mL d'acétate d'éthyle comme précédemment. Les phases organiques sont combinées et séchées sous pression réduite à 40°C à l'évaporateur rotatif [7]. Les résultats sont exprimés en g de composés phénoliques pour 100g de grignons frais. Le résidu sec est repris dans 5 mL de méthanol pour le dosage des phénols totaux.

2.2.8 Dosage des phénols totaux

Le dosage des phénols totaux est réalisé à partir du réactif de Folin-Ciocalteu. Selon le protocole de Box [8], 24 mL du jus de grignons préalablement délipidés sont mélangés à 36 mL de méthanol afin de constituer la fraction méthanol:jus (60:40, v/v). Après homogénéisation à 1000 rpm pendant 5 minutes, l'ensemble est complété par de l'eau distillée à 100 mL, jusqu'au trait de jauge; 5mL de cette solution sont ensuite mélangés à 2,5 mL de réactif de Folin-Ciocalteu dans une fiole de 50mL. Après homogénéisation et trois minutes d'attente,

1 mL d'une solution saturée en carbonate de sodium est additionné et l'ensemble et complété jusqu'au trait de jauge par de l'eau distillée. Après 1 heure à l'obscurité, l'absorbance est mesurée à 750nm.

Afin de pouvoir travailler sur de plus petits volumes, ce protocole a été modifié comme suit : 2,5 mL d'échantillon (jus de grignons d'olive dilué si nécessaire ou solution standard) sont mélangés à 0,125 mL de réactif de Folin-Ciocalteu. Après agitation et 3 minutes d'attente, 0,050 mL de carbonate de sodium sont ajoutés au mélange, agités, et l'ensemble est laissé 1 heure à l'obscurité à température ambiante. La lecture est réalisée à 750 nm.

La concentration en phénols totaux du jus de grignons est déterminée par une courbe d'étalonnage d'acide gallique. Une solution mère (10 mg.L^{-1}) est réalisée dans de l'eau distillée et sert à la réalisation de solutions filles permettant d'établir la gamme étalon. Le même protocole de Box modifié est utilisé.

3 Analyse chromatographique de la phase aqueuse des grignons d'olive

3.1 Préparation des échantillons

Tout échantillon avant injection est filtré sur filtres seringue PTFE 0,45µm puis 0,20µm. Les standards utilisés pour l'identification des composés phénoliques des grignons d'olive et pour les gammes étalon ont été préparés dans une solution méthanol:eau (20:80, v/v).

3.2 Méthodes

3.2.1 Conditions chromatographiques

Pour la séparation des composés phénoliques du jus de grignons d'olive, la phase mobile est constituée d'eau acidifiée (A, 0,5% d'acide formique) et d'acétonitrile (B). Un gradient de débit est utilisé en plus d'un gradient de solvant afin d'optimiser la séparation des composés. Le tableau suivant (II.2.) présente les conditions utilisées pour ces analyses. La détection spectrophotoscopique est faite sur la gamme de 200 à 800 nm avec une résolution de 1,2 nm. Les chromatogrammes sont obtenus à 280 nm et 330 nm, longueurs d'onde caractéristiques des composés phénoliques et des acides cinnamiques respectivement. La température de la colonne est de 35°C et 1 µL d'échantillon est injecté sans dilution.

Les molécules sont fragmentées jusqu'à la deuxième génération. L'énergie d'ionisation est de 50 eV à 100 eV en mode négatif. Le voltage du capillaire est de 2 kV et la température

de la source est de 365°C. Le débit de gaz est de 10 L/min et le voltage du skimmer est de 40 V. Les scans sont réalisés dans une gamme m/z de 100 à 800.

Tableau II.2. Gradient de solvant et de débit pour le dosage des composés phénoliques des grignons d'olive en UHPLC

Temps (min)	% A	% B	Débit (mL/min)
0	99	1	0,3
10	80	20	0,35
12,5	70	30	0,4
13,5	0	100	0,4
14,5	0	100	0,4

3.2.2 Gammes étalons

Selon le même gradient décrit ci-dessus, le dosage des composés phénoliques est réalisé à partir de gamme étalons. 10mg de standards de HT, de Tyr et des acides caféique et *p*-coumarique sont solubilisés dans 10 mL d'une solution méthanol:eau (20:80, v/v). Ces solutions mères servent à la réalisation de différentes courbes d'étalonnage.

4 Etude de la complexation des biophénols modèles par la β-cyclodextrine

4.1 Préparation des échantillons

Tyr et HT ont été choisi comme biophénols modèles des grignons d'olive. Les solutions de β-CD et de ces deux biophénols ont toujours été réalisées dans de l'eau distillée. Pour les études de la stœchiométrie et de la constante d'association, des solutions aqueuses de Tyr (1,0 mM) et de HT (0,5 mM) ont été réalisées dans l'eau. Des solutions aqueuses de β-CD à 0,5 mM et à 1,0 mM ont également été réalisées pour l'étude de la stœchiométrie.

Des solutions aqueuses de β-CD et de Tyr ou HT en concentrations équimolaires (5 mM) ont servi à l'étude de la complexation à l'état solide par atomisation et lyophilisation.

4.2 Méthodes

4.2.1 Méthode de Job

L'étude de la stœchiométrie entre la β-CD et les biophénols modèles est réalisée en solution, selon la méthode spectrophotométrique de Job. Des solutions équimolaires de β-CD et de biophénol (HT ou Tyr) sont mélangées selon un ratio biophénol/β-CD variant de 0,1 à 0,9. Le volume total de 10 mL reste constant ainsi que la concentration totale des solutions, égale à 1,0 mM ou 0,5 mM dans le cas de Tyr et HT respectivement. Après agitation, les différentes solutions sont lues au spectrophotomètre UV dans une cuve quartz de 10mm. Les absorbances

sont relevées à 280 nm pour Tyr et 292 nm pour HT et les variations ΔA sont calculées comme étant la différence entre l'absorbance à la longueur d'onde choisie du composé phénolique avec et sans β-CD. Les résultats sont confrontés au rapport molaire r, défini comme suit :

$$r = \frac{[BP]}{([BP] + [\beta - CD])}$$

Où :
[BP] : concentration en biophénols
[β-CD] : concentration en β-CD

4.2.2   Constante d'association K

La constante d'association K du complexe formé est mesurée à l'état liquide, au moyen du spectrophotomètre UV: les solutions de biophénols modèles de concentration fixe (1,0 mM pour Tyr et 0,5 mM pour HT) sont mélangées à des concentrations croissantes de β-CD (0 à 10mM). L'absorbance de chacune des solutions est lue à 280 nm et 292 nm pour Tyr et HT respectivement. La méthode Benesi-Hildebrand permet d'obtenir une relation linéaire entre la variation d'absorbance et la variable β-CD comme suit :

$$\frac{1}{\Delta A} = \frac{1}{\Delta \varepsilon C K [CD]} + \frac{1}{\Delta \varepsilon C}$$

Où:
$$K = \frac{[BP - CD]}{[AO][CD]}$$

$\Delta A = A - A_0$; avec A_0, l'absorbance du biophénol seul $= \varepsilon_{BP} C$

$\Delta \varepsilon = \varepsilon_{BP-CD} - \varepsilon_{BP}$

4.2.3   Complexation à l'état solide par atomisation

Les solutions (30mL) contenant de façon équimolaire (5 mM) le composé phénolique et la β-CD sont atomisées. La température de gaz en entrée est de 100°C causant une température en tête de 85°C. Le débit d'air est de 100 L/min, le taux de pulvérisation est de 100% et la pression interne est de 35mbar. Le débit d'alimentation moyen est de 0,5 mL/min. Une membrane vibrante dont la taille des pores est de 4μm a été sélectionnée. Les particules fines sont récupérées sous forme d'une poudre sèche grâce à un collecteur de particules électrostatique.

4.2.4   Complexation à l'état solide par lyophilisation

La température usuelle est de -50°C et la pression de 0,06 mBar. Les solutions congelées (30 mL) contenant de façon équimolaire (5 mM) le composé phénolique et la β-CD sont lyophilisées. L'eau est alors éliminée par sublimation.

5   Mise au point d'un nouveau procédé de complexation

5.1   Préparation des échantillons

5.1.1   Complexation de la β-CD à l'état solide avec les biophénols modèles

Pour l'étude sur les biophénols modèles, des solutions aqueuses (Tyr ou HT) de concentration 10 mM ont été réalisées pour avoisiner la concentration en phénols totaux du jus de grignons d'olive. 25 mL de solution sont utilisés pour chaque essai de l'étude du ratio molaire β-CD/biophénol.

Pour l'étude de l'effet de la concentration en biophénols, des solutions de 100mM de Tyr ou HT ont été réalisées. 10 mL de solution concentrée sont utilisés pour chaque essai

5.1.2   Complexation de la β-CD à l'état solide avec le jus de grignons d'olive

La concentration en phénols totaux du jus d'alperujo (grignons d'olive issus de moulin à centrifugation deux phases) a été estimée à 8,7 mM équivalent acide gallique.

Afin d'établir l'impact de la présence des protéines dans le jus de grignons, un échantillon déprotéiné a été préparé. Les protéines du jus sont éliminées par précipitation à l'éthanol 42% v/v. Après filtration et élimination des protéines, l'éthanol est éliminé à l'évaporateur rotatif à 40°C sous pression réduite. La concentration en phénols totaux du jus de grignons d'olive déprotéiné a été estimée à 8,7 mM équivalent acide gallique.

Les jus de grignons natif ou déprotéiné servent à l'étude de l'effet du ratio molaire β-CD/phénols sur l'extraction des composés phénoliques par la β-CD à l'état solide. 25 mL de jus sont utilisés pour chaque essai.

Pour l'étude de l'effet de la concentration en phénols, le jus de grignons d'olive a été concentré à l'évaporateur rotatif sous pression réduite à 35°C. La concentration finale du jus ainsi obtenu a été estimée à 96 mM équivalent acide gallique. 10 mL de solution concentrée sont utilisés pour chaque essai.

5.2   Méthodes

   5.2.1   Influence du ratio molaire β-CD : composés phénoliques

5.2.1.1. Sur les modèles tyrosol et hydroxytyrosol

   A 25 mL de solutions (10 mM) de Tyr ou HT est ajoutée la β-CD est ajoutée pour différents ratios molaires. Ainsi, pour une concentration en biophénol de 10 mM, la β-CD est ajoutée dans les proportions suivantes (Tableau II.3) :

Tableau II.3. Masse de β-CD ajoutée aux solutions modèles (10mM) pour l'étude du ratio molaire

Ratio molaire β-CD:phenol	1:1	3:1	5:1	10:1
m(β-CD) (g)	0,284	0,851	1,419	2,839

   L'ensemble est homogénéisé dans un ballon à 150 rpm à 20°C durant 3 heures. Un prélèvement du surnageant (50 µL) est effectué toutes les dix minutes durant la première heure puis toutes les heures jusqu'à 3 heures après arrêt de l'agitation et décantation du mélange. Ils permettent de faire en temps réel une approximation de la teneur en biophénols restante dans le surnageant par lecture au spectrophotomètre.

   En fin de manipulation, le mélange liquide-solide est filtré sur fritté (porosité 5) et le solide est séché à 35°C pendant 24 heures puis toutes les 2 heures jusqu'à stabilisation de sa masse (ratio m/m inférieur à 10%).

5.2.1.2. Sur le jus de grignons d'olive et le jus de grignons d'olive déprotéiné

   La concentration initiale en biophénols a été estimée à 8,7 mM équivalent acide gallique dans le jus de grignons et le jus exempt de protéine. La β-CD est ajoutée à un volume de 25 mL de jus dans les proportions suivantes (tableau II.4).

Tableau II.4. Masse de β-CD ajoutée aux jus de grignons (8,7mM) pour l'étude du ratio molaire

Ratio molaire β-CD:phenol	1:1	3:1	5:1	10:1
m(β-CD) (g)	0,247	0,742	1,237	2,475

   L'ensemble est homogénéisé dans un ballon à 150 rpm à 20°C durant 3 heures. Un prélèvement du surnageant (50 µL) est effectué toutes les dix minutes durant la première heure puis toutes les heures jusqu'à 3 heures après arrêt de l'agitation et décantation du mélange. Ils permettent de faire en temps réel une approximation de la teneur en phénols totaux restante du surnageant par dosage au réactif de Folin-Ciocalteu.

En fin de manipulation, le mélange liquide-solide est filtré sur fritté (porosité 5) et le solide est séché à 35°C pendant 24 heures puis toutes les 2 heures jusqu'à stabilisation de sa masse (ratio m/m inférieur à 10%).

5.2.2 <u>Influence de la concentration en biophénols</u>

Pour étudier l'impact de la concentration en biophénols sur leur complexation par la β-CD, celle-ci a été fixée à 100 mM pour les biophénols modèles. La concentration du jus de grignons est de 96 mM équivalent acide gallique.

5.2.2.1. Sur les modèles tyrosol et hydroxytyrosol

En accord avec les premiers résultats obtenus sur l'étude du ratio molaire, 10 équivalents molaires de β-CD offrent le meilleur rendement d'extraction des biophénols modèles à partir d'une solution aqueuse. Le ratio molaire 10:1 (β-CD:composés phénoliques) est donc choisi pour l'étude sur les biophénols modèles. Ainsi, 11,35g de β-CD sont ajoutés à 10 mL de solutions modèles concentrées (100 mM).

En fin de manipulation, chaque mélange liquide-solide est filtré sur fritté (porosité 5) et le solide est séché à 35°C pendant 24 heures puis toutes les 2 heures jusqu'à stabilisation de sa masse (ratio m/m inférieur à 10 %).

5.2.2.2. Sur le jus de grignons d'olive

Le ratio molaire 10:1 est donc choisi pour l'étude de l'effet de concentration en composés phénoliques du jus de grignons. Ainsi, 10,90 g de β-CD sont ajoutés à 10 mL de jus concentré (96 mM). En fin de manipulation, le mélange liquide-solide est filtré sur fritté (porosité 5) et le solide est séché à 35°C pendant 24 heures puis toutes les 2 heures jusqu'à stabilisation de sa masse (ratio m/m inférieur à 10 %).

6 Caractérisation des complexes (composé phénolique-β-CD) solides

Les poudres précédemment obtenues par lyophilisation, atomisation ou par une nouvelle méthode liquide-solide ont été caractérisées.

6.1 Préparation des échantillons

Pour les études RMN et MEB, les poudres n'ont pas subi de préparation particulière.

Pour l'étude au spectrophotomètre et en chromatographie, les poudres sont rincées par du méthanol et la solution est filtrée avant analyse.

Pour mesurer l'activité antiradicalaire, le DPPH est initialement solubilisé dans 100 % MeOH pour constituer une solution mère. Une solution fille (60 µM) est réalisée et est constituée d'un mélange méthanol:eau (50:50, v/v) afin d'éviter la précipitation de la β-CD. Des solutions aqueuses de 600 µM de HT sont réalisées à partir de HT standard ou des formes complexées à la β-CD solide.

6.2   Méthodes

6.2.1   Test DPPH

50 µL de solution de HT (600 µM) seul ou complexé à la β-CD sont ajoutés à une solution de DPPH (60 µM, 50% MeOH) de telle sorte que le volume final soit égal à 2 mL.

Les mesures sont réalisées au spectrophotomètre UV contre un blanc constitué à 50 % d'eau et 50 % de méthanol. Seuls les essais sur HT ont été réalisés, le test DPPH n'étant pas adapté au Tyr [9].

La stœchiométrie et l'activité anti-radicalaire (RSA) de HT sont déterminées comme suit :

$$n = \frac{A_0 - A_F}{\varepsilon_{DPPH} C} \qquad\qquad \% \, RSA = \frac{A_0 - A_F}{A_0} \times 100$$

Où:
A_0 = absorbance initial à 515nm (100% DPPH),
A_F = absorbance final à 515 nm,
C = concentration en HT

6.2.2   Calcul du taux de récupération de solide

Le taux de récupération de solide (SR) est défini pour les différentes techniques de séchage (lyophilisation, atomisation) et pour les solides obtenus à partir de notre procédé, basé sur le mélange composé phénolique-β-CD liquide-solide. Il décrit l'efficacité avec laquelle le solide composé de β-CD et de composés phénoliques est récupéré en fin de procédé. Il est exprimé en % de la masse initiale de solide:

$$SR \, (\%) = \frac{m(solide \; récupéré)}{m \, (solide \; initial)} \times 100$$

6.2.3   Calcul de la charge en biophénols et de l'efficacité d'extraction

50 mg de solide sont rincés par 2 mL de méthanol. L'ensemble est soumis aux ultrasons pendant 5 minutes. Après centrifugation (10 minutes, 3000 rpm), la concentration en biophénols de la fraction méthanolique est déterminée par lecture au spectrophotomètre à 275 nm ou

280 nm dans le cas de Tyr et HT respectivement. La concentration en biophénols est alors estimée à partir de leur coefficient d'extinction molaire respectif ($\varepsilon_{(Tyr)}$: 1414 $M^{-1}.cm^{-1}$; $\varepsilon_{(HT)}$: 2568 $M^{-1}.cm^{-1}$). Qe peut être exprimé pour 100 g de β-CD comme suit:

$$Qe = \frac{Cp.Vs}{m} \times 100$$

Avec:
Cp: la concentration en biophenols dans la fraction de rinçage
Vs: le volume de rinçage
m: la masse de solide rincé.

La solution méthanolique de rinçage des poudres issues de l'étude des jus de grignons est soumise au dosage des phénols totaux par le réactif de Folin-Ciocalteu après dilution dans de l'eau distillée.

L'efficacité d'extraction EE est alors déterminé comme étant le pourcentage de composés phénoliques retrouvés dans la totalité du solide récupéré par rapport à la masse initiale de composés phénoliques en solution avant ajout de β-CD,:

$$EE = Qe \times \frac{m(solide\ récupéré)}{Ci.Vi} \ x\ 100$$

Avec:
Ci, concentration initiale en compose phénolique à t_0
Vi volume initiale de la solution phénolique.

6.2.4   Etude des surfaces externes par Microscopie Electronique à Balayage

L'étude des surfaces externes est permise par la microscopie électronique à balayage. Différents grossissements ont été utilisés et aucune analyse n'a nécessité la métallisation superficielle des particules. Les micrographies obtenues sont étudiées par le logiciel Image J. Un minimum de 100 particules est mesuré en utilisant l'échelle micrométrique.

6.2.5   Etude des interactions entre les biophénols et la β-CD par RMN du solide

50mg d'échantillon (poudre sèche) sont placés dans un rotor en dioxide de zirconium (4 mm de diamètre extérieur) tournant à l'angle magique (Magic Angle Spinning, MAS) à une fréquence de 10 kHz. La technique de polarisation croisée (CP) [10] a été appliquée avec une rampe d'impulsion à ^{1}H commençant à 100 % de puissance puis diminuant à 50 % pendant le temps de contact (2 ms) afin d'éviter les inadéquations de Hartmann-Hahn [11,12]. Afin d'améliorer la résolution, une séquence, un découplage dipolaire GT8 de la séquence d'impulsion a été appliqué pendant le temps d'acquisition [13]. Pour obtenir de bons rapports signal-sur-bruit, 1000 spectres ont été accumulés en utilisant un délai de 2,5 secondes.

7 Digestion *in vitro* des composés phénoliques en présence ou non de β-cyclodextrine et étude sur la lignée Caco-2/TC7

Les digestions *in vitro* de HT et des grignons d'olive ont été réalisées à l'équipe Nutrition Obésité et Risque Thrombotique (NORT) de Marseille. L'impact de la β-CD sur le devenir du composé phénolique après un repas modèle a été étudié.

7.1 Préparation des échantillons

L'étude de digestion *in vitro* porte sur HT sous forme de standard ainsi que sur le jus des grignons d'olive, avec ou sans β-CD.

Le complexe HT-β-CD a été réalisé selon le protocole de lyophilisation précédent. Une solution aqueuse (125 mL) contenant de façon équimolaire la β-CD et le biophénol (5 mM) a été préparée puis congelée avant lyophilisation.

Après précipitation des protéines par 42 % d'éthanol (v/v) et élimination du solvant, une partie du jus des grignons (8,7mM équivalent acide gallique) a été réservée et congelée. 300 mL de ce jus sont dilués à 5 mM et 2,962g de β-CD sont ajoutés et l'ensemble est agité avant congélation et lyophilisation.

7.2 Méthodes

7.2.1 Digestion *in vitro*

7 mg de HT sont ajoutés à chaque digestion, qu'il soit sous forme standard, complexé ou apporté par les échantillons de jus de grignons d'olives. Le repas modèle est constitué de 6,7g de pomme de terre cuites en purée, 1,2g de steak haché à 5 % de matière grasse et 200mg d'huile d'olive raffinée (sans polyphénols).

Pour première étape orale, 32 mL de NaCl (0,9%) sont ajoutés au repas modèle. L'ensemble est homogénéisé 10 minutes à 160 va-et-vient/min à 37°C avant broyage à l'Ultra-Turrax® (Ika), 1 minute à 6 000 tours/min, pour mimer la mastication. La salive artificielle (2,5 mL) a ensuite été ajoutée au précédent mélange. L'ensemble est de nouveau homogénéisé à 37°C pendant 10 minutes à 190 rpm.

Pour l'étape gastrique, le pH est ajusté à 4 par addition d'acide chlorhydrique 1M. 2 mL de solution de pepsine (40 g.L^{-1}) sont ajoutés. L'ensemble est incubé à 37°C pendant 30 minutes sous agitation.

Pour l'étape intestinale, le pH est ajusté à 6 par addition de bicarbonate de sodium NAHCO$_3$, puis 9 mL de solution de bile (12 g.L^{-1}) et de pancréatine (3 g.L^{-1}) sont ajoutés ainsi que 4 mL de solution de bile (10 g.L^{-1}). Ce mélange est de nouveau agité à 37°C pendant 30 minutes.

Le mélange total obtenu constitue ce que l'on appelle « le digestat ». Les digestats sont finalement centrifugés à 3000 rpm pendant 1 heure à 10°C. Trois phases sont alors formées : le culot correspondant aux résidus solides, le surnageant, et une fine couche lipidique en surface. Le surnageant est récupéré et successivement filtré sur 0,8 µM et 0,2 µM. Le filtrat ainsi obtenu constitue « la fraction aqueuse ».

A chaque étape de la digestion, des aliquotes sont réalisés et congelé à -80°C pour les futures extractions et analyses. La fraction aqueuse est en partie conservée à -20°C pour la suite de l'étude sur cellules intestinales.

Chaque condition de digestion *in vitro* est répétée quatre fois.

7.2.2   Modèle *in vitro* d'absorption intestinale : les cellules Caco-2 clone TC7

7.2.2.1. *Culture cellulaire*

Les cellules Caco-2 clone TC7 sont issues d'un adénocarcinome colique humain. Elles ont la particularité de se différencier en entérocytes après avoir atteint la confluence. Les cellules sont initialement maintenues en phase de croissance dans des flasques de 25cm^3 avec du milieu complet de type DMEM supplémenté en acides aminés non essentiels (1 %), en antibiotiques (1 %) et en sérum de veau fœtal (16 %). Après que les cellules aient atteint 80 % de confluence, le tapis cellulaire est décollé par une solution de trypsine-EDTA à 0,25 %. Les cellules sont ensuite ensemencées dans chaque puits sur un insert poreux. Ils permettent un accès différentiel aux deux pôles des cellules et maximisent leur différentiation. Les cellules se multiplient durant les 7 premiers jours jusqu'au stade de confluence puis entrent en phase de différenciation durant laquelle les cellules se différencient en cellules de l'épithélium intestinal humain. Les cellules sont utilisées pour les expériences au bout de 21 jours de culture.

7.2.2.2. *Cytotoxicité*

Un test de cytotoxicité des fractions aqueuses récupérées lors des digestions *in vitro* a été effectué au préalable sur des cellules Caco-2 pour évaluer leur viabilité. En effet, la toxicité de cette phase est généralement liée à sa haute concentration en sels biliaires. Ce test est

indispensable avant toute étude d'absorption sur cellules et permet de déterminer la dilution de la fraction aqueuse nécessaire pour ne pas altérer les cellules durant l'expérience.

Le test se réalise sur une plaque de 96 puits contenant dans chacun d'eux des cellules Caco-2/TC7 (12 colonnes de 8 puits). Les fractions aqueuses sont diluées dans le milieu de culture cellulaire utilisé le jour de l'expérience (HBSS) puis 200 µL de fraction aqueuse sont déposés dans chaque puits et les plaques sont incubées pendant 6 heures à 37°C. 200 µL de milieu de culture seul sont déposés dans les puits. A la fin de l'incubation, chaque milieu est remplacé par 200 µL d'une solution de MTT (0,05 g.L^{-1}) et les plaques sont mises à incuber pendant 2 heures. Initialement jaune, les mitochondries encore actives dans les cellules vivantes transforment le MTT en cristaux de formazan, de couleur violet. En fin d'incubation, le milieu est éliminé et remplacé par 100 µL de DMSO pour solubiliser les cellules.

En fin de traitement, les plaques sont finalement lues après agitation sur un lecteur de plaque à 540 nm. La viabilité cellulaire est estimée par rapport à l'absorbance aux cellules témoin mises en contact avec le milieu de culture pur (100% de viabilité cellulaire).

Finalement, un échantillon est considéré cytotoxique lorsque la viabilité cellulaire est inférieure à 80%. La dilution de la fraction aqueuse est choisie comme étant la plus petite dilution permettant une viabilité cellulaire supérieure à 80%.

7.2.2.3. Absorption sur Caco-2/TC7

Ce test est réalisé dans des plaques 6 puits contenant 4 inserts. 2 mL de milieu sans sérum sont déposés du côté basolatéral. La fraction aqueuse est préalablement diluée dans de l'HBSS. 1 mL d'échantillon dilué est alors déposé sur les cellules, côté apical (représente la lumière intestinale). L'absorption cellulaire des composés phénoliques étudiés est mesurée à 2 heures, 4 heures et 6 heures. A ces temps, les milieux apicaux (1 mL) et basolatéraux (2 mL) sont récupérés dans chacun des 4 puits. Les cellules sont rincées dans 1 mL de PBS (tampon phosphate) puis 0,5 mL de PBS sont de nouveau ajoutés sur les cellules et ces dernières sont décollées de la membrane poreuse avec un grattoir et mises dans un eppendorf (Figure II.1). Chaque condition est répétée quatre fois.
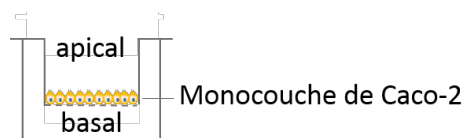

Figure II.1. Puits contenant les cellules Caco-2/TC7

L'ensemble des échantillons est conservé à -80°C avant extraction et analyse.

7.2.3   Extraction des milieux

Les milieux (0,2 mL) de l'étape orale, gastrique et duodénale sont extraits par 0,3mL d'éthanol contenant l'étalon interne. Pour l'étude des composés phénoliques des grignons, l'étalon interne est l'acide gallique. Tyr est l'étalon interne pour les études HT. Deux cents microlitres de *n*-hexane sont ensuite ajouté. L'ensemble est homogénéisé 10 minutes au vortex à la vitesse maximale. Après centrifugation (2500 rpm pendant 10 minutes à 4°C), la phase éthanol:eau est récupérée et le culot est repris dans 0,3 mL d'éthanol pur pour une extraction supplémentaire.

Les deux phases éthanoliques sont réunies et évaporées au Speed-Vac®. Le résidu sec est repris par 0,2mL d'eau.

Concernant les analyses de l'absorption par Caco-2/TC7, les milieux apicaux sont injectés directement. Les milieux basolatéraux (1900µL) sont séchés au Speed-Vac® et le résidu solide est repris dans 80µL d'eau avant injection. Les cellules ont été extraites selon un protocole inspiré de Mateos *et al*. (2011) [14]: après sonication des cellules dans 500 µL de PBS auxquels ont été ajoutés 50 µL d'étalon interne, l'ensemble est centrifugé à 7 000 rpm pendant 10 minutes à 4°C. Le surnageant contenant le contenu cellulaire est récupéré, concentré au Speed-Vac® et repris dans 50µL d'eau avant d'être injecté.

7.2.4   Analyses chromatographiques des milieux

L'analyse des différents milieux a été réalisée en UHPLC-DAD-MS.

7.2.4.1. Etude des grignons d'olive

Le gradient utilisé pour les grignons est le même que celui décrit précédemment (§ 3.2.1.). Le volume d'injection est de 1µL pour les milieux issus de la digestion *in vitro*, 5 µL pour les milieux apicaux, 8 µL pour les milieux basolatéraux et 10 µL pour les milieux cellulaires.

7.2.4.2. Etude de l'hydroxytyrosol

La séparation et la quantification de HT et l'identification de ses métabolites sont permises UHPLC-DAD-MS. Un gradient binaire est utilisé avec l'eau acidifiée (0,5% d'acide formique - A) et l'acétonitrile (B) comme solvant d'élution (tableau II.5).

Tableau II.5. Gradient de solvant et de débit pour le dosage de l'hydroxytyrosol en UHPLC

Temps (min)	% A	% B	Débit (mL/min)
0	99	1	0,3
2,4	70	30	0,3
3	0	100	0,3
3,5	0	100	0,3

La température de colonne est de 35°C. Le volume d'injection est de 1 µL pour les milieux issus de la digestion *in vitro* et 10 µL pour les milieux cellulaires, c'est-à-dire les milieux apicaux, basolatéraux et cellulaires.

7.2.5 Détermination de la bioaccessibilité et de la biodisponibilité

La bioaccessibilité est définie comme le pourcentage de la dose administrée au repas retrouvé dans la fraction aqueuse du digestat. Elle se calcule donc de la façon suivante :

$$\% \, bioaccessibilité = \frac{m(\text{composé cible dans la fraction aqueuse})}{m(\text{composé cible initialement administré})} \, x \, 100$$

L'absorption apparente peut être définie comme le pourcentage de la dose déposé en apical retrouvé dans le milieu basolatéral. Ce paramètre ne tient donc pas compte de la digestion *in vitro* préalable et se calcule comme suit :

$$\% \, absorption \, apprente = \frac{m(\text{composé cible dans le milieu basolatéral})}{m(\text{composé cible déposé en apical})} \, x \, 100$$

La biodisponibilité *in vitro* alors corrigée est définie comme étant le pourcentage de la dose administrée au repas retrouvé dans le milieu basolatéral :

$$\% \, biodisponibilité \, in \, vitro = \frac{m(\text{composé cible dans le milieu basolatéral})}{m(\text{composé cible initialement administré})} \, x \, 100$$

References

1. Suárez M, Romero M-P, Ramo T, Macià A, Motilva M-J. 2009. Methods for Preparing Phenolic Extracts from Olive Cake for Potential Application as Food Antioxidants. J. Agric. Food Chem. 57:1463–1472.

2. Official Method Ja 2a-46. 1989. Moisture. American Oil Chemists' Society, Champaign, IL, USA.

3. Alburquerque J. 2004. Agrochemical characterisation of "alperujo", a solid by-product of the two-phase centrifugation method for olive oil extraction. Bioresour. Technol. 91:195–200.

4. Federici E, Pepi M, Esposito A, Scargetta S, Fidati L, Gasperini S, Cenci G, Altieri R. 2011. Two-phase olive mill waste composting: Community dynamics and functional role of the resident microbiota. Bioresour. Technol. 102:10965–10972.

5. Benavente V, Fullana A. 2015. Torrefaction of olive mill waste. Biomass Bioenergy. 73:186–194.

6. International Organization for Standardization (ISO). 1988. ISO 659-1988 (E). Oilseeds -- Determination of hexane extract (or light petroleum extract), called 'oil content'.

7. Sannino F, De Martino A, Capasso R, El Hadrami I. 2013. Valorisation of organic matter in olive mill wastewaters: Recovery of highly pure hydroxytyrosol. J. Geochem. Explor. 129:34–39.

8. Box J.D. 1983. Determination of Total Phenolic Content in Olive Oil Samples by UV–visible Spectrometry and Multivariate Calibration - Springer. Water Res. 17:511–525.

9. Roche M, Dufour C, Mora N, Dangles O. 2005. Antioxidant activity of olive phenols: mechanistic investigation and characterization of oxidation products by mass spectrometry. Org. Biomol. Chem. 3:423.

10. Schaefer J, Stejskal EO. 1976. Carbon-13 nuclear magnetic resonance of polymers spinning at the magic angle. J. Am. Chem. Soc. 98:1031–1032.

11. Cook RL, Langford CH, Yamdagni R, Preston CM. 1996. A Modified Cross-Polarization Magic Angle Spinning 13 C NMR Procedure for the Study of Humic Materials. Anal. Chem. 68:3979–3986.

12. Peersen OB, Wu XL, Kustanovich I, Smith SO. 1993. Variable-Amplitude Cross-Polarization MAS NMR. J. Magn. Reson. A. 104:334–339.

13. Gerbaud G, Ziarelli F, Caldarelli S. 2003. Increasing the robustness of heteronuclear decoupling in magic-angle sample spinning solid-state NMR. Chem. Phys. Lett. 377:1–5.

14. Mateos R, Pereira-Caro G, Saha S, Cert R, Redondo-Horcajo M, Bravo L, Kroon PA. 2011. Acetylation of hydroxytyrosol enhances its transport across differentiated Caco-2 cell monolayers. Food Chem. 125:865–872.

Chapter III. Characterization of alperujo

.

The olive oil industry is associated with by-products whose quantity and physicochemical parameters are closely correlated with the harvest conditions, the cultivar variety and the olive oil mill system [1,2]. There are mainly two kinds of waste in traditional and three-phase mills, i.e. OMWW and olive pomace. The intensive production of OMWW contributed to the development of a new mill system in order to reduce the quantity of olive mill wastes. This new equipment based on two centrifugations, allows to obtain only one wet by-product composed of vegetation waters and solid olive fragments [3,4]. That two-phase olive pomace is also known as "alperujo".

The olive tree variety influences the composition [5,6]. Researchers observed that the phenolic content in olive oil is closely dependent on the cultivar and the fruit ripening. In particular, phenolic concentration decreases over time [7]. Others showed that the variety and harvest conditions influence the phenolic content and composition of OMWW [8] and olive pomace [9].

In collaboration with Afidol (Association Française Interprofessionnel De l'Olive) and C.T.O. (Centre Technique de l'Olivier), Aglandau has been selected to be the most important local variety (South-East of France) due to its excellent oil extraction yield and its adaptation to the Mediterranean climate [10]. The following results are the characteristics of alperujo from Aglandau variety. It was harvested in the middle of October (2014) to optimize its phenolic content.

1   Physicochemical parameters

Table III.1 shows the physicochemical parameters of alperujo. Many factors such as the plant variety, the harvest localization, the fruit maturity, the agricultural practices and the oil extraction conditions, affect the olive by-products composition and cause the wide ranges of values for each parameter.

Table III.1. Main physicochemical characteristics of alperujo from Aglandau variety

Parameters	Range of values	Results	References
Quantity of alperujo (kg per 100kg of olives)	72.5-85.0	85	[3,11–13]
pH	4.4-6.8	4.94 ± 0.01	[3,14]
Water content (% of FM)	49.6-75.0	69.74 ± 3.87	[3,13,15–19]
Seed (% of FM)	12.0-18.0	14.27 ± 1.04	[3,12,15]
Pulp (% of FM)	10.0-15.0	14.28 ± 1.12	[3]
Dry Matter (% of FM)	30.7-64.1	27.72 ± 1.42	[11,20]
Ash (% of FM)	1.4-4.0	1.05 ± 0.07	[3]

All data are the average of six determinations. FM: fresh matter.

The following analyses concerned the total phenolic content of the alperujo juice obtained after pressing. It was primarily estimated to $2.6g.L^{-1}$ gallic acid equivalent. During the laboratory move (second year of the thesis), a power failure caused the defrosting of all samples. The total phenolic content decreased but the phenolic profile remained similar than before the incident.

So, table III.2 presents the total phenolic content of the alperujo juice after the laboratory move. It has been measured for the juice and for its ethyl acetate extract. This solvent is recognized for its high selectivity for phenolic compounds [21,22].

The total phenolic content in alperujo juice is expressed as mass yield (from the ethyl acetate extraction) or gallic acid equivalent (Folin-Ciocalteu assays). The total phenolic contents of the ethyl acetate extract and the alperujo juice have been estimated at 0.097g/100mL and 0.15g/100mL respectively. Folin-Ciocalteu reagent can also be reduced by non-phenolic reductants, such as proteins or certain sugars which are presents in the alperujo juice that could overestimate its total phenolic content [23,24].

Table III.2. Total phenolic content before and after extracting the alperujo juice using ethyl acetate

Parameters	Range of values	Results	References
Ethyl acetate extraction (% of FM – mass yield)	0.58-1.12[a] 0.12-1.50[b]	0.40 ± 0.01[1] 0.79 ± 0.01[2]	[25,26]
Total phenolic content of the extract (% of FM – g.a.e.)	0.021-0.260[a] 0.01-1.01[b]	0.038 ± 0.003[1] 0.097 ± 0.008[2]	[26–29]
Total phenolic content of the TPOP juice (% of FM – g.a.e.)	0.021-0.260[a] 0.01-1.01[b]	0.062 ± 0.005[1] 0.159 ± 0.013[2]	[19,30–32]

All data are the average of six measurements. FM: fresh matter; g.a.e.: gallic acid equivalent; a: alperujo; b: OMWW; 1: g/100g of fresh matter; 2: g/100mL of fresh matter.

UHPLC analyses have been performed afterwards to profile phenolic compounds from the alperujo juice which is going to be the raw material for our following works.

2 Direct and rapid profiling of biophenols in olive pomace by UHPLC-DAD-MS

Abstract

Olive mill by-products are effluents generated during olive oil production process. The two-phase centrifugation system produces a semi-solid olive pomace called alperujo. This by-product is a combination of liquid and solid wastes derived from the three-phase manufacturing process. A direct and fast analytical method by UHPLC-DAD coupled with ESI/MS-MS has been developed for the profiling of phenolic compounds. Thirty-five metabolites belonging to phenyl alcohols, secoiridoids, flavonoids, and iridoids were identified as the main constituents of alperujo in 12 min, including *p*-coumaroyl aldarate and a verbascoside derivative found for the first time in alperujo and a new ligstroside derivative. Six quantitatively significant components were determined at concentrations ranging from 17.7 mg/L for *p*-coumaric acid to 370.7 mg/L for hydroxytyrosol. Our data confirm that alperujo is an interesting source of phenolic compounds that could be extracted for use as nutraceuticals.

2.1 Introduction

The Mediterranean landscape is since ancient time associated with the culture of olive trees. Today, it is estimated that nearly 98% of the global olive production originates in the Mediterranean basin, among which 73% in Southern Europe with Spain, Italy, and Greece as the main producers [33,34].

The ever-growing olive oil production is correlated with the accumulation of olive mill wastes, and several types of by-products may be generated depending on the process used. Three-phase mills, using large volumes of water to improve the feasibility and the efficiency of oil extraction [4,35], generate two by-products: the olive mill wastewater and a solid waste known as olive pomace composed of olive pulp, skins, and stones. The modern two-phase processing technique, requiring no addition of water during oil extraction, produces the wet olive pomace consisting of vegetation water and solid olive particles [3]. This new process is associated with a lower volume of by-products, thus minimizing the associated environmental impact. However, these by-products are still a major source of pollutants from oil mills, largely because of its phenolic compounds labeled as phytotoxic compounds [36]. On the other hand, alperujo provides a rich source of phenolic compounds (e.g., oleuropein, verbascoside, apigenin-7-glucoside, luteolin-7-glucoside, etc.) known to possess important health-promoting

properties by different mechanisms (antioxidant activity, modulation of a variety of cell signaling pathways) to protect against degenerative diseases [37–39].

The main methods proposed for determination of the phenolic compounds from alperujo include advanced chromatographic techniques coupled to mass spectrometry. Cardoso *et al*. (2005) investigated olive pulp and pomace by-products by electrospray ionization mass spectrometry, allowing the identification of common phenolic compounds and for the first time two oleoside derivatives [40]. Obied *et al*. (2007) achieved high resolution separation of 52 compounds from alperujo extracts in less than 60 min by chemical screening using reversed phase HPLC-diode array detection (RPLC-DAD) and HPLC-electrospray ionization mass spectrometry (RPLC-ESI-MS) [41]. Rubio-Senent *et al*. (2012) identified 26 phenolic compounds in 48 min by HPLC/MS after application of a process based on the hydrothermal treatment of alperujo and subsequent extraction by ethyl acetate [26]. Using the same pretreatment of alperujo, Rubio-Senent *et al*. (2013; 2015) identified also a polymeric phenolic fraction at the end of the separation [29] and were also able to isolate and identify some minor secoiridoids, such as oleuropein derivatives [42]. Besides HPLC-MS, capillary electrophoresis (CE) was also used for alperujo analysis. For instance, after ultrasound-assisted extraction, 20 biophenols were separated and identified in 11 min by CE-DAD [43].

The present study reports a rapid, reliable and efficient analytical method to extract and characterize the wet olive pomace by ultra-high performance liquid chromatography UHPLC-DAD coupled with ESI-MS/MS without any preliminary extraction procedure to preserve both the maximal content and integrity of its phenolic compounds.

2.2   Materials and methods

2.2.1   Chemicals

Alperujo was collected in October 2014 from *Aglandau* olives processed at a two-phase olive oil mill (Moulin Castelas, Baux- de-Provence, France). Samples were immediately frozen and stored at −20°C before chemical analyses. All solvents were of HPLC grade from VWR International (Darmstadt, Germany). *p*-Coumaric acid, caffeic acid, chlorogenic acid, gallic acid, 3,4 dihydroxybenzoic acid, HT, rutin, taxifolin, and vanillin were supplied by Sigma-Aldrich (Deisenhofer, Germany). Quinic acid, (E)-cinnamic acid, ferulic acid, homovanillic acid, syringic acid, vanillic acid, apigenin, luteolin, luteolin-7-O-glucoside, catechol, oleuropein, Tyr, and verbascoside were obtained from Extrasynthèse (Genay, France).

2.2.2 Two-phase olive pomace preparation

Two-phase olive pomace was pressed (Tompress, France) and filtered through celite on a Buchner funnel, then through a 0.2-μm PTFE filter (Alltech Associates, Deerfield, IL) prior to UHPLC analyses.

2.2.3 Two-phase olive pomace characterization in terms of phenolic compounds

2.2.3.1. Chromatographic and mass spectrometric conditions

UHPLC-DAD-MS analyses were performed using an Acquity UHPLC® system (Waters, Milford, MA, USA) linked to both a diode array detector (DAD 200–800 nm, Waters, Milford, MA, USA) and a Bruker Daltonics HCT Ultra Ion Trap Mass Spectrometer equipped with an Electron Spray Ionization (ESI) source operating in negative ion mode. The separation was performed on an Acquity C18 BEH column (1.7 μm, 2.1 × 50 mm). The solvents were (A) water/formic acid (99.5/0.5) and (B) acetonitrile. The gradient was linear, and the proportions of solvent B used were as follows: 0–10 min 1–20%, 10–12 min 20–30%, and 12–14 min 30-100%. The injection volume was 1 μL, and the column temperature was kept at 35 °C. Along the three steps of the gradient, the flow rate was 0.30, 0.35, and 0.40 mL/min. The spectroscopic detection was performed in the range 200–600 nm with a resolution of 1.2 nm. The concentrations of the main phenolic compounds were estimated from calibration curves (peak area vs. concentration) constructed with HT, Tyr, caffeic acid, and *p*-coumaric acid. The quantification of the glucoside forms of HT were undertaken as millimoles of HT equivalent per liter. Limits of detection (LOD) and quantification (LOQ) of these four standards were determined by the signal-to-noise (S/N) evaluations. Low concentrations were injected to attempt a S/N equal to 3 and 10 for LOD and LOQ, respectively (Table III.3). All analyses were run in triplicate.

Table III.3. Calibration curves, limits of detection (LOD) and quantification (LOQ) of standard biophenols

Standard	t_R (min)	λ_{max} (nm)	Calibration line	R	LOD (ng/μL)	LOQ (ng/μL)
HT	2.28	227, 280	$y = 2.093 \times 10^6 x - 1703.36$	0.9998	0.54	1.79
Tyr	3.23	227, 276	$y = 1.907 \times 10^6 x - 2540.69$	0.9996	2.35	7.84
Caffeic acid	4.11	239, 295sh, 324	$y = 2.285 \times 10^6 x - 2128.28$	0.9993	0.23	0.78
p-Coumaric acid	5.50	224, 309	$y = 6.891 \times 10^7 x + 2189.48$	0.9999	0.24	0.80

sh: shoulder; *y*: peak area; *x*: mass in milligrams.

ESI mass spectra were obtained at ionization energies of 50 and 100 eV in negative mode, the capillary voltage was 2 kV, the source temperature was 365°C, the drying gas was

introduced at a flow rate of 10 L/min and the skimmer voltage was 40 V. Scans were performed in the m/z range 100 - 800. Identification of phenolic compounds in samples was performed after standard injection from analysis of retention times, UV-visible spectra, MS molecular peaks and fragments, and comparison with literature data. Tentative identifications of new biophenols were deduced from MS fragmentation.

2.3   Results and discussion

2.3.1   Phenolic profiles in alperujo juice

In our UHPLC–MS method, LC and mass parameters for native alperujo juice have been optimized, such as injection volume of samples, flow rate of mobile phase, peak resolution, mass collision energy and fragmentation voltage. The optimized conditions showed appropriate fragmentation with the detection of the parent ion [M−H]− for all compounds over the 12 min runtime. The analysis of injected standards is summarized in Table III.4.

Table III.4. Retention times (t_R) and UV-visible characteristics of standard biophenols

Standard	t_R(min)	λ_{max} (nm)	
		Standard	Sample
Gallic acid	1.14	229, 271	nd
3,4-Dihydroxybenzoic acid	2.03	258, 294	nd
Hydroxytyrosol	2.28	227, 280	227, 280
Catechol	2.60	276	nd
Tyrosol	3.23	227, 276	224, 276
Chlorogenic acid	3.91	242, 301, 327	244, 296, 327
Vanillic acid	3.95	261, 293	nd
Caffeic acid	4.11	239, 295sh, 324	234, 295sh, 325
Syringic acid	4.49	227, 275	nd
Homovanillic acid	4.59	235, 280	nd
Vanillin	5.04	242, 280, 309	nd
p-Coumaric acid	5.50	224, 309	227, 309
Ferulic acid	6.41	238, 297sh, 324	237, 296sh, 322
Taxifolin	6.88	289	nd
Rutin	7.35	256, 354	nd
Luteolin-7-*O*-glucoside	7.76	255, 349	nd
Verbascoside	8.27	235, 290sh, 331	235, 291sh, 330
Oleuropein	10.38	235, 281	nd
(*E*)-Cinnamic acid	10.96	224, 278	nd
Luteolin	11.13	253, 348	nd

sh: shoulder, *nd:* not detected

Figure III.1 shows a typical chromatographic analysis with detection at 280 nm (total phenols) and 330 nm (hydroxycinnamic acids, flavones and flavonols). Table III.5 summarized

the phenolic compounds identified in the alperujo juice and their UHPLC-DAD-MS characteristics (peak numbering according to elution order).
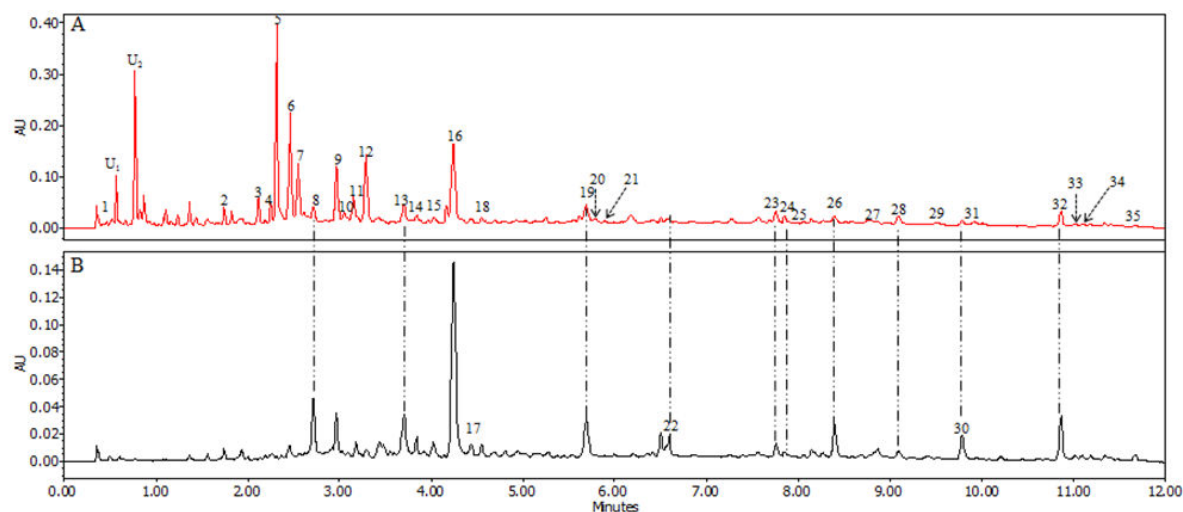
Figure III.1. UHPLC chromatograms of alperujo juice with detection at 280 nm (A) and 330 nm (B)

Table III.5. Retention times, UV-visible and MS data of alperujo phenolic compounds and other metabolites

No.	t_R (min)	Compound	λmax (nm)	m/z	fragments	References
1	0.46	Quinic acid	-	191	173, 127, 111	[44]
U1	0.52	Unknown 1	232, 267	191	173, 127, 111	
U2	0.77	Unknown 2	227, 279	191	173, 127, 111	
2	1.75	Verbascoside - Rha	234, 282, 308	477	459, 367, 161	[45]
3	2.12	Loganic acid glucoside	232, 283	537	375, 331, 179	[46]
4	2.25	Vanillic acid hexoside	254, 293	329	167, 151, 123, 108	
5	2.31	Hydroxytyrosol	227, 280	153		[16,29]
6	2.35	Hydroxytyrosol glucoside 1	231, 277	315	153, 123	[41,44]
7	2.46	Hydroxytyrosol glucoside 2	231, 279	315	153, 123	[41,44]
8	2.55	*p*-Coumaroyl aldarate	313	355	337, 209, 191, 147, 129	First report in olive, [47]
9	2.72	1-β-Glucosyl-acyclo-dihydroelenolic acid	236, 294	407	389, 375, 357, 313, 161	[40,42,44]
10	3.05	Hydroxylated DCMEA derivative	236	199	181, 155, 111	[48,49]
11	3.15	Verbascoside - CA	237, 281	461	315, 297, 161, 135	First report in olive, [50]
12	3.29	Tyrosol	227, 276	137	119	[46,48]
13	3.71	Feruloyl-hexoside	286, 320	401	355, 193	
14	3.73	Caffeoyl-hexoside	239, 286sh, 318	341	179, 135	
15	4.02	Chlorogenic acid	244, 296, 327	353	247, 163, 135, 109	[26]
16	4.24	Caffeic acid (CA)	238, 295sh, 325	179	163, 135	[41,51]
17	4.43	*p*-Coumaroyl-hexoside	240, 325	325	265, 163, 119	
18	4.55	Oleoside	236	389	345, 209, 165	[44,52]

19	5.69	*p*-Coumaric acid	227, 309	163	119	[16,26]
20	5.73	Oleoside deoxyriboside	239, 278	505	389, 345, 121	[46]
21	5.77	Oleuropein aglycone	245, 282	377	197, 153	[29,40,44]
22	6.60	Ferulic acid	237, 296sh, 322	193	149	[41,46]
23	7.75	Luteolin-O-rutinoside	246, 346	593	285	[16,26]
24	7.87	Luteolin-O-rutinoside	244, 346	593	285	[16,26]
25	8.18	Elenolic acid	244	241	209, 165, 139, 127, 121, 101	[22,48]
26	8.39	Verbascoside	235, 291sh, 330	623	461, 477, 315	[22,26]
27	8.82	Tetrahydro-oleuropein	246, 279	543	525, 513	[48]
28	9.17	Nüzhenide	246, 282, 334	685	523, 453, 421, 299	[53,54]
29	9.41	Oleuropein glucoside	250, 279	701	539, 377, 307, 275	[40]
30	9.79	Caffeoyl-6'-secologanoside	225, 290, 327	551	507, 389, 385, 341, 281, 251, 221, 179, 161	[26,41]
31	9.91	10-Hydroxy-DCMO aglycone	243, 281	335	199, 155, 111	[26,49,51,55]
32	10.86	Comselogoside	240, 313	535	491, 389, 345, 307, 265, 163	[29,41]
33	11.02	Oleuroside	244, 282	539	469, 437, 377, 307, 275	[48]
34	11.09	Ligstroside derivative	246, 277	655	517, 361, 291, 259	New compound
35	11.69	Ligstroside isomer	248, 282	523	453, 421, 299	[56]

sh: shoulder, CA : caffeic acid, DCMEA: decarboxymethyl elenolic acid, DCMO: decarboxymethyl oleuropein

The large number of peaks confirmed the complexity of alperujo juice in terms of its phenolic composition. Figure III.2 showed some chemical structures of common secoiridoids identified in alperujo.
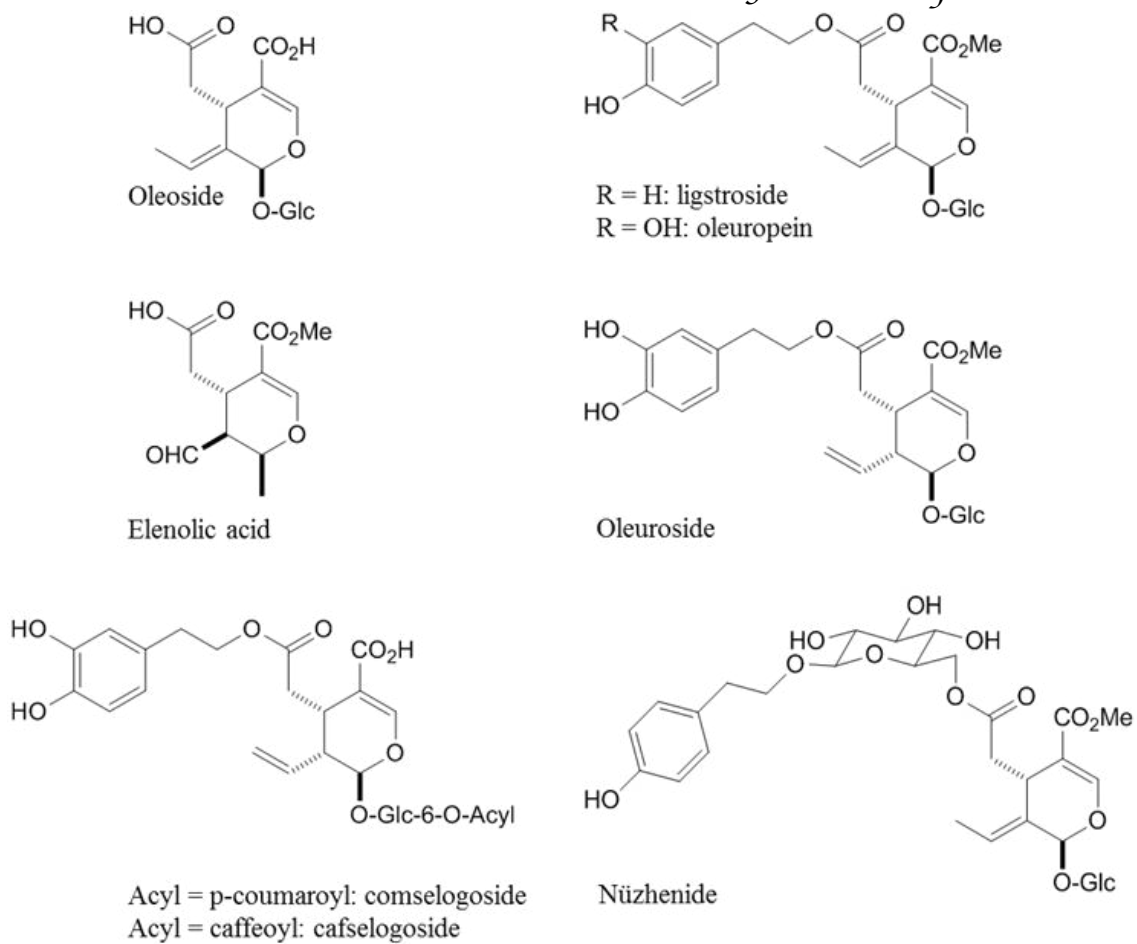
Figure III.2. Chemical structures of common secoiridoids in alperujo

2.3.2   Quinic acid and isomers at m/z = 191

Compound 1 assigned to quinic acid was not detected by DAD at 280 nm but its identity was confirmed by injection of the authentic standard. Two peaks at m/z = 191 and retention times of 0.52 and 0.77 min show the same parent ion and molecular fragments as quinic acid. However, they are detectable by DAD and slightly differ by their UV spectra (Figure III.3). These data did not permit their identification.

A/   Continuous line: Chromatogram (280nm)   C/   Continuous line: quinic acid
      Discontinuous line: EIC m/z 191   Discontinuous line: U_1
                                                          Dotted line: U_2
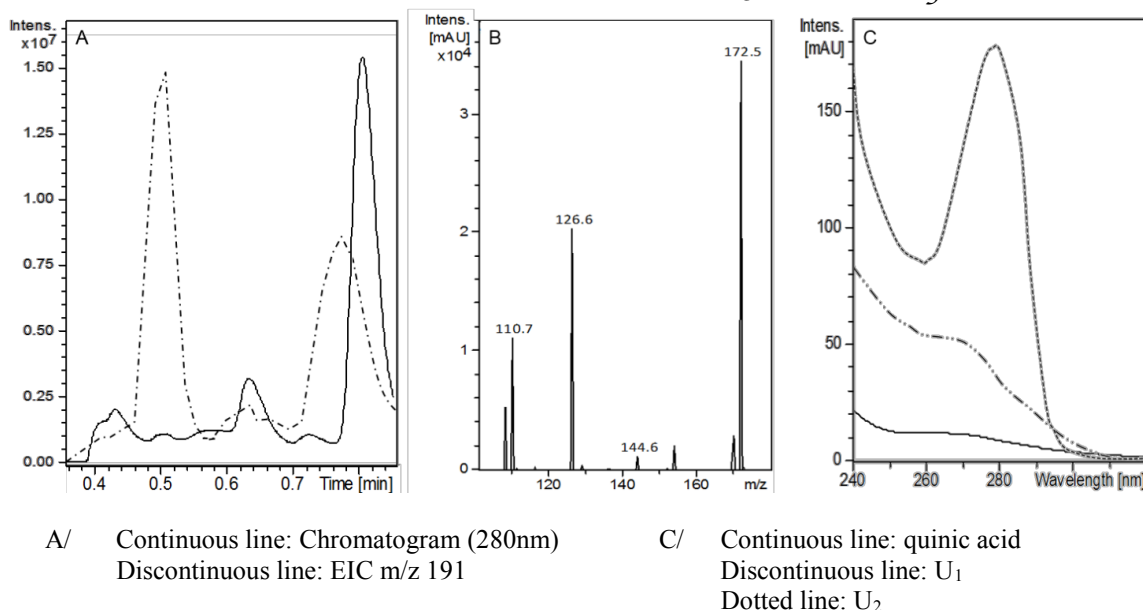
Figure III.3. Extracted ion chromatogram (EIC) at m/z = 191 and chromatogram at 280 nm (A), mass spectrum of quinic acid (B) and UV spectra of compounds at m/z = 191 (C)

2.3.3   Verbascoside and derivatives

Peak 2 displays a molecular ion at m/z = 477 consistent with hydrolysis of the rhamnose residue from verbascoside (m/z = 623) [45]. The ion fragments produced at 459 and 367 correspond to a loss of water and catechol respectively. Peak 11 (m/z = 461) may be identified as the verbascoside derivative formed after hydrolysis of the caffeic acid residue. According to literature, it has never been found in olive pomace but among others in ash (gender: Fraxinus) (Figure III.4) [50]. Its fragments at m/z = 315 and 297 correspond to the successive losses of Rha and H_2O.
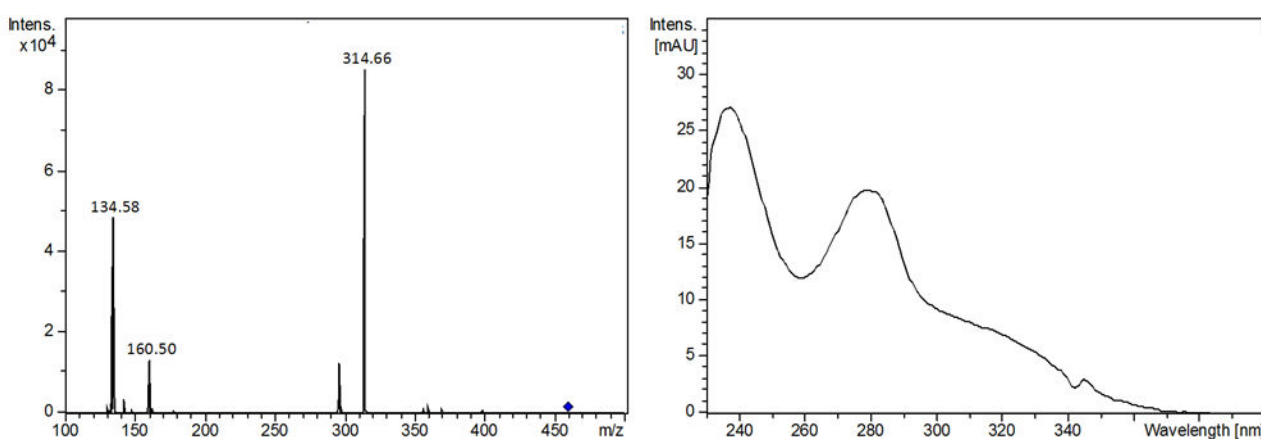
Figure III.4. MS/MS and UV absorption spectra of verbascoside - CA identified in alperujo (compound 11)

2.3.4   Phenolic alcohols and derivatives

In alperujo juice, phenolic alcohols are the main compounds, such as HT (peak 5) at m/z = 153 and its glucosides (peaks 6 and 7) at m/z = 315. HT-Glc are commonly identified in olive mill wastes [16,22] but are generally eluted before HT [38,57]. However, sometimes, the elution order can be reversed [48,52,55,59]. This phenomenon may be due to differences in chromatographic phase, particle shape and particle porosity among the different studies. Peak 12 was identified as Tyr by standard injection, which was confirmed by its molecular ion at m/z = 137. HT generated the most intense UV signal. The high concentrations of Tyr, HT and its glucosides confirm the interest of alperujo juice for applications in the food and cosmetic industries (Table III.6) [28,38].

Table III.6. UHPLC-DAD quantification of major phenolic compounds in alperujo juice (on fresh basis)

Phenolic compound	Content (mg/L)	Content (mM)
Hydroxytyrosol	370.7 ± 5.1	2.40 ± 0.03
Hydroxytyrosol glucoside 1	165.2 ± 1.2	1.07 ± 0.01
Hydroxytyrosol glucoside 2	88.3 ± 1.3	0.57 ± 0.01
Tyrosol	148.4 ± 1.0	1.08 ± 0.01
Caffeic acid	68.0 ± 1.0	0.38 ± 0.01
p-Coumaric acid	17.7 ± 0.5	0.11 ± 0.01

*Expressed as HT equivalent. Values are mean ± standard deviation from triplicate analyses.

2.3.5   Phenolic acids and derivatives

Peak 4 at m/z = 329 is consistent with a vanillic acid hexoside in agreement with its UV spectrum with absorption maxima at 254 and 285 nm and its fragment at m/z = 167 (vanillic acid). Additional fragment ions result from demethylation (-14 Da) and decarboxylation (-44 Da), which is characteristic of vanillic acid fragmentation.

Caffeic acid (peak 16) and *p*-coumaric acid (peak 19) were two of the main phenolic acids identified in alperujo [41]. Some of their hexosides (peaks 14 and 17) were also detected with their typical fragment ions featuring hexose loss and subsequent decarboxylation. The presence of chlorogenic acid (peak 15) and ferulic acid (peak 22) was confirmed by injection of internal standards.

A ferulic acid hexoside (peak 13) was detected as its formic acid ester at m/z = 401 (an artefact due to the use of HCO_2H for elution) and its typical fragment ions at m/z = 355 and

193 featuring the successive losses of formic acid and hexose. Another *p*-coumaric acid derivative was detected at m/z = 355 (peak 8) with its typical UV spectrum and MS fragments at m/z = 337 (loss of water), 209 and 191 (loss of *p*-coumaric acid with or without water addition) (Figure III.5).
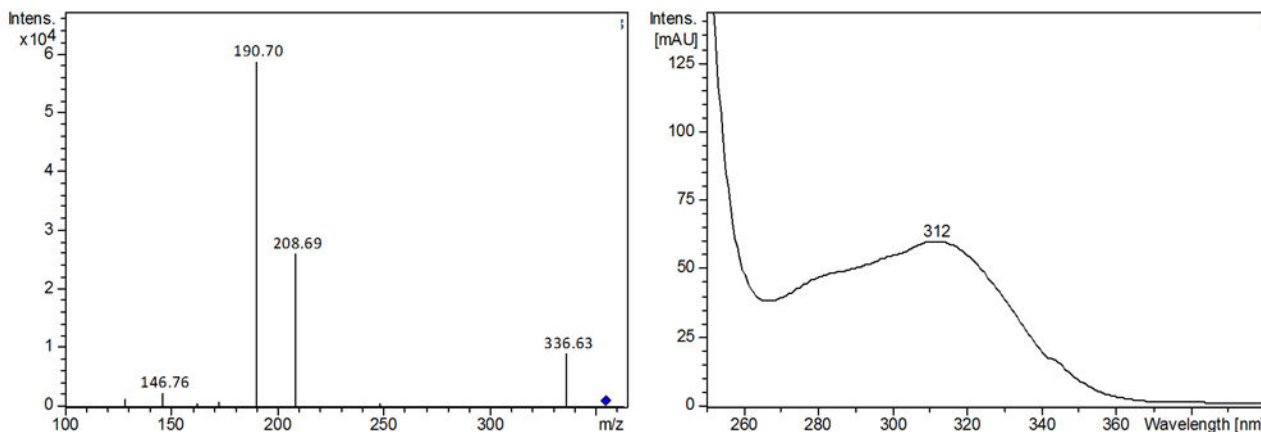
Figure III.5. MS/MS and UV absorption spectra of ρ-coumaroyl aldarate identified in alperujo (compound 8)

A compound with the same characteristics was already found in pineapple and assigned to *p*-coumaroyl aldarate [47]. In this work, it is evidenced for the first time in olive. Peak 30 (m/z = 551), which displays major fragments at m/z = 507 (-CO_2), 389 (loss of a hexose unit) and 179 (caffeic acid) unit, was identified to caffeoyl-6′-secologanoside. Finally, peak 32 was identified as comselogoside, the analog of peak 30 with a *p*-coumaric acid unit [47].

2.3.6   Flavonoids

With their major fragment at m/z = 285 and their UV absorption maxima at 245 and 345 nm, peaks 23 and 24 (m/z = 593) were identified as luteolin derivatives. The loss of 308 Da corresponds to the cleavage of a rutinosyl moiety. Thus, both peaks are proposed to be luteolin-O-rutinoside isomers [16].

2.3.7   Iridoids and derivatives

Iridoids are monoterpenes characterized by a cyclopentane ring. Ring opening leads to the secoiridoid class. Peaks 3, 9, 10, 18, 20, 21, 25, 27, 28, 29, 31, 33, 34 and 35 were identified as iridoid and secoiridoid derivatives. For instance, peak 3 (m/z = 537) is loganic acid glucoside. Its fragments at m/z = 375 and 331 feature hexose loss and subsequent decarboxylation. Peak 25 (m/z = 241) was identified as elenolic acid in agreement with the literature [49]. Peak 9 (m/z = 407, fragments at m/z = 389, 375, 357, 313 and 161) was previously described by several authors [40,44] and recently identified as 1-β-glucopyranosyl acyclodihydroelenolic acid [42].

Peak 10 displays a molecular ion at m/z = 199 and fragment ions at m/z = 181 and 155 that are typical of water loss and decarboxylation. It may be ascribed to a hydroxylated derivative of decarboxymethyl elenolic acid. Peak 18 could be assigned to oleoside with its molecular ion at m/z = 389 and fragment ions at m/z = 345, 209 and 165, respectively due to decarboxylation, glucose elimination and the combination of both. An oleoside deoxyriboside (m/z = 505, peak 20) was also detected [46]. Peak 21 was identified as the oleuropein aglycone (m/z = 377, fragment ions at m/z = 197 and 153 generated by glucose elimination and additional decarboxylation) [29,40,44]. Tetrahydro-oleuropein (peak 27) was detected with its molecular ion at m/z = 543 and its fragment at m/z = 525 (water loss). Peak 28 was ascribed to nüzhenide, an ester of elenolic acid glucoside and Tyr glucoside commonly found in olive seeds. Its molecular peak (m/z = 731) actually corresponds to the formate ester with fragments at m/z = 685 (nüzhenide), 523 (loss of glucose) and 299 (Tyr glucoside after loss of elenolic acid glucoside) [53,54]. The identification of peak 29 (m/z = 701) as oleuropein glucoside was consistent with the literature [40,60]. The hydroxy-decarboxymethyl oleuropein aglycone (peak 31) was also identified by comparison of its UV and mass spectra with literature data [49,51]. Peak 34 (m/z = 655) and peak 35 (m/z = 523) were also detected at the end of the elution. Peak 34 may be a ligstroside derivative as the molecular ion at m/z = 655 generated fragments at m/z = 517 (loss of Tyr), 361 (ligstroside after loss of glucose), 291 (ligstroside after loss of glucose and a $C_3H_2O_2$ moiety) and 259 (ligstroside after loss of $C_3H_2O_2$ and CH_3OH moieties) (Figure III.6). According to our knowledge, this potential ligstroside derivative has never been identified in alperujo juice. Peak 35 displays a molecular peak consistent with ligstroside although its fragments at m/z = 453, 421 and 299 rather suggest that it is an isomer [56]. Finally, peak 33 (m/z = 539) was identified as oleuroside, an oleuropein isomer, with a fragment ion at m/z = 377 consistent with a hexose loss [48,56].
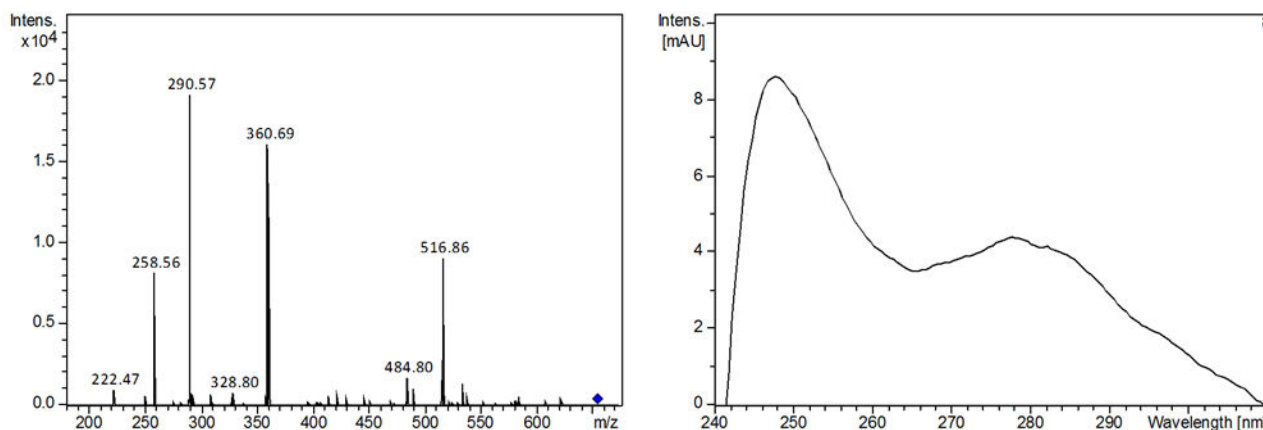
Figure III.6. MS/MS and UV absorption spectra of ligstroside derivative identified in alperujo (compound 34)

2.4   Conclusion

Alperujo juice was analyzed by UHPLC-DAD-MS/MS after a direct injection to preserve the maximal integrity of phenolic compounds and other olive metabolites. Despite the great structural diversity and complexity of alperujo juice, 35 olive metabolites have been separated and identified in only 12 min, including a newly discovered compound (probably a ligstroside derivative) and two compounds so far not reported in olive (*p*-coumaroyl aldarate and a verbascoside derivative). This analytical method confirms the high content of HT and its glucosides in alperujo juice with a total concentration estimated at about 4 mM. This method is simple, fast and effective and can thus be routinely applied in the lab and in the industry to the metabolic profiling of olive juice for the selection of samples according to their biophenol content.

References

1. Breton C.M., Warnock P., Jean A. 2012. Origin and History of the Olive. In Innocenzo Muzzalupo, ed., *Olive Germplasm - Olive Cultiv. Table Olive Olive Oil Ind. Italy*. InTech.

2. Veillet S, Tomao V, Bornard I, Ruiz K, Chemat F. 2009. Chemical changes in virgin olive oils as a function of crushing systems: Stone mill and hammer crusher. *Comptes Rendus Chim*. 12:895–904.

3. Dermeche S., Nadour M., Larroche C., F. Moulti-Mati, Michaud P. 2013. Olive mill wastes: Biochemical characterizations and valorization strategies. *Process Biochem*. 48:1532–1552.

4. Niaounakis M, Halvadakis CP. 2006. *Olive processing waste management literature review and patent survey*. Elsevier, Amsterdam; London.

5. Alcázar Román R., Amarós J.A., Pérez de los Reyes C., García Navarro F.J., Bravo S. 2014. Etude de la teneur en éléments majeurs et en éléments traces dans les feuilles d'olivier. *Olivae*.:1–7.

6. Servili M, Baldioli M, Selvaggini R, Macchioni A, Montedoro G. 1999. Phenolic Compounds of Olive Fruit: One- and Two-Dimensional Nuclear Magnetic Resonance Characterization of Nüzhenide and Its Distribution in the Constitutive Parts of Fruit. *J. Agric. Food Chem*. 47:12–18.

7. Zaringhalami S, Ebrahimi M, Piravi Vanak Z, Ganjloo A. 2015. Effects of cultivar and ripening stage of Iranian olive fruit on bioactive compounds and antioxidant activity of its virgin oil. *Int. Food Res. J*. 22.

8. Sannino F, De Martino A, Capasso R, El Hadrami I. 2013. Valorisation of organic matter in olive mill wastewaters: Recovery of highly pure hydroxytyrosol. *J. Geochem. Explor*. 129:34–39.

9. Leouifoudi I, Harnafi H, Zyad A. 2015. Olive Mill Waste Extracts: Polyphenols Content, Antioxidant, and Antimicrobial Activities. *Adv. Pharmacol. Sci*. 2015:1–11.

10. Conseil Oléicole International. 2012. *Politique-France: Description générale de l'oléiculture en France*.:11.

11. Di Giovacchino L. 2000. Technological aspects. *Handb. Olive Oil*. Springer, pp 17–59.

12. Di Giovacchino L. 2010. *Tecnologie di lavorazione delle olive in frantoio: rese di estrazione e qualità dell'olio*. Tecniche nuove, Milano.

13. Toscano P, Montemurro F. 2012. Olive Mill By-Products Management. In Muzzalupo Innocenzo, ed., *Olive Germplasm - Olive Cultiv. Table Olive Olive Oil Ind. Italy*. InTech.

14. Federici E, Pepi M, Esposito A, Scargetta S, Fidati L, Gasperini S, Cenci G, Altieri R. 2011. Two-phase olive mill waste composting: Community dynamics and functional role of the resident microbiota. *Bioresour. Technol*. 102:10965–10972.

15. Frankel E, Bakhouche A, Lozano-Sánchez J, Segura-Carretero A, Fernández-Gutiérrez A. 2013. Literature Review on Production Process To Obtain Extra Virgin Olive Oil Enriched in Bioactive Compounds. Potential Use of Byproducts as Alternative Sources of Polyphenols. *J. Agric. Food Chem*. 61:5179–5188.

16. Leouifoudi I, Zyad A, Amechrouq A, Oukerrou MA, Mouse HA, Mbarki M. 2014. Identification and characterisation of phenolic compounds extracted from Moroccan olive mill wastewater. *Food Sci. Technol. Camp*. 34:249–257.

17. Perez J, De La Rubia T, Hamman OB, Martinez J. 1998. Phanerochaete flavido-alba laccase induction and modification of manganese peroxidase isoenzyme pattern in decolorized olive oil mill wastewaters. *Appl. Environ. Microbiol*. 64:2726–2729.

18. Roig A, Cayuela ML, Sánchez-Monedero MA. 2006. An overview on olive mill wastes and their valorisation methods. *Waste Manag*. 26:960–969.

19. Vlyssides A., Loizides M, Karlis P. 2004. Integrated strategic approach for reusing olive oil extraction by-products. *J. Clean. Prod*. 12:603–611.

20. Bernal MP, García-Gomez A, Roig A, Paredes C, Cegarra J, Sangiorgi F. 2000. Changes in the composition of the wastes generated by different systems of the olive oil industry. *Proc 9th Intern Conf FAO ESCORENA Netw. Recycl. Agric. Munic. Ind. Residues Agric. RAMIRAN*., pp 220–222.

21. De Marco E, Savarese M, Paduano A, Sacchi R. 2007. Characterization and fractionation of phenolic compounds extracted from olive oil mill wastewaters. *Food Chem*. 104:858–867.

22. Suárez M, Romero M-P, Ramo T, Macià A, Motilva M-J. 2009. Methods for Preparing Phenolic Extracts from Olive Cake for Potential Application as Food Antioxidants. *J. Agric. Food Chem*. 57:1463–1472.

23. Padda MS, Picha DH. 2007. Methodology Optimization for Quantification of Total Phenolics and Individual Phenolic Acids in Sweetpotato (*Ipomoea batatas* L.) Roots. *J. Food Sci*. 72:C412–C416.

24. Georgé S, Brat P, Alter P, Amiot MJ. 2005. Rapid Determination of Polyphenols and Vitamin C in Plant-Derived Products. *J. Agric. Food Chem*. 53:1370–1373.

25. Lama-Muñoz A, Álvarez-Mateos P, Rodríguez-Gutiérrez G, Durán-Barrantes MM, Fernández-Bolaños J. 2014. Biodiesel production from olive–pomace oil of steam-treated alperujo. *Biomass Bioenergy*. 67:443–450.

26. Rubio-Senent F, Rodríguez-Gutíerrez G, Lama-Muñoz A, Fernández-Bolaños J. 2012. New Phenolic Compounds Hydrothermally Extracted from the Olive Oil Byproduct Alperujo and Their Antioxidative Activities. *J. Agric. Food Chem*. 60:1175–1186.

27. Jerman KT, Mozetič VB. 2011. Ultrasonic Extraction of Phenols from Olive Mill Wastewater: Comparison with Conventional Methods. *J. Agric. Food Chem*. 59:12725–12731.

28. Kalogerakis N, Politi M, Foteinis S, Chatzisymeon E, Mantzavinos D. 2013. Recovery of antioxidants from olive mill wastewaters: A viable solution that promotes their overall sustainable management. *J. Environ. Manage*. 128:749–758.

29. Rubio-Senent F, Rodríguez-Gutiérrez G, Lama-Muñoz A, Fernández-Bolaños J. 2013. Phenolic extract obtained from steam-treated olive oil waste: Characterization and antioxidant activity. *LWT - Food Sci. Technol*. 54:114–124.

30. Cioffi G, Pesca MS, De Caprariis P, Braca A, Severino L, De Tommasi N. 2010. Phenolic compounds in olive oil and olive pomace from Cilento (Campania, Italy) and their antioxidant activity. *Food Chem*. 121:105–111.

31. Filidei S, Masciandaro G, Ceccanti B. 2003. Anaerobic digestion of olive oil mill effluents: evaluation of wastewater organic load and phytotoxicity reduction. *Water. Air. Soil Pollut*. 145:79–94.

32. Salgado JM, Abrunhosa L, Venâncio A, Domínguez JM, Belo I. 2014. Screening of winery and olive mill wastes for lignocellulolytic enzyme production from Aspergillus species by solid-state fermentation. *Biomass Convers. Biorefinery*. 4:201–209.

33. Conseil Oléicole International. 2013. - ECONOMIE : 1,5 milliards d'oliviers dans le monde - Olive Info.

34. Ollivier D., Pinatel C., Ollivier V., Artaud J. 2014. Composition en acides gras et en triglycérides d'huiles d'olive vierges de 34 variétés et 8 Appellations d'Origine Françaises et de 2 variétés étrangères implantées en France: Constitution d'une banque de données (1ère partie). *Olivae.*:36–48.

35. Kapellakis IE, Tsagarakis KP, Crowther JC. 2008. Olive oil history, production and by-product management. *Rev. Environ. Sci. Biotechnol*. 7:1–26.

36. Alburquerque JA, Gonzálvez J, García D, Cegarra J. 2006. Measuring detoxification and maturity in compost made from "alperujo", the solid by-product of extracting olive oil by the two-phase centrifugation system. *Chemosphere*. 64:470–477.

37. Giordano E, Dangles O, Rakotomanomana N, Baracchini S, Visioli F. 2015. 3-O-Hydroxytyrosol glucuronide and 4-O-hydroxytyrosol glucuronide reduce endoplasmic reticulum stress *in vitro*. *Food Funct*. 6:3275–3281.

38. Obied HK, Allen MS, Bedgood, DR, Prenzler PD, Robards K. 2005b. Investigation of Australian Olive Mill Waste for Recovery of Biophenols. *J. Agric. Food Chem*. 53:9911–9920.

39. Visioli F, Bernardini E. 2011. Extra virgin olive oil's polyphenols: biological activities. *Curr. Pharm. Des*. 17:786–804.

40. Cardoso SM, Guyot S, Marnet N, Lopes-da-Silva JA, Renard CM, Coimbra MA. 2005. Characterisation of phenolic extracts from olive pulp and olive pomace by electrospray mass spectrometry. *J. Sci. Food Agric*. 85:21–32.

41. Obied HK, Bedgood DR, Prenzler PD, Robards K. 2007. Chemical screening of olive biophenol extracts by hyphenated liquid chromatography. *Anal. Chim. Acta*. 603:176–189.

42. Rubio-Senent F, Martos S, Lama-Muñoz A, Fernández-Bolaños JG, Rodríguez-Gutiérrez G, Fernández-Bolaños J. 2015. Isolation and identification of minor secoiridoids and phenolic components from thermally treated olive oil by-products. *Food Chem*. 187:166–173.

43. Priego-Capote F, Ruiz-Jiménez J, Luque de Castro M. 2004. Fast separation and determination of phenolic compounds by capillary electrophoresis–diode array detection. *J. Chromatogr. A*. 1045:239–246.

44. D'Antuono I, Kontogianni VG, Kotsiou K, Linsalata V, Logrieco AF, Tasioula-Margari M, Cardinali A. 2014. Polyphenolic characterization of olive mill wastewaters, coming from Italian and Greek olive cultivars, after membrane technology. *Food Res. Int*. 65:301–310.

45. Cardinali A, Pati S, Minervini F, D'Antuono I, Linsalata V, Lattanzio V. 2012. Verbascoside, Isoverbascoside, and Their Derivatives Recovered from Olive Mill Wastewater as Possible Food Antioxidants. *J. Agric. Food Chem.* 60:1822–1829.

46. Peralbo-Molina Á, Priego-Capote F, Luque de Castro MD. 2012. Tentative Identification of Phenolic Compounds in Olive Pomace Extracts Using Liquid Chromatography–Tandem Mass Spectrometry with a Quadrupole–Quadrupole-Time-of-Flight Mass Detector. *J. Agric. Food Chem.* 60:11542–11550.

47. Steingass CB, Glock MP, Schweiggert RM, Carle R. 2015. Studies into the phenolic patterns of different tissues of pineapple (*Ananas comosus* [L.] *Merr.*) infructescence by HPLC-DAD-ESI-MS n and GC-MS analysis. *Anal. Bioanal. Chem.* 407:6463–6479.

48. Kanakis P, Termentzi A, Michel T, Gikas E, Halabalaki M, Skaltsounis A-L. 2013. From Olive Drupes to Olive Oil. An HPLC-Orbitrap-based Qualitative and Quantitative Exploration of Olive Key Metabolites. *Planta Med.* 79:1576–1587.

49. Lozano-Sánchez J, Castro-Puyana M, Mendiola J, Segura-Carretero A, Cifuentes A, Ibáez E. 2014. Recovering Bioactive Compounds from Olive Oil Filter Cake by Advanced Extraction Techniques. *Int. J. Mol. Sci.* 15:16270–16283.

50. Sanz M, Simón BF, Cadahía E, Esteruelas E, Muñoz AM, Hernández T, Estrella I, Pinto E. 2012. LC-DAD/ESI-MS/MS study of phenolic compounds in ash (*Fraxinus excelsior* L. and *F. americana* L.) heartwood. Effect of toasting intensity at cooperage: LC-DAD/ESI-MS/MS of ash wood phenolic compounds. *J. Mass Spectrom.* 47:905–918.

51. Suárez M, Macià A, Romero M-P, Motilva M-J. 2008. Improved liquid chromatography tandem mass spectrometry method for the determination of phenolic compounds in virgin olive oil. *J. Chromatogr. A.* 1214:90–99.

52. Bouaziz M, Jemai H, Khabou W, Sayadi S. 2010. Oil content, phenolic profiling and antioxidant potential of Tunisian olive drupes. *J. Sci. Food Agric.* 90:1750–1758.

53. Silva S, Gomes L, Leitao F, Coelho AV, Boas LV. 2006. Phenolic Compounds and Antioxidant Activity of Olea europaea L. Fruits and Leaves. *Food Sci. Technol. Int.* 12:385–395.

54. Silva S, Gomes L, Leitão F, Bronze M, Coelho AV, Boas LV. 2010. Secoiridoids in olive seed: characterization of nüzhenide and 11-methyl oleosides by liquid chromatography with diode array and mass spectrometry. *Grasas Aceites.* 61:157–164.

55. Obied HK, Bedgood DR, Prenzler PD, Robards K. 2007. Bioscreening of Australian olive mill waste extracts: Biophenol content, antioxidant, antimicrobial and molluscicidal activities. *Food Chem. Toxicol.* 45:1238–1248.

56. Cardoso SM, Falcão SI, Peres AM, Domingues MRM. 2011. Oleuropein/ligstroside isomers and their derivatives in Portuguese olive mill wastewaters. *Food Chem.* 129:291–296.

57. El-Abbassi A, Kiai H, Hafidi A. 2012. Phenolic profile and antioxidant activities of olive mill wastewater. Food Chem. 132:406–412.

58. Aranda E, García-Romera I, Ocampo JA, Carbone V, Mari A, Malorni A, Sannino F, De Martino A, Capasso R. 2007. Chemical characterization and effects on *Lepidium sativum* of the native and bioremediated components of dry olive mill residue. Chemosphere. 69:229–239.

59. Savarese M, Demarco E, Sacchi R. 2007. Characterization of phenolic extracts from olives (*Olea europaea* cv. *Pisciottana*) by electrospray ionization mass spectrometry. Food Chem. 105:761–770.

60. Herrero M, Temirzoda TN, Segura-Carretero A, Quirantes R, Plaza M, Ibañez E. 2011. New possibilities for the valorization of olive oil by-products. J. Chromatogr. A. 1218:7511–7520.

Chapter IV. Study of biophenol-β-CD complexes in solution and in the solid state obtained by conventional process

1　Characterization of Hydroxytyrosol-β-cyclodextrin complexes in solution and in the solid state, a potential bioactive ingredient

Abstract

This study focused on characterizing the inclusion complexes between β-CD and HT in aqueous solution and for the first time in the solid state. In aqueous solution, the stoichiometry and association constant were determined by UV-visible spectroscopy. The results showed that HT and β-CD are able to form a 1:1 inclusion complex with an association constant of $33.2 \pm 3.7 \ M^{-1}$. In the solid state, the inclusion complexes prepared by freeze-drying and spray-drying of an equimolar mixture of both partners were characterized and compared by ^{13}C NMR and scanning electron microscopy (SEM). After dissolution, their radical scavenging activity was also determined by UV-visible spectroscopy. The results show that β-CD and drying processes have no effect on the efficiency of HT to reduce the DPPH radical. The solid state ^{13}C CP/MAS NMR data confirm the interactions between β-CD and HT and suggest the formation of inclusion complexes for both drying processes. However, the morphology of the solids obtained was significantly different, as spherical particles were formed by spray-drying while freeze-drying only provided irregular shapes.

1.1　Introduction

Phenolic compounds are the main class of secondary metabolites acting at low concentration in plant defenses against ultraviolet damage or predators. [1,2]. Abundant in fruits and vegetables, phenolic compounds are considered as the major (non-essential) micronutrients in the human diet [3,4]. Their daily consumption provides protection against cardiovascular disease, obesity and diabetes but also against neurodegenerative disorders such as Alzheimer's [5]. The specific benefits of the phenolic compounds typical of olive oil have led the European Food Safety Agency to issue a health claim about the relation between the dietary consumption of HT from olive oil and protection of blood lipids against oxidative damage. [6,7]. The antioxidant activity of phenolic compounds is closely related to their hydroxylation degree [8]. Thus, the catechol unit of HT is responsible for its general electron-donating capacity. This property underlies the ability of HT to scavenge the reactive oxygen species (ROS) involved in oxidative stress [9,10] and also possibly to modulate the expression of genes sensitive to redox regulation. Less fortunately, the catechol group is also responsible for the relatively sensitivity of HT to oxidation during food storage or processing.

To answer the current food industrial demand, olive biophenols, in particular HT, could be used as natural functional food additives or ingredients. However, adequate formulation may be required to increase their chemical stability and preserve their bioactivity. The utilization of encapsulated phenolic compounds, instead of free compounds, can overcome the drawbacks of their instability, but also alleviate unpleasant tastes or flavors, enhance their aqueous solubility and potentially control their release, improve their bioavailability and half-life *in vivo* and *in vitro* [11].

Being recognized as safe for food applications, CDs have been extensively studied as hosts for encapsulation [12,13]. CDs are natural cyclic oligosaccharides consisting of glucopyranose subunits bound through α-(1,4) links. CDs are obtained from the degradation of starch, for example by *Bacillus macerans* [12,14]. Their hydrophobic cavity can accommodate a variety of guest compounds to form inclusion complexes, while their hydrophilic outer surface provides aqueous solubility. Examples of phenolic compounds forming inclusion complexes with CDs in aqueous solution are rosmarinic acid [15], ferulic acid and gallic acid [16,17], resveratrol [18,19] and phenol-rich plant extracts [13,20–22].

With its 7 D-Glc subunits [23], β-CD has been chosen because of its internal diameter of about 6.6 Å, which is consistent with the molecular size of HT. A few works have investigated the β-CD–HT binding in aqueous solution. López-García *et al.* (2010) determined the corresponding binding constant using NMR and studied the protection afforded by β-CD to HT [24]. Rescifina *et al.* (2010) investigated the inclusion complexes of olive phenols with β-CD by NMR and molecular dynamics [25]. Formation of the HT-β-CD complex in solution does not guarantee its existence in the solid state. So far, this topic has not been addressed in the literature.

In this work, the encapsulation of HT into β-CD (Figure IV.1) in aqueous solution and in the solid state was investigated. In solution, the complex was characterized by its stoichiometry and stability constant obtained by UV-visible spectroscopy. Then, HT + β-CD powders were prepared by spray- or freeze-drying and the encapsulation yield and efficiency were assessed. The powders were characterized by solid state ^{13}C CP/MAS NMR. After dissolution, their free radical-scavenging ability was measured by UV-visible spectroscopy according to the DPPH test. Finally, the shape and size of the inclusion complexes in the solid state were determined by SEM.
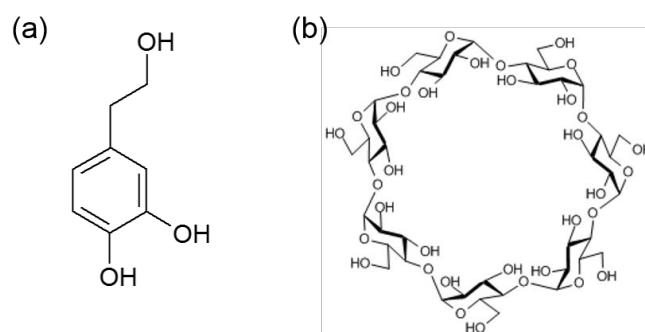
Figure IV.1. Chemical structures of hydroxytyrosol (a) and β-CD (b)

1.2   Materials and methods

1.2.1   Materials

HT was purchased from Extrasynthèse (Genay, France). β-CD was kindly given by Roquette Frères (Lesterm, France). 2,2-diphenyl-1-picrylhydrazyl was supplied from Sigma-Aldrich Co (St Louis, USA) methanol was purchased from Sigma-Aldrich Chimie (Fontenay sous Bois, France), and water was supplied by Fisher Scientific (Leics, UK). Folin-Ciocalteu reagent was purchased from Sigma-Aldrich Chemie GmBH (Buchs, Switzerland).

1.2.2   Spectrophotochemical analysis

UV-visible analyses were recorded using an Agilent 8453 spectrophotometer (Waldbronn, Germany) equipped with a magnetically stirred quartz cell (optical pathlength: 1 cm). The stoichiometry and stability constant of the HT - β-CD complex were calculated from the changes in absorbance monitored at 292 nm.

1.2.3   Preparation of the complexes in the solid state by spray- and freeze-drying

An equimolar aqueous solution of HT and β-CD (final concentration of each = 5 mM) was prepared and filtered through a 0.45 µM syringe filter (VWR International, North America, USA) before the drying processes.

1.2.3.1. Spray-drying conditions

The Nano Spray Dryer B-90 (Büchi, Switzerland) was operated with the long version of the drying chamber (height = 150 cm, diameter = 55 cm) with the following conditions: gas inlet temperature = 100°C (spray head temperature = 85°C), drying gas (air) flow rate = 100 L/min, feed rate = 0.5 mL/min, inside pressure = 35 mbar, spray rate = 100%, spray mesh corresponding to 4 µm size holes. The dried powder was collected from the cylindrical particle-collecting electrode using a particle scraper.

1.2.3.2. Freeze-drying conditions

The freeze-drying was performed using an ALPHA 1-4 LD plus (Christ Martin, Germany). The frozen samples were slowly dried at -50°C under 0.06 mbar.

1.2.3.3. Preparation of the physical mix

Accurately weighed equimolar amounts of HT and β-CD (0.1mmol each) were mixed using a mortar and pestle during 10 min.

1.2.4   Analysis of the inclusion complex in aqueous solution

1.2.4.1. Stoichiometry determination

For the calculation of the stoichiometry, equimolar freshly prepared aqueous solutions of β-CD and HT were mixed in various proportions in volumetric flasks (total volume = 10 mL). Thus, the mole fraction r of HT was varied from 0.1 to 0.9, while the sum of the total host and guest concentrations was held constant at 0.5 mM. The absorbance change δ was then measured and plotted against r (Job's plot).

1.2.4.2. Association constant determination

For the determination of the binding constant K, 0.5 mM aqueous solutions of HT containing β-CD in increasing concentration (0 – 10 mM) were prepared. The absorbance A was measured at 292 nm. The absorbance data were fitted with the Benesi-Hildebrand double reciprocal plot, as follows:

$$\frac{1}{\Delta A} = \frac{1}{\Delta \varepsilon C K [CD]} + \frac{1}{\Delta \varepsilon C}$$

Where:

$$K = \frac{[HT - CD]}{[HT][CD]}$$

C = total HT concentration, $\Delta A = A - A_0$, A_0 = absorbance of HT alone = $\varepsilon_{HT} C$, $\Delta \varepsilon = \varepsilon_{HT\text{-}CD} - \varepsilon_{HT}$

1.2.4.3. Hydrogen abstraction by DPPH

To 2 mL of a freshly prepared 0.06 mM solution of DPPH in MeOH - H_2O (1:1, v/v) was added 0.05 mL of a freshly prepared 0.6 mM solution of HT or HT + β-CD. After 60 min, the spectra were recorded for the determination of the stoichiometry (number of DPPH radicals reduced per HT molecule) and radical scavenging activity (RSA), as follows:

$$n = \frac{A_0 - A_F}{\varepsilon_{DPPH} C} \qquad\qquad \% RSA = \frac{A_0 - A_F}{A_0} \times 100$$

Where A_0 = initial absorbance at 515 nm (100% DPPH), A_F = final absorbance at 515 nm, C = HT concentration

    1.2.5   Analysis of solid inclusion complexes

1.2.5.1. Solid recovery

    Solid recovery (*SR*) of the spray-drying and freeze-drying processes was calculated as follow:

$$\% \, SR = \frac{\text{m}(recovered \ solid)}{\text{m}(initial \ solid)} \times 100$$

1.2.5.2. Extraction efficiency

    The extraction efficiency (*EE*) of the spray-drying and freeze-drying processes was estimated as described by da Rosa *et al*. (2013) [17]: samples of HT + β-CD powder (10 mg) were dissolved in 2 mL MeOH, sonicated for 5 min and centrifuged for 10 min at 3000 rpm. Then, the HT concentration was evaluated by UV-visible spectroscopy. The encapsulation efficiency was finally calculated:

$$\% \, EE \ = \ \frac{Cp \, .Vs}{m \, (dissolved \ solid)} \times \frac{m(recovered \ solid)}{Ci.Vi} \times \, 100$$

Where Cp is the HT concentration in the methanol fraction, Vs is the volume of methanol (2mL), m is the mass of dissolved solid (50 mg), Ci is the initial HT concentration and Vi is the initial HT volume.

1.2.5.3. Solid nuclear magnetic resonance

    The solid-state NMR spectra were obtained on a Bruker AvanceHD-400 MHz NMR spectrometer operating at a ^{13}C resonance frequency of 106 MHz and using a commercial Bruker double-channel probe. About 50 mg of samples were placed in zirconium dioxide rotors of 4-mm outer diameter and spun at a Magic Angle Spinning rate of 10 kHz. The CP technique [26] was applied with a ramped ^{1}H-pulse starting at 100% power and decreasing until 50% during the contact time (2 ms) in order to circumvent Hartmann-Hahn mismatches [27,28].

    To improve the resolution, a dipolar decoupling GT8 pulse sequence [29] was applied during the acquisition time. To obtain a good signal-to-noise ratio in ^{13}C CP/MAS experiment 1K scans were accumulated using a delay of 2.5 s. The proton relaxation time in the rotating frame (^{1}HT1 ρ) was measured by recording the carbon signal as a function of the ^{1}H spin-locking time in the range 0.1 − 15 ms (12 values), before the CP period in ^{13}C CP/MAS experiments. A frequency field of 65 kHz was used for the spin-lock field B1. The recycle delay was 10 s, the number of transients was 1024 and a contact time of only 0.4 ms was selected to minimize ^{1}H spin-diffusion. The carbon spin–lattice relaxation time in the rotating frame (^{13}CT1ρ) was measured using a standard CP pulse sequence with 0.4 ms contact time, proton

spin-locking interruption from 0.1 to 20 ms (16 values) over the cross-polarization period, and 10 s recycle delay. The chemical shifts were referenced to tetramethylsilane and calibrated with glycine carbonyl signal, set at 176.5 ppm.

1.2.5.4. Scanning electron microscopy (SEM) and size distribution

The outer structures of spray-dried and freeze-dried HT + β-CD particles were investigated by SEM using a Philips XL30 FEG at a 1 kV voltage. The microstructure was not coated and observed at different extensions. The spray-dried particle diameters were estimated by image analysis. The Image J software (an open source image processing program) was used and a minimum of 100 particles were measured using a calibrated micrometric scale. To ensure a good particle size distribution, size classes were selected each 0.2 μm from 0 to 3.4 μm.

1.3   Results and discussion

1.3.1   Stoichiometry and association constant determination

β-CD does not absorb the UV light but induces small changes in the UV spectrum of HT (i.e. bathochromic and hyperchromic shifts) that were ascribed to encapsulation. These absorbance changes as a function of β-CD concentration were used for the calculation of the stoichiometry and binding constant of the β-CD – HT complex. For the stoichiometry, the method of continuous variation, known as job's plot, was used. ΔA.[HT] was plotted against the mole fraction of HT (r) ranging from 0.1 to 0.9 (Figure IV.2). A symmetrical curve with a maximum at $r = 0.5$ evidenced the formation of a complex having a 1:1 stoichiometry in accordance with literature data [24].
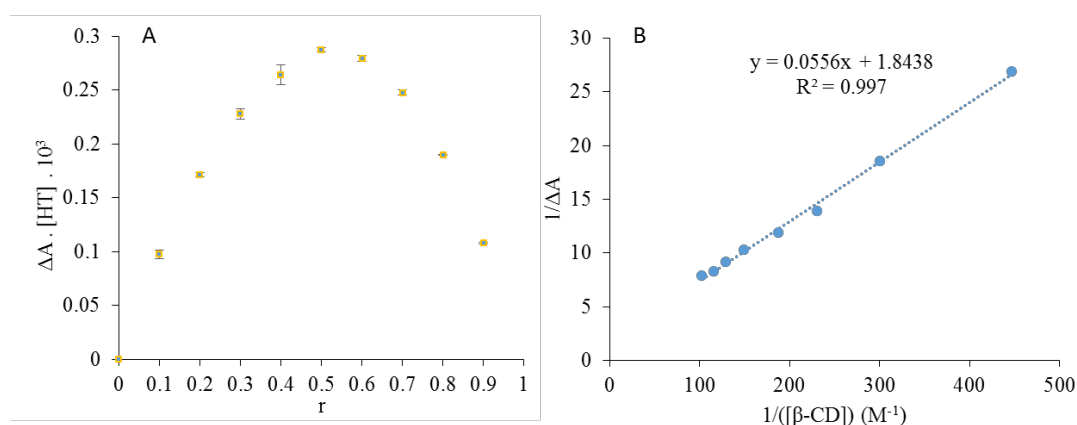
Figure IV.2. Job's plot (A) and Benesi-Hildebrand method (B) for the stoichiometry and the binding constant determination

Figure IV.2 also presents the linear Benesi-Hildebrand plot for the determination of the binding constant, which is simply deduced from the intercept/slope ratio: $K = 33.2 \ (\pm \ 3.7) \ M^{-1}$. Using NMR, López-García *et al*. (2010) obtained a close value of 43 ($\pm$ 1) M^{-1} [24].

1.3.2   Solid recovery and extraction efficiency

Spray- and freeze-drying processes were used to recover the HT - β-CD complexes as powders from aqueous solutions. Spray-drying is a fast thermal process whereas freeze-drying is a cold process requiring much more time. As shown in table IV.1, the latter provided better yields. Indeed, the spray-drying solid recovery was almost twice lower because only part of the powder was sent to the electrostatic receiver and actually recovered, while the rest remained on the top of the walls of the drying chamber and thus was lost. These results are in accordance with the literature. For instance, Wilkowska *et al*. (2016) prepared blueberry juice polyphenols encapsulated in β-CD by freeze-drying with a 82% production yield while Nunes *et al*. (2007) using spray-drying only obtained a 51% production yield of encapsulated lycopene [30,31].

Table IV.1. Solid recovery (S.R.) and extraction efficiency (E.E.) of spray- and freeze-drying processes

	Spray-drying	Freeze-drying
S.R. (%)	53.0	91.0
E.E. (%)	84.4 ± 3.2	89.6 ± 3.7

Moreover, low temperature may be more suitable for the preservation of thermally sensitive compounds such as HT. To our knowledge, no study has reported the extraction efficiency of HT into β-CD. However, our results are similar to literature data for other phenolic compounds such as gallic acid. Using HP-β-CD, Olga *et al*. (2015) reached a 89.2% *EE* by spray-drying while Rosa *et al*. (2013) obtained a slightly lower *EE* (80%) by freeze-drying [16,17].

1.3.3   Hydrogen abstraction by DPPH

Phenolic compounds can act as hydrogen donors or electron donors to radicals and other oxidizing species, thereby preventing the oxidation of important biomolecules such as polyunsaturated lipids. In plant, they also act as electron donors for the peroxidase-catalyzed reduction of hydrogen peroxide [32]. As a first approach, the free radical-scavenging ability of phenolic compounds can be assessed by monitoring the reduction of the stable colored DPPH radical in MeOH. As β-CD is insoluble in MeOH, a 1:1 MeOH - water mixture was used [33].

Table IV.2 shows the radical-scavenging percentage values and the stoichiometry *n* of HT samples. Freeze-dried and spray-dried HT + β-CD samples were compared with HT and a 1:1 HT + β-CD physical mix. The % *RSA* and *n* values were essentially the same for all samples. So, both encapsulation processes do not affect HT integrity and preserve its H-donating capacity. These results were in accordance with Kfoury *et al.* (2014) who showed that encapsulation into CDs did not change the antioxidant capacity of eugenol, caffeic acid or ferulic acid [34].

Table IV.2. DPPH assays: radical scavenging activity and stoichiometry of HT and HT+β-CD powders

	% R.S.A.	n_{tot}
HT (control)	83.25 ± 1.00	3.21 ± 0.09
Equimolar HT + β-CD mixture	85.99 ± 3.67	3.30 ± 0.16
Spray-dried HT + β-CD powder	83.02 ± 3.15	3.25 ± 0.04
Freeze-dried HT + β-CD powder	85.82 ± 3.67	3.27 ± 0.01

*% R.S.A: radical scavenging activity

Finally, the stoichiometry values of the different samples in MeOH – H_2O (1:1) are slightly higher than for HT in MeOH: $n \approx 2.5$ [35], which could point to an easier regeneration of the catechol nucleus from the *o*-quinone, possibly after tautomerization into a *p*-quinone methide followed by water addition (Figure IV.3).
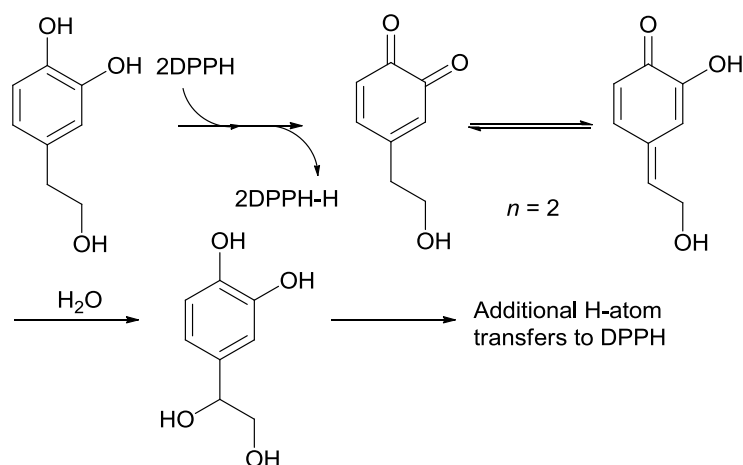
Figure IV.3. Possible fate of HT during its reaction with DPPH in MeOH – H2O (1:1)

1.3.4   Solid state NMR

The influence of mobility in the relative intensity of the host and guest signals can be probed in the kHz frequency ranges by measuring the ^1H and ^{13}C spin–locking (^1H T1ρ and ^{13}C T1ρ) relaxation times. ^1H T1ρ and ^{13}C T1ρ were chosen to probe spin diffusion and mobility,

respectively. Indeed, motion is the driving mechanism for ^{13}C T1ρ, because it is less influenced by spin diffusion than ^{1}H T1ρ since the spin diffusion rate increases with the magnetogyric ratio and natural isotopic abundance and is therefore higher for ^{1}H than for ^{13}C. HT and β-CD relaxation times were measured using the signals recorded at ca. 37 ppm and 102 ppm, respectively.

Table IV.3. Spin-diffusion (1HT1ρ) and mobility (13CT1ρ) for HT + β-CD solid samples

Samples	^{1}H T1ρ	(ms)	^{13}C T1ρ	(ms)
Physical mix	β-CD	4.5	β-CD	19.5
	HT	2.5	HT	2.6
Spray-dried sample	β-CD	4.5	β-CD	14.5
Freeze-dried sample	HT	2.5	HT	2.6
	β-CD	4.5	β-CD	14.5

In the case of the HT + β-CD physical mix, different ^{1}H T1ρ values were measured for β-CD and HT. This is consistent with 2 independent spin systems (no spin diffusion) and thus suggests that HT and β-CD do not interact. For both spray-dried and freeze-dried samples, similar ^{1}H T1ρ were measured for HT and β-CD, which clearly suggests a common spin system for both compounds. In other words, host - guest ^{1}H – ^{1}H distances are now small enough to allow spin diffusion, in agreement with the formation of an inclusion complex. ^{13}C T1ρ values are lower for HT than for β-CD in all samples with no clear influence of encapsulation. This is consistent with less restricted molecular motion for HT than for β-CD.

1.3.5   Scanning electron microscopy (SEM) and size distribution

The micrographs obtained by SEM showed two kinds of external structures according to the selected drying process. Freeze-dried particles (Figures IV.4 A and B) display irregular structures compared to spray-dried particles (Figures IV.4 C and D), which have spherical and indented shapes. The wrinkled surface of the spray-dried particles could be attributed to capillary forces and fast dehydration during the process [36,37].
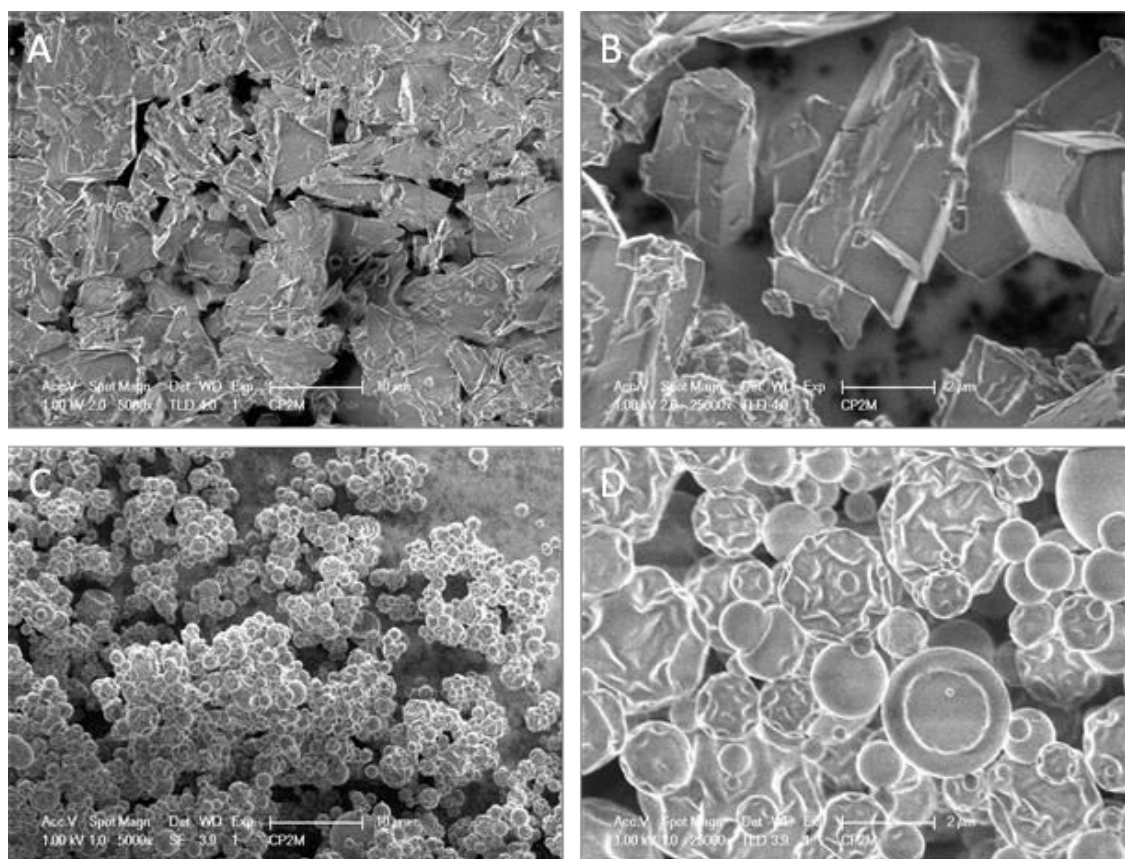
Figure IV.4. Scanning electron micrographs at 1 kV of freeze-dried (A,B) and spray-dried (C,D) HT + β-CD powders. Magnification: x5000 (A,C), x25000 (B,D)

The particle size is an important criteria in industry, influencing the solubility of the inclusion complex [38]. The diameter distribution of the spray-dried particles (Figure IV.5) was estimated using the calibrated scale on micrographs and the Image J software.
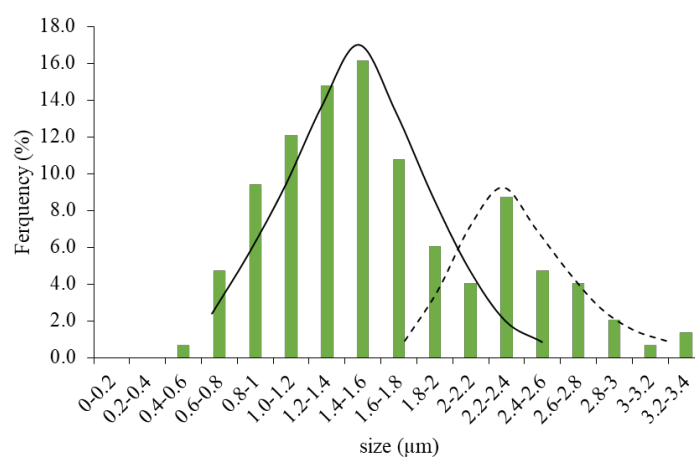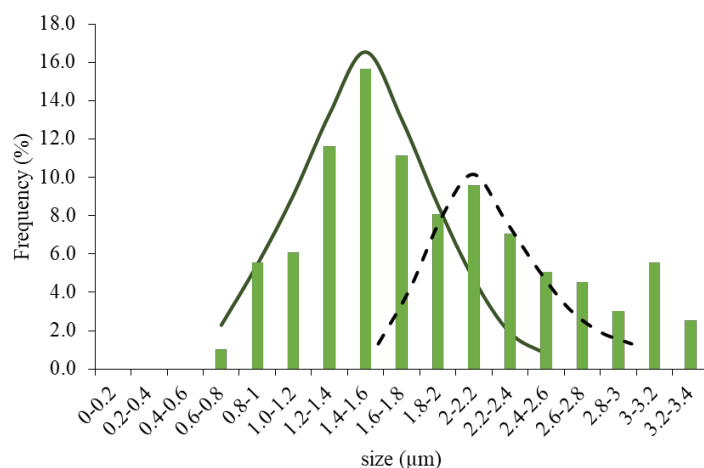

Figure IV.5. Diameter distribution in number for the spray-dried HT-β-CD complex determined by image analysis of SEM photographs

The particle diameters ranged from 0.4 to 3.4 µm, in agreement with previous data on the same spray-dryer [39,40]. More than 15% of particles had diameters between 1.4 and

1.6 μm, defining the first population mode. Moreover, particles with diameters distributed around 2.2 - 2.4 μm represented ca. 10% of the population. The size polydispersity is a frequent consequence of spray-drying [41,42].

1.4 Conclusion

Spectroscopic analyses provided evidence that HT and β-CD form a weak inclusion complex of 1:1 stoichiometry in aqueous solution. Based on the *K* value, the percentage of complex in solution from an equimolar (5 mM) mixture of both partners is lower than 20%. However, spray-drying or freeze-drying of such solutions allowed the simple preparation of HT + β-CD powders with HT encapsulated inside the macrocycle as evidenced by solid state ^{13}C CP/MAS NMR. Such preparations could express extended shelf-life for HT upon storage in the solid state. On the other hand, dissolution of the powders in MeOH – H_2O (1:1) show that the radical-scavenging activity of HT (and thus its chemical integrity) is fully preserved during the drying processes and that in solution HT is immediately released from its complex to express its bioactivity. SEM analysis indicated that freeze-dried particles were irregular in shape, whereas spray-dried particles displayed a spherical and smooth surface. Additional investigations will aim at showing whether those differences have an impact on the rate of dissolution and shelf-life of HT in the solid state. In conclusion, HT can form inclusion complexes with β-CD in aqueous solution and in the solid state, which could foster its development as a bioactive ingredient.

2 Case of tyrosol

The same complexation study has been led on Tyr (Figure IV.6).
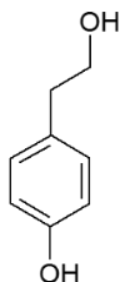
Figure IV.176. Chemical structure of tyrosol

2.1 Stoichiometry and association constant determination

β-CD can encapsulate Tyr in aqueous solution. In the case of Tyr, β-CD induced UV spectrum shifts, i.e. hyperchromic and batochromic shifts, which were higher than for HT (Figure IV.7).
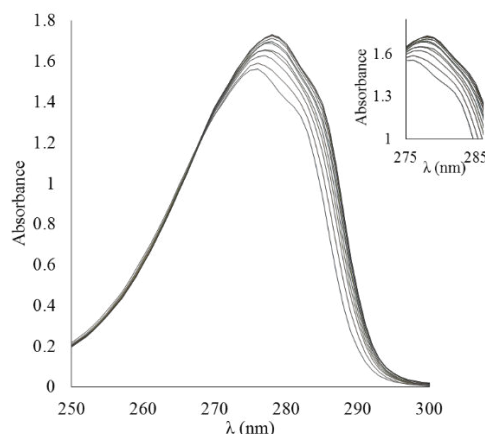
Figure IV.7. UV spectra of tyrosol in presence of increasing amounts of β-CD

These absorbance shifts increased with β-CD and allowed the calculation of the stoichiometry and binding constant of the β-CD-Tyr complex (Figure IV.8).
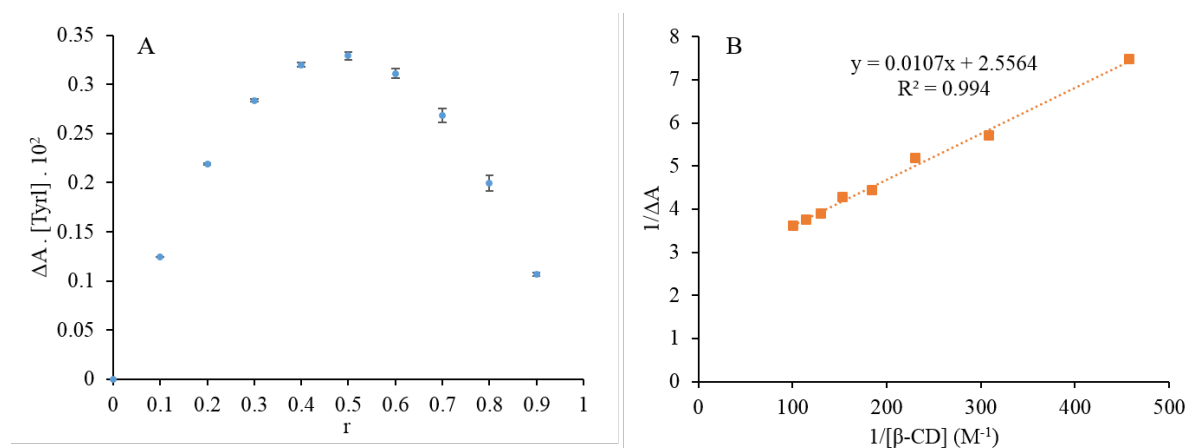
Figure IV.8. Job's plot (A) and Benesi-Hildebrand method (B) for the stoichiometry and the binding constant determination of tyrosol:β-CD complex

The β-CD - Tyr complex formed with a 1:1 stoichiometry (r= 0.5) had a binding constant K = 238.9 ± 18.5 M^{-1}, which is 7 times higher than for HT. García-Padial *et al*. (2013) calculated for Tyr and β-CD a binding constant of 211 ± 13 and 294 ± 63 M^{-1} in UV spectrometry and spectrofluorimetry respectively [43].

2.2   Solid recovery and extraction efficiency

The production of Tyr-β-CD complexes by spray- or freeze-drying led to similar yields than for HT-β-CD complexes. In the case of spray-drying, more powder remained on the wall and was lost. Extraction efficiency for spray-dried Tyr-β-CD powder was slight better (92.8 ± 2.1%) than for HT-β-CD (84.4 ± 3.2%). No difference was highlighted for freeze-dried particles.

Table IV.4. Production yield (P.Y.) and encapsulation efficiency (E.E.) of spray- and freeze-drying processes

	Spray-drying	Freeze-drying
SR (%)	52.0	88.0
EE (%)	92.8 ± 2.1	86.6± 5.3

2.3   Scanning electron microscopy (SEM) and size distribution

The micrographs of Tyr-β-CD complexes were realized with a more recent apparatus, Gemini SEM 500 (Zeiss®). As expected, two kinds of external structures have been observed according to the selected drying process (Figure IV.9).
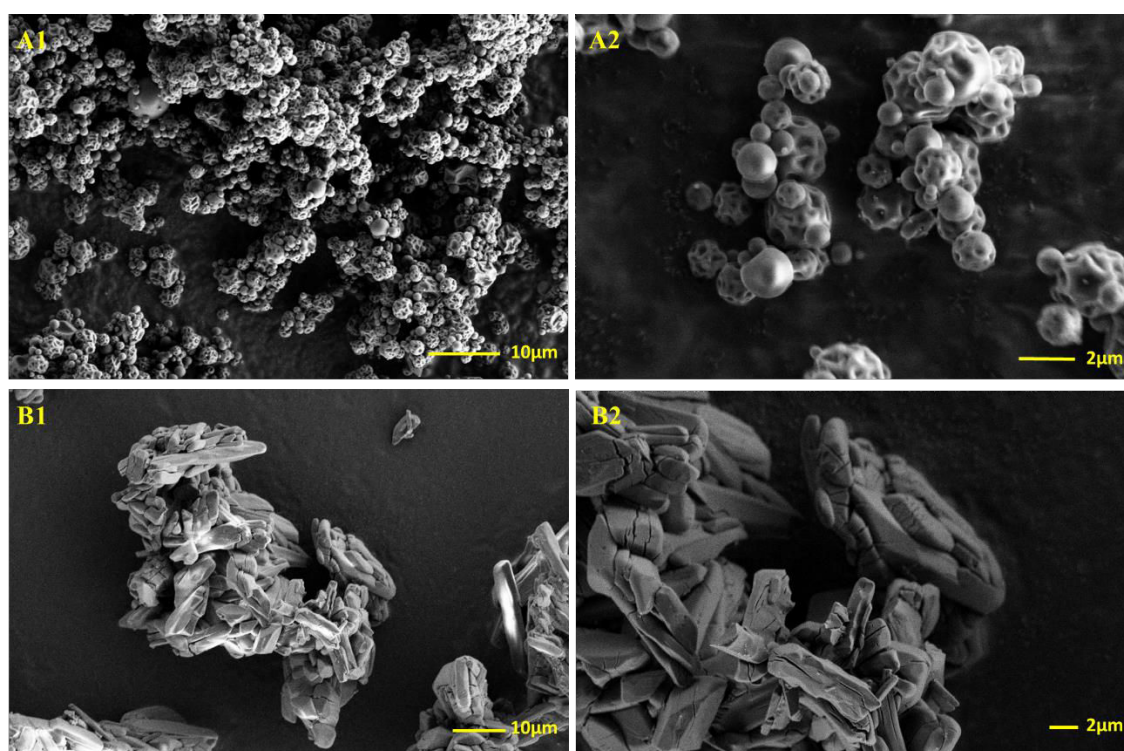
Figure VI.9. Scanning electron micrographs of spray-dried (A) and freeze-dried (B) Tyr+β-CD powders. Magnification x 1480 (A1), 5730 (A2), 1140 (B1) and 2870 (B2)

Freeze-dried particles (figure IV.9 B1 and B2) have irregular structures while spray-dried particles display spherical and indented shapes (figures IV.9-A). The external structure results from the slected drying process, explaining that HT-β-CD and Tyr-β-CD particles displayed similar similar shapes (Figure IV.10).

Figure IV.10. Diameter distribution in number for the spray-dried Tyr-β-CD complex determined by image analysis of SEM photographs

Spray-dried Tyr-β-CD particles defined two population modes, the first one between 1.4 to 1.6μm (more than 15%) and the second one around 2.0 to 2.2μm (almost 10%). So, spray-drying process leads to similar sized particles in either case.

2.4   Comparative conclusion

Tyr-β-CD complexes were produced according the same method than HT-β-CD complexes. It can be concluded that Tyr was more encapsulated inside the β-CD cavity, having a seven-time higher binding constant. HT possesses one more hydroxyl group at the *o*-position than Tyr, which makes HT more hydrophilic. The higher hydrophobicity of Tyr seems to be advantageous to interact with the β-CD cavity. In any case, the solid recovery was higher after freeze-drying. Spray-drying produced smaller particles. Besides, extraction efficiency was up to 84% in every instance.

References

1. Beart JE, Lilley TH, Haslam E. 1985. Plant polyphenols—secondary metabolism and chemical defence: Some observations. *Phytochemistry*. 24:33–38.

2. Lattanzio V, Kroon PA, Quideau S, Treutter D. 2008. Plant Phenolics– Secondary Metabolites with Diverse Functions. In Daayf, F and Lattanzio, V, eds, *Recent Adv. Polyphenol Res*. Wiley-Blackwell, Oxford, UK, pp 1–35.

3. Faridi Esfanjani A, Jafari SM. 2016. Biopolymer nano-particles and natural nano-carriers for nano-encapsulation of phenolic compounds. *Colloids Surf. B Biointerfaces*. 146:532–543.

4. Tsao R. 2010. Chemistry and Biochemistry of Dietary Polyphenols. *Nutrients*. 2:1231–1246.

5. de Mello Andrade JM, Fasolo D. 2014. Polyphenol Antioxidants from Natural Sources and Contribution to Health Promotion. *Polyphenols Hum. Health Dis*. Elsevier, pp 253–265. doi:10.1016/B978-0-12-398456-2.00020-7.

6. Bulotta S, Celano M, Lepore SM, Montalcini T, Pujia A, Russo D. 2014. Beneficial effects of the olive oil phenolic components oleuropein and hydroxytyrosol: focus on protection against cardiovascular and metabolic diseases. *J. Transl. Med*. 12:219.

7. EFSA Panel on Dietetic Products, Nutrition and Allergies (NDA). 2011. Scientific Opinion on the substantiation of health claims related to polyphenols in olive and protection of LDL particles from oxidative damage (ID 1333, 1638, 1639, 1696, 2865), maintenance of normal blood HDL cholesterol concentrations (ID 1639), mainte: Polyphenols in olive related health claims. *EFSA J*. 9.

8. Servili M, Sordini B, Esposto S, Urbani S, Veneziani G, Di Maio I, Selvaggini R, Taticchi A. 2013. Biological Activities of Phenolic Compounds of Extra Virgin Olive Oil. *Antioxidants*. 3:1–23.

9. Kitsati N, Mantzaris MD, Galaris D. 2016. Hydroxytyrosol inhibits hydrogen peroxide-induced apoptotic signaling via labile iron chelation. *Redox Biol*. 10:233–242.

10. O′Dowd Y, Driss F, Dang PM-C, Elbim C, Gougerot-Pocidalo M-A, Pasquier C, El-Benna J. 2004. Antioxidant effect of hydroxytyrosol, a polyphenol from olive oil: scavenging of hydrogen peroxide but not superoxide anion produced by human neutrophils. *Biochem. Pharmacol*. 68:2003–2008.

11. Munin A, Edwards-Lévy F. 2011. Encapsulation of Natural Polyphenolic Compounds; a Review. *Pharmaceutics*. 3:793–829.

12. Astray G, Gonzalez-Barreiro C, Mejuto JC, Rial-Otero R, Simal-Gándara J. 2009. A review on the use of cyclodextrins in foods. *Food Hydrocoll*. 23:1631–1640.

13. Ratnasooriya CC, Rupasinghe HPV. 2012. Extraction of phenolic compounds from grapes and their pomace using β-cyclodextrin. *Food Chem*. 134:625–631.

14. Szejtli J. 1988. *Cyclodextrin Technology*. 1, Springer Netherlands, Dordrecht.

15. Aksamija A, Polidori A, Plasson R, Dangles O, Tomao V. 2016. The inclusion complex of rosmarinic acid into beta-cyclodextrin: A thermodynamic and structural analysis by NMR and capillary electrophoresis. *Food Chem*. 208:258–263.

16. Olga G, Styliani C, Ioannis RG. 2015. Coencapsulation of Ferulic and Gallic acid in hp-β-cyclodextrin. *Food Chem*. 185:33–40.

17. da Rosa CG, Borges CD, Zambiazi RC, Nunes MR, Benvenutti EV, Luz SR da, D'Avila RF, Rutz JK. 2013. Microencapsulation of gallic acid in chitosan, β-cyclodextrin and xanthan. *Ind*. *Crops Prod*. 46:138–146.

18. Lu Z, Cheng B, Hu Y, Zhang Y, Zou G. 2009. Complexation of resveratrol with cyclodextrins: Solubility and antioxidant activity. *Food Chem*. 113:17–20.

19. Lucas-Abellán C, Mercader-Ros MT, Zafrilla MP, Gabaldón JA, Núñez-Delicado E. 2011. Comparative study of different methods to measure antioxidant activity of resveratrol in the presence of cyclodextrins. *Food Chem*. *Toxicol*. 49:1255–1260.

20. Kalogeropoulos N, Yannakopoulou K, Gioxari A, Chiou A, Makris DP. 2010. Polyphenol characterization and encapsulation in β-cyclodextrin of a flavonoid-rich Hypericum perforatum (St John's wort) extract. *LWT - Food Sci*. *Technol*. 43:882–889.

21. Mantegna S, Binello A, Boffa L, Giorgis M, Cena C, Cravotto G. 2012. A one-pot ultrasound-assisted water extraction/cyclodextrin encapsulation of resveratrol from Polygonum cuspidatum. *Food Chem*. 130:746–750.

22. Rajha HN, Chacar S, Afif C, Vorobiev E, Louka N, Maroun RG. 2015. β-Cyclodextrin-Assisted Extraction of Polyphenols from Vine Shoot Cultivars. *J*. *Agric*. *Food Chem*. 63:3387–3393.

23. Uekama K, Hirayama F, Irie T. 1998. Cyclodextrin drug carrier systems. *Chem*. *Rev*. 98:2045–2076.

24. López-García MÁ, López Ó, Maya I, Fernández-Bolaños JG. 2010. Complexation of hydroxytyrosol with β-cyclodextrins. An efficient photoprotection. *Tetrahedron*. 66:8006–8011.

25. Rescifina A, Chiacchio U, Iannazzo D, Piperno A, Romeo G. 2010. β-Cyclodextrin and Caffeine Complexes with Natural Polyphenols from Olive and Olive Oils: NMR, Thermodynamic, and Molecular Modeling Studies. *J*. *Agric*. *Food Chem*. 58:11876–11882.

26. Schaefer J, Stejskal EO. 1976. Carbon-13 nuclear magnetic resonance of polymers spinning at the magic angle. *J*. *Am*. *Chem*. *Soc*. 98:1031–1032.

27. Cook RL, Langford CH, Yamdagni R, Preston CM. 1996. A Modified Cross-Polarization Magic Angle Spinning [13] C NMR Procedure for the Study of Humic Materials. *Anal*. *Chem*. 68:3979–3986.

28. Peersen OB, Wu XL, Kustanovich I, Smith SO. 1993. Variable-Amplitude Cross-Polarization MAS NMR. *J*. *Magn*. *Reson*. *A*. 104:334–339.

29. Gerbaud G, Ziarelli F, Caldarelli S. 2003. Increasing the robustness of heteronuclear decoupling in magic-angle sample spinning solid-state NMR. *Chem*. *Phys*. *Lett*. 377:1–5.

30. Wilkowska A, Ambroziak W, Czyżowska A, Adamiec J. 2016. Effect of Microencapsulation by Spray-Drying and Freeze-Drying Technique on the Antioxidant Properties of Blueberry (*Vaccinium myrtillus*) Juice Polyphenolic Compounds. *Pol*. *J*. *Food Nutr*. *Sci*. 66.

31. Nunes IL, Mercadante AZ. 2007. Encapsulation of lycopene using spray-drying and molecular inclusion processes. *Braz*. *Arch*. *Biol*. *Technol*. 50:893–900.

32. Dangles O. 2012. Antioxidant Activity of Plant Phenols: Chemical Mechanisms and Biological Significance. *Curr. Org. Chem.* 16:692–714.

33. Ferreira F da R, Valentim IB, Ramones ELC, Trevisan MTS, Olea-Azar C, Perez-Cruz F, de Abreu FC, Goulart MOF. 2013. Antioxidant activity of the mangiferin inclusion complex with β-cyclodextrin. *LWT - Food Sci. Technol.* 51:129–134.

34. Kfoury M, Landy D, Auezova L, Greige-Gerges H, Fourmentin S. 2014. Effect of cyclodextrin complexation on phenylpropanoids' solubility and antioxidant activity. *Beilstein J. Org. Chem.* 10:2322–2331.

35. Roche M, Dufour C, Mora N, Dangles O. 2005. Antioxidant activity of olive phenols: mechanistic investigation and characterization of oxidation products by mass spectrometry. *Org. Biomol. Chem.* 3:423.

36. Foerster M, Gengenbach T, Woo MW, Selomulya C. 2016. The impact of atomization on the surface composition of spray-dried milk droplets. *Colloids Surf. B Biointerfaces.* 140:460–471.

37. Yang F, Liu X, Wang W, Liu C, Quan L, Liao Y. 2015. The effects of surface morphology on the aerosol performance of spray-dried particles within HFA 134a based metered dose formulations. *Asian J. Pharm. Sci.* 10:513–519.

38. Khadka P, Ro J, Kim H, Kim I, Kim JT, Kim H, Cho JM, Yun G, Lee J. 2014. Pharmaceutical particle technologies: An approach to improve drug solubility, dissolution and bioavailability. *Asian J. Pharm. Sci.* 9:304–316.

39. Bürki K, Jeon I, Arpagaus C, Betz G. 2011. New insights into respirable protein powder preparation using a nano spray dryer. *Int. J. Pharm.* 408:248–256.

40. Pérez-Masiá R, López-Nicolás R, Periago MJ, Ros G, Lagaron JM, López-Rubio A. 2015. Encapsulation of folic acid in food hydrocolloids through nanospray drying and electrospraying for nutraceutical applications. *Food Chem.* 168:124–133.

41. Huntington DH. 2004. The Influence of the Spray Drying Process on Product Properties. *Dry. Technol.* 22:1261–1287.

42. Yao Y, Zhao G, Yan Y, Chen C, Sun C, Zou X, Jin Q, Wang X. 2016. Effects of freeze drying and spray drying on the microstructure and composition of milk fat globules. *RSC Adv.* 6:2520–2529.

43. García-Padial M, Martínez-Ohárriz MC, Isasi JR, Vélaz I, Zornoza A. 2013. Complexation of tyrosol with cyclodextrins. *J. Incl. Phenom. Macrocycl. Chem.* 75:241–246.

Chapter V. Biophenols extraction using β-cyclodextrin in the solid state by a new process

One-step extraction of tyrosol and hydroxytyrosol from aqueous solution using β-cyclodextrin in the solid state

Aurélia Malapert, Emmanuelle Reboul, Olivier Dangles, Valérie Tomao (*future submission*).

New procedure for the biophenols extraction from alperujo using β-cyclodextrin in the solid state

Aurélia Malapert, Emmanuelle Reboul, Olivier Dangles, Valérie Tomao, (*future submission*).

1 One-step extraction of tyrosol and hydroxytyrosol from aqueous solution using β-cyclodextrin in the solid state

Abstract

The extraction of phenolic compounds from olive mill wastes is important not only to avoid environmental damages but also because of the intrinsic value of those biophenols, well-known for their high antioxidant potential and health benefits. This study focuses on tyrosol and hydroxytyrosol, two of the main phenolic compounds found in olive mill wastes. A new simple and eco-friendly extraction process of phenolic compounds from aqueous solution with native β-CD in solid state has been developed. Several β-CD/biophenol molar ratios and biophenol concentrations were investigated in order to maintain β-CD mostly in the solid state and optimize the extraction yield and the loading capacity of the sorbent. The extraction efficiencies of Tyr and HT were up to 61 % from an initial 100 mM biophenol solution with a total solid recovery higher than 90 % by using 10 molar equivalent of β-CD. The powder obtained could be directly used as a safe-grade phenol-rich source. The proposed process could be used as a model for extracting valuable biophenols from olive mill wastewater.

1.1 Introduction

In the Mediterranean basin, two of the main agricultural wastes are olive mill wastewaters and olive pomace, associated with olive oil production [1]. As much as 98% of olive phenolic compounds remain in wastes after olive mill processing and cause environmental damages upon spreading in fields [2]. The European Protection Agency (EPA), in collaboration with other organisms, has developed regulations and laws concerning the phenolic content in water [3].

Many studies worked on decreasing the pollutant character of olive mill effluents by removing phenolic compounds. Iboukhoulef *et al.* (2016) succeeded in reducing by more than 60% the phenolic content of olive mill wastewaters (OMWW) in 65 min, by using an oxidative Fenton process using Cu^{II} and hydrogen peroxide [4]. An optimized ozonolytic process also allowed removing more than 80% of the phenolic compounds [5]. On the other hand, physical technics, especially filtration-based methods, are commonly used for cleaning water effluents. For instance, Comandini *et al.* (2015) worked on the removal of phenolic compounds from OMWW by a first ultrafiltration followed by a reverse osmosis step ([6]). Ultrafiltration was used to reduce about 40% the phenolic compounds from the initial OMWW while reverse osmosis allowed to obtain on the one hand a phenolic-free permeate and on the other hand a

phenolic-rich concentrate. Other filtration methods rest on adsorption technologies. Aly *et al*. (2014) successively used columns of gravel, fine sand and a zeolite/acidified cotton mixture for removing pollutants from OMWW ([7]). Final steps with activated charcoal and lime led to safe effluents that could be used for irrigation. Abdelkreem (2013) dried the olive mill pomace to turn it into an adsorbent. They succeeded in removing 85% of the phenolic compounds from 25 mL OMWW by using 1 g of dried olive pomace [8]. Using the Granular Activated Carbon (GAC), Aliakbarian *et al*. (2011) removed 96% of phenolic compounds from OMWW and produced a clean water sample ([9]). Ena *et al*. (2012) compared GAC and *Azolla* to remove phenolic compounds from OMWW. GAC showed higher adsorption and desorption capacities than *Azolla* and the profile of retained phenolic compounds was found different according to the adsorbent used. While the total phenolic content was more than twice higher in *Azolla*-treated OMWW, HT was more abundant in GAC-treated OMWW ([10].

Apart from their polluting character, olive mill wastes have emerged as a valuable and economic source of natural phenolic compounds known for their diverse biological activities, including antioxidant, anti-inflammatory and antimicrobial properties. Among them, hydroxytyrosol is considered one of the most interesting phenolic compounds in olive oil and its by-products [11].

β-cyclodextrin (β-CD) is a cyclic oligosaccharide composed of 7 D-glucopyranose units connected by α-1,4 bonds. β-CD is Generally Recognized As Safe (GRAS) by the European Food Safety Agency (EFSA), which has defined an acceptable daily intake for β-CD of 5 mg/kg of body weight [12]. Because of its relatively nonpolar cavity and its hydrophilic outer surface, β-CD has a well-known ability to form inclusion complexes with a wide range of valuable compounds in aqueous solution and is nowadays commonly used as part of formulations for protecting or enhancing the solubility of guest compounds. β-CD also finds many applications in food processing for controlling flavor release or for reducing a bitter taste for example. Complex formation depends on size complementary and the development of stabilizing molecular interactions between host and guest [13].

β-CD is able to encapsulate phenolic compounds in aqueous solution and this property could be used for reducing their bitter taste [14]. Moreover, López-García *et al*. (2010) showed that β-CD could increase the antioxidant activity of HT by providing photoprotection ([15]).

Host-guest complexes can also be formed in the solid state for convenient handling and storage. Spray- and freeze-drying processes are commonly used and first require the mix of β-CD and phenol in aqueous solution. Over the last 10 years, works on phenolic compounds

from olive leaves [16], *Melissa Officinalis* leaves [17] and blueberry juice [18] have been reported. Hundre *et al*. (2015) also prepared β-CD-vanillin complexes by spray-drying, freeze-drying or by a combination of both, and concluded that the method selected has an impact on the external shape and thermal stability of the powder [19]. Other methods for preparing complexes in the solid state are the classical co-precipitation procedure, the paste technique or kneading, which consists in mixing host and guest with a small amount of water, and the solid phase complexation using a high level of mechanical energy to co-grind or extrude complexes. Only a few studies have focused on the solid complexes of HT and Tyr with β-CD. For instance, Garcia-Padial *et al*. (2013) prepared the solid Tyr-β-CD complex by co-evaporation and kneading [20].

In this study, a new simple and eco-friendly process was developed for the one-step extraction of olive phenolic compounds from an aqueous solution by directly forming a solid state complex with β-CD. The conditions were optimized in terms of phenol and β-CD concentration and molar ratio.

1.2   Material and methods

1.2.1   Materials

β-CD was kindly given by Roquettes Frères (Lesterm, France). Folin-Ciocalteu reagent was supplied by Sigma-Aldrich[®] (Sigma-Aldrich company Ltd, Great Britain). Analytical-grade methanol and water were from VWR[®] (Fontenay-sous-Bois, France) and Fisher Scientific[®] (Leics, UK) respectively. Tyr was supplied by Sigma-Adrich® (Deisenhofer, Germany) and HT was purchased from Extrasynthèse (Genay, France).

1.2.2   Spectroscopic analyses

UV analyses were performed on Agilent® 8453 UV-Visible spectrophotometer in a quartz cell (1 cm length). For quantification, the molar absorption coefficients of olive phenols were determined: $\varepsilon(Tyr) = 1414$ $M^{-1}.cm^{-1}$ at 275 nm, $\varepsilon(HT) = 2568$ $M^{-1}.cm^{-1}$ at 280 nm.

1.2.3   Standard solution

To optimize the phenol - β-CD molar ratio, 10 mM biophenol solutions (i.e. Tyr or HT) were prepared in 25 ml H_2O. Then, β-CD was added according to a β-CD/phenol molar ratio of 1:1; 3:1; 5:1; 10:1. The β-CD/phenol molar ratio of 1.4:1 corresponds to the β-CD limit of solubility (16 $g.L^{-1}$ at 20°C).

To optimize the phenolic concentration, 10 mL of a 100 mM phenol solution were mixed with β-CD at 20°C. The β-CD/phenol molar ratio of 10:1 was investigated for the Tyr and HT studies.

All analyses were performed on fresh standard solutions. Each analysis was repeated three times.

1.2.4 Kinetic procedure

Standard solutions were mixed with β-CD in the solid state at 20°C under stirring at 250 rpm. The phenol concentration in the supernatant was followed by UV/Vis spectroscopy over 3h. A brief supplementary centrifugation as well as dilution in water could be carried out if necessary.

1.2.5 Analysis of solid complexes

1.2.5.1. Solid and biophenol recovery procedure

At the end of kinetics, the biophenol + β-CD mixture was filtered on a glass filtering funnel (porosity 5). The recovered solid was dried at 35°C until the mass variation was less than 10%. The solid recovery was determined as a percentage of the initial solid amount (biophenol + β-CD). It was corrected for the solubilized β-CD amount (16 g L^{-1} at 20°C) to determine the true solid recovery efficiency.

1.2.5.2. Loading and extraction efficiencies

The final powders recovered from the kinetic procedure were analyzed to determine the amount of Tyr or HT retained by solid β-CD. Thus, 50 mg of powder were rinsed with 2 mL MeOH and filtered on a 0.2 μm PTFE syringe. The loading efficiency Qe (mmol/100 g) and the extraction efficiency (EE) were then calculated as follows:

$$Qe = \frac{Cp.Vs}{m} \times 100$$

and

$$EE = \frac{Cp.Vs}{m} \times \frac{m(recovered\ solid)}{Ci.Vi} \times 100$$

Where Cp = phenol concentration in the MeOH fraction, Vs = volume of MeOH (2 ml), Ci = initial phenol concentration, Vi = initial volume, m = mass of the rinsed powder.

1.2.5.3. Scanning electron microscopy

The solid particles obtained for a β-CD/tyrosol molar ratio of 10:1 were investigated by scanning electronic microscopy (SEM). A Gemini SEM (Zeiss$^{®}$) scanning electron microscopy was used with a voltage of 3 kV. The microstructure was not coated and was observed at different extensions.

1.3 Results and discussion

1.3.1 Influence of the β-CD/phenol molar ratio

Biophenols were extracted from 10 mM solutions containing various β-CD amounts over 3 h. The phenol concentration in the supernatant was plotted as a function of time (Figures V.1 and 2) respectively.
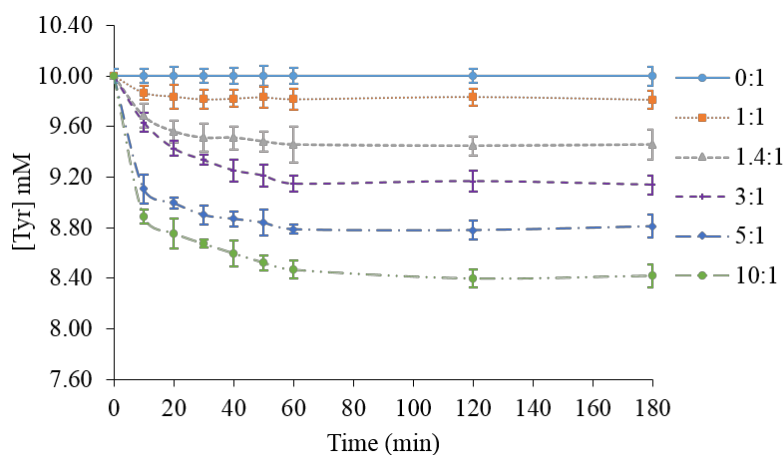
Figure V.1. Time-dependence of the tyrosol concentration according to the β-CD/tyrosol molar ratio
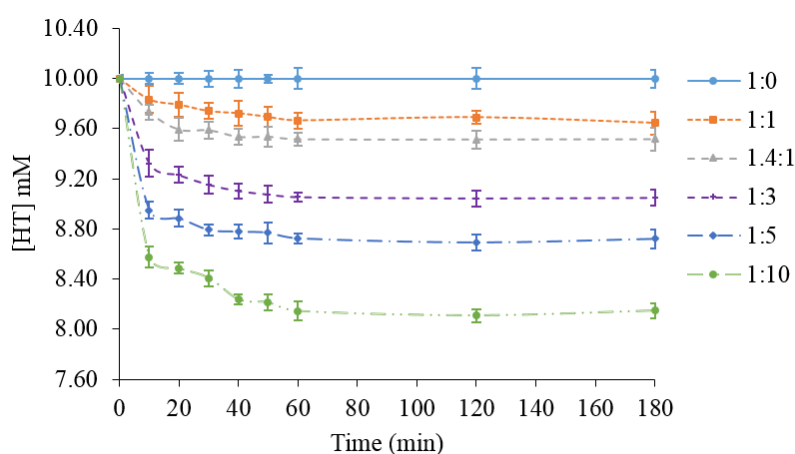
Figure V.2. Time-dependence of the hydroxytyrosol concentration according to the β-CD/hydroxytyrosol molar ratio

The studies of solid β-CD as a biophenol-extracting agent led to similar kinetic behaviors for Tyr and HT. Compared to standard solutions without β-CD (0:1), adding β-CD caused a fast decrease of the remaining biophenol concentration in the supernatant, which was complete after 60 min. This phenomenon could be explained by the fast adsorption of the phenols onto the solid particles, followed by the slower diffusion of the solution into the cavity of the extracting particles to reach the equilibrium state [21,22]. Our observations are in

agreement with the literature [23–25]. The β-CD/phenol molar ratios of 1:1 and 1.4:1 corresponded to β-CD below or at its solubility limit (16 g/L at 20°C) and thus did not allow the recovery of powders. However, shifts in the phenols' absorption bands consistent with the formation of inclusion complexes in solution were observed. At higher molar ratios, solid recovery was possible. Wang *et al*. (2014) studied the adsorption of phenols from wastewaters onto cross-linked β-CD - diphenylmethane diisocyanate polymer particles. The kinetics observed were similar with Tyr and HT ([26]).

As shown in Table V.1, the solid recovery increased with the β-CD/tyrosol molar ratio from 22.2% to 75.4% of the initial solid quantity (β-CD + tyrosol). After correction for the amount of solubilized β-CD, the values increased from 69.2% to 89.5%. For comparison, using freeze-drying, Jantarat *et al*. (2014) obtained a 95.7% yield for curcumin encapsulated into a β-CD derivative ([27]).

The extraction efficiency was calculated from the biophenol concentration in the rinsed MeOH fraction compared to the initial content. Results were in agreement with the kinetic data, showing an enhancement of the extraction efficiency at higher β-CD/Tyr molar ratio. Kumar *et al*. (2010) proposed that a higher adsorbent amount, although it offers a larger number of available binding sites, could generate partial aggregation ([28]). The loading efficiency (Qe), which decreased with the β-CD quantity, seemed to be consistent with this view.

Table V.1. Solid recovery, extraction and loading efficiencies for a 10 mM tyrosol solution

β-CD/Tyr ratio	Solid recovery (%)	Solid recovery efficiency (%)	Extraction efficiency (%)	Loading efficiency Qe	
				mmol/100g	mg/g
3:1	22.2 ± 3.9	69.2 ± 3.9	2.2 ± 0.2	2.9 ± 0.3	4.1 ± 0.4
5:1	51.7 ± 4.6	79.9 ± 4.6	6.1 ± 0.4	2.1 ± 0.1	2.9 ± 0.1
10:1	75.4 ± 5.1	89.5 ± 5.1	10.9 ± 1.2	1.3 ± 0.1	1.8 ± 0.1

The same analyses were carried out with the β-CD - HT powder and gave similar data (Table V.2).

Table V.2. Solid recovery, extraction and loading efficiencies for a 10 mM hydroxytyrosol solution

β-CD/HT ratio	Solid recovery (%)	Solid recovery efficiency (%)	Extraction efficiency (%)	Loading efficiency Qe	
				mmol/100g	mg/g
3:1	31.4 ± 4.8	78.4 ± 4.8	3.4 ± 0.3	3.2 ± 0.2	4.9 ± 0.3
5:1	57.4 ± 5.4	85.6 ± 5.4	7.1 ± 0.6	2.2 ± 0.0	3.4 ± 0.1
10:1	79.1 ± 3.1	93.2 ± 3.1	13.6 ± 1.3	1.5 ± 0.1	2.3 ± 0.1

Hence, it can be suggested that solid β-CD does not express selectivity in its extraction of Tyr or HT despite the higher affinity of the former for β-CD in aqueous solution, which is reflected by a ca. 10 times higher binding constant [20].

1.3.2   Influence of the biophenol concentration

According to the precedent results, the highest extraction efficiency was obtained with 10 molar β-CD equivalents. This condition was further tested with a concentrated Tyr solution (100 mM). The same study was carried out with a concentrated HT solution (100mM) (Figure V.3).
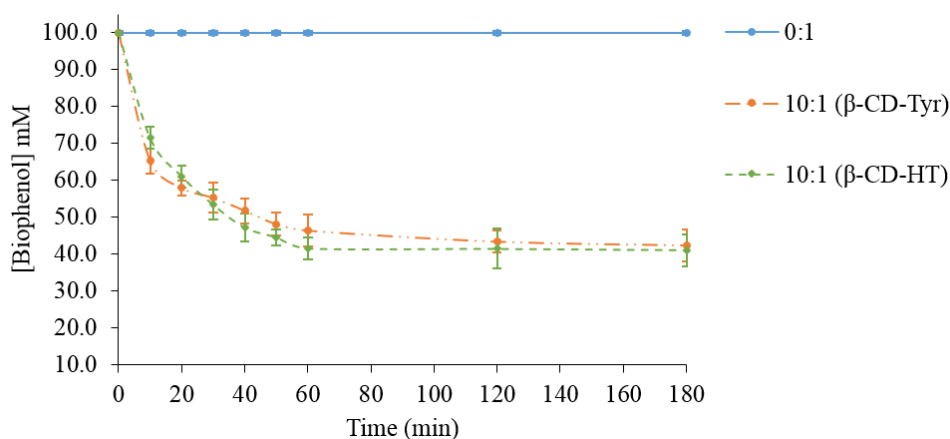
Figure V.3. Time-dependence of the biophenol concentration in a concentrated aqueous solution according to the β-CD/phenol molar ratio of 10:1

As expected, the biophenol concentration in the aqueous phase decreased when the β-CD amount increased. For the same β-CD/biophenol molar ratio, this decrease was significantly higher than in dilute biophenol solutions (10 mM, Figs V.1 and V.2). Table V.3 presents the powder analysis.

Table V.3. Solid recovery, extraction and loading efficiencies for 100 mM tyrosol or hydroxytyrosol solutions

Phenols	β-CD/Phenol molar ratio	Solid recovery (%)	Solid recovery efficiency (%)	Extraction efficiency (%)	Loading efficiency Qe	
					mmol/100g	mg/g
Tyr	10:1	91.7 ± 6.2	93.1 ± 6.2	61.9 ± 4.9	5.9 ± 0.1	8.2 ± 0.1
HT	10:1	92.2 ± 3.1	93.6 ± 3.1	61.7 ± 3.1	5.9 ± 0.1	9.1 ± 0.2

Working with concentrated solutions of phenols allowed better extraction yields over 61% for the molar ratios of 10:1, respectively. The loading efficiency Qe was still higher than in any experiment starting from a 10 mM tyrosol solution. The assays on a concentrated hydroxytyrosol solution gave almost identical results as for tyrosol.

1.3.3   Scanning electron microscopy (SEM)

The following SEM micrographs compare the external shape of native β-CD with those of the solid particles obtained from the extraction of Tyr (Figure V.4).
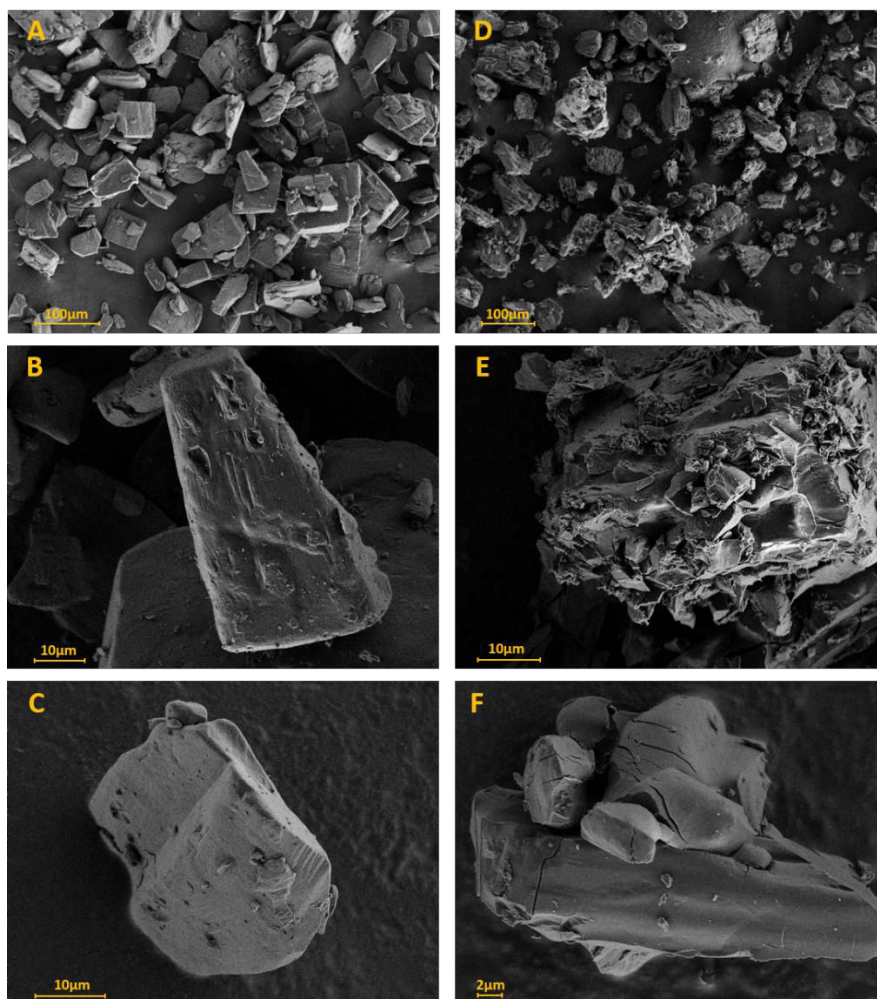
Figure V.4. Scanning electron micrographs of β-CD (A) and the powder recovered after extraction of tyrosol from a 100mM aqueous solution (10:1 β-CD/tyrosol molar ratio) magnification x 167 (A), x 1290 (B), x 1860 (C), x140 (D), x1630 (E)and x3170 (F)

Native β-CD had a microsized angular shape, giving geometrical structures. The solid β-CD-Tyr particles also displayed the microsized morphology. However, the external surface is very irregular and striated compared to native β-CD. This characteristic could be caused by Tyr particles deposited onto the β-CD particles.

1.4   Conclusion

This work describes a one-step procedure for the concomitant removal of olive phenols from wastewater and formulation of these micronutrients in a native β-CD matrix. It is based on the affinity of solid β-CD for olive phenols. This procedure is very simple, environment-

friendly (as no organic solvent is involved) and probably much cheaper than the preparation of phenol-β-CD powders by spray- or freeze-drying processes. It could then be applied to agricultural wastewaters for the recovery of high value phenolic compounds for use as food supplements.

2 New procedure for the biophenols extraction from alperujo using native β-cyclodextrin in the solid state

Abstract

This work focuses on the use of β-cyclodextrin (β-CD) in the solid state to act as a biophenol-extracting agent from alperujo. The feasibility of this procedure was evaluated by UV spectroscopy and UHPLC-DAD analyses. After optimizing the process in terms of β-CD/phenol molar ratio and phenol concentration, solid β-CD succeeded in extracting until 20% of HT and its glycoside forms from a concentrated alperujo juice. Solid β-CD could then act as an economic and efficient phenol-extracting agent and in consequence, as an innovative process to reduce the environmental impact of olive mills. In addition, the safe-grade phenol-rich powder obtained could be directly used as food additive or supplementary food.

2.1 Introduction

Olive oil industry is currently considered as one of the major pollutant sector in Mediterranean basin [29]. The main olive mill wastes are olive pomace and olive mill wastewaters (OMWW) [30,31]. Produced in large quantities (until 120L/100kg olive fruits) in traditional mills and three phase centrifuge mills, OMWW were the most known olive wastes for their large production and their pollutant character before the 90s [32,33]. Thus, two-phase centrifuge system was developed in order to reduce the OMWW production, by avoiding the water addition during olive oil extraction [34]. The only by-product generated called "alperujo" is composed of olive vegetation water and solid olive pieces [35]. This waste is still considered as pollutant for its high phenol content [36].

However, olive biophenols are recognized as efficient antioxidants and mainly remain in the olive mill wastes [37,38]. Among them, HT is the target of several studies, having a high antioxidant potential [39,40]; some phenolic acids such as caffeic acid, chlorogenic acid, vanillic acid; secoiridoids of which the most famous are oleuropein, ligstroside and their derivatives, are also considered [41].

β-CD composed of 7 D-glycopyranose units connected by α-1,4 bonds, is a cyclic oligosaccharide and is widely used to be low cost, safe-grade (GRAS) and to form inclusion complexes, receiving the guest molecule in its hydrophobic cavity [42,43,44]. β-CD can protects the guest against oxidative degradation and can enhance its bioavailability by improving its water solubility [45]. Some studies worked on the ability of β-CD to encapsulate

phenolic compounds in solution. Barão *et al.* (2014) who compared α-CD (6 sub-units) and β-CD observed a higher affinity of oleuropein for β-CD [46]. López-García *et al.* (2010) demonstrated a photoprotective action of β-CD on HT in solution [15]. The solid form of CD + guest complex is common for nutraceutical or food applications. In this way, the recovery of solid β-CD complexes is generally allowed by spray- [47] or freeze-drying [16].

This work focuses on the development of a new simple and eco-friendly process to recover biophenols from alperujo with β-CD in the solid state. The experiments were followed by UV spectroscopy and UHPLC-DAD analyses.

2. Material and methods

2.1.1   Materials

β-CD was kindly given by Roquettes Frères (Lesterm, France). Folin-Ciocalteu reagent was supplied by Sigma-Aldrich® (Sigma-Aldrich company Ltd, Great Britain). Analytical-grade methanol, acetonitrile were from VWR® (Fontenay-sous-Bois, France), water and ethanol from Fisher Scientific® (Leics, UK) respectively. Tyr, caffeic acid, *p*-coumaric acid and gallic acid were supplied by Sigma-Adrich® (Deisenhofer, Germany) and HT was purchased from Extrasynthèse (Genay, France).

2.1.2   Spectroscopic analyses

UV analyses were performed on Agilent® 8453 UV-Visible spectrophotometer in a quartz cell (1 cm length). Thanks to the total phenolic content determination (Folin-Ciocalteu method), the molar absorption coefficient of alperujo was estimated: ε(alperujo) = M^{-1} cm^{-1} at 277nm in gallic acid equivalent (g.a.e.).

2.1.3   Preparation of alperujo samples

Alperujo (Aglandau variety, 72% of moisture) was manually pressed, then filtered on celite and passed through 0.45μm and 0.2μm paper filters (VWR). The AF indicates the aqueous fraction obtained from alperujo.

A protein-free alperujo sample was also investigated. Ethanol was added to a final proportion of 42% to precipitate proteins (removed by centrifugation) and ethanol was evaporated under vacuum. PF refers to this protein-free alperujo solution.

To 25mL of AF or PF (8.7mM g.a.e.) was added β-CD according to a β-CD/phenol molar ratio of 1:1, 3:1, 5:1, 10:1.

To optimize the phenolic concentration, 10mL of 96mM C-AF were mixed with β-CD at 20°C. The β-CD/phenol molar ratio of 10:1 was investigated.

All analyses were performed on fresh alperujo solutions. Each analysis was repeated three times.

2.1.4 Total phenolic content

As commonly, the total phenolic content was measured with the Folin-Ciocalteu reagent. According to the modified Box protocol [48], 2.5ml of diluted sample were mixed with 0.125mL of Folin-Ciocalteu reagent. After three minutes, 0.050mL of a 35% sodium carbonate solution was added. After 1h in a dark room, the absorbance was measured at 750nm against a blank. Quantitative analysis was allowed by a calibration curve of gallic acid.

2.1.5 UHPLC-DAD analyses

Analyses were performed using an Acquity UHPLC® system (Waters, Milford, MA, USA) linked to both a diode array detector (DAD: 200–800 nm, Waters, Milford, MA, USA). The separation was performed on an Acquity C18 BEH column (50x2.1 mm i.d., 1.7 µm). The solvents were (A) water/formic acid (99.5/0.5) and (B) acetonitrile. The gradient was linear and the proportions of solvent B used were: 0–10 min: 1–20%, 10–12 min: 20-30%, 12–14 min: 30-100%. The injection volume was 1 µL and the column temperature was kept at 35°C. Along the 3 steps of the gradient, the flow rate was 0.30, 0.35 and 0.40 mL/min. The spectroscopic detection was performed in the range 200-600 nm with a resolution of 1.2 nm. The concentrations of the main phenolic compounds, i.e. HT, Tyr, caffeic and *p*-coumaric acids were estimated from calibration curves (peak area vs. concentration). All analyses were run in triplicate.

2.1.6 Kinetic procedure

Sample solutions were mixed with β-CD in the solid state at 20°C under stirring at 250 rpm. The phenol concentration in the supernatant was followed by UV/Vis spectroscopy over 3h. A brief supplementary centrifugation as well as dilution in water could be carried out if necessary.

2.1.7 Analysis of solid complexes

2.1.7.1. Solid and biophenol recovery procedure

At the end of kinetics, the olive phenol + β-CD mixture was filtered on a glass filtering funnel (porosity 5). The recovered solid was dried at 35°C until the mass variation was less than 10%. The solid recovery was determined as a percentage of the initial solid amount. It was

corrected for the solubilized β-CD amount (16 g L^{-1} at 20°C) to determine the true solid recovery efficiency.

2.1.5.2. *Loading and extraction efficiencies*

The final powders recovered from the kinetic procedure were analyzed to determine the exact amount of phenols (Folic-Ciocalteu method) retained by solid β-CD. Thus, 50 mg of powder were rinsed with 2 mL MeOH and filtered on a 0.2 μm PTFE syringe. The loading efficiency Qe (mmol / 100 g) and the extraction efficiency (EE) were then calculated as follows:

$$Qe = \frac{Cp.Vs}{m} \times 100$$

and

$$EE = \frac{Cp.Vs}{m} \times \frac{m(recovered\ solid)}{Ci.Vi} \times 100$$

Where Cp is the total phenolic content (gallic acid equivalent) in the MeOH fraction, Vs = volume of MeOH (2 ml), Ci = initial phenol concentration, Vi = initial volume, m = mass of the rinsed powder.

2.2   Results and discussion

2.2.1   Influence of the phenol - β-CD molar ratio

Figure V.5 presents the biophenol extraction from alperujo samples according to several β-CD/biophenol molar ratios over 3 h.
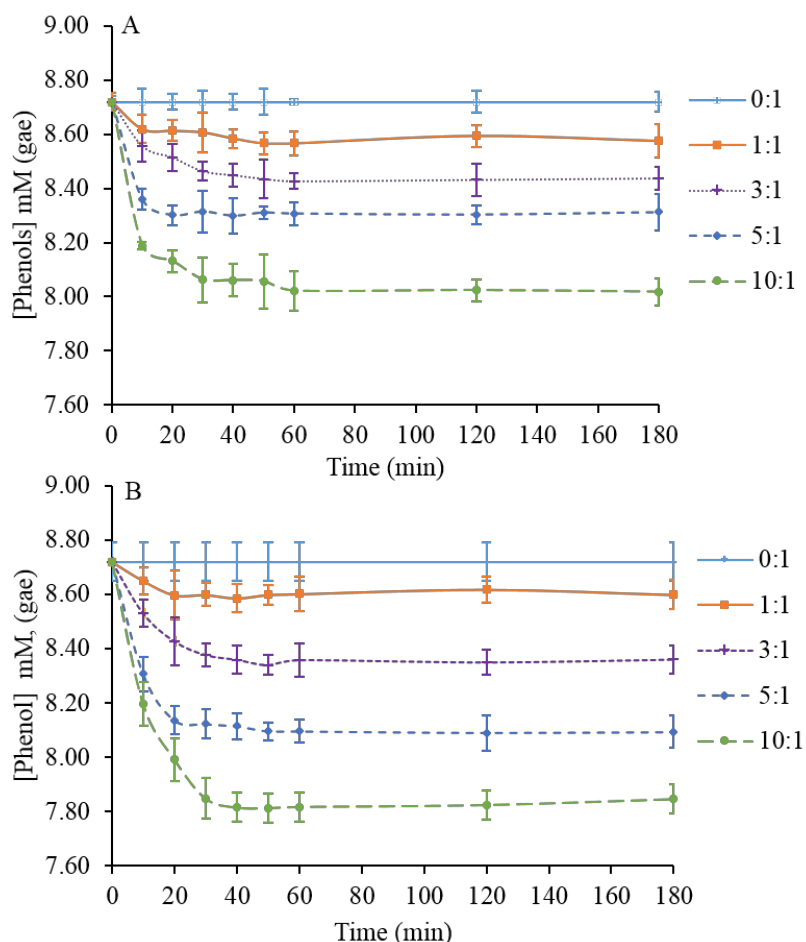
Figure V.5. Time-dependence of the phenol concentration according to the β-CD/phenol molar ratio for AF (A) and PF (B)

One β-CD molar equivalent was below its solubility limit (16 g/L at 20°C). However, no solid powder was also recovered from the β-CD/phenol molar ratio 3:1. So, the β-CD solubility seemed to be higher in aqueous plant extract. The absorbance shifts could then be the results of the formation of inclusion complexes in solution. Similar kinetic behaviors were obtained for AF and PF. The phenol concentration in the supernatant decreased with the β-CD/phenol molar ratio for 60min. Similar kinetics were obtained in literature about the phenol removal from an aqueous solution by using modified β-CD. Researchers succeeded to remove phenols from an aqueous solution in around one hour for reaching equilibrium [23,49].

The solid recovery, the extraction and loading efficiencies for AF and PF are presented in table V.4.

Table V.4. Solid recovery, extraction and loading efficiencies for an 8.7mM AF or PF solution

	β-CD/Phenol molar ratio	Solid recovery (%)	Solid recovery efficiency (%)	Extraction efficiency (%)	Loading efficiency Qe (mmol/100g)	(mg/g)
AF	5:1	12.8 ± 1.2	41.7 ± 1.2	2.6 ± 0.2	2.8 ± 0.3	4.7 ± 0.6
	10:1	52.9 ± 3.1	69.1 ± 2.1	4.9 ± 0.3	0.8 ± 0.0	1.4 ± 0.1
PF	5:1	13.6 ± 2.4	42.5 ± 2.4	2.9 ± 0.2	3.3 ± 0.4	5.8 ± 0.6
	10:1	59.7 ± 2.7	75.9 ± 2.7	5.6 ± 0.6	0.8 ± 0.1	1.4 ± 0.1

The solid recovery was possible from the β-CD/phenol molar ratio of 5:1. Thus, 12.8% to 52.9% of the initial solid quantity were recovered for AF. After correction for the amount of solubilized β-CD, the values increased from 41.7% to 69.2 %. Similar data were obtained for PF condition. For comparison, using freeze-drying, Wilkowska *et al*. (2016) obtained a 78.1% yield for bluerberry (poly)phenols encapsulated into β-CD and Borghetti *et al*. (2009) obtained a 77% yield using spray-drying for quercetin-β-CD complexes [18,50].

The extraction efficiency (EE) was determined from the phenol concentration in the rinsed MeOH fraction compared to the initial content. EE increased at higher β-CD/phenol molar ratio, from 2.6% to 4.9% (for AF); and Qe conversely decreased. Similar values were obtained for PF. The β-CD/phenol molar ratio of 10:1 offered the higher extraction efficiency.

These kinetic procedures for the phenols extraction using solid β-CD led to conclude that the presence of protein had no significant effect on the phenol recovery.

2.2.2 Influence of the biophenol concentration

The β-CD/phenol molar ratio of 10:1 offered the higher extraction efficiency and has been tested with a concentrated alperujo fraction (C-AF, 96mM g.a.e.). Figure V.6 showed the phenol concentration in the supernatant plotted as a function of time.
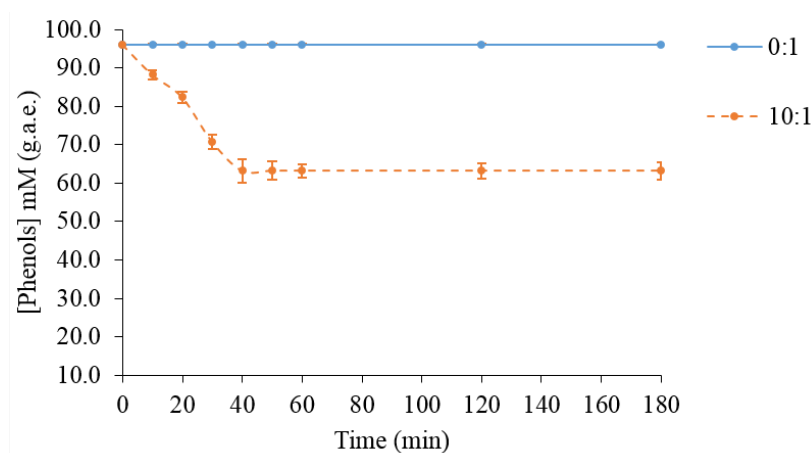
Figure V.6. Time-dependence of phenol concentration in a concentrated AF according to the β-CD/phenols molar ratio

As before, the concentration in the supernatant decreased with solid β-CD over time and the procedure was complete for one hour. Solid recovery increased from 73.9 % to 75.4% after correcting with the solubility limit. A higher extraction efficiency of 30.9 % was reached for the molar ratio 10:1 by working with concentrated AF. The loading efficiency of 6.6 mg g.a.e./g of solid was also higher than in any assays realized in a dilute alperujo sample.

Table V.5. Solid recovery, extraction and loading efficiencies for C-AF

	β-CD/phenol molar ratio	Solid recovery (%)	Solid recovery efficiency (%)	Extraction efficiency (%)	Loading efficiency Qe	
					mmol/100g	mg/g
C-AF	10:1	73.9 ± 2.1	75.4 ± 2.1	30.9 ± 1.7	3.8 ± 0.1	6.6 ± 0.2

2.2.3   UHPLC-DAD analyses

The powder recovered from a 96 mM C-AF mixed with 10 β-CD equivalents (10:1, β-CD/phenol molar ratio) was selected for the accurate chromatographic analysis of its phenolic content. Figure V.7 shows the chromatograms of C-AF (red) and the rinsed MeOH fraction (black).

These analyzes was performed thanks to a method previously developed for the fast determination of the phenolic compound profile of two-phase olive mill by-products [51].
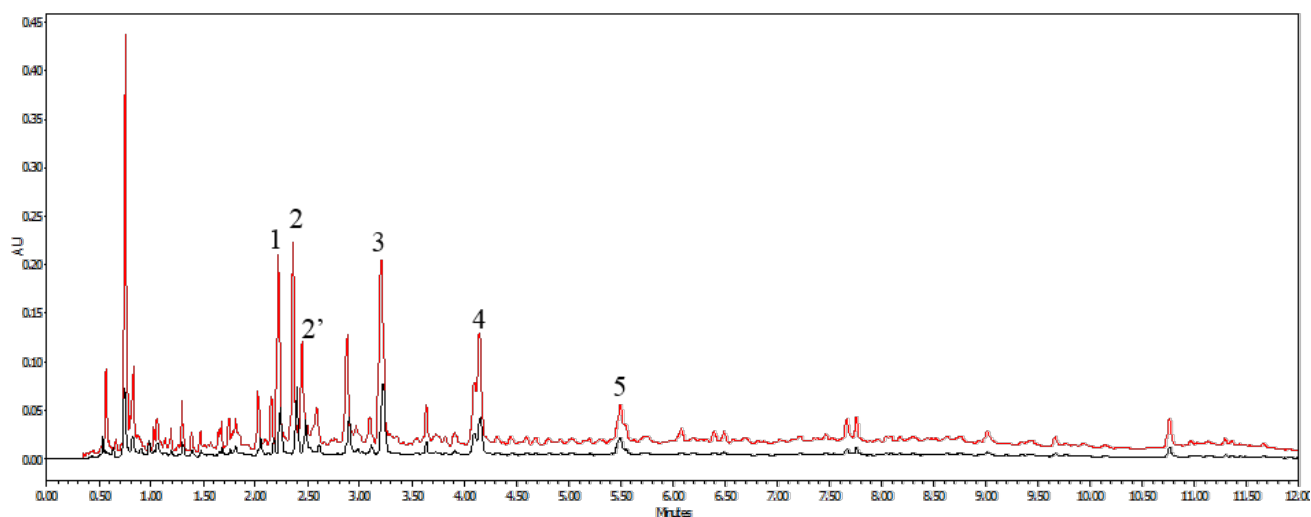
1: HT; 2: HT-glucoside (HT-Glc); 2': HT-Glc isomer; 3: Tyr; 4: caffeic acid; 5: p-coumaric acid.

Figure V.7. UHPLC-DAD chromatograms of C-AF (red) and of the rinsed MeOH fraction (black) (280nm)

The 6 most abundant biophenols, i.e., HT, HT-Glc, Tyr, caffeic cid and p-coumaric acid were ranged from 77.1 mg L^{-1} for *p*-coumaric acid to more than 2500 mg L^{-1} for tyrosol in C-AF.

Almost 16 % and 20 % of HT and its glucosides respectively, and almost 27 % and 32 % of caffeic acid and *p*-coumaric acid were extracted from C-AF (Table V.6.).

Table V.6. Concentration and extraction efficiency of the six major phenols of alperujo

	C-AF (mg.L^{-1})			MeOH (mg.L^{-1})*			EE (%)		
HT	1197.2	±	17.5	189.3	±	13.9	15.8	±	1.2
HT-Glc1	1170.9	±	44.7	232.9	±	15.4	19.9	±	1.3
HT-Glc2	705.4	±	43.1	133.7	±	10.8	19.0	±	1.5
Tyr	2534.1	±	120.1	552.9	±	46.9	21.8	±	1.9
Caffeic acid	107.3	±	7.2	28.8	±	3.6	26.8	±	3.4
p-coumaric acid	77.1	±	3.9	24.8	±	1.6	32.1	±	2.1
Total	5792.0	±	236.4	1162.3	±	92.2	20.0	±	0.8

*rinse MeOH fraction. Related to the total solid recovered

The inside distribution of each main phenolic compounds in C-AF and the rinsed methanol fraction were compared (Figure V.8). Tyr represented 46% of the total of the six main phenolic compounds in C-AF, while HT and its glucosides almost 20%. Smaller portions of both cinnamic acids i.e. caffeic and *p*-coumaric acids were quantified (1.2% and 1.5%). No significant difference was observed between the phenolic profile of C-AF and of the solid phenol-β-CD particles recovered.
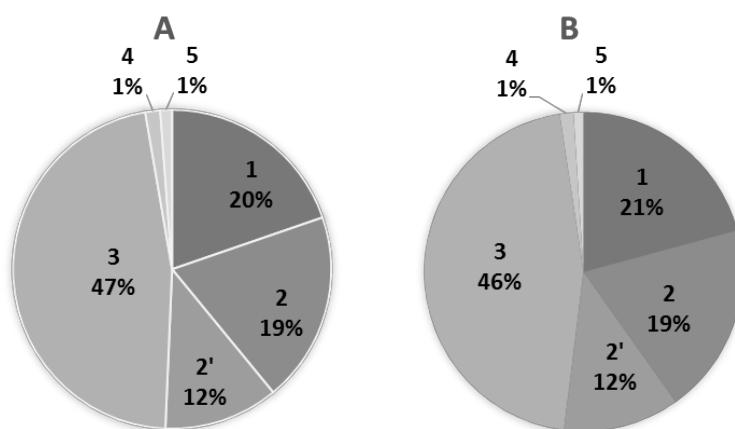
A: C-AF; B: solid recovered; 1: HT; 2: HT-Glc; 2': HT-Glc isomer; 3: Tyr; 4: caffeic acid; 5: p-coumaric acid.

Figure V.8. Relative distributions of the six major phenolic compounds in C-AF (A) and in the solid recovered (B)

2.3 Conclusion

The use of native β-CD in the solid state as a phenol-extracting agent has been evaluated on the aqueous fraction from alperujo. A pre-concentration step was required before mixing phenolic solution with the solid β-CD. More than 20% of alperujo phenolic compounds, including HT and its glucosides, were extracted by β-CD in the solid state. This procedure

offered a new simple and eco-friendly pathway to extract phenolic compounds from olive by-products. Furthermore, the phenol-rich powder recovered could then be reserved for food or nutraceutical industries.

References

1. Tsagaraki E, Lazarides HN, Petrotos KB. 2007. Olive mill wastewater treatment. *Util. - Prod. Treat. Waste Food Ind.* Springer, pp 133–157.

2. Rodis PS, Karathanos VT, Mantzavinou A. 2002. Partitioning of Olive Oil Antioxidants between Oil and Water Phases. *J. Agric. Food Chem.* 50:596–601.

3. Organization WH, others. 2008. *Guidelines for drinking-water quality [electronic resource]: incorporating 1st and 2nd addenda, vol. 1, Recommendations.* World Health Organization.

4. Iboukhoulef H, Amrane A, Kadi H. 2016. Removal of phenolic compounds from olive mill wastewater by a Fenton-like system $H_2O_2/Cu(II)$—thermodynamic and kinetic modeling. *Desalination Water Treat.* 57:1874–1879.

5. Chedeville O, Debacq M, Porte C. 2009. Removal of phenolic compounds present in olive mill wastewaters by ozonation. *Desalination.* 249:865–869.

6. Comandini P, Lerma-García MJ, Massanova P, Simó-Alfonso EF, Gallina Toschi T. 2015. Phenolic profiles of olive mill wastewaters treated by membrane filtration systems. *J. Chem. Technol. Biotechnol.* 90:1086–1093.

7. Aly AA, Hasan YNY, Al-Farraj AS. 2014. Olive mill wastewater treatment using a simple zeolite-based low-cost method. *J. Environ. Manage.* 145:341–348.

8. Abdelkreem M. 2013. Adsorption of Phenol from Industrial Wastewater Using Olive Mill Waste. *APCBEE Procedia.* 5:349–357.

9. Aliakbarian B, Casazza AA, Perego P. 2011. Valorization of olive oil solid waste using high pressure–high temperature reactor. *Food Chem.* 128:704–710.

10. Ena A, Pintucci C, Carlozzi P. 2012. The recovery of polyphenols from olive mill waste using two adsorbing vegetable matrices. *J. Biotechnol.* 157:573–577.

11. Fernández-Bolaños JG, Marset A, López-García MÁ, López Ó. 2012. *Biological Properties of Hydroxytyrosol and Its Derivatives.* INTECH Open Access Publisher.

12. EFSA Panel on Food Additives and Nutrient Sources added to Food (ANS), Mortensen A, Aguilar F, Crebelli R, Di Domenico A, Dusemund B, Frutos MJ, Galtier P, Gott D, Gundert-Remy U, Leblanc J, Lindtner O, Moldeus P, Mosesso P, Parent-Massin D, Oskarsson A, Stankovic I, Waalkens-Berendsen I, Woutersen RA, Wright M, Younes M, Boon P, Chrysafidis D, Gürtler R, Tobback P, Arcella D, Rincon AM, Lambré C. 2016. Re-evaluation of β-cyclodextrin (E 459) as a food additive. *EFSA J.* 14.

13. Zarzycki PK, Fenert B ena, Głód BK. 2016. Cyclodextrins-based nanocomplexes for encapsulation of bioactive compounds in food, cosmetics, and pharmaceutical products: principles of supramolecular complexes formation, their influence on the antioxidative properties of target chemicals, and recent advances in selected industrial applications. *Encapsulations.* Elsevier, pp 717–767. doi:10.1016/B978-0-12-804307-3.00017-X.

14. Rescifina A, Chiacchio U, Iannazzo D, Piperno A, Romeo G. 2010. β-Cyclodextrin and Caffeine Complexes with Natural Polyphenols from Olive and Olive Oils: NMR, Thermodynamic, and Molecular Modeling Studies. *J. Agric. Food Chem.* 58:11876–11882.

15. López-García MÁ, López Ó, Maya I, Fernández-Bolaños JG. 2010. Complexation of hydroxytyrosol with β-cyclodextrins. An efficient photoprotection. *Tetrahedron*. 66:8006–8011.

16. Mourtzinos I, Salta F, Yannakopoulou K, Chiou A, Karathanos VT. 2007. Encapsulation of Olive Leaf Extract in β-Cyclodextrin. *J. Agric. Food Chem*. 55:8088–8094.

17. Mourtzinos I, Papadakis SE, Igoumenidis P, Karathanos VT. 2011. Encapsulation of Melissa Officinalis leaf's active compounds in β-cyclodextrin and modified starch. *Procedia Food Sci*. 1:1679–1685.

18. Wilkowska A, Ambroziak W, Czyżowska A, Adamiec J. 2016. Effect of Microencapsulation by Spray-Drying and Freeze-Drying Technique on the Antioxidant Properties of Blueberry (*Vaccinium myrtillus*) Juice Polyphenolic Compounds. *Pol. J. Food Nutr. Sci*. 66.

19. Hundre SY, Karthik P, Anandharamakrishnan C. 2015. Effect of whey protein isolate and β-cyclodextrin wall systems on stability of microencapsulated vanillin by spray–freeze drying method. *Food Chem*. 174:16–24.

20. García-Padial M, Martínez-Ohárriz MC, Isasi JR, Vélaz I, Zornoza A. 2013. Complexation of tyrosol with cyclodextrins. *J. Incl. Phenom. Macrocycl. Chem*. 75:241–246.

21. Ahmaruzzaman M. 2008. Adsorption of phenolic compounds on low-cost adsorbents: A review. *Adv. Colloid Interface Sci*. 143:48–67.

22. Soto ML, Moure A, Domínguez H, Parajó JC. 2011. Recovery, concentration and purification of phenolic compounds by adsorption: A review. *J. Food Eng*. 105:1–27.

23. Aoki N, Murai H, Hattori K. 2010. Removal of Phenolic Compounds from Aqueous Solutions using Ionic Interaction between Cyclodextrin Derivatives and Chitosan. *Trans. Mater. Res. Soc. Jpn*. 35:809–812.

24. Romo A, Peñas FJ, Isasi JR, García-Zubiri IX, González-Gaitano G. 2008. Extraction of phenols from aqueous solutions by β-cyclodextrin polymers. Comparison of sorptive capacities with other sorbents. *React. Funct. Polym*. 68:406–413.

25. Xiaohong LI, Baowei Z, Kun ZHU, Xuekui HAO. 2011. Removal of nitrophenols by adsorption using β-cyclodextrin modified zeolites. *Chin. J. Chem. Eng*. 19:938–943.

26. Wang H, Wang Y, Zhou Y, Han P, Lü X. 2014. A Facile Removal of Phenol in Wastewater Using Crosslinked β-Cyclodextrin Particles with Ultrasonic Treatment: Removal of Phenol in Wastewater Using β-CD. *CLEAN - Soil Air Water*. 42:51–55.

27. Jantarat C, Sirathanarun P, Ratanapongsai S, Watcharakan P, Sunyapong S, Wadu A. 2014. Curcumin-Hydroxypropyl-beta-Cyclodextrin Inclusion Complex Preparation Methods: Effect of Common Solvent Evaporation, Freeze Drying, and pH Shift on Solubility and Stability of Curcumin. *Trop. J. Pharm. Res*. 13:1215.

28. Kumar NS, Suguna M, Subbaiah MV, Reddy AS, Kumar NP, Krishnaiah A. 2010. Adsorption of Phenolic Compounds from Aqueous Solutions onto Chitosan-Coated Perlite Beads as Biosorbent. *Ind. Eng. Chem. Res*. 49:9238–9247.

29. Azbar N, Bayram A, Filibeli A, Muezzinoglu A, Sengul F, Ozer A. 2004. A review of waste management options in olive oil production. *Crit. Rev. Environ. Sci. Technol*. 34:209–247.

30. Moral PS, Méndez MVR. 2006. Production of pomace olive oil. *Grasas Aceites*. 57:47–55.

31. Volpe M, D'Anna C, Messineo S, Volpe R, Messineo A. 2014. Sustainable Production of Bio-Combustibles from Pyrolysis of Agro-Industrial Wastes. *Sustainability*. 6:7866–7882.

32. Di Giovacchino L. 2000. Technological aspects. *Handb*. *Olive Oil*. Springer, pp 17–59.

33. Topi D, Beqiraj I, Seiti B, Halimi E, others. 2014. Environmental impact from olive mills waste disposal, chemical analysis of solid wastes and wastewaters. *J*. *Hyg*. *Eng*. *Des*. 7:44–48.

34. Borja R, Raposo F, Rincón B. 2006. Tecnología de tratamiento de los efluentes líquidos y residuos sólidos resultantes del proceso de elaboración del aceite de oliva por centrifugación en dos fases. *Grasas Aceites*. 57:32–46.

35. Doula MK, Moreno-Ortego JL, Tinivella F, Inglezakis VJ, Sarris A, Komnitsas K. 2017. Olive mill waste: recent advances for the sustainable development of olive oil industry. *Olive Mill Waste*. Elsevier, pp 29–56. doi:10.1016/B978-0-12-805314-0.00002-9.

36. Alburquerque J. 2004. Agrochemical characterisation of 'alperujo', a solid by-product of the two-phase centrifugation method for olive oil extraction. *Bioresour*. *Technol*. 91:195–200.

37. Obied HK, Allen MS, Bedgood DR, Prenzler PD, Robards K, Stockmann R. 2005a. Bioactivity and Analysis of Biophenols Recovered from Olive Mill Waste. *J*. *Agric*. *Food Chem*. 53:823–837.

38. Priego-Capote F, Ruiz-Jiménez J, Luque de Castro M. 2004. Fast separation and determination of phenolic compounds by capillary electrophoresis–diode array detection. *J*. *Chromatogr*. *A*. 1045:239–246.

39. Achmon Y, Fishman A. 2015. The antioxidant hydroxytyrosol: biotechnological production challenges and opportunities. *Appl*. *Microbiol*. *Biotechnol*. 99:1119–1130.

40. Bulotta S, Celano M, Lepore SM, Montalcini T, Pujia A, Russo D. 2014. Beneficial effects of the olive oil phenolic components oleuropein and hydroxytyrosol: focus on protection against cardiovascular and metabolic diseases. *J*. *Transl*. *Med*. 12:219.

41. Natella F, Nardini M, Di Felice M, Scaccini C. 1999. Benzoic and Cinnamic Acid Derivatives as Antioxidants: Structure−Activity Relation. *J*. *Agric*. *Food Chem*. 47:1453–1459.

42. Zhongxiang Fang, Bhesh Bhandari. 2010. Encapsulation of polyphenols – a review. *Trends Food Sci*. *Technol*. 21:510–523.

43. Ratnasooriya CC, Rupasinghe HPV. 2012. Extraction of phenolic compounds from grapes and their pomace using β-cyclodextrin. *Food Chem*. 134:625–631.

44. Szejtli J. 1990. The cyclodextrins and their applications in biotechnology. *Carbohydr*. *Polym*. 12:375–392.

45. Lesmes U, McClements DJ. 2009. Structure–function relationships to guide rational design and fabrication of particulate food delivery systems. *Trends Food Sci*. *Technol*. 20:448–457.

46. Barão CE, Paiva-Martins F, Zanin GM, Moraes FF. 2014. Determination of the inclusion complex constant between oleuropein and cyclodextrins by complexation theory. *J. Incl. Phenom. Macrocycl. Chem.* 78:465–470.

47. Mourtzinos I, Papadakis SE, Igoumenidis P, Karathanos VT. 2011. Encapsulation of Melissa Officinalis leaf's active compounds in β-cyclodextrin and modified starch. *Procedia Food Sci.* 1:1679–1685.

48. Box J.D. 1983. Determination of Total Phenolic Content in Olive Oil Samples by UV–visible Spectrometry and Multivariate Calibration - Springer. *Water Res.* 17:511–525.

49. Oughlis-Hammache F, Senhadji-Kebiche O, Ali SA, Lahlou H, Benamor M. Removal of Phenol from Aqueous Solutions by Polymer Inclusion Membranes (PIMs): Modeling of the Extraction Process.

50. Borghetti GS, Lula IS, Sinisterra RD, Bassani VL. 2009. Quercetin/β-Cyclodextrin Solid Complexes Prepared in Aqueous Solution Followed by Spray-drying or by Physical Mixture. *AAPS PharmSciTech.* 10:235–242.

51. Malapert A, Reboul E, Loonis M, Dangles O, Tomao V. 2017. Direct and Rapid Profiling of Biophenols in Olive Pomace by UHPLC-DAD-MS. *Food Anal. Methods.* doi:10.1007/s12161-017-1064-2.

Chapter VI. *In vitro* bioavailability of phenolic compounds from alperujo

1 Effect of foods and β-cyclodextrin on the bioaccessibility and the uptake by Caco-2 cells of hydroxytyrosol from either a pure standard or from alperujo

Abstract

HT bioaccessibility and absorption by the intestinal cells have been studied using an *in vitro* digestion model and Caco-2 TC7 monolayers cells in culture, in the presence or absence of β-CD and foods. HT was either provided as a pure standard or in an alperujo powder. The presence of foods significantly decreased both the HT bioaccessibility and absorption (-20% and -10%, respectively), while β-CD had no effect. Moreover, the presence of other compounds from alperujo in the intestine compartment reduced HT absorption by Caco-2 cells compared to pure standard (-60%). The final bioavailability of HT, defined as its quantity at the basolateral side of cultured cell monolayers compared to the initial amount in the test meal, was 6.9±0.4%, 31.1±1.1% and 40.9±1.5% when HT was from alperujo, or a pure standard administered with or without food, respectively. The high metabolism of HT by the Caco-2/TC7 cells was responsible for its reduced bioavailability.

1.1 Introduction

Two-phase olive pomace, also called alperujo, is one of the most abundant industrial Mediterranean pollutants. It is produced in large quantity in two-phase centrifuge mills and is composed of olive vegetation water and solid olive pieces [1]. Nevertheless, this system allows reducing the water consumption and then the quantity of olive mill wastes compared to both traditional and three-phase centrifuge systems. Its pollutant character is especially due to its high phenolic content. Interestingly, lots of work have demonstrated the great interest of these phenolic compounds because of their high health benefits [2].

In order to valorize these co-products, the phenolic composition of alperujo has been extensively characterized, thus confirming that it can be an interesting source of valuable compounds for the nutraceutical, cosmetic and food industries. The major phenolic compounds identified into olive mill wastes wereHT and Tyr, both belonging to the phenyl alcohol family, as well as *p*-hydroxycinnamic acids such as caffeic acid and derivatives [3,4]. These molecules display a catechol unit that confer them a reducing (electron-donating) character tightly related to their bioactivity (e.g., their antioxidant potential) [5]. HT has received a health claim by the European Food Safety Agency (EFSA) due to its high ability to scavenge reactive oxygen

species and to reduce the risks of cardiovascular disease [6–8]. However, the electron-donating properties of olive phenols make them sensitive to oxidation. Hence, investigating the influence of the food matrix, including food ingredients used for formulation purposes, on the stability and bioavailability of olive phenols is a relevant issue.

CDs are natural cyclic oligosaccharides made of D-glucose units bound by α-1,4 linkages and mainly used in the agro-food and pharmaceutical industries to form inclusion complexes (IC) with bioactive compounds, to enhance their stability and solubility [9,10]. β-CD (7 D-glucose units) is the most used CD because of its low price, its availability and its ability to form inclusion complexes with a large range of medium-sized compounds (MM < 800 g/mol) [11]. β-CD can also be used to facilitate polyphenol extraction from plants, such as resveratrol from grape pomace [12–14].

In vitro digestion studies can be carried out to assess the bioaccessibility of a given compound, *i.e.* the fraction of the ingested dose that is transferred from the food matrix to the aqueous phase or to mixed micelles (combining bile acids and lipid digestion products). This fraction is considered as available for subsequent absorption by the enterocytes, which can be investigated using the Caco-2 cell model. Bioaccessibility and intestinal absorption are two critical steps governing a compound bioavailability, *i.e.* the fraction of the ingested dose (native forms + metabolites) that reaches the general blood circulation and/or target tissues [15].

In this work, we investigated the effects of foods, β-CD and plant matrix on the bioaccessibility and the intestinal absorption of HT (from a standard powder and from a local alperujo).

1.2   Materials and Methods

1.2.1   Materials

β-CD was given from Roquette Frères (Lestern, France). HT was kindly provided by Pr. Francesco Visioli (IMDEA, Madrid, Spain). Tyr and gallic acid were supplied from Sigma-Aldrich Co (St Louis, USA). Pepsin, porcine pancreatin, porcine bile extract, water, formic acid, ethanol and acetonitrile were purchased from Sigma-Aldrich (Fontenay sous Bois, France). Dulbecco's modified Eagle's medium (DMEM) containing 4.5 g/L glucose and trypsin-EDTA (500 mg/L and 200 mg/L, respectively), non-essential amino acids, penicillin/streptomycin and PBS were purchased from Life Technologies (Illkirch, France). Fetal bovine serum (FBS) came from PAA (Vélizy Villacoublay, France). Olive pomace was collected from the Castelas mill equipped with a two-phase centrifuge system (Baux-de-Provence, France). Foods were purchased from a local supermarket.

1.2.2   Preparation of the alperujo sample

Alperujo (Aglandau variety, 72% of moisture, stored in cheesecloth canvas) was manually pressed, then filtered on celite and passed through 0.45μm and 0.2μm paper filters (VWR). Ethanol was added to a final proportion of 42% to precipitate proteins (removed by centrifugation). After ethanol evaporation under vacuum, the aqueous alperujo sample was frozen at -20°C.

1.2.3   Preparation of the inclusion complexes

An aqueous equimolar (5 mM) solution of HT and β-CD was stirred at 200 rpm for 1h at room temperature, then freeze-dried. The inclusion complex was recovered in a solid form and kept in amber flask at -20°C until use.

The protein-free alperujo sample was diluted to reach a total phenol concentration of 5 mM in gallic acid equivalent. Then, β-CD was added to the sample in the same concentration and the solution was stirred at 200 rpm for 1h at room temperature. After freeze-drying, the alperujo + β-CD sample was stored at -20°C in amber glass. For comparison, an alperujo extract without β-CD was also freeze-dried.

1.2.4   Simulated digestion

The meal, when present, was composed of pureed potatoes (6.7 g), cooked minced beef (1.2 g) and refined olive oil (0.2 g). HT and alperujo samples with or without β-CD were added so as to reach 7 mg of HT in the meal. The simulated digestion was carried out as described previously [16]. All analyses were run in quadruplicate. Aliquots from oral, gastric and duodenal steps were taken up and frozen at -80°C until use.

1.2.5   Cell culture and uptake experiments

The human colon adenocarcinoma cell line Caco-2 TC-7 was cultured on transwell membrane (six-well plate, 1 mm pore size polycarbonate membrane; Becton Dickinson) to obtain confluent and differentiated cell monolayers as previously described [17].

Cytotoxicity of digestion samples on Caco-2/TC7 was primarily evaluated to determine the suitable dilution of the phenolic aqueous fractions in HBSS before adding them to the apical side of cell monolayers. These results showed that 1/20 and 1/10 dilutions were required for HT and alperujo samples, respectively (data not shown). To avoid any interference with DMEM or serum components, the phenolic aqueous fractions were diluted in HBSS and Caco-2 cells received HBSS in both chambers 12h before the experiments. At the beginning of each

experiment, cell monolayers were washed twice with 1 mL of PBS and received 1 mL of diluted aqueous fraction. Finally, cell monolayers were incubated at 37°C for 2h, 4h and 6h. After the incubation period, apical and basolateral solutions were harvested. Cell monolayers were washed twice with 1 mL of PBS and scraped in 0.5 mL of PBS. All samples were stored at -80°C until use.

1.2.6   Analyses of HT and alperujo samples

1.2.6.1. Extraction of digestion and cell media samples

Phenolic compounds were extracted from salivary, gastric and duodenal steps as follows: 0.3 mL ethanol was added to 0.2 mL of sample. The internal standards were respectively tyrosol and gallic acid for HT and alperujo samples. *n*-Hexane (0.2 mL) was added and the mixture was homogenized for 10 min using a vortex blender at maximal speed. After centrifugation (2500 rpm for 10 min at 4°C), the lower phase was collected and the sediment further extracted with 0.3 mL ethanol and additional vortexing for 10 min. The two ethanol phases were pooled, evaporated to dryness using a Speed-Vac®, and the dried extracts dissolved in 200 µL H₂O and frozen at -80°C before analysis. Apical media were directly injected. Basolateral media (1900 µL) were primarily dried using a Speed-Vac® and the residues dissolved in 80 µL H₂O.

The PBS fractions containing harvested cells (500 µL) were sonicated with 50 µL of internal standard for 10 min at room temperature and centrifuged at 7000 rpm for 10 min at 4°C [18]. Supernatants were recovered and evaporated to dryness, then dissolved in 50 µL H₂O and frozen at -80°C before analysis.

1.2.6.2. Chromatographic analysis

All extracts were analyzed by UHPLC-DAD-MS using an Acquity UHPLC® system linked to both a diode array detector and a Bruker Daltonics HCT Ultra Ion Trap mass spectrometer equipped with an Electron Spray Ionization (ESI) source operating in negative mode. The separation was performed on an Acquity C18 BEH column (50x2.1 mm i.d., 1.7 µm). The solvents were (A) water/formic acid (99.5/0.5) and (B) acetonitrile. For alperujo analyses, the proportions of solvent B used were: 0-10 min: 1-20%, 10-12 min: 20-30%, 12-14 min: 30-100%. The injection volume was 1 µL for all samples and 10 µL for cells and basolateral extracts. The column temperature was kept at 35°C. Along the 3 steps of the gradient, the flow rate was 0.30, 0.35 and 0.40 mL/min. Chromatograms were acquired at 280 nm. The spectroscopic detection was performed in the range 200-800 nm with a resolution of

1.2 nm. HT concentrations were estimated from a calibration curve (peak area vs. concentration) constructed with HT standard with R values greater than 0.99. Homovanillyl alcohol and homovanillyl alcohol glucuronide were quantified as HT equivalent [19]. For HT analyses, the same conditions conditions were used and the flow rate was constant at 0.30 mL/min. The proportions of B were: 0 – 2.4 min: 1-30%, 2.4 – 3 min: 30-100%.

1.2.6.3. Mass spectrometry

ESI mass spectra were obtained in the following conditions: ionization energy = 50 or 100 eV, capillary voltage = 2 kV, source temperature = 365°C. The drying gas was introduced at a flow rate of 10 L/min and the skimmer voltage was 40V. Scans were performed in the *m/z* range 100 – 2000.

1.2.6.4. Calculation and statistics

All the *in vitro* experiments were run in quadruplicate. Results were expressed as means and standard deviations. Differences between means were assessed using ANOVA followed by the post-hoc Tukey test for parametric data. P values under 0.05 were considered significant. The bioavailability was assessed by the ratio between the amount of phenolic compounds in the basolateral side and the initial amount added to the apical side or to the meal.

1.3 Results

1.3.1 HT bioaccessibility in the oral, gastric and duodenal compartments

The digestion of the HT in the 3 compartments was assessed with free HT and CD-bound HT. The influence of the meal on HT bioaccessibility was also evaluated with the HT-β-CD complex (HTCD). Figure VI.1 shows the percentage of remained HT in each compartment. In the mouth compartment, β-CD seems to act as a protective agent for HT within the meal, HT recovery being 87.6 % (± 1.2) and 96.4 % (± 1.1) for HT and HTCD respectively ($p < 0.0001$). In the absence of food (HTCD-FF), β-CD provided a weaker but still significant protective effect. In the gastric compartment, HT recoveries in this step were 91.3 % (± 2.7), 94.9 % (± 1.9) and 97.7 % (± 2.7) for HT, HTCD and HTCD-FF, respectively. No significant benefit of β-CD were observed. Conversely, the presence of food had a negative effect on HT recovery (HTCD *vs* HTCD-FF, $p < 0.05$). Finally, except for the HTCD condition, the stability of HT was not significantly different in the duodenal compartment at pH 6 compared to the gastric one. The total apparent losses in the aqueous fractions were 37.2 % (± 1.0), 33.6 % (± 0.9) and 13.5 % (± 3.2) for HT, HTCD and HTCD-FF respectively. There was thus no difference regarding HT bioaccessibility between free HT and its β-CD complex. However, the

absence of food significantly improved HT bioaccessibility compared to the other conditions ($p < 0.0001$).
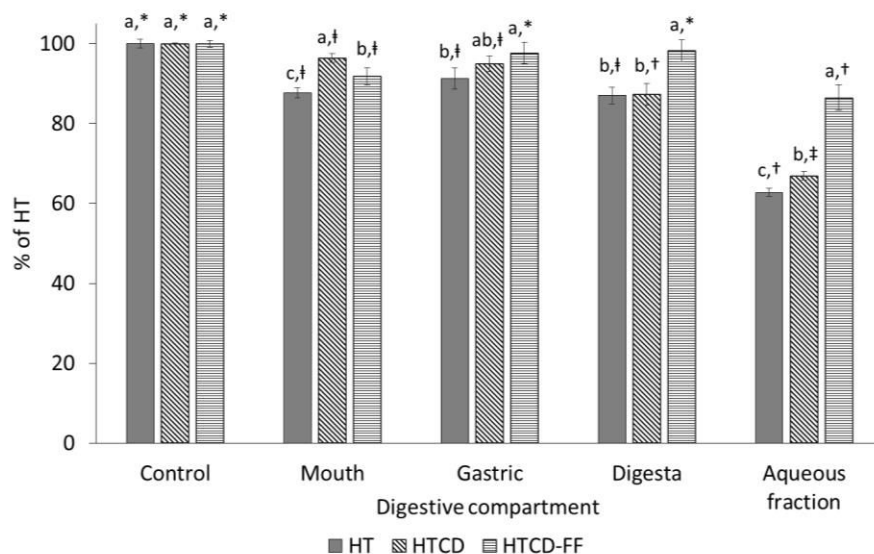
Values are expressed as mean ± SD of quadruplicate measurements. Different letters indicate a significant difference according to Tukey test ($p \leq 0.05$) between all conditions for each compartment. Different symbols indicate a significant difference according to Tukey test ($p \leq 0.05$) between all compartments for each condition.

Figure VI.1. Bioaccessibility of HT from standard powder in each digestive compartment

Figure VI.2 presents the bioaccessibility of HT from an alperujo powder during the same digestion steps.
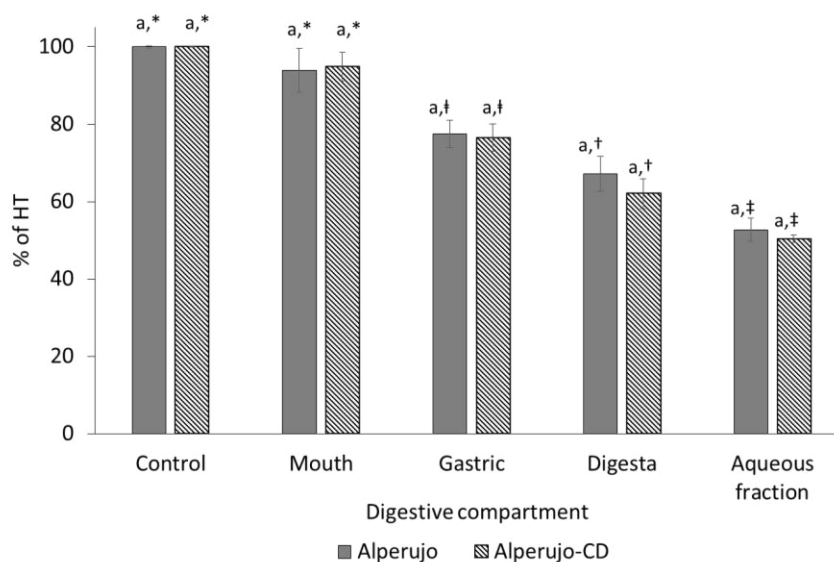
Values are expressed as mean ± SD of quadruplicate measurements. Different letters indicate a significant difference according to Tukey test ($p \leq 0.05$) between all conditions for each compartment. Different symbols indicate a significant difference according to Tukey test ($p \leq 0.05$) between all compartments for each condition.

Figure VI.2. Bioaccessibility of HT from alperujo powder in each digestive compartment

There was no significant influence of β-CD on HT recovery from alperujo in the different compartments. As for pure HT, no degradation was observed in the mouth while an

190

important loss was observed in the duodenal compartment. HT recovery from alperujo samples in the gastric compartment and in the aqueous phase decreased from 77.2 % (± 2.8) to 52.6 % (± 2.3) and from 76.4 % (± 2.7) to 50.3 % (± 1.2) for alperujo and alperujo-CD, respectively. HT recovery from alperujo samples decreased along digestion (p < 0.0001). The stability of HT into the alperujo samples appeared less important than for pure HT (p < 0.001).

1.3.2   HT absorption by Caco-2 TC7 cells

The absorption and metabolism of HT were studied using differentiated Caco-2 TC7 cell monolayers. Bioavailability was determined as the quantity of targeted compounds in the basolateral side *vs*. the initial amount added to the meal. The aqueous fractions obtained from the precedent digestion studies were used to study HT absorption into the enterocytes after a 1/10 or a 1/20 dilution for alperujo and HT samples, respectively. Thus, the cells received about 5.1-5.3, 6.0 and 6.7 µg/mL of HT from meals containing HT, HTCD or alperujo and from HTCD-FF, respectively. UHPLC-DAD-MS analyses allowed to identify homovanillyl alcohol (HVA) as a O-methylether metabolite of HT, giving a parent ion [M-H]$^-$ at *m/z* 167 and a fragment ion at *m/z* 153 (HT).

Figure VI.3 shows the quantity of HT and HVA recovered at the apical and basolateral sides of the cells. Each quantity was expressed as a percentage of the initial HT concentration at the apical side. For all conditions, a significant decrease of the HT content was observed at the apical side (more than 85%, p > 0.05) after 6h incubation. Concomitantly, a significant increasing quantity of HT was recovered at the basolateral side (>40%). The curve profiles highlight the time-dependent transport of HT from the apical to basolateral side. No significant difference was observed at the basolateral side between the three HT samples. HVA was the only HT metabolite observed in our conditions. It was mainly recovered at the apical side reaching about 32.8± 1.2%, 37.5± 4.1% and 40.3± 2.5% of the initial HT content for the HTCD-FF, HTCD and HT conditions, respectively. The lower percentage of HVA that appeared in the aqueous fraction without meal was due to the higher initial quantity of HT in this condition.
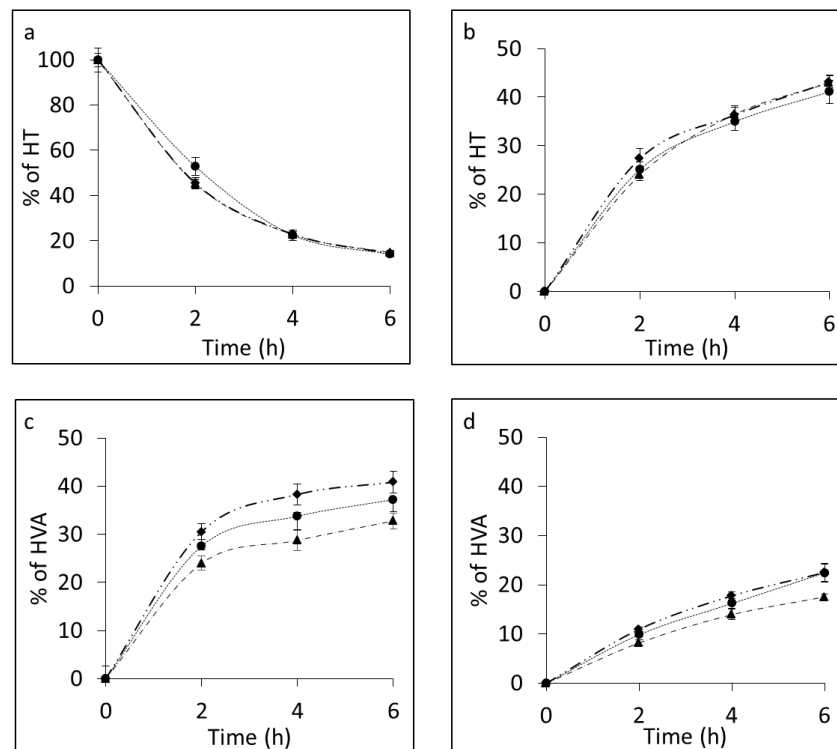
(a) Quantity of HT at the apical side; (b) Quantity of HT at the basolateral side; (c) Quantity of HVA at the apical side; (d) Quantity of HVA at the basolateral side. All results are expressed in percent of the initial HT amount at the apical side. (◆) HT meal; (●) HTCD meal; (▲) HTCD-FF. Values are expressed as mean ± SD of quadruplicate measurements.

Figure VI.3. Absorption and metabolism by Caco-2 TC7 cells of HT from HT standard samples

In the case of HTCD-FF, the initial HT amount was higher (+26%) compared to other conditions. The final HT amounts at the basolateral side were about 2.2 µg for HT and HTCD and 2.9 µg for HTCD-FF, respectively. Thus, the absorption of native HT from HTCD-FF increased over 30% (p < 0.0001) compared to conditions containing foods. The transport of HT through the intestinal barrier was also concentration-dependent. The same amount of HVA was approximately produced whatever the initial HT concentration. The amount of native HT at the basolateral side reached 65.7± 2.1%, 63.9± 1.4% of the initial apical content for HT and HTCD, and 71.0± 0.8% for HTCD-FF. The analysis of cell contents revealed neither HT nor HT metabolite: more than 99% of HT and its metabolite were recovered in the apical and basolateral compartments.

The absorption of HT from alperujo samples by Caco-2 cells was also evaluated, as shown in Figure VI.4.
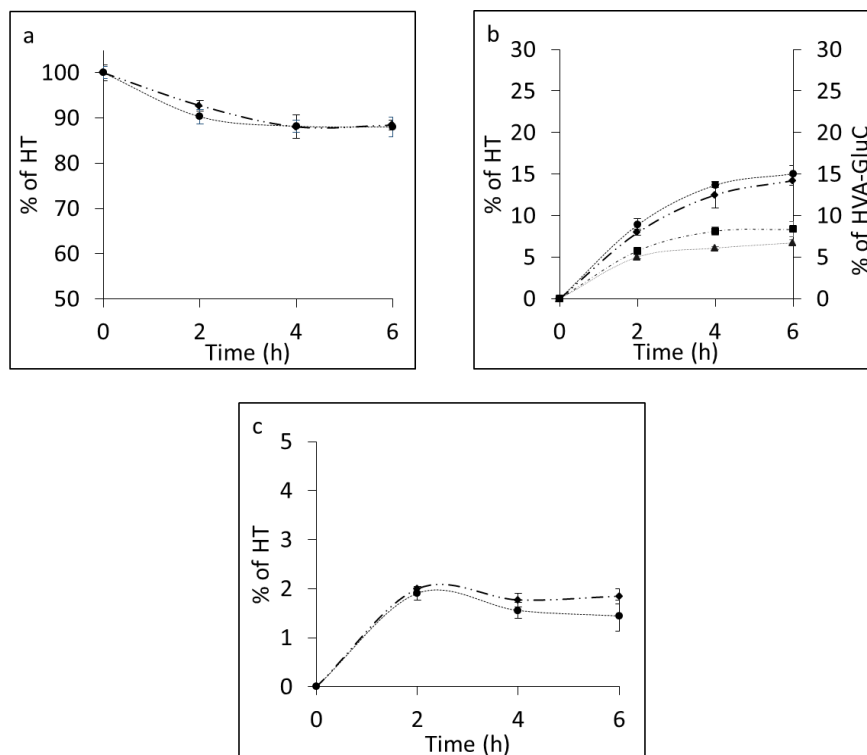
(a) Quantity of HT at the apical side; (b) Quantity of HT and homovanillyl alcohol glucuronide (HVA-GlcU) at the basolateral side; (c) Quantity of HT in the cytosolic compartment of Caco- 2 TC7 cells. All results are expressed in percent of the initial HT amount at the apical side. (●) HT from alperujo, (♦) HT from alperujo-CD; (▲) HVA-GlcU from alperujo (■) HVA-GlcU from alperujo-CD. Values are expressed as mean ± SD of quadruplicate measurements.

Figure VI.4. Absorption and metabolism by Caco-2 TC7 cells of HT from alperujo samples

The initial HT amount was around 6 µg at the apical side of the cells. The general curve profile indicates a time-dependent transport of HT. No significant difference regarding the amounts of both HT and its metabolite was found between alperujo and alperujo-CD samples in all culture media over time. About 0.88±0.05 µg and 0.91±0.04 µg of HT were recovered at the basolateral side for alperujo and alperujo-CD conditions, respectively. So, 14.4± 0.8% and 15± 0.5% of the initial apical HT amount from alperujo samples crossed the cell monolayers ($p > 0.05$). Despite the higher HT load in the alperujo conditions (about 6 µg *vs* 5.1-5.3 µg for alperujo conditions, HT and HTCD), the amount of HT absorbed was about 2.5-fold less important than for HT and HTCD conditions, *i.e.* the absorption rate decreases by more than 60% ($p < 0.0001$). Homovanillyl alcohol glucuronide (HVA-GlcU) was identified according to its molecular ion $[M-H]^-$ at *m/z* 343 and its fragment ions $[M-H-GlcU]^-$ at *m/z* 167 (HVA) and 153 (HT), characteristic of the homovanillyl moiety. This HT metabolite was only found in the basolateral compartment and was estimated at 6.9± 0.4% and 7.3± 0.3% of the initial apical HT amount for alperujo and alperujo-CD, respectively. The total amount of unmetabolized HT at the basolateral side was 68.8± 1.5% and 69.8±2.6 % for alperujo and alperujo-CD, respectively.

So, β-CD had no significant effect on the HT metabolism rate. In these conditions and conversely to the standard samples, a low amount of HT was recovered into Caco-2 cells. Moreover, the total recovery of HT in these three compartments exceeds 110 % after 6h of incubation (p < 0.0001). This may be explained by the fact that a partial metabolization of other compounds from alperujo could generate HT.

1.4   Discussion

The first step of HT digestion occurs in the mouth. Mastication favors interactions between the phenolic compounds, food, saliva and dioxygen. In this compartment, the protective effect of β-CD observed in our study may be linked to its ability to build a protective shell around HT, thereby limiting its contact with potential food prooxidants such as iron species.

In the stomach, food disintegration intensifies due to the periodic and synchronized contractions of its wall, the acidic environment and the enzymatic activity [20]. The *in vitro* digestion of HT standard confirmed that HT is stable in the acidic conditions of the gastric compartment, which is in accordance with previous data [21]. The recovery of HT after the gastric step was almost total, in agreement with Pereira-Caro *et al*. who obtained a recovery rate higher than 99 % in their *in vitro* digestion study without food [22]. In our work, the small loss (lower than 5%) in the gastric compartment may be due to interactions between HT and the food matrix.

In our duodenal conditions, the HT recovery did not significantly decrease. Several studies have shown that HT was not stable in neutral or mildly alkaline conditions. In their work on the digestion of phenolic compounds from olive oil, Soler *et al*. (2010) observed a loss of HT in alkaline conditions [23]. Corona *et al*. (2006) also observed that the amounts of HT and its derivatives progressively decreased during digestion by pancreatin (pH 7.5), reaching a total apparent loss of 20.3% after 2h for HT. This value took into account the formation of 3,4-dihydroxyphenylacetic acid (DOPAC) as a side-product of HT [24]. In our cases, no DOPAC formation was observed. We suggest that the total apparent losses in the aqueous fractions were the result of the partition of HT after the centrifugation step.

The comparative study of the HT standard and the HTCD sample showed a slight effect of β-CD on the final bioaccessibility of HT. β-CD is mainly used in the pharmaceutical industry to protect bioactive compounds and increase their water solubility and consequently their bioavailability [25]. As a cyclic starch derivative, β-CD may be partially hydrolyzed during

digestion. However *in vivo*, β-CD is mainly not digested in the upper gastrointestinal tract and can reach the large intestine where it is metabolized by the microflora fermentation [26-28]. Besides possible β-CD digestion, dilution is the major factor triggering the release of the guest compound from a CD complex [29]. This factor should be very important in our study because HT has only a weak affinity for β-CD (binding constant $< 10^2$ M^{-1} [30]). Overall, the bioaccessibility of HT from HTCD was not significantly increased compared to the free HT standard without β-CD.

In the absence of food, the bioaccessibility of HT was increased by almost 20% compared to the same sample in the presence of food. Many macromolecular food components can bind phenolic compounds and retain them within the food matrix. In this work, potato is a source of starch, which is known to retain phenolic compounds [31]. Similarly, beef is rich in proteins, which have a general affinity for phenols [32,33]. The clear influence of the food matrix on the bioaccessibility of dietary plant phenols such as HT outlines the importance of including real meal components in *in vitro* digestion studies.

The study with alperujo samples was carried out in the presence of food. In each compartment, HT from alperujo samples was generally less bioaccessible than from free standard. Indeed, although alperujo samples are protein-free, they contain fibers and sugars, which could interact with the meal components and the digestive enzymes (possibly slowing down protein and starch digestion), thereby reducing the bioaccessibility of phenolic compounds [2]. The apparent loss of HT bioaccessibility from alperujo powders (compared to the standard) was also higher (+10%). Again, no significant effect of β-CD was observed.

Caco-2 TC7 cells were then chosen as a suitable model to follow the absorption of target compounds through the intestinal barrier. HT was brought to the cells as an aqueous fraction obtained from our previous digestion study. The study of HT and its β-CD complex within a meal revealed that HT was largely absorbed through Caco-2 cells and partly metabolized into homovanillyl alcohol due to the catechol-O-methyltransferase (COMT) activity of the enterocytes. Most of the HT recovered at the basolateral side was unmetabolized (over 60%) and HVA was recovered in the two culture media, especially in the apical compartment. These data are in agreement with previous results. Indeed, Manna *et al*. (2000) observed that 25% of HT reached the basolateral side of Caco-2 cells after 1h, 90% of which being unmetabolized. They also identified HVA as a metabolite. They determined that HT reaches the basolateral side through passive diffusion and that this transport was time- and concentration-dependent

[34]. Corona *et al.* (2006) also observed 90% of unmetabolized HT at the basolateral side of the cells after the phenolic compounds were added to the apical side from a standard buffered solution [24]. Finally, Mateos *et al.* (2011) observed that 59% of HT from apical side (initial concentration = 50 µM) reached the basolateral side after 4h of incubation, with almost 20% recovered as O-methylether and 80% as unmetabolized HT [35]. In our study, for HT, HTCD and HTCD-FF conditions, the transport of unmetabolized HT from the apical to the basolateral side of Caco-2 cells ranged from 25.4± 1.5% to 42.3± 0.8% over 2 to 6h. The difference regarding HT absorption rates in our study compared to previous data is likely explained by the fact that HT was just dissolved in an aqueous buffer (HBSS or PBS) in previous studies, while we used a more complex mixture obtained from *in vitro* digestion.

In the case of HT from alperujo powders, we observed the appearance of HVA-GlcU as a HT metabolite. Moreover, the transport of HT from the apical to basolateral side ranged from 8.4± 0.6% to 14.7± 0.5% over 2 to 6h. This lower transport rates compared to HT standard conditions can be the result of a competition between HT and other alperujo components to cross the intestinal cells. The same phenomenon was observed when comparing the absorption of pure diosmetin and diosmetin from a rosemary extract [36]. Interestingly, a small amount of HT from alperujo was recovered into the harvested Caco-2 cells and the total recovery of HT exceeded 100%. If metabolized, HT-glucoside that is also present in alperujo extract (data not shown) could be a source of HT, which would explain this result.

Finally, it is interesting to compare two methods to calculate the *in vitro* bioavailability of HT, by making a ratio with either the initial HT apical content during the absorption experiments or the initial HT amount brought via the meal (Table VI.1). The second method allows to correct the common overestimation of the *in vitro* bioavailability when considering uniquely the absorption step and not the whole digestion process (Table VI.2).

Table VI.1. Bioavailability of phenolic compounds as percentage of HT initial apical amount

Samples	HT	HVA
HT	42.6 ± 2.5	22.2 ± 2.5
HTCD	41.4 ± 3.0	23.4 ± 2.0
HTCD-FF	43.0 ± 0.7	17.5 ± 0.6
Alperujo	14.4 ± 0.8	
Alperujo-CD	15.0 ± 0.5	

Values are expressed as mean ± SD of quadruplicate measurements.

Table IV.2. Bioavailability of phenolic compounds as percentage of HT initial amount in the test meal.

Samples	HT	HVA
HT	31.1 ± 1.1	16.2 ± 1.3
HTCD	30.9 ± 1.8	17.5 ± 1.4
HTCD-FF	40.9 ± 1.5	16.7 ± 0.6
Alperujo	6.9 ± 0.4	
Alperujo-CD	7.3 ± 0.3	

Values are expressed as mean ± SD of quadruplicate measurements.

The second values were decreased by more than 25% and 50% for HT standard and alperujo samples, respectively. This analysis confirmed that HT was more bioavailable when it was brought as a pure standard form than as a plant extract. The absence of food also participated in increasing the final HT bioavailability. HT bioavailability from the alperujo samples was lower, likely because of possible interactions between HT and other alperujo components and/or competition between them for absorption by Caco-2 cells [23].

1.5   Conclusion

In summary, β-CD did not modify the bioaccessibility and the bioavailability of HT from alperujo, in the presence or in the absence of foods. Conversely, interactions between food components (probably potato starch and beef proteins) and phenolic compounds were shown to decrease HT bioaccessibility. These interactions have a strong impact on HT final bioavailability, the HT amount absorbed by the intestinal cells being strongly dependent on the bioaccessible HT content. Besides, HT was more bioaccessible and better absorbed by enterocytes from a pure form than from an alperujo powder, in which it likely competes with other phenolic compounds for uptake by intestinal cells. HT absorption was time- and concentration-dependent. HVA was the only metabolite observed when HT was from a pure standard and HVA-GlcU was detected when HT was provided via alperujo powders. The low bioavailability of HT reflected its high metabolization in the intestine and the potential competition with other dietary plant phenols.

Our data have dietary significance as plant phenol supplements are usually consumed within a meal and under the form of complex mixtures, rather than individual supplements taken at fast.

2   Effect of β-cyclodextrin on the bioaccessibility and the uptake by Caco-2 cells of main phenolic compounds from alperujo

Abstract

Alperujo is one of the most studied olive by-products due to its high content in interesting phenolic compounds. This study focused on HT-Glc, Tyr, caffeic and *p*-coumaric acids from local alperujo powders. Phenolic compounds were complexed or not with β-CD, used as a protective agent, before we assessed their bioaccessibility (i.e. the percentage of molecule found in the aqueous phase of the digesta) and uptake by intestinal cells using an *in vitro* digestion model and Caco-2 TC7 monolayers cells in culture, respectively. Our results showed that β-CD had no effect on the bioaccessibility of HT-Glc, Tyr, caffeic and *p*-coumaric acids. HT-Glc and caffeic did not cross Caco-2 cell monolayers. Ferulic acid was identified as the main caffeic acid intestinal metabolite and was absorbed through intestinal cell monolayers (≈20%). Interestingly, β-CD moderately but significantly improved the local absorption of Tyr and *p*-coumaric acid (2.4% and 6.9%, respectively, p<0,05), even if their final bioavailability (expressed as bioaccessibility x absorption by Caco-2 cells) was not significantly modified (16.2 ± 0.6% vs 16.8 ± 0.5% for Tyr and 32.0 ± 3.2% vs 37.2 ± 3.2% for *p*-coumaric acid, from alperujo and alperujo-CD, respectively). Overall, we showed that β-CD did not negatively interfere with phenolic compounds. Besides, phenolic compound high metabolism by the Caco-2 cells as well as competition between molecules for absorption were likely responsible for their moderate bioavailability.

2.1   Introduction

Nearly 98% of the global olive production originates in the Mediterranean basin, among which 73% in Southern Europe with Spain, Italy and Greece as the main producers [37,38]. Alperujo is a two-phase olive mill waste composed of olive vegetation water and solid skins, pulp and seeds fragments [1]. Because of its high moisture and high phenolic content, this semi-solid leftover is considered as one of the largest Mediterranean pollutant [2].

Many studies confirmed the potential of alperujo as a concentrated and economic source of olive and olive oil phenolic compounds. Phenyl alcohols and cinnamic acids -

including HT, Tyr, caffeic acid and *p*-coumaric acid and their glycosidic forms (such as HT-Glc) - are the main phenolic families found in this olive pomace [3,4] (Figure VI.5).
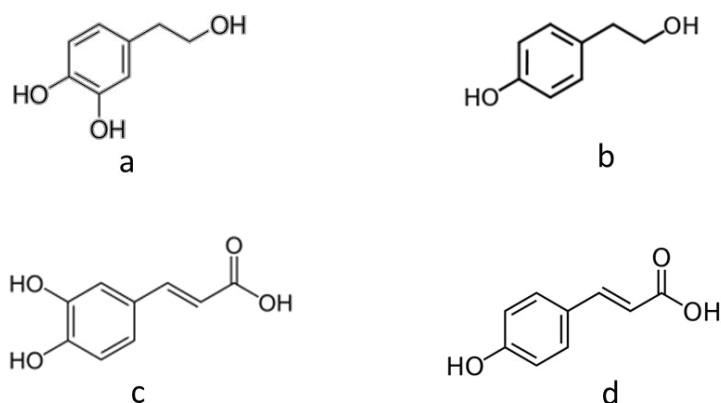
Figure VI.5. Chemical structures of hydroxytyrosol (a), Tyrosol (b), caffeic acid (c) and p-coumaric acid (d). The glucoside unit can be attached to one of the three HT hydroxyl units

All these biophenols were previously associated with health benefits such as anti-inflammatory, antidiabetic, cardioprotective or cell-apoptosis-reducing activities thank to their ability to reduce oxidative stress and improve the antioxidant status of individuals [7–11]. These phenols are thus considered as interesting bioactive compounds for food, cosmetic as well as pharmaceutic industries.

CDs are cyclic oligosaccharides composed of monomeric units of glucopyranose connected by α-1,4glycosidic bonds. All hydroxyl groups are steered to the exterior of the cavity, making CD hydrophilic [12,13]. Conversely, CD cavity, which is constituted by carbons, hydrogen atoms and glycosidic oxygen bridges, is more hydrophobic and rather apolar [14]. CDs can act as encapsulation agents for several compounds that are able to enter in the cavity. CDs thus have been extensively studied during the last decades [15–17]. Composed of 7 glucopyranose units, β-CD is the most common CD because of its low price, its safety and its efficiency to form inclusion complexes with a wide range of medium-sized compounds (MM < 800 g/mol) [13]. Their use as protective agent for phenolic compounds has been investigated recently [41]. Furthermore, CDs could enhance the extraction of phenolic compounds when CDs are used in aqueous solution as extraction solvent matter or as a pre-treatment in fresh plant material [14]. Studies highlighted the stability improvement

of phenolic compounds when they form inclusion complexes with CDs [30,41], which could be interesting to extract and protect phenols during storage periods [42-44]. Furthermore, it has been accepted that the bioavailability of nutrients such as (poly)phenols can be enhanced in presence of CDs which can improve their water solubility [45,46].

Phenolic compound bioavailability is still only partly understood and can be very low. As HT bioavailability has been studied in details previously [34,47-49], we focused in this study on i) the fate during the digestion process and ii) the absorption of four other major phenolic compounds from alperujo (variety: Aglandau), i.e. HT-O-Glc, Tyr, caffeic acid and *p*-coumaric acid, in the presence or absence of β-CD, using an *in vitro* digestion model and a human intestinal cell model in culture.

2.2   Materials and Methods

2.2.1   Supplies

β-CD was from Roquette Frères (Lestern, France). HT, Tyr, caffeic acid, *p*-coumaric acid and gallic acid were supplied from Sigma-Aldrich Co (St Louis, USA). Water, formic acid, ethanol and acetonitrile were purchased from Sigma-Aldrich (Fontenay sous Bois, France). Dulbecco's modified Eagle's medium (DMEM) containing 4.5 g/L glucose and trypsin-EDTA (500 mg/L and 200 mg/L, respectively) were purchased from BioWhittaker (Fontenay-sous-Bois, France), fetal bovine serum (FBS) came from Biomedia (Issy-les-Moulineaux, France), and non-essential amino acids, penicillin/streptomycin, Hanks' Balanced Salt Solution (HBSS) and phosphate-buffered saline (PBS) were purchased from Gibco BRL (Cergy-Pontoise, France). Pepsin, porcine pancreatin and porcine bile extract were purchased from Sigma- Aldrich Co (St Louis, USA). Alperujo was collected from the Castelas mill equipped with a two-phase centrifuge system (Baux-de-Provence, France). Foods were purchased from a local supermarket.

2.2.2   Preparation of alperujo sample

Alperujo (72% of moisture) contained in cheesecloth canvas was firstly pressed and filtered through celite followed by a passage through 0.45μm and 0.2μm (VWR). Ethanol was added in final proportion of 42% v/v to removed proteins. Ethanol was then evaporated and the aqueous alperujo fraction was frozen at -20°C.

2.2.3   Preparation of inclusion complexes

The protein-free alperujo aqueous fraction was diluted to reach a total phenolic content of 5mM in gallic acid equivalent. Then, β-CD was added in the sample to reach a molar ratio of 1:1 and was stirred at 200 rpm for 1h at room temperature. After freeze-drying, alperujo-CD powder was stored at -20°C in amber glass. In parallel, a freeze-dried powder of alperujo aqueous fraction without β-CD was also realized.

2.2.4   Preparation of the test meals for *in vitro* digestion

Meal was composed of 6.7 g of pureed potatoes, 1.2 g of fried minced beef and 0.2 g of refined olive oil. Alperujo samples, with or without β-CD, were added in such a way that almost 9.7mg of HT-Glc, 12.3mg of Tyr, 0.8mg of caffeic acid and 0.5mg of *p*-coumaric acid were added to the meal.

2.2.5   Simulated digestion

The simulated digestion was realized as described by Gonçalves *et al*. (2013) with minor changes. Briefly, meal components (including phenolic samples) were mixed with 32 mL of NaCl 0.9%. The mixture was dispersed with Ultra-Turrax® (Ika) and 2.5 ml of artificial saliva (pH 7) was added to the mixture. The sample was incubated for 10min at 37°C in a shaking incubator. The pH of the gastric medium was adjusted to 4 ± 0.02 with HCl 1M. Then, 2 mL of porcine pepsin (40 mg/mL in 0.1 M HCl) was added and the homogenate was incubated at 37°C in a shaking incubator for 30min simulating the gastric step. The pH of the mixture was raised to 6 ± 0.02 with $NaHCO_3$ 0.9M and 9ml of a mixture of porcin bile extract and pancreatin (2mg/mL pancreatin and 12mg/mL bile extract in 0.1M trisodium citrate, pH 6) and 4mL of porcine bile extract (0.1 g/ml) were added. Samples were incubated in a shaking incubator at 37°C for 30 min to complete the digestion process. The final mixture represented the digesta and was centrifuged (3000rpm for 1h12min) to isolate aqueous fraction. Finally, the aqueous fraction was successively passed through 0.8μm and 0.2μm filters (Milipore) [17].

All analyses were run in quadruplicate. Aliquots from salivary, gastric and duodenal steps were realized and frozen at -80°C until use.

2.2.6   Cell culture and uptake experiments

The human colon adenocarcinoma cell line Caco-2 TC-7 were grown in DMEM supplemented with 16% (v/v) fetal bovine serum (FBS), 1% (v/v) nonessential amino acids

and 1% (v/v) antibiotics (complete medium). Cells were seeded at a density of 15 000 cells/well and grown on transwell membrane (six-well plate, 1mm pore size polycarbonate membrane; Becton Dickinson) and were incubated in humidified atmosphere of 5% CO_2 and 95% air at 37°C during 21 days to obtain confluent and differentiated cell monolayers.

Cytotoxicity of digestion samples on Caco-2/TC7 was primarily evaluated to determine the suitable dilution of aqueous fractions in HBSS before adding them to the apical side of cell monolayers. These results showed that 1/10 dilution was required for alperujo samples (data not shown). To avoid any interference with DMEM or serum components, aqueous fractions were diluted in HBSS and Caco-2 cells received HBSS in both chambers 12h before the experiments. At the beginning of each experiment, cells monolayers were washed twice with 1mL of PBS and received 1mL of diluted aqueous fraction. Finally, cells monolayers were incubated at 37°C for 2h, 4h and 6h. After the incubation period, apical and basolateral were harvested. Cell monolayers were washed twice with 1mL of PBS and harvested by scraping in 0.5mL of PBS. All samples were stored at -80°C until use [17].

2.2.7   Analyses of alperujo samples

2.2.7.1. Extraction of digestion and cell media samples

Phenolic compounds were extracted from salivary, gastric and duodenal steps as follows: 0.3 mL of ethanol was added to 0.2mL of sample. The internal standard was gallic acid. 0.2mL of *n*-hexane was added and the mixture was homogenized for 10 min using a vortex blender at maximal speed. After centrifugation (2 500rpm for 10 min at 4°C), the lower phase was collected. The solid bottom was re-extracted with 0.3mL of ethanol and re-vortexed for 10min. The second ethanol phase recovered was pooled to the previously collected phase. After evaporation to dryness using a Speed-Vac®, the dried extracts were dissolved in 200µL of water and frozen at -80°C before analysis. Apical mediums were directly injected. Basolateral media (1900µL) were primarily dried using a Speed-Vac® and the dried residues were dissolved in 80µL of water to concentrate them.

Inspired by Gallardo E. *et al*. (2016), the PBS fractions containing harvested cells (500µL) were sonicated with 50µL of internal standard for 10min at room temperature and centrifuged at 7000rpm for 10min at 4°C [47]. Supernatants were recovered and evaporated to dryness, then dissolved in 50µL of water and frozen at -80°C before analysis.

2.2.7.2. Chromatographic analysis

All extracts were analyzed by UHPLC-DAD-MS using an Acquity UHPLC® system linked to both a diode array detector and a Brucker Daltonics HCT Ultra Ion Traps mass

spectrometer equipped with an Electron Spray Ionization (ESI) source operating in negative ion mode. The separation was performed on an Acquity C18 BEH column (50x2.1 mm i.d., 1.7 μm). The solvents were (A) water/formic acid (99.5/0.5) and (B) acetonitrile. For alperujo analyses, the proportions of solvent B used were: 0–10 min: 1–20%, 10–12 min: 20-30%, 12–14 min: 30-100%. The injection volume was 1 μL for all samples and 10μL for cells and basolateral extracts. The column temperature was kept at 35°C. Along the 3 steps of the gradient, the flow rate was 0.30, 0.35 and 0.40 mL/min. Chromatograms were acquired at 280nm. The spectroscopic detection was performed in the range 200-800 nm with a resolution of 1.2 nm. The concentrations of phenolic compounds were estimated from calibration curves (peak area vs. concentration) Tyr, caffeic and *p*-coumaric acids with R values greater than 0.99 [19].

2.2.7.3. Mass spectrometry

ESI mass spectra were obtained at ionization energies of 50 and 100eV, the capillary voltage was 2kV, the source temperature was 365°C, the drying gas was introduced at a flow rate of 10 L/min and the skimmer voltage was 40V. Scans were performed in the m/z range 100 – 2000.

22.7.4. Calculation and statistics

All the *in vitro* experiments were run in quadruplicate. Results were expressed as means and standard deviations. Differences between means were assessed using ANOVA followed by the post-hoc Tukey test for parametric data. P values under 0.05 were considered significant. Two methods were used for the bioavailability calculation, i.e. a ratio between the mass of phenolic compounds in the basolateral side and the initial mass added in the apical side and, the ratio between the phenolic mass at the basolateral side against the initial one added to the meal.

2.3   Results

2.3.1   HT-Glc, Tyr, caffeic acid and *p*-coumaric acid bioacessibility

Figure VI.6 shows the bioaccessibility of HT-Glc, Tyr, caffeic and *p*-coumaric acids in each digestive compartment during the digestion process.
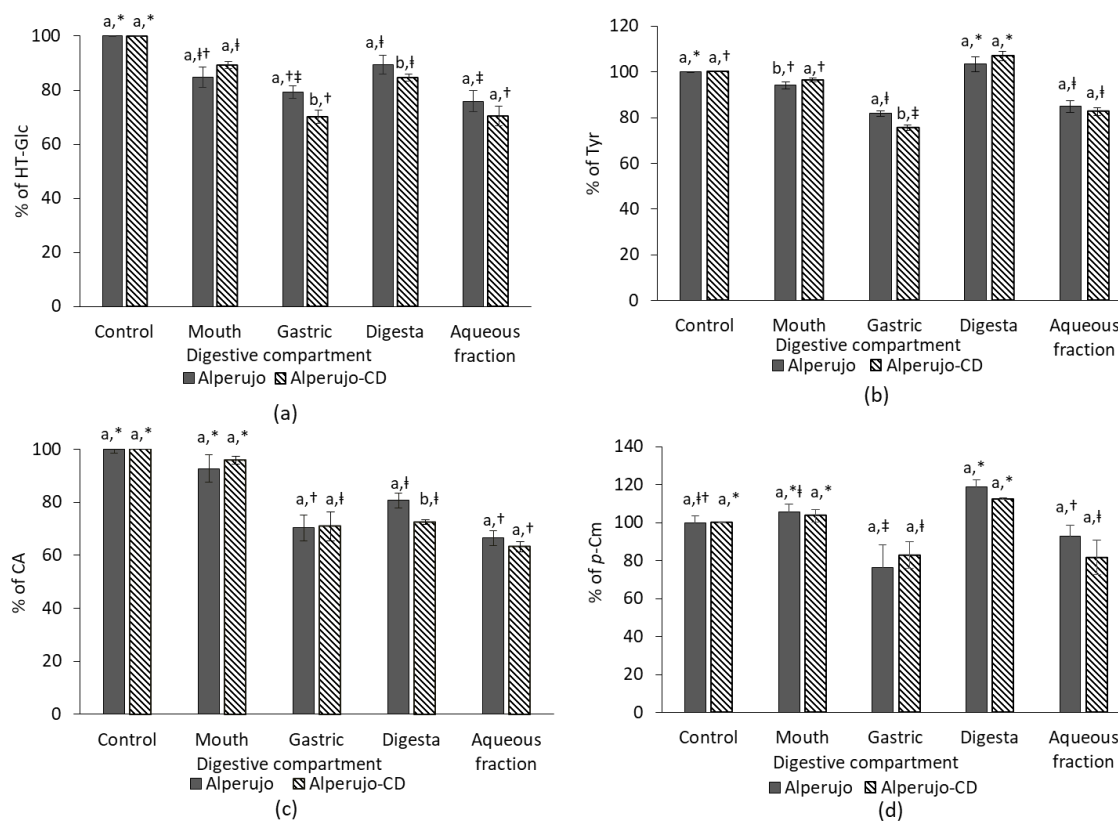
(a) Bioaccessibility of HT-Glc; (b) Bioaccessibility of Tyr; (c) Bioaccessibility of caffeic acid; (d) Bioaccessibility of *p*-coumaric acid. Values are expressed as mean ± SD of quadruplicate measurements. Different letters indicate a significant difference according to Tukey test (p ≤ 0.05) between all conditions for each compartment. Different symbols indicate a significant difference according to Tukey test (p ≤ 0.05) between all compartments for each condition.

Figure VI.6. Evaluation of the phenols bioaccessibility from alperujo juice powders in each digestive compartment

The presence of β-CD has no effect in the different compartment and on the final aqueous bioaccessibility of HT-Glc, Tyr, caffeic acid and *p*-coumaric acid during the digestion process. On average, HT-Glc concentration decreased during the digestion process to reach a bioaccessibility of 73.2 ± 4.5%. Almost 83.7 ± 2.4% of Tyr was recovered in the final aqueous phase at duodenal step. As Tyr, *p*-coumaric acid, which is a monohydroxy cinnamic acid, was highly soluble in the aqueous phase and was recovered at more than 87.9 ± 7.5 % while caffeic acid recovery was about 64.9 ± 2.9%. The amounts of Tyr and *p*-coumaric acid recovered in digestas seemed to be higher than the initial quantity (Tyr from alperujo-CD and *p*-coumaric acid from alperujo, p < 0.05).

2.3.2   HT-Glc, Tyr, caffeic acid and *p*-coumaric acid uptake by Caco-2/C 7 cells

Bioavailability of HT-Glc, Tyr, caffeic acid and *p*-coumaric acid was also evaluated in Caco-2 cells using the previous aqueous fractions from *in vitro* digestions. According to preliminary cytotoxicity assays, a 1:10 dilution of the aqueous fractions was required to perform the study. Our results showed that each phenolic compound exhibited the same absorption behavior whether it was from alperujo or from alperujo-CD powder. Therefore, figure VI.7 presents the recovery of these phenolic compounds for the alperujo condition only.
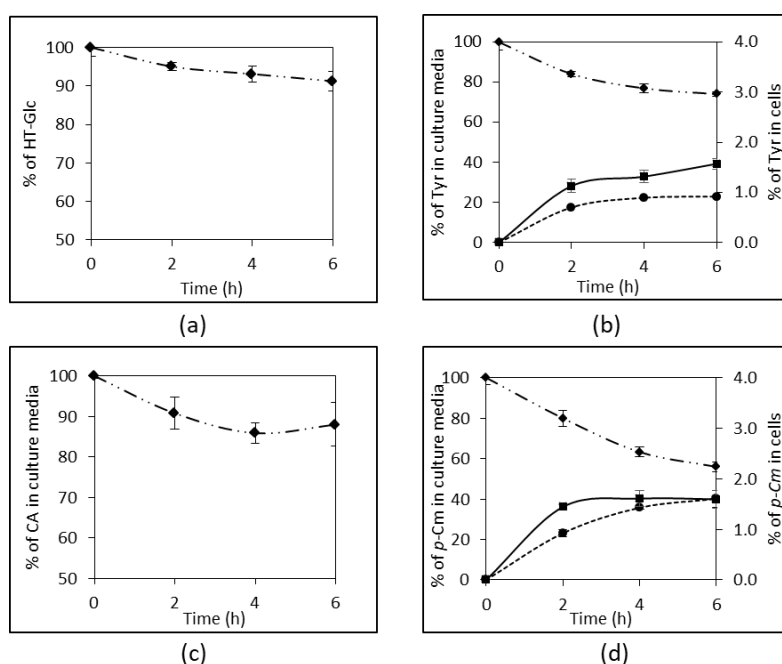
(**a**) Case of HT-Glc; (**b**) Case of Tyr; (**c**) Case of caffeic acid; (**d**) Case of *p*-coumaric acid. All results are expressed in percent of the initial amount in the apical side. (◆) for the apical side; (●) for the basolateral side; (■) for the Caco-2/TC7 cells. Values are expressed as mean ± SD of quadruplicate measurements.

Figure VI.7. Phenolic compounds recovery in apical side, basolateral side and Caco-2/TC7 cells

After a 6-h incubation period on cell monolayers, a decrease of HT-Glc and caffeic acid amounts of about 10% ($p < 0.05$) and 18% ($p < 0.052$), respectively, was measured in the apical media (Figures VI.7.a and 3.c). However, neither HT-Glc nor caffeic acid was recovered in the cytosolic compartment of the cells or in the basolateral media.

Conversely, both Tyr and *p*-coumaric acid were found in the cytosolic compartment of Caco-2 cells after a 6h-incubation period: 1.6 ± 0.1% and 1.4 ± 0.1% = for Tyr, and 1.6 ± 0.1% and 1.8 ± 0.2% = for *p*-coumaric acid, from alperujo and alperujo-CD respectively

(Figures VI.7.b and 3.d). Both were more recovered in the basolateral side after 6h, in higher amount when they were from alperujo-CD than from alperujo, i.e. $25.2 \pm 0.9\%$ and $22.8 \pm 0.9\%$ for Tyr (p < 0.022) and $48.7 \pm 1.7\%$ and $41.8 \pm 1.9\%$ for *p*-coumaric acid (p < 0.006) from alperujo-CD and alperujo, respectively. Our data also showed that the absorption of Tyr and *p*-coumaric acid into Caco-2 cells and their passage in the basolateral side were time-dependent. Moreover, the total recovery of Tyr and *p*-coumaric acid in these three compartments was nearly 100%, suggesting that no metabolism occurred in the intestinal cells.

Three metabolites of caffeic acid were identified in culture media. Ferulic acid, which is a methylated caffeic acid, was recognized with its deprotonated mass [M-H]- at 193Da and its UV spectrum. Two other compounds at m/z 306Da were fragmented at m/z 288Da, 272Da, 254Da and at 179Da characteristic of the caffeic acid unit. They were then assigned as CA metabolites. Figure VI.8 shows the amounts of ferulic acid and the both isomers of caffeic acid derivatives in culture media cells. They were expressed as caffeic acid equivalent.
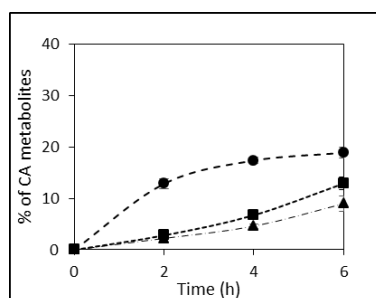
(●) for ferulic acid in the basolateral side; (■) for caffeic acid derivative isomer 1 in cells; (▲) for caffeic acid derivative isomer 2 in cells. Values are expressed in caffeic acid equivalent as mean ± SD of quadruplicate measurements.

Figure VI.8. Metabolites of caffeic acid in culture media of alperujo condition

Ferulic acid found at the basolateral side represented almost $19.5 \pm 1.4\%$ and $23.4 \pm 1.5\%$ (caffeic acid equivalent) of the initial caffeic acid amount in the apical side, from alperujo and alperujo-CD respectively (p < 0.0001). The two other caffeic acid derivatives found into the cells represented about $12.9 \pm 1.3\%$ and $9.0 \pm 1.5\%$ of initial caffeic acid, for the isomers 1 and 2, respectively. Taking into account the presence of the three metabolites, the total recovery of caffeic acid was $128.9 \pm 4.2\%$ (p < 0.0001).

2.3.3   Calculation of phenolic compounds bioavailability

The following tables VI.3 and 4 show the bioavailability of phenolic compounds calculated according to their amounts added at the apical side or in the initial meal.

Table VI.3. Bioavailability of phenolic compounds as percentage of their initial apical amount

Samples	Tyr	*p*-coumaric acid	Ferulic acid
Alperujo	22.8 ± 0.9^a	41.8 ± 1.9^a	19.5 ± 1.4^a
Alperujo-CD	25.2 ± 0.9^b	48.7 ± 1.7^b	23.4 ± 1.5^b

Values are expressed as mean ± SD of quadruplicate measurements. Different letters indicate a significant difference according to Tukey test ($p \leq 0.05$) between the both alperujo conditions for each phenolic compound.

Table VI.4. Bioavailability of phenolic compounds as percentage of their initial amount in the test meal

Samples	Tyr	*p*-coumaric acid	Ferulic acid
Alperujo	16.2 ± 0.6^a	32.0 ± 3.2^a	8.9 ± 0.5^a
Alperujo-CD	16.8 ± 0.5^a	37.2 ± 3.2^a	10.0 ± 1.0^a

Values are expressed as mean ± SD of quadruplicate measurements. Different letters indicate a significant difference according to Tukey test ($p \leq 0.05$) between the both alperujo conditions for each phenolic compound.

The *in vitro* bioavailability has been firstly calculated taking to account the phenolic amount recovered in the basolateral compartment compared to the initial amount provided at the apical side. *p*-Coumaric acid displayed a bioavailability higher than 40% whether it was from alperujo or alperujo-CD. Caffeic acid, which is another cinnamic acid, was not bioavailable, while ferulic acid which was identified as a caffeic acid metabolite showed an absorption efficiency of about 20% of the initial caffeic acid amount. Tyr also displayed a bioavailability higher than 20%. In all cases, the phenolic compounds from alperujo-CD condition were better absorbed than from the alperujo condition ($p < 0.05$ for Tyr and *p*-coumaric acid from alpejuro and alpejuro-CD, respectively).

The second way to calculate the bioavailability was to compare the Tyr, caffeic acid, *p*-coumaric acid and ferulic acid content at the basolateral side of cell monolayers to the initial amount of phenol provided in the meal. With this calculation, no significant difference was showed between these phenolic compounds whether they were from alperujo or alperujo conditions.

2.4   Discussion

This study explored the *in vitro* bioaccessibility and bioavailability of HT-Glc, Tyr, caffeic acid and *p*-coumaric acid from the alperujo powders. No significant effect of β-CD was observed on the phenolic recovery at each digestive step, from the mouth to the duodenal compartment. The amounts of all of them decreased during the digestion process to reach an

average aqueous bioaccessibility of 73.2 ± 4.5%, 83.7 ± 2.4%, 64.9 ± 2.9% and 87.9 ± 7.5% for HT-Glc, Tyr, caffeic acid and *p*-coumaric acid respectively.

Caffeic acid and *p*-coumaric acid are two cinnamic acids distinguishable by their hydroxyl numbers on the phenyl unit. *p*-Coumaric acid was more bioaccessible compared to the dihydroxylated forms, i.e. caffeic acid, from alperujo samples (+25%). D'Antuono *et al*. (2016) observed that Tyr exhibited a higher bioaccessibility (+16%) than HT when they performed an *in vitro* digestion of table olives [50]. These results confirm that mono-hydroxylated phenols as *p*-coumaric acid and Tyr gives are more stable during digestion than their di-hydroxylated homologues, i.e. caffeic acid and HT respectively. Moreover, their mass ratios in the digesta reached or exceeded 100%, which can reflect the hydrolysis of other phenolic compounds from alperujo samples resulting in both Tyr and *p*-coumaric acid release. In fact, an apparent decrease observed for the comselogoside signal could be the sign of its hydrolysis into *p*-coumaric acid aglycon for example, which would explain the higher quantity of *p*-coumaric acid compared to its initial amount in the digesta.

We then aimed at evaluating the bioavailability of HT-Glc, Tyr, caffeic acid and *p*-coumaric acid in a Caco-2 TC7 cell model. These cells were chosen as a suitable model to follow the absorption of target phenolic compounds through the intestinal barrier [51,52]. The Tyr apical to basolateral transport through Caco-2 cells reached almost 22.8 ± 0.9% of its initial apical content in 6 hours. Furthermore, it was also recovered in the cellular compartment. Consistently with the results obtained by Corona *et al*. (2009), no metabolite was recovered in to Caco-2 cells. Besides, we observed a time-dependent decrease of the HT-Glc amount at the apical side, but no HT-Glc was recovered in cells or at the basolateral side. O-β-D-Glucosides of dietary plant phenols are resistant to acid hydrolysis and reach the intestine in their intact form. In general, they are not or only slightly absorbed because of their polarity and size, while aglycones, released by the action of intestinal β-glucosidase, can be absorbed [53,54]. Manna *et al*. (20009) observed that HT and Tyr was absorbed by passive diffusion [34]. Besides, a direct transport through the Na+-dependent D-glucose transporter was evidenced as a minor absorption route for quercetin O-β-D-glucosides [32], which may also be a transport route for HT-Glc.

Both cinnamic acids were behaving very differently depending on the molecule, caffeic acid being not bioavailable whereas *p*-coumaric acid was highly absorbed and transported through Caco-2 cells even though its initial amount was lower. In reason of the low water solubility of caffeic acid, its bioavailability is known to be poor or even non-

existent [56,57]. Konishi *et al*. (2004) worked with a 5mM caffeic acid solution at the apical side of the cells and showed that caffeic acid absorption was more efficient with a proton gradient (apical: pH 6; basolateral: pH 7.4) [58]. Tsukagoshi *et al*. (2007) compared the uptake by Caco-2 cells of hydroxyl derivatives of benzoic and cinnamic acids. They observed that the di-hydroxylation of benzoic or cinnamic acids decreased drastically their uptake by cells. Thus, the hydroxylation degree and position affect the affinity of these phenolic acids for the monocarboxylic acid transporters (MCTs) probably due to the change in lipophilicity [59]. No metabolite was found for *p*-coumaric acid whereas an important metabolism was assigned for caffeic acid, which reduced its bioavailability as an intact molecule. Our results revealed that the total recovery of caffeic acid and its metabolites exceeded 100%. Ferulic acid, which can also result from catechol-O-methyltransferase (COMT) activity, and caffeic derivative isomers, could then come from the metabolism of caffeic acid or its derivatives naturally found in alperujo as caffeoyl-6'-secologanoside. Indeed, this molecule was previously identified in the alperujo with which we worked [19].

The uptake study allowed to highlight a better absorption of Tyr, *p*-coumaric acid and ferulic acid from alperujo-CD condition than from the alperujo condition without β-CD. Shulman *et al*. (2011) observed that HP-β-CD improved the naringenin absorption through the gut epithelium by 11-fold [60]. Lee *et al*. (2007) increased the absorption of isoflavones from a Soy extract in rats of about 126% by complexing them with β-CD [61]. The main recognized β-CD advantage regarding the phenolic compounds formulation is to improve their bioavailability by increasing their apparent water solubility, their dissolution rate and/or their permeability [45,62,63]. Our lower improvement rates could be due to the higher hydrophilic character of our studied compounds compared to flavonoids which can more easily form inclusion complexes with β-CD.

Finally, the *in vitro* bioavailability calculation method (expressed as bioaccessibility x absorption by Caco-2 cells), allowed to correct the common overestimation of the phenolic compound bioavailability by considering the effects of the digestion process. Even though the *in vitro* bioavailability for each phenolic compound was not significantly different whether alperujo was administered with or without β-CD, values were higher from the alperujo-CD condition than alperujo without CD. This absence of significance may be due to the low amounts of phenolic compounds recovered in the basolateral chamber compared to the initial ones brought to the meal. However, this calculation confirmed that among the studied compounds, *p*-coumaric acid was the more bioavailable, followed by Tyr and ferulic

acid. The differences of bioavailability may be due to the interactions that occur between phenolic compounds between them and with other alperujo constituents as well as to their difference of polarity [23].

2.5   Conclusion

When ingested concomitantly to a meal, β-CD seems to have no significant effect on the bioaccessibility of phenolic compounds from alperujo. β-CD increased the bioavailability of Tyr, *p*-coumaric and ferulic acids but the difference remained non-significant. However, it has been observed that β-CD was able to locally increase the Tyr, *p*-coumaric acid and ferulic acid absorption through intestinal cells ($p < 0.05$). Furthermore, the absorption of Tyr, ferulic acid and *p*-coumaric acid were time-dependent. Finally, the bioavailability of phenolic compounds and metabolites from alperujo determined as a ratio between their basolateral and their initial meal amounts were as follows: *p*-coumaric acid > Tyr > ferulic acid. The moderate bioavailability of these compounds (8.9 to 37.2%) could result from their low water solubility, their high metabolism in the intestine and the possible competition between them and the other foods and alperujo compounds for absorption.

References

1. Niaounakis M, Halvadakis CP. 2006. *Olive processing waste management literature review and patent survey*. Elsevier, Amsterdam; London.

2. Dermeche S., Nadour M., Larroche C., F. Moulti-Mati, Michaud P. 2013. Olive mill wastes: Biochemical characterizations and valorization strategies. *Process Biochem*. 48:1532–1552.

3. Ghanbari R, Anwar F, Alkharfy KM, Gilani A-H, Saari N. 2012. Valuable Nutrients and Functional Bioactives in Different Parts of Olive (Olea europaea L.)?A Review. *Int. J. Mol. Sci*. 13:3291–3340.

4. Leouifoudi I, Zyad A, Amechrouq A, Oukerrou MA, Mouse HA, Mbarki M. 2014. Identification and characterisation of phenolic compounds extracted from Moroccan olive mill wastewater. *Food Sci. Technol. Camp*. 34:249–257.

5. Malapert A, Reboul E, Dangles O, Tomao V. 2016. An overview of the analysis of phenolic compounds found in olive mill by-products. *Trends Chromatogr*. 10:81–94.

6. Giordano E, Dangles O, Rakotomanomana N, Baracchini S, Visioli F. 2015. 3-O-Hydroxytyrosol glucuronide and 4-O-hydroxytyrosol glucuronide reduce endoplasmic reticulum stress *in vitro*. *Food Funct*. 6:3275–3281.

7. Jemai H, El Feki A, Sayadi S. 2009. Antidiabetic and Antioxidant Effects of Hydroxytyrosol and Oleuropein from Olive Leaves in Alloxan-Diabetic Rats. *J. Agric. Food Chem*. 57:8798–8804.

8. Visioli F, Bernardini E. 2011. Extra virgin olive oil's polyphenols: biological activities. *Curr. Pharm. Des*. 17:786–804.

9. Iacovino R, Rapuano F, Caso J, Russo A, Lavorgna M, Russo C, Isidori M, Russo L, Malgieri G, Isernia C. 2013. β-Cyclodextrin Inclusion Complex to Improve Physicochemical Properties of Pipemidic Acid: Characterization and Bioactivity Evaluation. *Int. J. Mol. Sci*. 14:13022–13041.

10. Patil JS, Kadam DV, Marapur SC, Kamalapur MV. 2010. Inclusion complex system; a novel technique to improve the solubility and bioavailability of poorly soluble drugs: a review. 2:29–34.

11. Szejtli J. 2004. Past, present and future of cyclodextrin research. *Pure Appl. Chem*. 76.

12. Munin A, Edwards-Lévy F. 2011. Encapsulation of Natural Polyphenolic Compounds; a Review. *Pharmaceutics*. 3:793–829.

13. Pinho E, Grootveld M, Soares G, Henriques M. 2014. Cyclodextrins as encapsulation agents for plant bioactive compounds. *Carbohydr. Polym*. 101:121–135.

14. Ratnasooriya CC, Rupasinghe HPV. 2012. Extraction of phenolic compounds from grapes and their pomace using β-cyclodextrin. *Food Chem*. 134:625–631.

15. Rein MJ, Renouf M, Cruz-Hernandez C, Actis-Goretta L, Thakkar SK, da Silva Pinto M. 2013. Bioavailability of bioactive food compounds: a challenging journey to bioefficacy: Bioavailability of bioactive food compounds. *Br. J. Clin. Pharmacol.* 75:588–602.

16. Goncalves A, Gleize B, Roi S, Nowicki M, Dhaussy A, Huertas A, Amiot M-J, Reboul E. 2013. Fatty acids affect micellar properties and modulate vitamin D uptake and basolateral efflux in Caco-2 cells. *J. Nutr. Biochem.* 24:1751–1757.

17. Goncalves A, Margier M, Tagliaferri C, Lebecque P, Georgé S, Wittrant Y, Coxam V, Amiot M-J, Reboul E. 2016. Pinoresinol of olive oil decreases vitamin D intestinal absorption. *Food Chem.* 206:234–238.

18. Gallardo E, Sarria B, Espartero JL, Gonzalez Correa JA, Bravo-Clemente L, Mateos R. 2016. Evaluation of the Bioavailability and Metabolism of Nitroderivatives of Hydroxytyrosol Using Caco-2 and HepG2 Human Cell Models. *J. Agric. Food Chem.* 64:2289–2297.

19. Malapert A, Reboul E, Loonis M, Dangles O, Tomao V. 2017. Direct and Rapid Profiling of Biophenols in Olive Pomace by UHPLC-DAD-MS. *Food Anal. Methods.* doi:10.1007/s12161-017-1064-2

20. Drechsler KC, Ferrua MJ. 2016. Modelling the breakdown mechanics of solid foods during gastric digestion. *Food Res. Int.* 88:181–190.

21. Gómez-Romero M, García-Villalba R, Carrasco-Pancorbo A, Fernández-Gutiérrez A. 2012. Metabolism and bioavailability of olive oil polyphenols. *Olive Oil-Const. Qual. Health Prop. Bioconversions.* InTech.

22. Pereira-Caro G, Sarri? B, Madrona A, Espartero JL, Escuderos ME, Bravo L, Mateos R. 2012. Digestive stability of hydroxytyrosol, hydroxytyrosyl acetate and alkyl hydroxytyrosyl ethers. *Int. J. Food Sci. Nutr.* 63:703–707.

23. Soler A, Romero MP, Macià A, Saha S, Furniss CSM, Kroon PA, Motilva MJ. 2010. Digestion stability and evaluation of the metabolism and transport of olive oil phenols in the human small-intestinal epithelial Caco-2/TC7 cell line. *Food Chem.* 119:703–714.

24. Corona G, Tzounis X, Assunta Dess? M, Deiana M, Debnam ES, Visioli F, Spencer JPE. 2006. The fate of olive oil polyphenols in the gastrointestinal tract: Implications of gastric and colonic microflora-dependent biotransformation. *Free Radic. Res.* 40:647–658.

25. Zhongxiang Fang, Bhesh Bhandari. 2010. Encapsulation of polyphenols – a review. *Trends Food Sci. Technol.* 21:510–523.

26. Flourié B, Molis C, Achour L, Dupas H, Hatat C, Rambaud JC. 1993. Fate of β-cyclodextrin in the human intestine. *J. Nutr.* 123:676–680.

27. Joint FAO/WHO Expert Committee on Food Additives, World Health Organization, International Program on Chemical Safety. 2009. *Safety evaluation of certain food additives*. World Health Organization, Geneva.

28. Magnúsdóttir A, Másson M, Loftsson T. 2005. The conventional model of drug/cyclodextrin complex formation (salicylic acid/β-cyclodextrin inclusion complex). *Expert Opin. Drug Deliv.* 2.

29. Shimpi S, Chauhan B, Shimpi P. 2005. Cyclodextrins: application in different routes of drug administration. *Acta pharmaceutica*. 2:139–156.

30. López-García MÁ, López Ó, Maya I, Fernández-Bolaños JG. 2010. Complexation of hydroxytyrosol with β-cyclodextrins. An efficient photoprotection. *Tetrahedron*. 66:8006–8011.

31. Manach C, Scalbert A, Morand C, Rémésy C, Jiménez L. 2004. Polyphenols: food sources and bioavailability. *Am. J. Clin. Nutr.* 79:727–747.

32. Bohn T. 2014. Dietary factors affecting polyphenol bioavailability. *Nutr. Rev.* 72:429–452.

33. Jakobek L. 2015. Interactions of polyphenols with carbohydrates, lipids and proteins. *Food Chem.* 175:556–567.

34. Manna C, Galletti P, Maisto G, Cucciolla V, D'Angelo S, Zappia V. 2000. Transport mechanism and metabolism of olive oil hydroxytyrosol in Caco-2 cells. *FEBS Lett.* 470:341–344.

35. Mateos R, Pereira-Caro G, Saha S, Cert R, Redondo-Horcajo M, Bravo L, Kroon PA. 2011. Acetylation of hydroxytyrosol enhances its transport across differentiated Caco-2 cell monolayers. *Food Chem.* 125:865–872.

36. Pérez-Sanchez A, Borras-Linares I, Barrajon-Catalan E, Arraez-Roman D, Gonzalez-Alvarez I, Ibanez E, Segura-Carretero A, Bermejo M, Micol V. 2017. Evaluation of the intestinal permeability of rosemary (*Rosmarinus officinalis* L.) extract polyphenols and terpenoids in Caco-2 cell monolayers. In Medina, MA, ed., *PLOS ONE*. 12:e0172063.

37. Conseil Oléicole International. 2013. - ECONOMIE : 1,5 milliards d'oliviers dans le monde - Olive Info.

38. Ollivier D., Pinatel C., Ollivier V., Artaud J. 2014. Composition en acides gras et en triglycérides d'huiles d'olive vierges de 34 variétés et 8 Appellations d'Origine Françaises et de 2 variétés étrangères implantées en France: Constitution d'une banque de données (1ère partie). *Olivae*.:36–48.

39. Uekama K, Hirayama F, Irie T. 1998. Cyclodextrin drug carrier systems. *Chem. Rev.* 98:2045–2076.

40. Szejtli J. 1988. *Cyclodextrin Technology*. 1, Springer Netherlands, Dordrecht.

41. Mangolim CS, Moriwaki C, Nogueira AC, Sato F, Baesso ML, Neto AM, Matioli G. 2014. Curcumin–β-cyclodextrin inclusion complex: Stability, solubility,

characterisation by FT-IR, FT-Raman, X-ray diffraction and photoacoustic spectroscopy, and food application. *Food Chem*. 153:361–370.

42. Ferreira F da R, Valentim IB, Ramones ELC, Trevisan MTS, Olea-Azar C, Perez-Cruz F, de Abreu FC, Goulart MOF. 2013. Antioxidant activity of the mangiferin inclusion complex with β-cyclodextrin. *LWT - Food Sci. Technol*. 51:129–134.

43. Mourtzinos I, Salta F, Yannakopoulou K, Chiou A, Karathanos VT. 2007. Encapsulation of Olive Leaf Extract in β-Cyclodextrin. *J. Agric. Food Chem*. 55:8088–8094.

44. Mourtzinos I, Makris DP, Yannakopoulou K, Kalogeropoulos N, Michali I, Karathanos VT. 2008. Thermal Stability of Anthocyanin Extract of Hibiscus sabdariffa L. in the Presence of β-Cyclodextrin. *J. Agric. Food Chem*. 56:10303–10310.

45. Carrier RL, Miller LA, Ahmed I. 2007. The utility of cyclodextrins for enhancing oral bioavailability. *J. Controlled Release*. 123:78–99.

46. Zhang H, Hou Y, Liu Y, Yu X, Li B, Cui H. 2010. Determination of Mangiferin in Rat Eyes and Pharmacokinetic Study in Plasma After Oral Administration of Mangiferin-Hydroxypropyl-Beta-Cyclodextrin Inclusion. *J. Ocul. Pharmacol. Ther*. 26:319–324.

47. Gallardo E, Sarria B, Espartero JL, Gonzalez Correa JA, Bravo-Clemente L, Mateos R. 2016. Evaluation of the Bioavailability and Metabolism of Nitroderivatives of Hydroxytyrosol Using Caco-2 and HepG2 Human Cell Models. *J. Agric. Food Chem*. 64:2289–2297.

48. Khymenets O, Crespo MC, Dangles O, Rakotomanomana N, Andres-Lacueva C, Visioli F. 2016. Human hydroxytyrosol's absorption and excretion from a nutraceutical. *J. Funct. Foods*. 23:278–282.

49. Pereira-Caro G, Sarriá B, Madrona A, Espartero JL, Escuderos ME, Bravo L, Mateos R. 2012. Digestive stability of hydroxytyrosol, hydroxytyrosyl acetate and alkyl hydroxytyrosyl ethers. *Int. J. Food Sci. Nutr*. 63:703–707.

50. D'Antuono I, Garbetta A, Ciasca B, Linsalata V, Minervini F, Lattanzio VMT, Logrieco AF, Cardinali A. 2016. Biophenols from Table Olive cv *Bella di Cerignola* : Chemical Characterization, Bioaccessibility, and Intestinal Absorption. *J. Agric. Food Chem*. 64:5671–5678.

51. Turco L, Catone T, Caloni F, Consiglio ED, Testai E, Stammati A. 2011. Caco-2/TC7 cell line characterization for intestinal absorption: How reliable is this *in vitro* model for the prediction of the oral dose fraction absorbed in human? *Toxicol. In vitro*. 25:13–20.

52. Gonzales GB, Van Camp J, Vissenaekens H, Raes K, Smagghe G, Grootaert C. 2015. Review on the Use of Cell Cultures to Study Metabolism, Transport, and Accumulation of Flavonoids: From Mono-Cultures to Co-Culture Systems: Cell co-cultures for flavonoid research…. *Compr. Rev. Food Sci. Food Saf*. 14:741–754.

53. Kumar S, Pandey AK. 2013. Chemistry and Biological Activities of Flavonoids: An Overview. *Sci. World J.* 2013:1–16.

54. Huynh N, Van Camp J, Smagghe G, Raes K. 2014. Improved Release and Metabolism of Flavonoids by Steered Fermentation Processes: A Review. *Int. J. Mol. Sci.* 15:19369–19388.

55. Day AJ, Gee JM, DuPont MS, Johnson IT, Williamson G. 2003. Absorption of quercetin-3-glucoside and quercetin-4′-glucoside in the rat small intestine: the role of lactase phlorizin hydrolase and the sodium-dependent glucose transporter. *Biochem. Pharmacol.* 65:1199–1206.

56. Wang S-J, Zeng J, Yang B-K, Zhong Y-M. 2014. Bioavailability of caffeic acid in rats and its absorption properties in the Caco-2 cell model. *Pharm. Biol.* 52:1150–1157.

57. Prasadani WC, Senanayake CM, Jayathilaka N, Ekanayake S, Seneviratne KN. 2017. Effect of three edible oils on the intestinal absorption of caffeic acid: An *in vivo* and *in vitro* study. In Caruso, C, ed., *PLOS ONE*. 12:e0179292.

58. Konishi Y, Kobayashi S. 2004. Transepithelial Transport of Chlorogenic Acid, Caffeic Acid, and Their Colonic Metabolites in Intestinal Caco-2 Cell Monolayers. *J. Agric. Food Chem.* 52:2518–2526.

59. Tsukagoshi K, Endo T, Kimura O. 2016. Uptake of Hydroxy Derivatives of Benzoic Acid and Cinnamic Acid by Caco-2 cells via Monocarboxylic Acid Transporters. *J. Pharm. Drug Res.* 1:9–18.

60. Shulman M, Cohen M, Soto-Gutierrez A, Yagi H, Wang H, Goldwasser J, Lee-Parsons CW, Benny-Ratsaby O, Yarmush ML, Nahmias Y. 2011. Enhancement of Naringenin Bioavailability by Complexation with Hydroxypropoyl-β-Cyclodextrin. In Deli, MA, ed., *PLoS ONE*. 6:e18033.

61. Lee S-H, Kim YH, Yu H-J, Cho N-S, Kim T-H, Kim D-C, Chung C-B, Hwang Y-I, Kim KH. 2007. Enhanced Bioavailability of Soy Isoflavones by Complexation with β-Cyclodextrin in Rats. *Biosci. Biotechnol. Biochem.* 71:2927–2933.

62. Tiwari G, Tiwari R, Rai A. 2010. Cyclodextrins in delivery systems: Applications. *J. Pharm. Bioallied Sci.* 2:72.

63. Challa R, Ahuja A, Ali J, Khar RK. 2005. Cyclodextrins in drug delivery: An updated review. *AAPS PharmSciTech*. 6:E329–E357.

64. Soler A, Romero MP, Macià A, Saha S, Furniss CSM, Kroon PA, Motilva MJ. 2010. Digestion stability and evaluation of the metabolism and transport of olive oil phenols in the human small-intestinal epithelial Caco-2/TC7 cell line. *Food Chem.* 119:703–714.

General discussion

Two-phase olive pomace, also called 'alperujo', is a new kind of olive mill waste composed of olive peels, pulp, seeds, vegetation water and traces of olive oil. The main valorization pathways of olive pomace are the second oil extraction leading to the "olive-pomace oil" [4], the combustion [5] that produces energy and its application on soil as fertilizer [6]. However, alperujo is also recognized as a phenolic-rich matter with a total phenolic content from 0.021 to 0.26 g/100g [7–9]. Indeed, most part of olive phenolic compounds (almost 98%) remain in the olive mill by-products after the oil extraction [1]. Furthermore, because of the high sensitivity of phenolic compounds in particular to oxidation, protection means are often used to preserve their integrity. β-CD, which is a oligosaccharide composed of 7 monomeric unit of glucopyranose, is defined by its conical shape, exhibiting a hydrophilic external structure and a hydrophobic cavity [10]. These properties make β-CD a good host to form inclusion complexes with small guest molecules (less than 800 g/mol) that protects them and enhances their water solubility [11–13]. Several studies focused on the inclusion complex formation between CDs and olive phenolic compounds. They mainly showed that β-CD was often more suitable than other CDs to encapsulate phenolic compounds and that a 1:1 stoichiometry occurred. In most cases, the inclusion complex is formed in water solution, by mixing β-CD and the guest phenolic compound in equimolar ratio. A drying process such as freeze-drying or spray-drying is the main way to finally obtain a solid form of inclusion complexes [14,15].

During that thesis, studies on the feasibility to recover phenolic compounds from alperujo samples into a final solid form by using a green and simple procedure based on the native β-CD as a solid extraction agent. First, pressing alperujo has been considered as a good way to obtain a phenolic-rich water solution. This aqueous sample has been used as the raw material for all our studies. The solid residue from the alperujo pressing could be used to recover the rest of phenolic compounds by solid-liquid extraction [16–18] or as combustible to produce energy [5]. The physicochemical characterization and the phenolic profile of alperujo juice have been firstly performed (Part 1). A direct and fast analytical method has been developed and led to identify 35 compounds in only 12 minutes in the alperujo juice

using a UHPLC-DAD-MS system. HT and Tyr are the two main phenyl alcohols found in the alperujo juice, followed by caffeic acid and *p*-coumaric acid belonging to the cinnamic acid family. HT and its glucosides have been quantified over 620 mg.L^{-1} HT equivalent. The sum of each major phenolic amount has been estimated higher than 850 mg.L^{-1}. Data confirmed that the alperujo juice obtained by pressing alperujo is a phenolic-rich aqueous fraction that could be used as an economic source of high value compounds.

HT and Tyr have been determined as the two major biophenols of the alperujo juice. Furthermore, HT has been usually associated with great bioactive properties. Thus, the two HT and Tyr have been selected as two biophenol models to study the formation of β-CD inclusion complex in solution (Part 2). This oligosaccharide is commonly used as part of formulations to form inclusion complexes in solution. This ability is especially due to its conical structure offering a hydrophobic cavity. The main common way to produce solid inclusion complexes is to mix β-CD with the guest compound in solution and to dry the whole in order to recover the guest-β-CD complexes in a solid form. The characterization of HT-β-CD complexes in solution and in the solid state obtained by usual drying processes, were carried out. A 1:1 stoichiometry and an association constant Ka of 33.2 (± 3.7) M^{-1} have been provided by spectroscopic analyses. Then, freeze-drying and spray-drying processes have been compared to the formation of solid HT-β-CD complex particles. Freeze-drying allowed a better solid recovery while spray-drying generated smaller and spherical particles. Nevertheless, both of them led to similar encapsulation efficiencies (higher than 84%) and generated β-CD complexes without modifying the antioxidant activity of HT. ^{13}C CP/ MAS NMR study finally confirmed that both drying processes produced HT-β-CD inclusion complexes. The same spectroscopic and microscopic analyses were carried out onto Tyr-β-CD complexes. The drying processes influenced the size and external shape of solid inclusion complexes. A 1:1 stoichiometry occurred between Tyr and β-CD and exhibited a Ka of 238.9 (± 18.5) M^{-1}. So, mixing β-CD with HT or Tyr in solution always led to the formation of biophenol-β-CD complex in our conditions. Furthermore, the association constant was ten times higher in the case of Tyr-β-CD complexes. The fact of lacking a

hydroxyl unit reduces the water solubility of Tyr that enhances its ability to enter and have a stronger interaction in the hydrophobic cavity of β-CD.

In order to avoid the drying step, which is currently used to obtain solid complexes, and to extract biophenols from olive mill by-products via a simple and eco-friendly process, the use of native β-CD in the solid state has been evaluated. The first assays were carried out onto biophenols models (Part 3). A new and eco-friendly process to extract phenolic compounds from an aqueous solution by using native β-CD in the solid state has been developed. Several β-CD/phenolic compounds molar ratios have been tried between the phenolic solution and the solid-state β-CD. Only one filtration step was required after mixing both components in solution. Results showed that Tyr and HT present in a water solution could be quickly and efficiently extracted by native β-CD kept in the solid state. The final filtration step allowed to recover more than 90% of solid particles and to extract more than 60% of Tyr or HT from a 100mM biophenol solution and 10 molar equivalents of β-CD. The final loading efficiency in these conditions was higher than 9 mg of biophenol/g of β-CD.

The same experiments have been carried out on the alperujo juice (Part 4). As observed for model solutions, native β-CD in the solid state allowed to extract phenolic compounds from the rich and complex alperujo juice. Results showed that removing protein from TPOP juice did not improve the phenolic extraction. Even if the solubility of β-CD increased in the plant extract, it has been possible to recover a final phenolic compound-β-CD powder whose loading efficiency reached 6.5 mg/g in gallic acid equivalent from a concentrated alperujo juice (96Mm g.a.e.) and 10 molar equivalents of β-CD. The chromatographic analyses have been performed to determine in which proportions each targeted phenolic compound (i.e. HT, HT-Glc, Tyr, caffeic and *p*-coumaric acids) was retained. More than 20% of the total of targeted phenolic compounds were extracted. Almost 15% of HT and 20% of its glucosides from the alperujo juice were extracted and were finally found in the alperujo-β-CD powder. Furthermore, the profile and distribution in the β-CD powder were similar to those of the initial alperujo juice. A non-selective character of the solid β-CD seems to occur for the phenolic compounds extraction.

Results obtained from model solutions or alperujo juice have been compared. First, the kinetic behaviors of the phenolic compounds extraction were the same whether β-CD was added to the models or alperujo samples. This new simple and eco-friendly process proved to be fast, for the extraction equilibrium was achieved in less than an hour. Furthermore, results showed that the extraction efficiency has been increased with the β-CD/phenolic compounds molar ratio and that it was more efficient for Tyr and HT models. Alperujo juice is a rich and complex solution where many compounds can enter in competition with phenolic ones to interact with β-CD. Landi *et al*. (2009) compared the phenol extraction from model solutions and wastewaters on granular activated carbon assisted with ultrasounds, and observed that the extraction efficiency was higher in the case of model solutions. Indeed, organic matter of studied wastewaters saturated sorbent pores and then limited the adsorption of the targeted molecules [19]. Finally, the loading efficiency Qe which represents the quantity of biophenols per g of β-CD progressed in return of the extraction efficiency, being higher for small amounts of β-CD. In excess, solid β-CD particles could interfere with one another for the antioxidant extraction. Alperujo juice composition could be assimilated to the one of olive mill wastewaters. It is a complex mix of water and sugars [20–22], protein [23] and mineral salts [24,25]. These components could interfere with β-CD, entering in competition with phenolic compounds to access to retention sites. In both studies, concentrating phenolic aqueous samples allowed to improve almost five folds the loading efficiency from either a biophenol model solution or alperujo juice. This new simple and eco-friendly process is a fast and easy procedure to efficiently recover phenolic compounds from a natural water solution and leading to a safe and high added value product.

Finally, the bioaccessibility and bioavailability of HT and of the other main phenolic compounds from alperujo juice were determined by *in vitro* digestion studies followed by absorption by Caco-2/TC7 cells in culture. These two parameters are decisive for benefiting of an antioxidant potential after consuming active compounds. Firstly, HT was studied from either a pure standard or alperujo juice, and the influence of both β-CD and foods on its bioaccessibility and bioavailability were evaluated. Results showed that β-CD did not disturb HT bioaccessibility (i.e. the percentage of the ingested dose found in the aqueous phase of

the digesta) and bioavailability (defined as its quantity at the basolateral side of cultured cell monolayers compared to the initial amount brought by the meal), while the presence of foods significantly decreased both of about 20% and 10%, respectively. Bringing HT in a full plant extract such as alperujo juice decreased its intestinal bioaccessibility, which could be the results of the possible interactions between HT and other alperujo compounds such as fibers. A higher part of HT could then be complexed with food and alperujo constituents and be finally remain in the unabsorbed intestinal solid residue. Subsequently to the *in vitro* digestion, the intestinal absorption study revealed a time- and dose-dependent absorption of HT. Furthermore, a high metabolism occurred whether HT was from a pure standard of alperujo samples. Manna *et al*. (2000) worked on olive biophenols and observed that HT passed through Caco-2 monolayers by passive diffusion. They also observed that their absorptions were time- and dose-dependent [26,27]. Besides, metabolism involving COMT has been highlighted by the appearance of homovanillyl alcohol and homovanillyl alcohol glucuronide as metabolites of HT from pure standard and alperujo, respectively. In literature, digestion studies of olive phenolic compounds from pure standards or olive derivative matrices showed that olive phenols, even if they could cross enterocytes, underwented metabolism resulting on their transformation and/or conjugation in the small intestine. Their final bioavailability were then modified [28–30]. Furthermore, our *in vitro* studies showed that HT was about four-times more bioavailable from a pure standard (more than 30%) than from a plant extract (almost 7.0%). This phenomenon could be the result of competition between HT and other components from alperujo to cross the intestinal cells as observed by Pérez-Sanchez and colleagues for a rosemary extract [31].

The intestinal absorption of HT from alperujo juice revealed that its recovery (i.e. the HT amount in the apical side, basolateral side and cells) exceeded 100%. We supposed that other phenolic compounds from that olive pomace could be a source of HT if metabolized by the intestinal cells. Thus, the analyses of other mains phenolic compounds, i.e. HT-Glc, Tyr, caffeic acid and *p*-coumaric acid have been also performed. Once again, no significant effect of β-CD has been observed during the *in vitro* digestions. The higher Tyr and *p*-

coumaric acid mass recoveries during the digestion process compared to the initial ingested dose could also be the results of the metabolism of other alperujo compounds. For instance, comselogoside was identified in the alperujo juice. Its amount decreased over the digestion and *p*-coumaric acid could be one of its metabolites. Intestinal absorption studies by Caco-2 TC7 cells were also carried for these phenolic compounds. Firstly, analyses informed about the limiting impact of the catechol unit on the phenolic absorption. In fact, Tyr was more absorbed about 2 times than HT, and *p*-coumaric acid was largely absorbed, while caffeic acid was not. Other researchers observed that the di-hydroxylation of benzoic or cinnamic acids was unfavorable for their uptake certainly because of their higher hydrophilicity and lower affinity for cellular transporters as MCTs decrease in lipophilicity [32]. Furthermore, a time-dependent decrease of HT-Glc occurred in the apical side while none was recovered in cells and in basolateral side. O-β-D-Glucosides is a natural phenols form in dietary plant suitable, which improve their water solubility and stability. It is known that they are stable in acid and alkaline digestive conditions resistant. They are mainly found in the intestine in their intact form, but they are so rarely absorbed because of their large size and their polarity. However, their cleavage and the release of the aglycone (i.e. HT) can be the result of the action of intestinal β-glucosidase, which would thus explain that HT recovery from alperujo samples exceeded 100%. Because of the absence in cells of HT-Glc and HT, LPH that is found in the small intestinal brush border, could be involved in the apical metabolism of HT-Glc and led to its time-dependent decrease and to a HT release that could then be absorbed by passive diffusion.

Even if a high metabolism has been commonly observed, other phenolic compounds from alperujo juice displayed a high bioavailability (> 8.9%) except for caffeic acid. However, their metabolites can exhibit interesting antioxidant potential, as ferulic acid that is one of caffeic acid metabolites [33]. Interestingly, it has been observed that β-CD significantly increased the intestinal absorption rates of Tyr and *p*-coumaric acid as well as of ferulic acid. Finally, the calculation was corrected with the initial phenolic amount brought to the meal. Thus, the "real" bioavailability has been determined up to32% for *p*-coumaric

acid followed by Tyr (higher than 16%) and HT (higher than 14.4%) from alperujo samples, without any significant difference whether they were administrated with or without β-CD. So, the method used to evaluate and calculate the fate of phenolic compounds in the gastrointestinal tract is an important parameter. In fact, we suggest that the numerous studies realized *in vitro* digestion without food overestimated the bioaccessibility of phenolic compounds, in particular by ruling out the natural interactions occurring between phenolic and food compounds, such as proteins or fibers [34,35].

Overall, competition occurred between all foods and alperujo compounds, which induced a decrease of the final bioavailability of phenolic compounds. As it could be interesting to consume antioxidants from alperujo to take advantage of their antioxidant power and their synergic potential activity, we recommend to consume these β-CD-phenolic complexes at fast for reducing their potential interaction with other components and optimizing their final bioavailability.

All these studies allowed to firstly demonstrate the high potential of the aqueous phase of alperujo as a rich and economic source of phenolic compounds. Based on the use of native β-CD in the solid state, a new simple and eco-friendly procedure has been developed and allowed to efficiently extract phenolic compounds from aqueous media and to finally obtain a phenol-rich powder. The optimum has been reached in one hour and this process only consisted in firstly mixing both β-CD in the solid state and the phenolic solution and finally filtering the mix for recovering a β-CD-phenolic compound powder. This solid form is suitable for many industrial uses. That procedure could then be an interesting way to avoid solvents and costly techniques and to respond to the current industrial demands. The phenol-β-CD powder could also be interesting for industrial formulations

General conclusion and perspectives

Olive oil is one of the most studied ingredients of the Mediterranean diet because of its high value content in active molecules, such as phenolic compounds. The olive oil production is associated with large waste productions. The two-phase olive mill system is a new kind of mill developed to reduce the effluent amount. Two-phase olive pomace, also called 'alperujo', is composed of olive pieces and vegetation waters. While olive oil is associated with health benefits, olive mill wastes possess larger amounts of phenolic compounds.

β-Cyclodextrin has been selected as a safe oligosaccharide commonly used in agroindustry for its ability to form complexes with other molecules and to improve their solubility and stability. β-CD inclusion complexes are often processed in solution with the target compounds, and the whole is generally dried to produce an active powder.

In order to characterize the biophenols behavior in presence of β-cyclodextrin, first HT-β-CD or Tyr-β-CD complexes in solution and in the solid state (spray- and freeze-drying) have been evaluated. Secondly, complexes produced by a new process using β-cyclodextrin in the solid state have been studied; the method has been optimized with selected biophenols and then with alperujo juice. Based on the molar ratio mix between a biophenol-rich solution and 10 molar equivalents of native β-cyclodextrin in the solid state, this procedure led to extract more than 60% of biophenols from a model solution and more than 20% of the total phenolic compounds from the alperujo juice in one hour. One final filtration step enabled the recovery of a high added value powder composed of antioxidants and β-cyclodextrin. In the case of alperujo, the final phenolic content reached 6.6 mg of biophenols (gallic acid equivalent) per gram of powder.

Finally, the *in vitro* studies showed an unfavourable effect of consuming phenolic compounds with foods regarding their bioaccessibility and bioavailability. Results also confirmed that β-cyclodextrin did not disturb the gastrointestinal fate of phenolic compounds after ingestion. Furthermore, β-CD increased locally the intestinal absorption of some alperujo phenolic compounds such as Tyr or *p*-coumaric acid.

The use of native β-cyclodextrin in the solid state allows the extraction of high added values compounds such as phenolic compounds by a fast and simple procedure. The mix between β- cyclodextrin and the concentrated alperujo juice followed by a filtration are the two only steps for this new process. It allows to recover a phenolic-rich powder in only one hour without using any organic solvent or expensive technics, which are often used for extracting phenolic compounds from plant materials. Finally, this eco-friendly technique leads to a

β-CD-phenolic compound powder which could be used in food industries to increase the stability and the quality of some preparations. Furthermore, nutraceutical use could be considered to improve the nutritional intake.

Following this work, several perspectives could be considered. First, in the short term, the effects of ultrasounds on the extraction efficiency of the process could be evaluated.

Structural and conformational aspects of phenol-β-CD complexes obtained in this thesis could be explored. Differential Scanning Calorimetry (DSC) or Fourier-Transform InfraRed spectroscopy (FR-IR) could be carried out to clarify what type of interactions occurred in that biophenol-β-CD powders, such as adsorption and/or inclusion complex formation.

After a patentability study and in the case of its validation, pre-pilot scale assays could follow to determine the conditions of the proposed procedure for a larger scale.

In a long-term view, studies on β- cyclodextrin as an oligosaccharide could be expanded to include polysaccharides such as potato, corn or pea starches which are also GRAS and current ingredients in many food preparations. Their variable amylose content could certainly lead to various kinds of starch-phenolic compounds complexes that could be a way to produce time-dependent delivery systems allowing to control the release of phenolic compounds.

References

1. Rodis PS, Karathanos VT, Mantzavinou A. 2002. Partitioning of Olive Oil Antioxidants between Oil and Water Phases. *J. Agric. Food Chem.* 50:596–601.

2. Fernandez-Bolanos J, Felizón B, Brenes M, Guillén R, Heredia A. 1998. Hydroxytyrosol and tyrosol as the main compounds found in the phenolic fraction of steam-exploded olive stones. *J. Am. Oil Chem. Soc.* 75:1643–1649.

3. Schievano A, Adani F, Buessing L, Botto A, Casoliba EN, Rossoni M, Goldfarb JL. 2015. An integrated biorefinery concept for olive mill waste management: supercritical CO_2 extraction and energy recovery. *Green Chem.* 17:2874–2887.

4. Niaounakis M, Halvadakis CP. 2006. *Olive processing waste management literature review and patent survey*. Elsevier, Amsterdam; London. [cited 6 November 2014]. Available from http://www.sciencedirect.com/science/book/9780080448510.

5. Intini F., Kühtz S., Rospi G. 2011. Energy recovery of the solid waste of the olive oil Industries–LCA analysis and carbon footprint assessment. *J. Sustain. Energy Environ.* 2.:157–166.

6. Roig A, Cayuela ML, Sánchez-Monedero MA. 2006. An overview on olive mill wastes and their valorisation methods. *Waste Manag.* 26:960–969.

7. Cioffi G, Pesca MS, De Caprariis P, Braca A, Severino L, De Tommasi N. 2010. Phenolic compounds in olive oil and olive pomace from Cilento (Campania, Italy) and their antioxidant activity. *Food Chem.* 121:105–111.

8. Malapert A, Reboul E, Dangles O, Tomao V. 2016. An overview of the analysis of phenolic compounds found in olive mill by-products. *Trends Chromatogr.* 10:81–94.

9. Salgado JM, Abrunhosa L, Venâncio A, Domínguez JM, Belo I. 2014. Screening of winery and olive mill wastes for lignocellulolytic enzyme production from Aspergillus species by solid-state fermentation. *Biomass Convers. Biorefinery.* 4:201–209.

10. Szente L, Szejtli J. 2004. Cyclodextrins as food ingredients. *Trends Food Sci. Technol.* 15:137–142.

11. Astray G, Gonzalez-Barreiro C, Mejuto JC, Rial-Otero R, Simal-Gándara J. 2009. A review on the use of cyclodextrins in foods. *Food Hydrocoll.* 23:1631–1640.

12. Olga G, Styliani C, Ioannis RG. 2015. Coencapsulation of Ferulic and Gallic acid in hp-b-cyclodextrin. *Food Chem.* 185:33–40.

13. Zhongxiang Fang, Bhesh Bhandari. 2010. Encapsulation of polyphenols – a review. *Trends Food Sci. Technol.* 21:510–523.

14. Oehlke K, Adamiuk M, Behsnilian D, Gräf V, Mayer-Miebach E, Walz E, Greiner R. 2014. Potential bioavailability enhancement of bioactive compounds using food-grade engineered nanomaterials: a review of the existing evidence. *Food Funct.* 5:1341.

15. Szejtli J. 1988. *Cyclodextrin Technology*. 1, Springer Netherlands, Dordrecht.

16. Lafka T-I, Lazou AE, Sinanoglou VJ, Lazos ES. 2011. Phenolic and antioxidant potential of olive oil mill wastes. *Food Chem*. 125:92–98.

17. Mulinacci N, Innocenti M, La Marca G, Mercalli E, Giaccherini C, Romani A, Erica S, Vincieri FF. 2005. Solid Olive Residues: Insight into Their Phenolic Composition. *J. Agric. Food Chem*. 53:8963–8969.

18. Priego-Capote F, Ruiz-Jiménez J, Luque de Castro M. 2004. Fast separation and determination of phenolic compounds by capillary electrophoresis–diode array detection. *J. Chromatogr. A*. 1045:239–246.

19. Landi M. 2009. Phenol removal by adsorption on granular activated carbon enhanced with ultrasound.

20. Bouknana D, Hammouti B, Salghi R, Jodeh S, Zarrouk A, Warad I, Aouniti A, Sbaa M. 2014. Physicochemical characterization of olive oil mill wastewaters in the eastern region of Morocco. *J Mater Env. Sci*. 5:1039–1058.

21. Rubio-Senent F, Rodríguez-Gutiérrez G, Lama-Muñoz A, Fernández-Bolaños J. 2015. Pectin extracted from thermally treated olive oil by-products: Characterization, physico-chemical properties, *in vitro* bile acid and glucose binding. *Food Hydrocoll*. 43:311–321.

22. Rubio-Senent F, Rodríguez-Gutiérrez G, Lama-Muñoz A, García A, Fernández-Bolaños J. 2015. Novel pectin present in new olive mill wastewater with similar emulsifying and better biological properties than citrus pectin. *Food Hydrocoll*. 50:237–246.

23. Fernández-Bolaños J, Rodríguez G, Rodríguez R, Guillén R, Jiménez A. 2006. Extraction of interesting organic compounds from olive oil waste. *Grasas Aceites*. 57:95–106.

24. Alburquerque J. 2004. Agrochemical characterisation of "alperujo", a solid by-product of the two-phase centrifugation method for olive oil extraction. *Bioresour. Technol*. 91:195–200.

25. Davies LC, Vilhena AM, Novais JM, Martins-Dias S. 2004. Olive mill wastewater characteristics: modelling and statistical analysis. *Grasas Aceites*. 55.

26. Manna C, Galletti P, Maisto G, Cucciolla V, D'Angelo S, Zappia V. 2000. Transport mechanism and metabolism of olive oil hydroxytyrosol in Caco-2 cells. *FEBS Lett*. 470:341–344.

27. Visioli F, Galli C, Bornet F, Mattei A, Patelli R, Galli G, Caruso D. 2000. Olive oil phenolics are dose-dependently absorbed in humans. *FEBS Lett*. 468:159–160.

28. Gallardo E, Palma-Vald?s R, Espartero JL, Santiago M. 2014. *In vivo* striatal measurement of hydroxytyrosol, and its metabolite (homovanillic alcohol), compared with its derivative nitrohydroxytyrosol. *Neurosci. Lett*. 579:173–176.

29. Gómez-Romero M, García-Villalba R, Carrasco-Pancorbo A, Fernández-Gutiérrez A. 2012. Metabolism and bioavailability of olive oil polyphenols. *Olive Oil-Const. Qual. Health Prop. Bioconversions*. InTech.

30. Soler A, Romero MP, Macià A, Saha S, Furniss CSM, Kroon PA, Motilva MJ. 2010. Digestion stability and evaluation of the metabolism and transport of olive oil phenols in the human small-intestinal epithelial Caco-2/TC7 cell line. *Food Chem*. 119:703–714.

31. Pérez-Sanchez A, Borras-Linares I, Barrajon-Catalan E, Arraez-Roman D, Gonzalez-Alvarez I, Ibanez E, Segura-Carretero A, Bermejo M, Micol V. 2017. Evaluation of the intestinal permeability of rosemary (Rosmarinus officinalis L.) extract polyphenols and terpenoids in Caco-2 cell monolayers. In Medina, MA, ed., *PLOS ONE*. 12:e0172063.

32. Tsukagoshi K, Endo T, Kimura O. 2016. Uptake of Hydroxy Derivatives of Benzoic Acid and Cinnamic Acid by Caco-2 cells via Monocarboxylic Acid Transporters. *J. Pharm. Drug Res.* 1:9–18.

33. Kikuzaki H, Hisamoto M, Hirose K, Akiyama K, Taniguchi H. 2002. Antioxidant Properties of Ferulic Acid and Its Related Compounds. *J. Agric. Food Chem.* 50:2161–2168.

34. Attri S, Singh N, Singh TR, Goel G. 2017. Effect of *in vitro* gastric and pancreatic digestion on antioxidant potential of fruit juices. *Food Biosci.* 17:1–6.

35. Domínguez-Avila JA, Wall-Medrano A, Velderrain-Rodríguez GR, Chen C-YO, Salazar-López NJ, Robles-Sánchez M, González-Aguilar GA. 2017. Gastrointestinal interactions, absorption, splanchnic metabolism and pharmacokinetics of orally ingested phenolic compounds. *Food Funct.* 8:15–38.

List of figures

List of tables

List of abbreviations

ABC	*ATP binding cassette*
AF	*Alperujo fraction*
β-CD	*β-cyclodextrin*
BCRP	*Breast cancer resistant proteins*
C-AF	*Concentrated-alperujo Fraction*
CBG	*Cytosolic β-glucosidase*
COMT	*Catechol O-methyl transferase*
CP/MAS	*Cross polarization/Magic angle spinning*
3,4-DHPEA-AC	*3,4-dihydroxyphenylethanol-acetate*
3,4-DHPEA-EA	*3,4-dihydroxyphenylethanol-elenolic acid monoaldehyde*
3,4-DHPEA-EDA	*3,4-dihydroxyphenyl ethyl alcohol-elenolic acid di-aldehyde*
DGM	*Dynamic gastric model*
DMEM	*Dulbecco modified Eagle medium*
DMSO	*Dimethylsulfoxide*
DOPAC	*3,4-dihydroxyphenylacetic acid*
DPPH	*2,2-diphenyl-1-picrylhydrazyl*
EE	*Extraction efficiency*
EFSA	*European Food Safety Agency*
EGCG	*Epigallocatechin gallate*
ESI	*Electrospray Ionization*
ESI-TOF/MS	*Electrospray time of flight mass spectrometry*
EtOH	*Ethanol*
FBS	*Fœtal bovine serum*
g.a.e.	*Gallic acid equivalent*
GC	*Gas chromatography*
Glc	*Glucose*
GlcU	*Glucuronide*
GLUT	*Glutathione-S-transferase*
p-gp	*p-glycoproteins*
GRAS	*Generally recognized as Safe*
HBSS	*Hank's balanced salt solution*
HP-β-CDs	*hydroxypropyl derivative of β-cyclodextrin*
HPEA-EDA	*p-hydroxyphenylethanol-elenolic acid dialdehyde*
HPLC	*High performance liquid chromatography*
HPLC-DAD-MS	*High performance liquid chromatography coupled with a diode array detector and a mass spectrophotometer*
HT	*Hydroxytyrosol*
HTCD	*HT-β-CD complex*

HTCD-FF	HT-β-CD complex – food-free
HT-Glc	Hydroxytyrosol-O-β-glucoside
HVA	Homovanillyl alcohol
HVA-GlcU	Homovanillyl alcohol glucuronide
JECFA	Joint FAO/WHO Expert Committee on Food Additives
K	Association constant
LPH	Lactase phlorizin hydrolase
MCT	Monocarboxylic transporters
MeOH	Methanol
MRP	Multidrug resistance associated proteins
MTT	Methylthiazolydiphenyl-tetrazolium
NMR	Nuclear magnetic resonance
OAT	Organic anion transporters
OATP	Organic anion transporters polypeptides
OMWW	Olive mill wastewaters
PBS	Phosphate-buffered saline
PF	Protein-Free alperujo juice
POS	Postprandial oxidative stress
PTFE	Polytetrafluoroethylene
PY	Production yield
Qe	Loading efficiency
QTOF-MS/MS	Quadrupole time of flight mass spectrometry
RSA	Radical scavenging activity
Rt	Retention time
SEM	Scanning electron microscopy
SD	Stadard deviation
SULT	Sulfatotransferase
TIM	TNO intestinal model
Tyr	Tyrosol
UGT	UDP-glucuronyltransferases
UHPLC	Ultra high performance liquid chromatography
UHPLC-DAD	Ultra high performance liquid chromatography coupled with a diode array detector
UHPLC-DAD-MS	Ultra high performance liquid chromatography coupled with a diode array detector and a mass spectrophotometer
US	Ultrasounds
UV/Vis	Ultra-Violet/Visible

Abstract: In relation to the current environmental issues of industrial effluents, the interest of new management pathways of by-products is still growing. Two-phase olive pomace also called 'alperujo' is one of the main industrial pollutants in the Mediterranean basin, associated with the olive oil production.

The first part of this thesis highlighted the high potential of alperujo to be considered as a phenolic-rich source. Then, β-CD has been chosen to extract olive biophenols from alperujo. The behaviour of β-CD with olive phenols has been firstly studied with biophenol models, i.e. tyrosol and hydroxytyrosol by usual spray- and freeze-drying processes. The ability of β-CD to form complexes in the solid state has been revealed by UV spectroscopy and ^{13}C CP/MAS NMR analyses. The use of β-CD in the solid state as phenol-extracting agent was evaluated. Over 60% and 20% of phenolic compounds were extracted from biophenol model solutions and alperujo juice respectively. This one-step procedure led to the concomitant removal of olive phenols from wastewaters and to recover food-grade biophenol-rich powders. Successively, *in vitro* bioavailability studies revealed the downside of combining food with biophenols whereas β-CD allowed to increase the intestinal absorption of some phenols, such as tyrosol and *p*-coumaric acid. Therefore, it has been shown in this work that alperujo is a phenolic-rich source and that native β-CD in the solid state could be recognized as an efficient, green and safe-grade extraction agent leading to the recovery of high values added products by a simple one-step procedure.

Keywords: Alperujo, two-phase olive pomace, phenolic compounds, β-cyclodextrin, inclusion complex, green extraction, bioavailability, valorization.

Résumé: Avec les problématiques environnementales actuelles associées aux effluents industriels, l'intérêt de nouveaux moyens de management des déchets grandit continuellement. Le grignon d'olive deux-phase aussi appelé « alperujo », est un des principaux polluants industriels du bassin Méditerranéen, lié à la production d'huile d'olive. La première partie de cette thèse a souligné le haut potentiel des grignons d'olive comme source riche en composés phénoliques. β-CD a été choisi pour extraire les biophénols présents des grignons. Le comportement de la β-CD avec les phénols de l'olive a été tout d'abord étudié avec des biophénols modèles, le tyrosol et l'hydroxytyrosol, par des procédés classiques, que sont l'atomisation et la lyophilisation. La capacité de la β-CD à former des complexes avec les biophénols modèles a été confirmée par des analyses UV spectroscopique et de RMN ^{13}C CP/MAS. L'utilisation de la β-CD native à l'état solide comme agent d'extraction des phénols a été évaluée. Plus de 60% et de 20% des composés phénoliques ont été extraits par la β-CD solide à partir de solutions de biophénols modèles et du jus d'alperujo respectivement. Cette procédure en une étape a conduit à l'enlèvement concomitant phénols de l'olive d'eaux usées et à la récupération de poudres riches en biophénols et de qualité alimentaire. A la suite, des études de biodisponibilités *in vitro* ont révélé l'effet négatif de consommer les biophénols avec des aliments tandis que la β-CD a permis d'augmenter l'absorption intestinale de certains composés, comme le tyrosol et l'acide *p*-coumarique. Ainsi, il a été montré dans cette étude que les grignons d'olive constituent une source riche en composés phénoliques, abondante et économique, et que la β-CD native à l'état solide pourrait être reconnue comme agent d'extraction efficace, écologique et sain, conduisant à la récupération de produits à hautes valeurs ajoutées par une simple procédure en une étape.

Mots clés : Alperujo, grignons d'olive deux phases, composés phénoliques, b-cyclodextrine, complexe d'inclusion, éco-extraction, biodisponibilité, valorisation.